Development and characterisation of a low-shear mycobacterial biofilm model

Daire M. Cantillon

A thesis submitted in partial fulfilment of the requirements of the University of Brighton and the University of Sussex for the degree of Doctor of Philosophy at the Brighton and Sussex Medical School.

May 2017

Abstract

Tuberculosis (TB) is a bacterial disease that primarily affects the lungs and is caused by the bacillus *Mycobacterium tuberculosis (M.tb).* Approximately 1 in 3 people are latently infected globally, with 1.5 million people dying from active TB in 2015 alone. Prolonged therapy of at least six months with four antimicrobial drugs is required to successfully treat disease. This lengthy drug treatment is necessary to remove sub-populations of *M.tb* that are tolerant to antimicrobial drugs and as a result persist through drug therapy. Despite the hypothesised clinical significance of drug tolerant *M.tb* sub-populations *in vivo*, drug development models for TB fail to account for these complex mycobacterial populations. Drug discovery models currently focus on planktonic bacterial growth systems that do not likely represent *M.tb in vivo* at which chemotherapy is targeted. The research presented in this thesis utilised a three-dimensional Rotary Cell Culture System (RCCS) to model mycobacterial growth in low shear conditions. *Mycobacterium bovis* (*M. bovis*) BCG was cultured in the RCCS optimised to induce biofilm formation, which was confirmed by scanning electron microscopy. *M. bovis* BCG biofilms were harvested after 21 days, homogenised to planktonic cell suspensions and antimicrobial susceptibility testing measured using culture, luminescent and colorimetric assays. Biofilm-derived bacilli were tolerant to isoniazid and streptomycin, a phenotype that could be rescued by passaging in drug-free media. Transcriptional profiling of mycobacterial biofilms in comparison to stationary phase bacilli revealed that the stress response transcriptional regulators SigB and SigE were upregulated, as well as the ESX5 secretion system implicated in virulence. Isocitrate lyase, an essential glyoxylate shunt enzyme required for virulence *in vivo* and implicated in antimicrobial tolerance, was also induced in biofilm growth. Mammalian cell entry genes were downregulated, as well as dihydrofolate reductase, an enzyme required for the activation of the anti-tuberculous drug pretomanid. Macrophages exposed to biofilm supernatants significantly induced TNFα but not IL-1β, suggesting a novel role for mycobacterial biofilms in host inflammatory responses. Finally, the role of a novel nuclease, *nuc,* was shown to not significantly increase rates of drug resistance in the laboratory strain *M.tb* H37Rv. This work shows that low shear, rotary cell culture induces mycobacterial biofilm formation *in vitro* generating drug-tolerant bacteria that may more accurately represent *in vivo* drug-tolerant *M.tb* than traditional *in vitro* models. The results contribute novel research to the role of biofilm formation in TB, the clinical relevance of which is still not fully understood.

Table of contents

Table of Figures

Table of Tables

Commonly used abbreviations

ADC	Albumin, dextrose, catalase
AGP	Arabinogalactan-peptidoglycan
AST	Antimicrobial Susceptibility Testing
ATP	Adenosine Triphosphate
BCA	Broth Culture Assay
BTG	BacTiter Glo
CFU/mL	Colony Forming Units/mL
CL2	Category Level 2
CL3	Category Level 3
CLP-10	Culture Filtration Protein-10
dH_2O	Distilled H_2O
DMSO	Dimethyl Sulfoxide
DU1/2	Duplication 1/2
ECM	Extracellular Matrix
EMB	Ethambutol
ESAT-6	Early Secretory Antigenic Target 6
ESX-1	ESAT-6 Secretion System 1
ETBU	Ethambutol
EUCAST	European Committee on Antimicrobial Susceptibility Testing
FCS	Foetal Calf Serum
GTC	Guanidine Thiocyanate
IFN-γ	Interferon gamma
IGRA	Interferon Gamma Release Assay

INH	Isoniazid (Isonicotinic acid hydrazide)
IL-12	Interleukin 12
IMS	Industrial Methylated Spirits
LA	Luria Bertani Agar
LAM	Lipoarabinomannan
LB	Luria Bertani Broth
LM	Lipomannan
LPS	Lipopolysaccharide
LTBI	Latent Tuberculosis Infection
MB	Methylene Blue
MDR-TB	Multidrug Resistant TB
M. bovis BCG	*Mycobacterium bovis* BCG
M.tb	*Mycobacterium tuberculosis*
MIC	Minimum Inhibitory Concentration
MTZ	Metronidazole
NRP	Non-Replicating Persistence
OADC	Oleic acid, albumin, dextrose, catalase
O.D.	Optical Density
OFLO	Ofloxacin
ORF	Open Reading Frame
PAMP	Pathogen Associated Molecular Pattern
PBS	Phosphate Buffered Saline
PBMCs	Peripheral Blood Mononuclear Cells
PCR	Polymerase Chain Reaction

PDDP	Phenotypic Drug Discovery Program
PE	Proline Glutamate rich protein
PPE	Proline-Proline Glutamate rich protein
PGL	Phenolic Glycolipid
PKS	Polyketide synthase
PMA	Phorbol 12-myristate 13-acetate
PZA	Pyrazinoic Acid
rATP	recombinant Adenosine Triphosphate
RCCS	Rotary Cell Culture System
RIF	Rifampicin
RLU	Relative Luminescence Units
ROS	Reactive Oxygen Species
RPM	Revolutions per Minute
RPMI Media	Roswell Park Memorial Institute med
RPMI FCS GLU	RPMI media 10% Foetal Calf Serum, 2mM Glutamine
SEM	Standard Error of the Mean
SDEV	Standard Deviation
SNP	Small nucleotide polymorphism
STREP	Streptomycin
TAE	Tris, Acetic Acid and EDTA Buffer
TC	Tissue Culture
TDDP	Target-based Drug Discovery Program
TDM	Trehalose 6, 6′-Dimycolate

TNFα	Tumour Necrosis Factor alpha
TLR	Toll-like receptor
TST	Tuberculin Skin Test
UNICEF	United Nations International Children's Emergency Fund
WGS	Whole Genome Sequencing
WHO	World Health Organisation
XDR-TB	Extensively Drug Resistant TB

Acknowledgements

First and foremost, I would like to thank my supervisor Simon for all his help and support throughout my PhD. His door has always been open and he never seemed to get annoyed by my persistent hounding over the past three and a half years. I would also like to thank Ian and Mel for all their support throughout my PhD. I have been truly lucky to have had you all as my supervisors.

I would also like to thank my family and my partner Ruairi for putting up with me missing birthdays, christenings and weddings over lab work- the end is nearly in sight!

I'd like to acknowledge all my friends in Brighton who have been a massive support for me through the past few years, namely Leticia, Heena, Julia, Caroline, Maria, Niall, Barry, Rich and Terri, as well as all the PhD students here in the Medical Research Building. A special thanks to Ben Alberts for the help with the ELISAs.

Go raibh mile maith agaibh a chairde!

Finally, I'd like to dedicate this thesis to my Dad, who died shortly after my viva. I am happy he got to see me pass my viva and I know he would be proud.

Publications

Castaneda-Garcia, A., A. I. Prieto, J. Rodriguez-Beltran, N. Alonso, D. Cantillon, C. Costas, L. Perez-Lago, E. D. Zegeye, M. Herranz, P. Plocinski, T. Tonjum, D. Garcia de Viedma, M. Paget, S. J. Waddell, A. M. Rojas, A. J. Doherty and J. Blazquez (2017). "A non-canonical mismatch repair pathway in prokaryotes." Nat Commun **8**: 14246.

Author’s declaration

I declare that the research contained in this thesis, unless otherwise formally indicated within the text, is the original work of the author. The thesis has not been previously submitted to this or any other university for a degree, and does not incorporate any material already submitted for a degree.

Signed:

Dated:

Chapter 1: Introduction

1.0 Tuberculosis- A Global Problem

Tuberculosis (TB) is an infectious disease caused by a group of genetically related bacterial pathogens belonging to the *Mycobacterium tuberculosis* complex (MTBC), with *Mycobacterium tuberculosis (M.tb)* the most common aetiological agent (Brudey, Driscoll et al. 2006). Approximately 90% of TB is pulmonary, although *M.tb* can disseminate throughout the body and cause disease at sites distal to the lung (Ducati, Ruffino-Netto et al. 2006). The World Health Organisation (WHO) declared TB a global health emergency in 1993, when TB was identified as the cause of death of 2 million people globally (Zumla, Mwaba et al. 2009). The mortality rate of TB decreased by 22% between 2000 and 2015 due to a series of health interventions such as increased testing and treatment programs as well as supervised therapy programs to reduce patient attrition (Karumbi and Garner 2015). However, TB was still responsible for 1.4 million deaths in 2015 as well as an additional 0.4 million deaths in people living with HIV/AIDS (World Health Organisation, 2016). Despite this significant decrease in mortality, TB remains in the top ten causes of death globally(World Health Organisation, 2017). Reducing TB worldwide was a United Nations Millennium Development Goal and is a recent UN Sustainable Development Goal (Basu Roy, Brandt et al. 2016) highlighting the global impact of this disease. Approximately 98% of the burden of disease is distributed across low to middle income countries, Figure 1.1, although TB disproportionately affects the poorest in high income countries (World Health Organisation 2013). In 2015, six countries accounted for 60% of new TB cases diagnosed- India, Indonesia, China, Nigeria, Pakistan and South Africa.

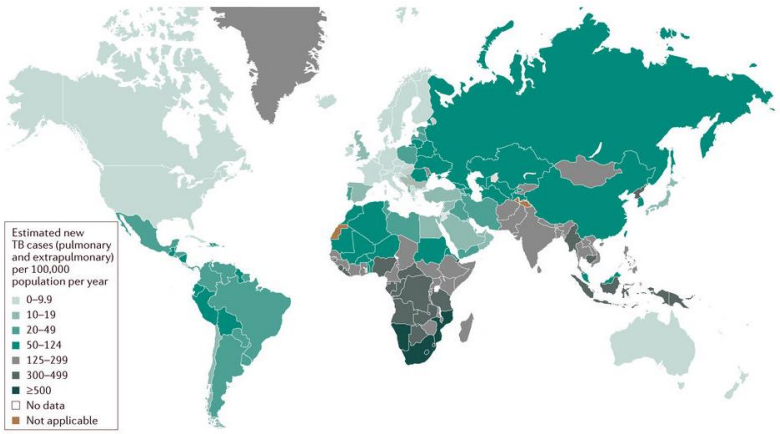

Figure 1.1: The global burden of disease primarily affects low to middle income countries (World Health Organisation 2016).

1.1 *Mycobacterium tuberculosis*

The *M.tb* bacillus is a non-motile bacillus which is 0.3- 0.6 µm in width and 1-4 µm in length. *M.tb is* a slow-growing mycobacterium with a doubling time of approximately 24 hours (in both infected animal models and *in vitro*) (Cole, Brosch et al. 1998) and possesses a unique, waxy, hydrophobic cell wall. The *M.tb* bacillus only weakly stains Gram positive, and must be identified using a Ziehl Neelson (ZN) stain, also known as the Acid Fast stain (Ducati, Ruffino-Netto et al. 2006). Carbol fuschin is taken up by all cells present, staining them red. Acid alcohol decolourises all non-acid fast cells while mycobacteria retain the red stain due to the presence of mycolic acids in the cell envelope, which binds the dye. *M.tb* was first identified as the causative agent of TB by Robert Koch; a discovery which earned him the Nobel Prize in Physiology or Medicine in 1905*(Ritacco and Kantor 2015).* The *M.tb* genome sequence was first published in 1998 and was shown to be composed of 4.4 million base pairs, encoding approximately 4,000 genes (Cole, Brosch et al. 1998). Analysis of the genome sequence showed extensive lipid-orientated functions; in summary, 250 genes were identified to be involved in lipid metabolism, of which 39 genes were central to polyketide metabolism, which is required for the production of cell envelope lipids. Several chromosome-encoded drug resistance mechanisms were identified, including drug-modifying enzymes such as β-lactamase and aminoglycoside transferases, as well as drug efflux pump systems, including ATP Binding Cassette (ABC) transporters (Cole, Brosch et al. 1998).

1.1.1 Mycobacterial cell envelope

The cell envelope of *M.tb* is a complex layered structure composed of numerous macromolecules and lipids, Figure 1.2. Adjacent to the cytoplasm is the mycobacterial inner plasma membrane (MIM) that encloses cellular contents. The MIM is a lipid bilayer plasma membrane that is 6-7 nm in diameter and is composed of conventional plasma membrane lipids such as phosphatidylethanolamine (PE) and phosphatidylinositol (PI). However, these membranes are unique in structure as they have additional phosphatidylinositol mannosides (PIMs) which have only been identified in mycobacteria (Morita, Fukuda et al. 2011). Importantly, the presence of PIMs reduces the fluidity of the lipid bilayer which could reduce influx of molecules, such as antimicrobial drugs, into the bacillus (Bansal-Mutalik and Nikaido 2014).

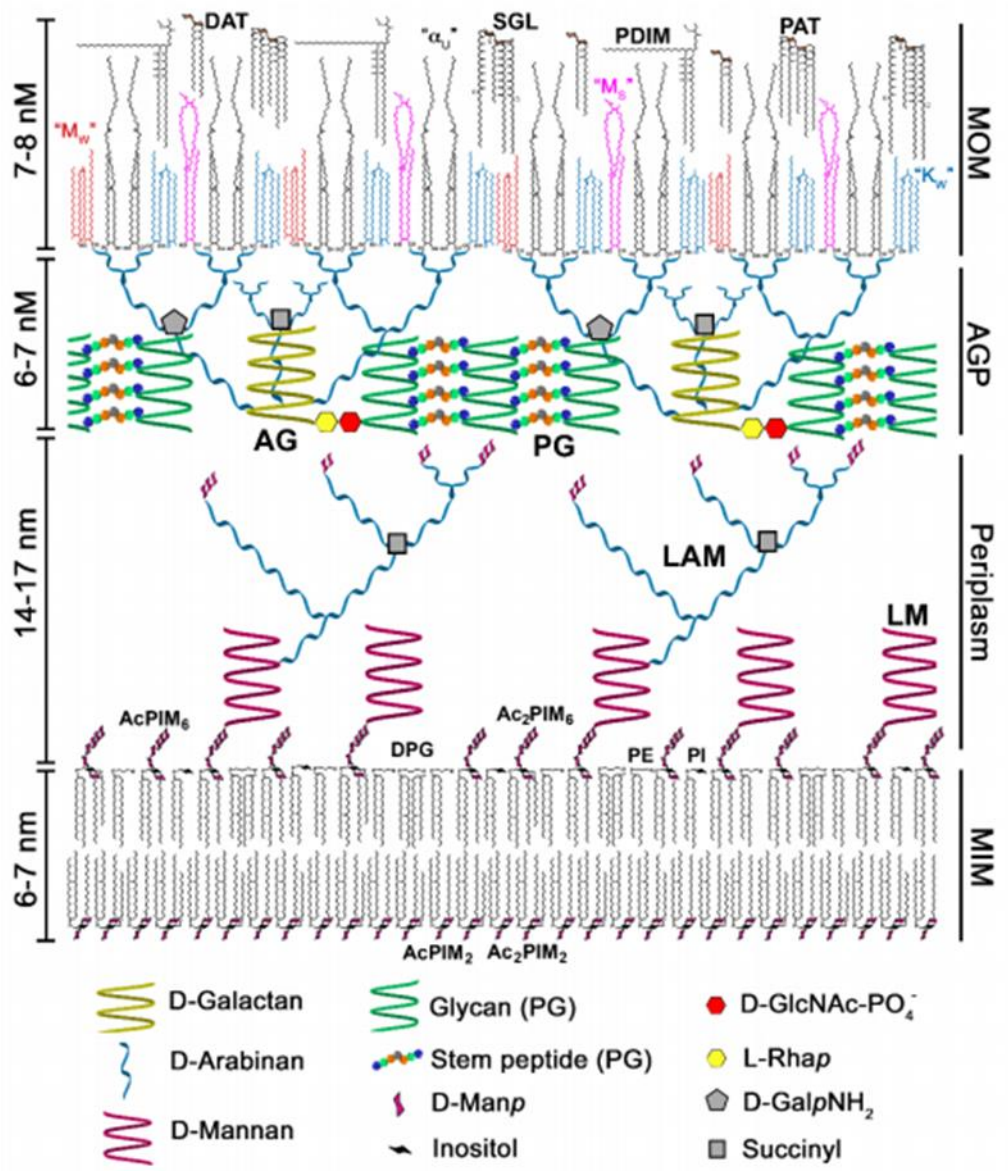

Figure 1.2: Cross-section of the mycobacterial cell envelope

"MIM" is the mycobacterial inner membrane and encloses the cytoplasm. The periplasm or periplasmic space facilitates the transition of "MOM", or mycobacterial outer membrane components from the cytosol. The arabinogalactan peptidoglycan layer (AGP) aids in maintaining cell integrity and anchors mycolic acids that form the inner leaflet of the MOM. The outer leaflet is composed of a diverse range of lipids such as diacyl trehalose (DAT), sulphated trehalose glycolipids (SGLs) and pthiocerol dimycocerosates (PDIMs). Figure taken from Minnikin 2015.

Extending out 14-17 nm from the MIM is the periplasmic space, Figure 1.2. Lipids such as PE, PI and PIMs are anchored in the outer leaflet of the MIM, and extend out into the periplasmic space where they serve to secure the glycolipids lipomannan (LM) and lipoarabinomannan (LAM) (Mishra, Driessen et al. 2011). LM and LAM are major cell envelope components that also serve as potent virulence factors during incidents of

human infection; LAM has been shown *in vitro* to inhibit the expression of the cytokines tumour necrosis factor α (TNFα) and interleukin 12 (IL-12) in lymphocytes (Knutson, Hmama et al. 1998). The various macromolecules and lipids required to construct the mycobacterial outer membrane (MOM) are first synthesised in the cytosol and transported out of the cell. Thus, the periplasmic space facilitates the transition of these molecules out of the cell and is a zone of intense metabolic activity (Minnikin 2015).

On the exterior surface of this first membrane, the periplasmic space extends outward from the cell where there is a section of arabinogalactan and peptidoglycan (AGP), Figure 1.2. Peptidoglycan is a crucial component of the bacterial cell wall in most species of bacteria where it functions to maintain cell shape and integrity in response to cell turgor (Vollmer, Blanot et al. 2008). It is formed by glycan strands cross-linked by short peptides, with the glycan itself being made up of repeating units of N-acetylglucosamine (NAG) and N-acetylmuramic acid (NAM) (Prescott 2005). Mycobacterial peptidoglycan is unusual in that up to 80% of its glycan strands are connected via 3-3 crosslinks as opposed to 4-3 cross links present in the peptidoglycan in the cell walls of most other bacterial species' (Sambou, Dinadayala et al. 2008). This feature of mycobacterial peptidoglycan can be exploited for treatment of TB; D, D carboxypeptidase, the enzyme responsible for this 4-3 cross linkage, is inhibited by the β-lactam antimicrobial drug meropenem *in vitro* when supplemented with a β-lactamase inhibitor in *M.tb* (Kumar, Arora et al. 2012). This combination therapy is indicated for the treatment of extensively drug- resistant TB (XDR-TB). Drug resistant TB is discussed in detail below.

Arabinogalactan is a highly branched oligosaccharide that is formed from the two monosaccharides, arabinose and galactose. NAG anchors molecules of the polysaccharide galactan, which in turn anchors long arabinan molecules that are added via numerous enzymatic steps, which include the arabinofuronosyl transferases EmbA and EmbB. Both of these enzymes are targeted by the first-line antimycobacterial drug ethambutol. Mutations in the genes encoding EmbA and EmbB are associated with ethambutol antimicrobial resistance, highlighting the role the mycobacterial cell membrane plays in druggable targets (Ramaswamy, Amin et al. 2000), (Sreevatsan, Stockbauer et al. 1997).

Within the membrane, not all galactan molecules are bonded to arabinan to form arabinogalactan. These arabinan-free galactans can be conjugated with succinyl or galactosamine groups, which generates further molecular diversity within the cell wall layer (Kaur, Guerin et al. 2009). Arabinogalactan possesses a reducing functional

group that attaches to peptidoglycan in the AGP layer through a specific diglycosylphosphoryl bridge, Figure 1.2, L-Rhap-D-GlcNAc, while its non-reducing end covalently binds mycolic acids in the mycobacterial outer membrane (MOM) (Minnikin 2015). The extensive cross-linking within peptidoglycan and arabinogalactan suggests dense scaffolding between these molecules that facilitate the compaction of large molecules of AGP within the relatively limited space available of 6-7 nm (Kaur, Guerin et al. 2009).

Mycolic acids are branched 60-90 carbon molecules (Barry, Crick et al. 2007) that are characteristic lipids of *Mycobacterium* species and are partly responsible for the waxy, hydrophobic characteristics of the mycobacterial cell wall (Hett and Rubin 2008). Indeed, mycolic acids have been shown to account for up to 60% of the dry weight of mycobacteria (Draper 1998) and are covalently bound to arabinogalactan molecules form the inner leaflet of the MOM, Figure 1.2. Two enzyme complexes are central to the synthesis of mycolic acids; fatty acid synthase I (FAS I) and fatty acid synthase II (FAS II) (Schweizer and Hofmann 2004). FAS I and FAS II generate the fatty acid backbone of mycolic acid, with subsequent processing by a number of enzymes leading to alpha-, methoxy- and keto- mycolic acids. The structural variation amongst these three groups of mycolic acids allows for the development of varied conformations, facilitating tight packaging of mycolic acids, thus enhancing the MOM hydrophobicity (Minnikin 2015).

The presence of a stable mycolic acid inner leaflet of the MOM acts as a base for interactions with a diverse range of free fatty acids that form the outer leaflet of the MOM (Minnikin 2015). Straight chain fatty acids such as diacyl trehalose (DAT) and pentaacyl trehalose (PAT) can insert into the outer leaflet, increasing steric stability of the membrane (Minnikin 1982), while phthiocerol dimycocerosates (PDIMs) are >90 carbon glycolipids that anchor into the mycolic acid portion of the MOM that are potent antigenic molecules (Ridell, Wallerstrom et al. 1992). In addition to the unique cell wall, *M.tb* bacilli possess a capsule composed of polysaccharide, protein and to a lesser extent lipids (Daffe and Etienne 1999). Importantly, this glycan rich capsule can reduce phagocytosis by macrophages, suggesting a host evasion role of this capsular structure (Stokes, Norris-Jones et al. 2004).

1.1.2 Pathogenesis of TB

M.tb is spread through aerosol formation when an individual with an active pulmonary TB infection coughs. Clinical signs of active pulmonary TB include night sweats, fever, anorexia, haemoptysis, sputum production and chronic cough (Lawn and Zumla 2011). Infection is initiated when individuals inhale *M.tb* bacilli, where they reach the alveolar sac. From this point onwards, a number of pathophysiological outcomes are possible, Figure 1.3.

(I) *M.tb* in the alveolar sac can be successfully destroyed by alveolar macrophages and the innate immune system (*M.tb* sterilisation);

(II) *M.tb* may survive within the human lung without causing active disease. Such individuals are asymptomatic and non-infectious and are classed as latent TB infection;

(III) Finally, *M.tb* may resist phagocytosis by alveolar macrophages, undergo intracellular replication and cause active TB (Ewer, Millington et al. 2006).

Development of active TB leads to organised cellular structures within the lung known as granulomas, which are the pathological hallmark of TB infection. Granulomas are formed in response to failed initial immunological attempts to eradicate bacilli in the lung. Infected pulmonary cells such as alveolar macrophages and type II pneumocytes release chemokines and cytokines such as TNF-α and IFN-γ to recruit additional subsets of immune cells that drive granuloma formation (Cooper, Mayer-Barber et al. 2011). The granuloma is mainly composed of blood-derived macrophages, epithelioid cells that are terminally differentiated macrophages, multinucleated giant cells and T and B-lymphocytes, Figure 1.4. A central, necrotic zone of *M.tb*-containing macrophages is surrounded by a rim of T and B-lymphocytes, “foamy” macrophages (lipid droplet loaded cells with a “foamy” microscopic appearance) and fibroid cells. The pathogen-host relationship inside a granuloma is dynamic, with continued host cell death and cellular recruitment occurring, as well as vascularisation and tissue remodelling continuously occurring (Ehlers and Schaible 2012).

Granulomas are dynamic structures and have a number of variable outcomes, Figure 1.5. A granuloma may successfully contain *M.tb* without any immediate or potential disease progression; it may successfully result in the sterilisation of bacilli contained within its structure; or, the centre of a granuloma may lose structural integrity and cause the breakdown of the lung caseum, in a process known as caseation (Ehlers and Schaible 2012). All granulomatous structures that form in TB result in permanent tissue destruction and loss of subsequent function but it is caseating granulomas that are a

feature of active disease and disease transmission. Granulomas may break down into nearby bronchioles, leading to expectoration of granulomatous components and *M.tb* bacilli. This liquefaction of lung tissue is also associated with high levels of multiplication of bacilli that utilise sudden exposure to host nutrients to replicate; *M.tb* growth is very profuse, leading to clumps of bacilli forming at the air-caseum interface, and also throughout the liquefied granuloma (Canetti 1955, Grosset 2003). One or more granulomas can form in pulmonary TB throughout the course of disease and in numerous locations within the lung. Therefore, granulomas have been shown to vary both spatially and temporally within an infected lung. This has significant impact on the pharmacokinetics of antimicrobial drugs within the lung as their physical properties can dictate their tissue penetration and efficacy (Dartois 2014). Furthermore, the various microenvironments generated through the heterogeneous pathology of a granuloma may alter bacterial metabolism and thus the pharmacodynamics of TB chemotherapy (Lenaerts, Barry et al. 2015).

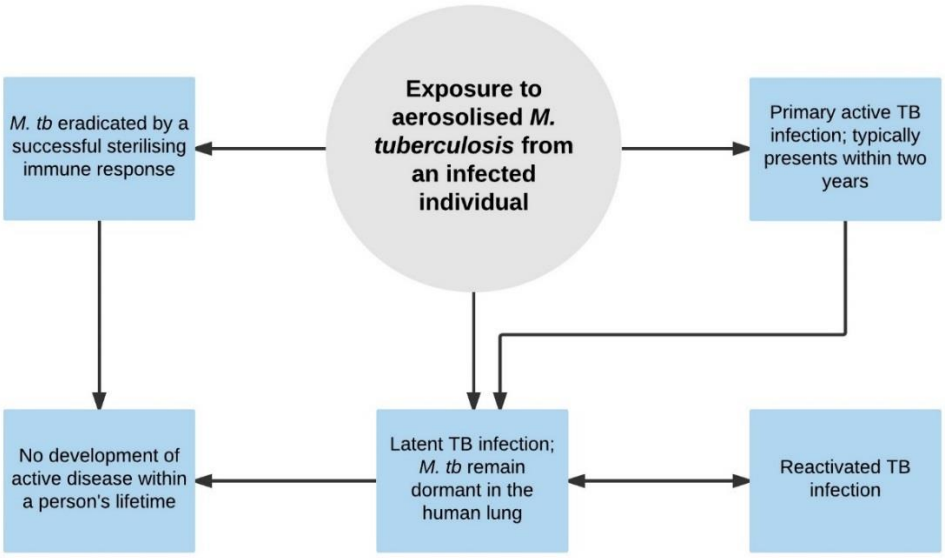

Figure 1.3: Possible outcomes of *Mycobacterium tuberculosis* exposure

The outcome of exposure to *M.tb* is variable, with a number of possible disease states. Bacilli may be cleared successfully by the innate immune response with no development of disease; active TB infection may develop with onset of disease typically within two years of exposure; an individual may develop asymptomatic latent TB that can progress to reactivated TB. TB infection. Co-infection with HIV increases likelihood of latent TB developing to active disease (Ai, Ruan et al. 2016).

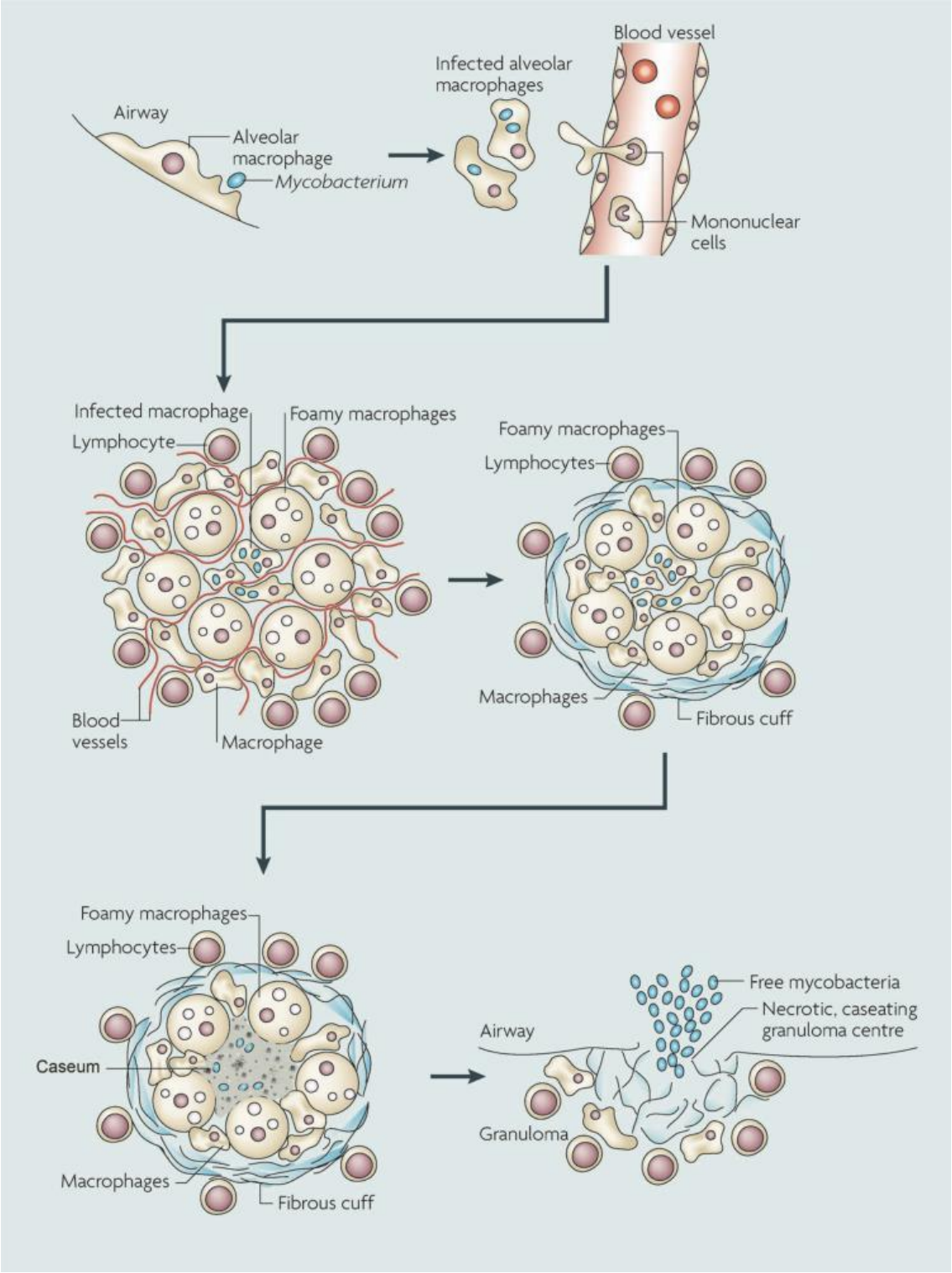

Figure 1.4: Granuloma formation during *Mycobacterium tuberculosis* infection

If the immune response by alveolar macrophages fails to eradicate *M.tb,* active TB infection can develop that involves the recruitment and differentiation of a number of lymphocytes. Extensive tissue remodelling driven by cytokine production and inflammation occurs with deposition of a fibrous cuff that encapsulates the granuloma. Progression of disease leads to caseation of the granuloma and expectoration of bacilli into the airway. Figure taken from (Russell, Cardona et al. 2009).

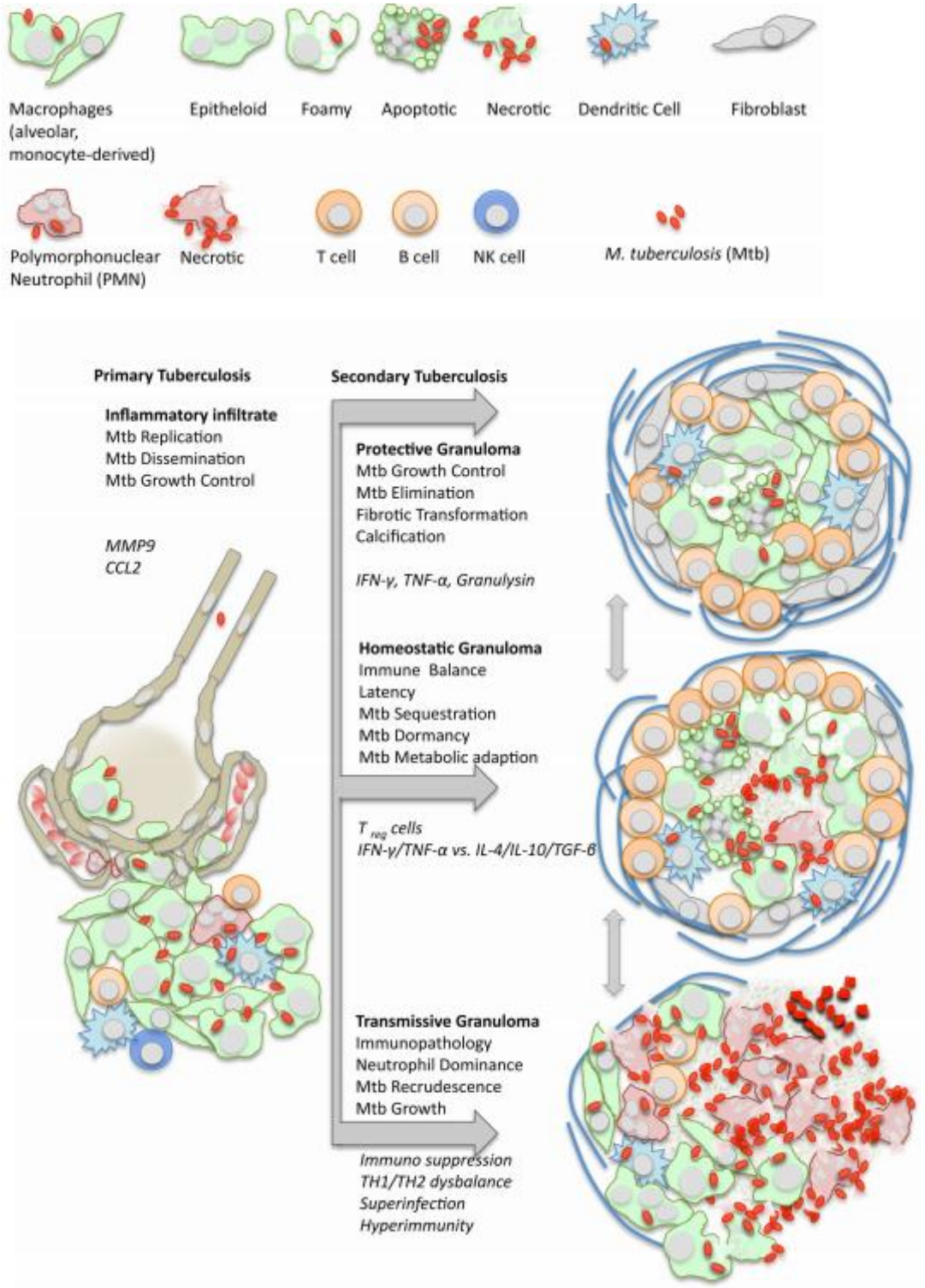

Figure 1.5: The possible fates of a tuberculous granuloma

A number of outcomes are possible for a tuberculous granuloma. A protective granuloma can successfully control and eliminate *M.tb*, and become fibrotic and calcified. A homeostatic granuloma can form where there is successful suppression, but not eradication, of *M.tb* within a granuloma. Finally, a caseating granuloma can occur where the granuloma structure breaks leading to expectoration of virulent, infectious bacilli. Image taken from (Ehlers and Schaible 2012).

1.1.3 Latent TB infection

It is estimated that 1 in 3 people worldwide are believed to be infected with TB, although only 10% of these will go on to develop active TB infection with the remainder of infected individuals having an asymptomatic and non-infectious disease state known as latent TB infection (LTBI) (Barry, Boshoff et al. 2009). LTBI is associated with an absence of clinical symptoms of active TB but does carry a risk of disease progression to active TB within an individual's lifespan, Figure 1.3, especially if co-infection occurs with HIV (Woldehanna and Volmink 2004). People with LTBI remain a significant reservoir of *M.tb* that impacts attempts to eradicate TB. LTBI can be diagnosed for by one of two assays; the Tuberculin Skin Test (TST) and the Interferon γ Release Assay (IGRA).

The TST involves a sub-dermal application of purified protein derivatives (PPD) from *M.tb* that induce a delayed hypersensitivity reaction. The scale of this reaction, or induration, corresponds to an immune response to *M.tb* suggesting an individual has had a previous exposure and may have LTBI (Nayak and Acharjya 2012). This test can infer current LTBI or a recent TB exposure; however, a positive TST can result from environmental exposure to non-tuberculous mycobacteria or vaccination with *Mycobacterium bovis* Bacillus Calmette-Guérin (*M. bovis* BCG) (Farhat, Greenaway et al. 2006). Furthermore, the accuracy of this diagnostic test is reduced in children and people living with HIV (Matteelli, Sulis et al. 2017).

Alternatively, an interferon γ release assay (IGRA) can be used to test for LTBI. IGRAs are *in vitro* assays that quantify the amount of IFN-γ released by a patients' effector T cells in response to specific *M.tb* antigens (Pai, Riley et al. 2004, Halevy, Cohen et al. 2005). IGRAs are more specific than the TST and do not tend to cross react in BCG-vaccinated individuals, but are relatively more expensive and can be difficult to conduct in resource-limited scenarios (Rangaka, Wilkinson et al. 2012).

Both TST and IGRA have respective advantages (such as the lower cost of TST and higher accuracy of IGRA) but both tests have poor predictive value in LTBI progression to active TB infection (Trajman, Steffen et al. 2013), and neither test can distinguish between a cleared TB infection and LTBI (Mack, Migliori et al. 2009). More sensitive, specific and robust tests are required in order to increase LTBI detection rates (Pai and Sotgiu 2016).

1.1.3.1 Vaccination as a strategy to prevent TB

The *M. bovis* BCG vaccine is a live, attenuated strain of *M. bovis* that has lost key virulence mechanisms, discussed in detail further on in this introduction. It is administered to infants in the first year of life who live in TB-endemic countries or regions with high rates of TB, and it is particularly effective against childhood TB especially against disseminated TB to the brain (TB meningitis) (Trunz, Fine et al. 2006). The BCG vaccine has been reported to demonstrate variable efficacy rates; it protects 20% of children from infection, and protects 50% of vaccinated children who do get infected from developing active TB disease (Roy, Eisenhut et al. 2014). However, protection varies among geographical regions (Zodpey and Shrikhande 2007). Sixteen new vaccine candidates are currently in active clinical development but, to date, no vaccine has superseded BCG (Frick 2015).

1.2 Regulatory basis of *M. bovis* BCG avirulence

M. bovis BCG is an attenuated strain of the virulent pathogen *M. bovis*. It was isolated by Calmette and Guérin in 1919 through 239 consecutive sub-passages of *M. bovis* on a glycerine-bile-potato based medium and was first used as a vaccine in humans against TB in 1921 (Calmette 1926). *M. bovis* is a virulent species of the *Mycobacterium* genus that can cause active TB infection in humans, but mainly causes disease in both domesticated and wild animals. Its attenuated form, *M. bovis* BCG ("Bacillus Calmette Guérin"), has to date been used to vaccinate over 3 billion people across 180 countries (Eisenach, Crawford et al. 1986; Zwerling, Behr et al. 2011). Today, several sub-strains of *M. bovis* BCG exist due to continuous sub-culturing in various laboratories over the past century (Lugosi 1992). These strains are now divergent enough from each other to vary in antigenicity, lipid content and the host immune responses they elicit when used as vaccines (Chen, Islam et al. 2007), (Aguirre-Blanco, Lukey et al. 2007). The Pasteur, Japanese and Glaxo strain are the most commonly used daughter strains for vaccination purposes (Magdalena, Supply et al. 1998); it was the Pasteur sub-strain of *M. bovis* BCG that was used in this PhD research in the development and characterisation of a novel, low-shear mycobacterial biofilm.

1.2.1 The avirulent *M. bovis* BCG

M. bovis BCG has had variable success as a vaccine. Vaccine efficacy correlates with strain type and antigenicity, as well as age of administration and age of exposure to virulent *M.tb* (Colditz, Berkey et al. 1995). The *M. bovis* BCG genome has been sequenced and analysed by a number of research groups in an attempt to characterise genomic alterations that arose during passaging by Calmette and Guerin that led to loss of virulence in order to elucidate mechanisms that underpin TB virulence and host immunoprotective strategies. *M. bovis* BCG has been shown to have 99.9% sequence similarity with *M.tb* (Brosch, Gordon et al. 2007), with several key mutations identified that differentiate *M. bovis* BCG from virulent *M. bovis*, as well as mutations and genetic alterations that lead to variation within strain types of *M. bovis* BCG (Liu, Tran et al. 2009, Oettinger, Jorgensen et al. 1999).

1.2.2 Genomic modifications contribute to loss of virulence in *M. bovis* BCG

Several modifications occurred in the *M. bovis* genome that led to the attenuated strain *M. bovis* BCG. Three regions of difference (RD1, RD2, RD3) in the genome were identified as absent in *M. bovis* BCG compared to virulent *M. bovis* and *M.tb* (Mahairas, Sabo et al. 1996). The RD1 locus is absent in all daughter strains of *M. bovis* BCG propagated in laboratories around the world (Pym, Brodin et al. 2002). RD1, is a 9.5-kb region that is conserved in all virulent clinical and laboratory strains of *M. bovis* and *M.tb* but is absent from *M. bovis* BCG (Pym, Brodin et al. 2002). Restoration of RD1 in *M. bovis* BCG shifted the protein expression profile to one similar to virulent *M.tb* and *M. bovis*, indicating RD1 deletion results in loss of virulence. Ten genes were also strongly repressed on re-introduction of RD1 into BCG, suggesting at least one regulatory ORF present in RD1 (Magdalena, Supply et al. 1998). Based on this research, Mahairas *et al* concluded that RD1 either contained one or more genes directly involved in virulence or contained one or more genes involved in the regulation of virulence genes; or a combination of these two hypotheses (Mahairas, Sabo et al. 1996). Through further investigation of RD1 complementation in *M. bovis* BCG, it was demonstrated that ESX-1, a mycobacteria-specific secretion system that is responsible for secretion of the two antigens ESAT-6 and CFP10, were both absent in *M. bovis* BCG (Harboe, Oettinger et al. 1996). A functional ESX-1 system has been shown to be crucial in mediating pathogen host interactions (Simeone, Bottai et al. 2009). Both *M.tb* and *M. bovis* BCG complemented with a functional RD1 operon can translocate from inside phagosomes of infected macrophages into the cytosol, a key step in the

pathogenesis of TB. Non-pathogenic mycobacteria and *M. bovis* BCG that lack an ESX-1 secretion system remain in the macrophage phagosome, leading to bacterial death, ultimately reducing their pathogenicity (Simeone, Bobard et al. 2012; Houben, Demangel et al. 2012).

The re-introduction of RD1 into *M. bovis* BCG does not, however, restore full virulence, suggesting that there are other genetic factors associated with the loss of virulence (Pym, Brodin et al. 2002, Kozak, Alexander et al. 2011).

Pathogenic mycobacteria such as *M.tb* secrete virulence factors through a range of secretory systems, known as type VII secretion systems (Ligon, Hayden et al. 2012). *M.tb* bacilli possess five type VII secretion systems, ESX1-5, that are necessary to transport substrates through the thick mycobacterial cell envelope. All of these ESX secretion systems share a core set of genes that are necessary for these systems to function, including two *esx* genes that encode secreted ESAT6-like proteins of approximately 100 amino acids in length (Houben, Korotkov et al. 2014). ESX secretion systems are named after the first of these secreted proteins to be identified, the 6kDa early secreted antigenic target (ESAT6 encoded by *esxA*) (Sorensen, Nagai et al. 1995; Groschel, Sayes et al. 2016). *Esx* genes are adjacently encoded in pairs per secretion system, with the most well described being the secretion of ESAT6 (*esxA*) and CFP10 (*esxB*). These ESX proteins dimerise to form a functional virulence factor but importantly are capable of effecting virulence as homodimers; ESAT6 has been shown to exhibit a leukocidin-like effect on neutrophils, inducing apoptosis through increased intracellular Ca2+ accumulation (Renshaw, Lightbody et al. 2005; Francis, Butler et al. 2014). Specifically, the ESX1 secretion system has been shown to be essential for phagosomal rupture within the host macrophage, allowing *M.tb* to escape into the cytoplasm and avoid destruction through macrophage defences (Simeone, Bobard et al. 2012). The ESX1 secretion system loci responsible for ESAT6 and CFP10 are located in the Region of Difference 1 (RD1) in *M.tb* that importantly is not present in *M. bovis* BCG. This has been shown to be key to the loss of virulence of *M. bovis* BCG, highlighting the role ESX secretion systems play in virulence (Pym, Brodin et al. 2002).

The ESX5 secretion system is found in all slow growing mycobacteria (Gey Van Pittius, Gamieldien et al. 2001). The ESX-5 secretion system is responsible for the secretion of proteins that are required for the uptake of nutrients from the environment (Ates, Ummels et al. 2015), as well as the secretion of a range of Proline Glutamate rich and Proline Proline Glutamate rich proteins (PE and PPE proteins respectively). PE and PPE proteins are secreted into the extracellular environment and are implicated in

virulence, host colonisation and pathogen-host interactions (Bottai, Di Luca et al. 2012). The ESX-5 secretion system has been primarily investigated in *M. marinum.* Abdullah *et al* showed that ESX5 suppresses IL-6, IL-12 and TNFα in THP-1 cells (a human monocytic cell line) infected with *M. marinum*, likely through repression of Toll-like receptor (TLR) signalling (Abdallah, Savage et al. 2008). The authors also noted that deletion of the ESX5 in *M. marinum* significantly impaired macrophage cell death compared to *M. marinum* wildtype, suggesting ESX5 plays a role in host cell survival. Building on this, Abdullah *et al* went on to show that in *M. marinum,* unlike ESX1, ESX5 was not required for phagolysosome rupture and bacterial escape into the cytosol. However, ESX5 was shown to induce caspase-independent cell death in infected THP-1 cells (Abdallah, Bestebroer et al. 2011). This research using *M. marinum* suggests that the ESX5 secretion system, consisting of esxJ and esxM, contributes to virulence through suppression of innate immune system cytokine secretion and of host cell viability upon infection. The ESX5 secretion system was further characterised by Bottai *et al* in *M.tb*, where the authors showed that disruption of the ESX5 secretion system impaired *M.tb* virulence, PPE protein secretion and cell wall integrity in both an infected macrophage model and a Severe Combined Immunodeficiency Disease (SCID) mouse model, (Bottai, Di Luca et al. 2012).

The genome of *M. bovis* BCG is approximately 30 kb larger than virulent *M. bovis* (Garnier, Eiglmeier et al. 2003) despite RD deletions. This increase in genomic size is due to two independent tandem duplications, DU1 and DU2. Because of these duplication events, *M. bovis* BCG is diploid for a minimum of 58 genes, and is diploid for its origin of replication, *oriC* within DU1. Duplication events are an important mechanism that contributes to genome plasticity, augmenting gene dosage within a cell and even generating novel protein products through gene fusion (Brosch, Gordon et al. 2000). In total, 736 single nucleotide polymorphisms (SNPs) were identified in BCG Pasteur compared to *M. bovis*, with 83% of these SNPs occurring in genes; 68% of these SNPs were shown to be non-synonymous (Leung, Tran et al. 2008). One such missense mutation is in the start codon of *sigK*, where the ATG has been replaced by ATA. As a result of this mutation, BCG Pasteur is unable to express the major antigens MPB70 and MPB83 (Charlet, Mostowy et al. 2005), a secreted soluble protein and membrane bound glycosylated lipoprotein respectively that are highly homologous at the genetic and amino acid sequence level across virulent mycobacteria (Wiker 2009). These lipoproteins may play a role in colonisation of host tissues, as these antigens can bind specific cell surface receptors and disturb cell adhesion, allowing penetration of bacilli through tissues (Wiker 2009).

PhoP forms part of a two-part component transmembrane histidine kinase system together with PhoR, and are responsible for the transcriptional regulation of ~2% of the *M.tb* genome (Cimino, Thomas et al. 2012). When *PhoP* was disrupted in *M.tb,* mutant strains could not replicate *in vitro* in mouse bone marrow-derived macrophages but could still survive, implicating PhoP in the persistence of *M.tb* but not in intracellular survival (Perez, Samper et al. 2001). The gene *phoP* is expressed to higher levels in *M. bovis* BCG Tokyo compared to *M. bovis* BCG Pasteur. A genomic duplication event, DU2, occurred that included upstream elements of *phoP* in BCG Tokyo that increased transcription of PhoP, but did not occur in BCG Pasteur (Brosch, Gordon et al. 2007). *M. bovis* BCG Tokyo elicits a more potent immunogenic effect than *M. bovis* BCG Pasteur that may be a result of this increased gene dosage effect (Ritz, Hanekom et al. 2008), This suggests that variation in *phoP* amongst *M. bovis* BCG strains leads to altered regulation of gene transcription and virulence compared to *M.tb* and *M. bovis*.

1.3 The innate immune system in TB

The innate immune system plays an important role in host defence against TB infection that was first shown by a tragic accident in 1930, Lubeck, Germany. 251 newborn babies were accidentally vaccinated orally with live *M. tuberculosis* instead of the actual vaccine, *M. bovis* BCG. In total, 72 of the 251 infants died because of active TB infection; a further 135 infants developed active TB infection but recovered. Interestingly, 44 of those 251 infants that were exposed did not develop any clinical symptoms of TB but did become Tuberculin Skin Test positive, indicating an exposure to TB (Fox, Orlova et al. 2016). This *M.tb* dose was administered at day 10 of life, where it is known that adaptive immunity is immature and not fully functional, thus highlighting the importance of innate immunity in protecting against TB disease (Basha, Surendran et al. 2014).

The clinical outcomes are variable for an exposure to *M.tb*, Figure 1.3. The innate immune system is crucial, as this is the first host response to invading *M.tb.* In order for innate immune cells such as alveolar macrophages to phagocytose invading bacilli, they must first recognise *M.tb* as a non-self-antigen. Pathogen Associated Molecular Patterns (PAMPs) are conserved molecules expressed on the surface on the bacillus that are recognised by specific host cell receptors known as pattern recognition receptors (PRRs) (Akira, Uematsu et al. 2006; Medzhitov and Janeway 2000). PRRs are a diverse group of receptors including mannose receptors, TLRs and NOD-like receptors.

1.3.1 *M.tb* survive phagocytosis and replicate intracellularly

Mannose receptors on alveolar macrophages recognise and bind to mycobacterial mannose-capped lipoarabinomannan molecules that are a key component of the cell wall, and are a hallmark of all pathogenic mycobacteria (Strohmeier and Fenton 1999). Human macrophages primarily phagocytose *M.tb* using mannose receptors in conjunction with complement 3, (Schlesinger 1993). Unlike mannose receptors, TLRs are not directly involved in alveolar macrophage phagocytosis but rather augment the immune responses upon binding to PAMPs (Sibille and Reynolds 1990). There are currently 11 identified human TLRs, with TLRs 2, 4 and 9 responsible for recognition of mycobacterial antigens or PAMPs (Juarez, Nunez et al. 2010). TLR 2 has been shown through mycobacterial cell wall fraction activation to be necessary for TNF-α production, a key cytokine involved in a protective response in initial TB infection (Underhill, Ozinsky et al. 1999).

Following *M.tb* recognition via alveolar macrophage PRRs, phagocytosis commences. Macrophage phagocytosis should end in the destruction of the microbe. However, *M.tb* has evolved to an intracellular pathogenic life cycle being able to subvert the phagocytosis process, and instead utilises phagocytosis as a survival mechanism to replicate within the lung (Scherr, Jayachandran et al. 2009). *M.tb* are phagocytosed and internalised in an early phagosome, where they are destined to progress to a mature phagosome and fuse with a lysosome, forming a phagolysosome. *M.tb* however, can inhibit phagosome maturation and prevent destruction from lysosomal hydrolases and acidification of the phagolysosome (Armstrong and Hart 1971), (Clemens and Horwitz 1995). Phosphatidylinositol 3-phosphate kinase (PI3P) is an essential component of the phagolysosome membrane that regulates host trafficking from the phagosome to the lysosome, through acting as a docking site for several proteins required for phagosome-lysosome fusion (Roth 2004; Wurmser, Gary et al. 1999). *M.tb* inhibits PI3P accumulation on phagosomal membranes through two mechanisms. Firstly, mycobacterial antigens such as lipoarabinomannan (LAM) can interfere with the PI3P kinase enzyme cascade, blocking PI3P accumulation on the phagosomal membrane (Fratti, Chua et al. 2003). Secondly, *M.tb* secrete SapM, a eukaryotic-like phosphatase that may hydrolyse PIP3 from vesicle membranes, inhibiting phagosome-lysosome interactions (Saleh and Belisle 2000; Vergne, Chua et al. 2005).

1.3.2 The role of IL-1β and TNFα in *M.tb* infection

Cytokine and chemokine production are central to the host response in *M.tb* infection and are crucial mediators in both early infection and chronic disease (Cooper 2009). TNFα is pro-inflammatory cytokine produced by a number of lymphocytes with mononuclear macrophages secreting the highest amount in granulomatous tissues (Vassalli 1992). TNFα is a pleiotropic cytokine with diverse roles in TB infection. Excessive levels exacerbates clinical symptoms of TB through enhanced tissue damage, while inhibition of TNFα can allow *M.tb* to proliferate through inhibition of key innate immune system pathways. This was described initially in a TNFα deficient (TNFα-/-) mouse model where TNFα-/- mice infected with *M.tb* were significantly more susceptible to infection, along with extensive necrosis in the lungs and widespread dissemination of *M.tb* to other organs (Bean, Roach et al. 1999). The role TNFα plays in human infection was evidenced with the use of anti-TNFα drugs used to treat inflammatory conditions such as rheumatoid arthritis; active TB infection was induced in individuals who had previously existing latent TB infection (Miller and Ernst 2009). As previously stated, inhibition of an effective phagocytosis pathway is not maintained throughout TB infection. However, the innate immune system has been shown to enhance the microbicidal activities of infected macrophages. Although T cells and natural killer cells are major sources of IFN (Fenton, Vermeulen et al. 1997), infected macrophages secrete IFNγ and importantly TNFα in response to infection. TNFα initiates macrophage activation, which leads to an upregulation of microbicidal activities such as increased phagosome maturation and fusing with lysosomes, which have increased reactive oxygen and nitrogen species generation exacerbating their cidal effects for *M.tb* (Adams and Hamilton 1984). Not only is TNFα crucial in mounting an early inflammatory response, it has been shown to regulate the release of interleukins (ILs) and chemokines that are responsible for cell recruitment to the site of infection to mount a further antimycobacterial response, and ultimately functions in granuloma formation (Roach, Bean et al. 2002).

IL-1β is a major mediator of the innate immune system response to TB infection, alongside TNFα. Macrophage TLR-4 binding to specific PAMPs triggers synthesis of an IL-1β pre-cursor molecule after TLR-4 activation. Cleavage of this IL-1β pre-cursor molecule to its active form, IL-1β, is dependent on activation of caspase-1, which in turn is activated through the formation of a protein complex known as an inflammasome that forms independently through cellular recognition of PAMPs (Contassot, Beer et al. 2012). The role of IL-1β has been characterised through the use of transgenic mice studies. Bourigalt *et al* showed that mice that were deficient for IL-1β and IL-1α, a

closely related cytokine with similar cellular functions to IL-1 β, rapidly succumbed to infection with *M.tb* (Bourigault, Segueni et al. 2013). However, when infected with *M. bovis* BCG could survive infection without mortality, suggesting that the role of IL-1β in host survival to infection depends on the virulence of the strain. In contrast, TNFα deficient mice were unable to survive infection with either *M.tb* or *M. bovis* BCG. Both TNFα and IL-1β are important pro-inflammatory mediators of the innate immune response to *M.tb* infection, but vary in their responses. IL-1 signalling is not crucial to the immediate host response to *M. bovis* BCG, while TNFα is, as TNFα deficient mice cannot survive *M. bovis* BCG infection. Interestingly, IL-1β induces protective immunity in macrophages in response to mycobacterial infection through increased TNFα secretion and upregulation of infected macrophage expression of TNFα-associated surface receptors (Jayaraman, Sada-Ovalle et al. 2013). TNFα signalling has been shown to induce apoptosis in infected macrophages through caspase-3 (a key enzyme in programmed cell death activation) which acts to restrict bacterial replication. Given that TNFα does not rely on IL-1β to exert its antimycobacterial activity but IL-1 relies on TNFα, the differential expression of these cytokines can impact on the development of active TB infection, bacterial proliferation and immune responses within the host tissues (Kleinnijenhuis, Joosten et al. 2009).

1.4 Treatment of TB

TB is a treatable and curable disease, however, in order to achieve successful sterilisation multiple antibiotics must be administered for at least six months. The standard TB drug regimen is isoniazid (INH), rifampicin (RIF), pyrazinamide (PZA) and ethambutol (EMB) for the first two months (intensive phase) followed by four months of INH and RIF only (continuation phase) (Aquinas 1982, Zumla; Raviglione et al. 2013).

1.4.1 Isoniazid (INH)

Isoniazid, or isonicotinylhydrazide (INH), is a pro-drug that requires activation within the bacillus to exert its effects. INH is composed of a pyridine ring with a hydrazine side group, and both of these structures are required for INH antimicrobial action (Zumla, Raviglione et al. 2013). Once inside the bacillus through passive diffusion, INH is converted to an isonicotinic aryl radical via the bacterial catalase-peroxidase enzyme KatG with concomitant production of carbon, nitrogen and oxygen based free radicals (Wengenack and Rusnak 2001). While these radicals can attack and damage a number

of cellular macromolecules such as lipids and proteins, inhibition of mycolic acid synthesis is the primary mode of action. INH conversion via KatG in the presence of NAD^+ leads to potent inhibition of an enoyl acyl carrier protein reductase, InhA, a key enzyme of the type II Fatty Acid Synthesis (FAS-II) system in *M.tb* (Banerjee, Dubnau et al. 1994). InhA is required for the synthesis of mycolic acids and cell wall biosynthesis; interference in this process will be cidal to bacilli. The efficacy of INH is dependent on the metabolic state of the bacillus. Actively growing *M.tb* require continual cell wall synthesis, and the introduction of INH to these bacilli exerts a bactericidal effect. Slow growing or non-dividing bacilli however, may have little on-going cell wall biosynthesis and so INH would exert a bacteriostatic effect (Yamori, Ichiyama et al. 1992; Ahmad, Klinkenberg et al. 2009). Additionally, pro-drug activation maybe affected by the bacterial metabolic state, as highlighted by mutations in KatG that confer INH resistance. Mutations in the *katG* gene reduce enzyme activity, abrogating INH conversion and thus reducing efficacy while also allowing this catalase-peroxidase enzyme to function in bacillus-protective mechanisms, such as degradation of host macrophage peroxides (Ng, Cox et al. 2004).

1.4.2 Rifampicin (RIF)

Rifampicin (RIF) is a potent antimicrobial compound which is used to treat numerous pathogenic mycobacterial infections such as Bruruli ulcer (*M. ulerans*) and leprosy (*M. leprae)* (Addison, Pfau et al. 2017), (Ramu, Sreevatsa et al. 1981). RIF was first discovered in 1965 as a metabolite of the Gram positive bacterium *Amycolatopsis rifamycinica* (Saxena, Kumari et al. 2014). RIF binds to the β-subunit of the bacterial RNA polymerase, inhibiting mRNA elongation and ultimately preventing protein synthesis (Blanchard 1996). Mutations arising in the *rpoB* gene encoding the subunit targeted by RIF lead to a structural change in the RIF binding sight, leading to antimicrobial resistance (Telenti, Imboden et al. 1993). Importantly, RIF has activity against both actively growing and non-dividing bacilli (Hu, Liu et al. 2015).

1.4.3 Pyrazinamide (PZA)

Pyrazinamide (PZA) was first used to treat TB in the 1950's and its introduction led to a reduction from 9 months of standard chemotherapy to 6 months Zhang, Wade et al. 2003). PZA is a nicotinamide analogue pro-drug that requires conversion to its active form pyrazinoic acid by the *M.tb* enzyme pyrazinamidase, encoded by the gene *pncA*

(Whitfield, Soeters et al. 2015). Pyrazinamidase is not found in other mycobacterial species, making *M.tb* the only pathogen PZA is prescribed to treat. In the acidic environment of a granuloma, pyrazinoic acid slowly diffuses out of the bacilli, becomes protonated, and is taken up again by bacilli. The protonated pyrazinoic acid is actively pumped out of the cell, and cycling of PZA derivatives are hypothesised to disrupt cellular energetics and membrane transport leading to bacterial death. Importantly, PZA is effective against non-replicating bacilli that are difficult to eradicate in TB (Mitchison 1985). PZA has also been shown to bind to the ribosomal protein S1, which is crucial in trans-translation. Trans-translation differs to canonical protein translation in that it is required to increase the availability of scarce ribosomes in non-replicating organisms (Shi, Zhang et al. 2011). Resistance occurs through single nucleotide polymorphisms (SNPs) throughout the *pncA* gene that encodes pyrazinamidase reducing binding site compatibility with PZA (Rajendran and Sethumadhavan 2014).

1.4.4 Ethambutol (EMB)

Ethambutol (EMB) was first identified in 1961 as an antimycobacterial drug through testing on the fast growing *M. smegmatis*, with clinical use starting in 1966 (Forbes, Kuck et al. 1962). EMB primarily inhibits the transfer of arabinogalactan into the cell wall and thus exhibits a bacteriostatic effect on actively growing bacilli. EMB-resistant strains were shown to possess mutations in the *embCAB*, a 10-kb operon that encodes a mycobacterial arabinosyl transferase suggesting that this enzyme is primarily targeted by EMB (Telenti, Philipp et al. 1997). Further sequencing of EMB-resistant strains however have shown resistance occurring without *embCAB* mutations, suggesting that there may be alternative EMB targets in the mycobacterial cell that have yet to be identified (Ramaswamy, Amin et al. 2000).

1.5 Drug Resistance in TB

Antimicrobial drug resistance, well characterised in pathogenic bacteria, is identified as an increase in MIC for one or more antimicrobial drugs, rendering those antimicrobials as less efficacious or altogether ineffective (Pratt 2000). *M.tb* does not harbour antibiotic-resistance plasmids, and antibiotic resistance has been shown to evolve through *de novo* mutations in the *M.tb* genome (Ramaswamy and Musser 1998), (Muller, Borrell et al. 2013). In 2014, the WHO estimated that of 9 million people diagnosed with TB infection, 480,000 were multidrug-resistant cases (World Health

Organisation 2014). Multidrug resistant TB (MDR-TB) is resistant to at least isoniazid and rifampicin, while extensive multidrug resistant TB (XDR-TB) is resistant to isoniazid and rifampicin, at least one fluoroquinolone and at least one of three second line injectable agents (World Health Organisation 2014). Diagnosis and appropriate treatment of drug resistant TB provide major challenges in the eradication of TB. Characterising what antibiotics MDR-TB isolates are susceptible to takes at least two weeks from time of sample collection, while establishing what XDR-TB isolates are resistant to may take months as extended *in vitro* antimicrobial susceptibility testing is required (Goloubeva, Lecocq et al. 2001). This delay in appropriate antibiotic selection has significant clinical implications, where treatments do not align with local resistance patterns for MDR-TB and XDR-TB, further fuelling drug resistance emergence (Chihota, Muller et al. 2012).

1.5.1 Treatment of drug resistant TB

The WHO have classified anti-TB drugs into first- and second- line drugs. First line antibiotics include the standard oral administered regimen of INH, RIF (as rifabutin and rifapentine), PZA and EMB and are known as Group 1 agents. Second line agents are composed of groups 2-5, Table 1.1 (World Health Organisation 2014). Patients with MDR-TB are treated for a minimum of 20 months, which is considerably longer than the six months required to sterilise drug-sensitive TB. MDR-TB regimens typically comprise of a group 2 injectable agent such as amikacin, a fluoroquinolone from group 3, and an oral bacteriostatic from group 4 with para-aminosalicylic acid most commonly selected. Group 5 agents are not routinely recommended for treatment of MDR-TB (World Health Organisation 2014). The evidence for these drugs' efficacy is based on *in vitro* or animal model data, with limited clinical data on efficacy or safety and tend to be included in regimens where a complete regimen cannot be designed from groups 2- 4.

Streptomycin, a group 2 agent, was the first antibiotic used to treat TB. Streptomycin is produced by the bacterium *Streptomyces griseum* and inhibits bacterial protein synthesis by binding to the 16S rRNA of the 30S subunit of the bacterial ribosome, inducing structural alterations of the ribosome. Codon misreading ensues, leading to protein synthesis inhibition and cell death (Sharma, Cukras et al. 2007). From 1946 to 1948, under the leadership of Geoffrey Marshall and Philip D'Arcy Hart, the MRC Tuberculosis Research Unit carried out a randomised, double-blind placebo controlled clinical trial that is regarded as the first randomised clinical trial (Crofton 2006). Despite

some patients being cured, streptomycin resistance emerged throughout monotherapy, emphasising the need to treat TB with more than one anti-TB drug.

GROUP NAME	ANTI-TB AGENT
GROUP 1 First-line oral anti-TB drugs	Isoniazid Rifampicin Ethambutol Pyrazinamide Rifabutin* Rifapentine*
GROUP 2 Injectable anti-TB drugs	Streptomycin Kanamycin Amikacin Capreomycin
GROUP 3 Fluoroquinolones	Levofloxacin Moxifloxacin Gatifloxacin
GROUP 4 Oral bacteriostatic second-line anti-TB drugs	Ethionamide Prothionamide Cycloserine Tetrizidone Para-aminosalicylic acid Para-aminosalicylate sodium
GROUP 5 Anti-TB drugs with limited data on efficacy or safety	Bedaquiline Delamanid Linezolid Clofazimine Amoxicillin/clavulanate Imipenim/cilastatin Meropenem High dose isoniazid Thioacetazone Clarithromycin

Table 1.1: WHO recommended grouping of anti-TB Drugs

Group 1 is used for standard therapy of drug sensitive TB. Rifabutin and Rifapentine have similar activity to rifampicin. Groups 2- groups 5 are used to form individualised treatment regimens for MDR-TB and XDR-TB. Table taken from (World Health Organisation 2014).

1.5.2 Deficit in anti-TB drugs

New, potent anti-TB drugs are needed to shorten treatment times and combat MDR-TB and XDR-TB. Only two new anti-TB drugs have been released for clinical use in the past 45 years; delamanid and bedaquiline (Tiberi, Buchanan et al. 2017). Delamanid is a nitroimadazo-oxole derivative pro-drug that must be activated by the bacillary enzyme deazaflavin dependent nitroreductase, forming a reactive intermediate that inhibits mycolic acid synthesis (Xavier and Lakshmanan 2014). Bedaquiline is a diarylquinoline that targets the mycobacterial ATP synthase, inhibiting bacterial respiration- importantly it is effective at sterilising non-replicating or slow-metabolising bacilli (Andries, Verhasselt et al. 2005). Drug resistance has however been identified for both bedaquiline and delamanid (Veziris, Bernard et al. 2016), thus restricting their use. As well as a deficit of new anti-TB drugs, *in vitro* models that are based upon bacillary growth and metabolism in the lung are required to elucidate antimicrobial tolerance and screen novel anti-TB compounds (Mitchison 2004).

1.6 Antimicrobial Drug Tolerance

Antimicrobial drug tolerant bacteria are a proportion within a bacterial population that are transiently tolerant to antimicrobial drugs. Importantly these drug tolerant sub-populations remain genetically identical to the drug-susceptible bacteria in the same population of cells and thus it is distinct from drug resistance (Amato, Fazen et al. 2014). Antimicrobial drug tolerance was first identified by Joseph Bigger in 1944, when he was investigating the limited efficacy of penicillin in treating staphylococcal infections compared to its high rate of success in treating gonorrhoea. Bigger added penicillin to a culture of *Staphylococcus pyogenes* and observed lysis of the culture. He plated this lysed culture onto agar and saw that a small number of colonies had developed. The colonies were transferred into broth and again treated with penicillin. The same observation was recorded again- that the culture lysed but a small population of bacteria had survived treatment. Bigger termed this sub-population of penicillin-tolerant colonies “persisters” so as to discriminate them from penicillin resistant mutants (Bigger 1944). Since then, antimicrobial tolerant or “persister” cells have been identified in numerous bacterial species such as *Staphylococcus aureus* (Conlon, Rowe et al. 2016), *E. coli* (Kaldalu, Joers et al. 2016) and *Pseudomonas aeruginosa* (Mlynarcik and Kolar 2016) as well in the fungal pathogen *Candida albicans* (Al-Dhaheri and Douglas 2008). It is clear across bacterial and fungal species where persister cells have been identified, that antimicrobial tolerance is a transient phenotype in a sub-population of

cells within a genetically identical population. The observation that the progeny of these drug tolerant cells retain sensitivity to the drug suggests that drug tolerance results from changes in phenotype, rather than genome associated modifications in drug resistance (Lewis 2008; Roberts and Stewart 2005).

1.6.1 Antimicrobial drug tolerance in TB

M.tb bacilli must adapt to many different environments during infection, from phagocytosis by macrophages to extracellular existence within host sputum. The complex disease pathology of TB generates heterogeneous microenvironments within a tuberculous granuloma; oxygen limitation, nitrosative stress and nutrient starvation have all been identified as factors that impact on mycobacterial metabolism and growth (Voskil, Visconti et al. 2004; Timm, Post et al. 2003; Garton, Waddell et al. 2008). *M.tb* are exposed to these environmental stresses to varying degrees during infection, generating heterogeneous sub-populations of *M.tb* that are genetically identical but are phenotypically diverse (Dhar, McKinney et al. 2016; Islam, Richards et al. 2012). These sub-populations that may be non-replicating, hypoxic, nutrient-starved or actively-growing are all affected differently by antibiotics, and as such TB could be perceived as a polymicrobial infection consisting of multiple potentially drug-tolerant sub-populations of bacilli that requires diverse and sustained drug action to successfully sterilise TB infection (Evangelopoulos, da Fonseca et al. 2015).

Seminal research into antimicrobial tolerance in *M.tb* infection *in vivo* was performed by Jindani *et al* in 1980. Viable counting of *M.tb* in human sputa from day 0 (treatment naïve) through to day 14 of treatment was performed by Jindani *et al* in 124 patients in Nairobi in 1974 (Jindani, Aber et al. 1980). Patients were treated with 22 regimens of INH, RIF, PZA, EBU or STREP, alone or in combinations, and colony counts of viable TB were performed every 2 days up to day 14 after start of drug therapy. Patients treated with INH only and INH and RIF showed a rapid decline in CFU/mL during the initial 2 days of treatment (phase 1), followed by a much slower decline in cell numbers (phase 2), Figure 1.6 (Hu, Coates et al. 2008). The authors reasoned that rapidly growing bacilli were killed during the first two days of INH treatment, while in phase 2 non-dividing or slowly metabolising bacilli were only slowly sterilised by INH, i.e. drug efficacy here is based on predicted bacterial factors such as metabolic or respiratory state of bacilli in the lung (Jindani, Dore et al. 2003). The presence of these “persistent” bacilli that survive through early drug therapy may explain why standard treatment for TB takes six months. A greater understanding of these processes might help novel drug

regimens to be designed that target these persister bacilli, potentially shortening treatment times.

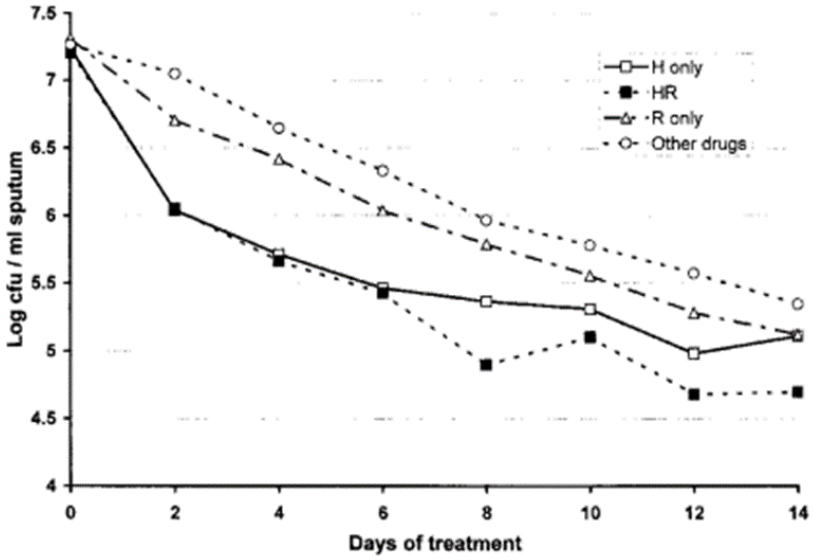

Figure 1.6: Bi-phasic kill curve of *M.tb* in human sputa during treatment

Viable counting *M.tb* derived from human sputa resulted in a bi-phasic kill curve, with phase 1 (day 0-2) showing a rapid decline in hypothesised actively-growing bacilli and phase 2 (day 2-14) showing a reduced rate of kill compared to phase 1. This may be due to drug tolerant sub-populations of *M.tb* that persist through treatment. H: INH only; HR: INH and RIF; R: RIF only. Other drugs include streptomycin, pyrazinamide and ethambutol. Y-axis is log colony forming units/mL sputum. Figure taken from Jindani, Dore et al. 2003.

1.6.2 The transcriptome of TB in human sputa

Transcriptional analyses of *M.tb* isolated from human sputa indicated distinct changes in respiratory and metabolic states compared to log phase *in vitro* cultures of *M.tb*, with a shift in metabolism from actively metabolising, replicating bacteria to fatty acid/cholesterol metabolising, slowly dividing bacilli (Garton, Waddell et al. 2008). This fatty acid metabolism transcriptome correlated with microscopy findings revealing that *M.tb* derived from human sputa were rich in lipid bodies. These sub-populations of lipid-rich bacteria, described as “fat and lazy” due to lipid body inclusions and slow metabolism, have been observed to accumulate triacylglycerol *in vitro*. This lipid storage mechanism may aid in the long-term survival of bacilli, through changing metabolic states from actively growing to slow- or non-dividing (Daniel, Deb et al. 2004, Sirakova, Dubey et al. 2006). The enzyme triacylglycerol synthase 1 is encoded in the DosR operon, a collection of approximately 50 genes that are transcribed under hypoxia and associated with long-term survival of *M.tb* (Bartek, Rutherford et al. 2009).

M.tb spreads through aerosolised sputa during coughing and analysis of *M.tb* in sputa can provide a snapshot of the expectorated bacilli. This is important for two reasons; it allows characterisation of bacilli destined to infect a new host, and can describe in part the metabolic states of bacilli in the lung. Mycobacteria have been shown to accumulate intracellular triacylglycerol inclusions known as lipid bodies (Garton, Christensen et al. 2002), and these have been reported to accumulate under hypoxic, acidic, static growth and nitrosative stresses (Daniel, Deb 2004; Sirakova, Dubey et al. 2006). The presence of these in bacilli that are in a non-replicating state surviving these stresses implicate lipid bodies in persistence and thus antimicrobial drug tolerance. Lipid body positive bacilli are readily seen in human sputum (a mean of 45% of bacilli ±STDEV of 20%), and at comparable levels to *in vitro* models of *M.tb* persistence (Garton, Waddell et al. 2008). The frequency of lipid body bacilli within sputum correlates with "time to positivity", which is the length of time from the beginning of culture incubation to the detection of bacterial growth; the higher the percentage of lipid body bacilli within a sputum samples the longer the time to positivity, suggesting that these bacilli were non-replicating. Transcriptional profiling of *M.tb* in human sputum showed a significant decrease in gene expression associated with aerobic respiration and ribosomal function, while an increase in genes associated with cholesterol utilisation and β-oxidation metabolism. Importantly, this research showed that *M.tb* in sputa is not primarily composed of aerobic, actively dividing bacilli but does in fact contain non-replicating persister bacilli at levels proportional to the amount of lipid bodies detected (mean 45% ± STDEV 20%).

Transcriptional analysis of *M.tb* in human sputa not only elucidates metabolic states of bacilli within the lung, but can also predict early drug efficacy (Honeyborne, McHugh et al. 2016). Profiling of TB patients' sputa showed drug induced changes to expression at day 3 that was not present at days 7 or 14, suggesting that bacilli with a drug-responsive phenotype at day 3 were presumably killed by day 7. Furthermore, the transcriptional profile of bacilli pre-antibiotic treatment resembled bacilli at days 7 and 14 implying that *M.tb* that were exhibiting a phenotype allowing survival post day 3 were already present in the lung before chemotherapy (Honeyborne, McHugh et al. 2016). Diverse *M.tb* transcriptional profiles were seen within this cohort of fifteen patients during chemotherapy, and these RNA signatures may align with disease severity or predict treatment success.

1.6.2.1 The DosR regulon

A mycobacterial genetic programme has been identified that is induced in response to nitric oxide exposure and hypoxia (Boon and Dick 2002). DosR, a transcription regulator of approximately 50 genes, has been shown to be responsible for inducing a non-replicating survival phenotype (Boon and Dick 2012). Collectively known as the DosR regulon, transcription initiation is controlled by a two-component system made up of the histidine kinases DosS and DosT which are redox and hypoxia sensing proteins respectively (Voskuil, Schnappinger et al. 2003; Shiloh, Manzanillo et al. 2008). The DosR regulon is hypothesised to be important in energy homeostasis as well as controlling redox balance, and is also required by *M.tb* upon resumption of replication and growth (Leistikow, Morton et al. 2010). Despite its discovery and characterisation, the role of DosR knockout mutants remains ambiguous. DosR knockout mutants show a drastic reduction in cell viability, as well as a lack of induction of the genes that compose the rest of the DosR regulon (Boon and Dick 2002). Bacilli appear unable to recover from hypoxia-induced dormancy, which suggests that DosR is essential for cycling between replicating and non-replicating states. DosR mutants were also shown to have increased virulence in a mouse model of infection (Parish, Smith et al. 2003), while the opposite was true in infected guinea pigs, where DosR mutants were shown to be attenuated (Malhotra, Sharma et al. 2004). This inter-species variation could be due to different TB lung pathologies, as mice do not form human-like hypoxic caseating granulomas, while guinea pigs do. This suggests that the role of DosR is likely to be throughout infection in hypoxic, complex granulomas rather than in an acute progressive infection in mice (Boon and Dick 2012).

1.7 *In vitro* models of mycobacterial drug tolerance/persistence

As discussed above, the dynamic environments encountered by bacilli during infection in the lung likely lead to the generation of multiple phenotypically distinct sub-populations of *M.tb.* Many of these conditions, such as hypoxia, nutrient limitation and variation in pH, have been mimicked *in vitro* to generate models that represent likely environments encountered by *M.tb* in the lung, Table 1.2.

Title	Author	Year	Organism	Condition	Drugs tested	Tolerance to
Evaluation of a nutrient starvation model of *Mycobacterium tuberculosis* persistence by gene and protein expression profiling	Betts JC et al	2002	*M.tb*	nutrient starvation	INH, RIF, MTZ	INH, RIF
A novel *in vitro* multiple-stress dormancy model for *Mycobacterium tuberculosis* generates a lipid-loaded, drug-tolerant, dormant pathogen	Deb et al	2009	*M.tb*	Hypoxia, high CO2, low pH and nutrient starvation	INH, RIF	INH, RIF
Potassium availability triggers *Mycobacterium tuberculosis* transition to, and resuscitation from, non-culturable (dormant) states	Salina et al	2014	*M.tb*	low potassium	INH, RIF, BZT	INH, RIF, BZT
Growth of *Mycobacterium tuberculosis* biofilms containing free mycolic acids and harbouring drug-tolerant bacteria	Ojha et al	2008	*M.tb*	Thiol-reductive stress, Biofilm	INH, RIF	INH, RIF
Thiol reductive stress induces cellulose-anchored biofilm formation in *Mycobacterium tuberculosis*	Trivedi et al	2016	*M.tb*	Biofilm	INH, RIF, ETB	INH, ETB

Table 1.2: Summary of *in vitro* mycobacterial persistence models that measured drug tolerance

"Condition" corresponds to the environment used to induce persistence; INH: Isoniazid; RIF: Rifampicin; ETB: Ethambutol; BZT: Benzothiazinone

1.7.1 The Wayne Model

The Wayne Model was one of the first *in vitro* models developed to investigate persister cell phenotypes in *M.tb*. In order to induce a persister-like phenotype, oxygen was limited *in vitro* by culturing *M.tb* in sealed tubes. Culture vessels with specific agitation and a defined headspace: media volume ratio were used to induce a shift down in *M.tb* metabolism through two distinct phases. *M.tb* grown in a highly aerobic environment will rapidly die when suddenly transferred to anaerobic conditions, but if the O_2 gradient is gradually depleted the bacilli will adapt without rapid cell death (Wayne 1976). The Wayne model builds on this through using gentle agitation of cultures to ensure a homogenous distribution of bacilli while the O_2 is depleting. Two distinct phases were describe in this model; Non-replicating persistence (NRP) 1 and 2. NRP 1 corresponds to a dissolved O_2 saturation of 1%, or a microaerobic environment where turbidity increased but without an increase in DNA replication (as measured by incorporation of a radioactive labelled DNA base into the genome) or CFU. Further depletion of dissolved O_2 to 0.06% corresponded to NRP2, an anaerobic phase, where no changes in culture turbidity or increases in DNA replication were observed. Interestingly, these NRP bacteria exhibited drug tolerance to INH and RIF likely due to minimal cell wall

biosynthesis and protein synthesis (the respective targets of these two antimicrobial drugs) and sensitivity to metronidazole, showing that these bacilli were anaerobic as metronidazole is usually only effective against anaerobically respiring bacteria (Wayne and Hayes 1996).

1.7.2 The Nutrient Starvation Model

M.tb bacilli within a lung lesion or cavity are likely to be subject to nutrient deprivation especially when compared to the nutritional environment of culturing *in vitro*. Nutrient starvation of *M.tb* was initially carried out by Loebel *et al* in 1933 where *M.tb* respiration rates were shown to drop to a basal level when re-suspended only in phosphate buffered saline (PBS), with return to an active metabolic state when cells were transferred to nutrient-rich media (Loebel, Shorr et al. 1933). Based on this work, a Nutrient Starvation model was developed by Betts *et al* to further investigate drug tolerance phenotypes in *M.tb* and to screen novel antimycobacterial compounds against persister bacilli (Betts, Lukey et al. 2002).

Seven-day-old *M.tb* nutrient rich cultures were pelleted by centrifugation, washed twice in PBS, then re-suspended in PBS and incubated at 37°C in sealed bottles for up to six weeks. Nutrient deprived cultures failed to decolourise methylene blue suggesting a rapid decrease in respiration rates of the bacilli had occurred, nor was there metabolism of O_2 in the media or vessel headspace. This is a key difference between this model and the Wayne model discussed above where O_2 depletion was required for the persister phenotype to be induced. These six-week old nutrient starved cultures were then treated with rifampicin, isoniazid or metronidazole. No decrease in viability (CFU) was observed for INH or RIF treatment. Unlike the Wayne model-derived bacilli, metronidazole had no effect on the viable counting of these nutrient-starved cultures. The redox indicator Methylene Blue showed nutrient-starved cultures were aerobic that explained why metronidazole was not effective (Betts, Lukey et al. 2002).

1.7.3 Multiple Stress Model

The Wayne Model and nutrient starvation model focus only on one environmental stress and do not represent multiple challenges that may induce persistence *in vivo*, such as phagocytosis, nitrosative and oxidative stress or variation in pH. A multiple stress model was developed by Deb *et al* to investigate *M.tb* persistence in conditions

of low oxygen (5%), high carbon dioxide (10%), low nutrient availability (10% Dubos media supplemented with Dubos albumin, no glycerol) and low pH of 5.0 (Deb, Lee et al. 2009). Bacilli were shown to have tolerance to both RIF and INH after 18 days incubation in this multiple stress model, with a loss of acid fastness and accumulation of intracellular lipid bodies. As stated already, lipid bodies are found in *M.tb* that are stained directly from human sputum and may provide a source of cellular energy to bacilli that enter a non-dividing persister metabolic state (Garton, Christensen et al. 2002).

1.7.4 Potassium Deficiency Model

The potassium ion K^+ is an important ion in bacterial cell physiology, and is crucial for maintaining intracellular pH, electrochemical gradient across the cell membrane, proton motive force and controlling osmotic pressure within the cell (Castaneda-Garcia, Do et al. 2011), (Epstein 2003). Low K+ environments may be relevant *in vivo*, as shown by transcriptional profiling of K^+-related *M.tb* related genes in a mouse model and in the human lung (Karakousis, Yoshimatsu et al. 2004; Garton, Waddell et al. 2008). Growth of *M.tb* in aerobic cultures that are deficient in K^+ generated populations of bacilli that were non-culturable (NC) on solid agar, however, the bacteria could be propagated in liquid culture (Salina, Waddell et al. 2014). These NC bacilli exhibited tolerance in response to INH and benzothiazinone (BTZ), with NC cultures experiencing a one-log reduction in cells/mL compared to a 2.5-log reduction for aerobic non-NC cultures. No tolerance was observed with RIF treatment however, with both cultures showing a 2.5 log reduction in cells/mL. Transcriptional analyses of this low K^+, NC cultures compared to *in vitro* aerobic log-phase cultures showed physiological adaptations of *M.tb* to this NC state. Genes induced and up-regulated in *M.tb* in other models of persistence such as the Wayne model and nutrients starvation model and stationary phase cultures were induced or up-regulated in this NC state (Muttucumaru, Roberts et al. 2004), (Betts, Lukey et al. 2002), (Voskuil, Visconti et al. 2004). Metabolic pathways such as glycolysis and protein synthesis were repressed, with adoption of an anaerobic state even though this K+ model was aerobic; the lack of K+ may inhibit the use of the proton motive force to generate ATP via respiration, but rather rely on alternative ATP generating pathways (Salina, Waddell et al. 2014).

1.8 Biofilms in disease

Biofilms are complex communities of bacteria that aggregate together or on a surface and are embedded within a self-produced extracellular matrix (ECM) (Davey and O'Toole G 2000). Biofilms are organised spatially, with populations of genetically identical bacteria showing diverse metabolic activity according to where they are localised within the biofilm (Hall-Stoodley, Costerton et al. 2004).Biofilms are important clinically because they allow pathogenic bacteria to not only colonise medical devices and implants, but also host tissues Fux, Costerton et al. 2005. Biofilm-associated infections are a major source of nosocomial infection, with 95% of urinary tract infections associated with a urinary catheter reporting the presence of a biofilm, and 80% of pneumonias associated with mechanical ventilation also indicating the presence of a biofilm structure (Bauer, Torres et al. 2002). Bacteria have been shown to attach to a surface using specific colonisation factors such as pili. Colonisation occurs through cell replication, leading to microcolony formation, followed by the generation of an ECM that physically protects cells from environmental insults, such as antimicrobials or host immune system attacks (Mulcahy, Charron-Mazenod et al. 2008), (Leid, Willson et al. 2005). Residence within a biofilm generates phenotypic cellular heterogeneity as access to nutrients varies throughout the biofilm, resulting in altered gene expression in response to the localised microenvironment of the bacteria (Stewart and Franklin 2008).

1.8.1 The role of biofilms in TB

Bacterial persistence within biofilms has been well documented for numerous bacterial pathogens such as *Pseudomonas aeruginosa* (Brooun, Liu et al. 2000), *E. coli* (Shah, Zhang et al. 2006) and *Staphylococcus aureus* (Conlon, Rowe et al. 2016). However, the role biofilms play in inducing the development of antimicrobial-tolerant sub-populations of bacilli in TB infection is not fully understood. TB is a chronic infection that requires high concentrations of antimicrobial drugs for long treatment times, is found to be recalcitrant to antibiotics and can subvert the immune system to further disease, all of which are clinical features of a biofilm-associated disease (Islam, Richards et al. 2012). Canetti *et al* described large clusters of *M.tb when* histologically examining TB infected lungs consistent with microscopic evidence of biofilm growth in the human lung (Canetti, Gay et al. 1972). *In vivo* evidence in infected guinea pigs suggests that drug-tolerant bacilli that survive chemotherapy exist in microcolonies in the acellular rim of granulomatous tissue (Lenaerts, Hoff et al. 2007), while *M.tb* isolated

from patients with active TB infection were shown to possess pili, which are an important host colonisation factor that facilitates attachment of bacteria to host tissues (Alteri, Xicohtencatl-Cortes et al. 2007). This mounting catalogue of evidence for mycobacterial biofilm formation *in vivo* highlights the need for *in vitro* models of mycobacterial biofilm formation, in order to elucidate drug tolerance and cell survival mechanisms that may occur in mycobacterial colonisation of the human lung. In order to develop new antimicrobials that can shorten this six-month chemotherapy treatment time, it is crucial that *in vitro* models of drug-tolerant bacilli are developed and the role of biofilms in this process investigated.

1.8.2 Mycobacteria exhibit a natural propensity to form multicellular structures

Mycobacteria, such as *M. bovis* BCG and *M.tb,* exhibit a propensity to grow in long rope or cord-like structures that leads to progressive cell aggregation and biofilm formation via a process known as cording (Caceres, Vilaplana et al. 2013). While strains such as *M.tb* and *M. bovis* BCG readily exhibit this cording phenomenon when cultured *in vitro*, the role of cording and subsequent biofilm formation *in vivo* in the pathogenesis of human TB infection is less well understood. During the 1930s, a clinical isolate of *M.tb* named H37 was serially passaged on various media types to differentiate this *M.tb* H37 isolate into an avirulent variant now designated H37Ra and a variant that retained its virulence, designated H37Rv (Steenken, Oatway et al. 1934). Interestingly, the avirulent variant displayed an altered colony morphology to H37Rv, and failed to exhibit cording that was normally seen in the original *M.tb* H37 and H37Rv variant strain (Middlebrook, Dubos et al. 1947). Various researchers in the following decades investigated the effects of this H37Ra variant *in vivo* and demonstrated that the variant lacking a cording phenotype had decreased rabbit, guinea pig (Steenken, Oatway et al. 1934) and mouse (Larson and Wicht 1964) animal model virulence. This strain could still infect macrophages, however it failed to replicate within this intracellular environment (McDonough, Kress et al. 1993).

During the 1950s, Hubert Bloch and colleagues (Noll, Bloch et al. 1956) had identified a membrane associated lipid called “cord factor” that was later identified as trehalose 6,6′-dimycolate (TDM). TDM was subsequently found to play a wide and varied role in the pathogenesis of *M.tb*; it is found in virulent, but not avirulent strains of *M.tb,* and was shown to be directly responsible for the development of cording morphology (Bloch 1955). This factor was shown to enhance disease severity of both acute and chronic TB in a mouse model (Bloch and Noll 1955) and the removal of TDM from bacilli in *M.tb*

abrogated their capability to survive within macrophages (Indrigo, Hunter et al. 2002). Meanwhile, Georges Canetti built upon the *in vivo* data obtained in murine models (Bloch and Noll 1955) by providing direct evidence of *M.tb* cording in human sputa through micrographs, stating that “the caseum was full of colonies of bacilli” (Canetti 1955). The role of biofilms and *M.tb* would not be investigated until 2008, where seminal work by (Ojha, Baughn et al. 2008) showed that *in vitro* biofilm growth of *M.tb* harboured drug-tolerant mycobacteria, with this research discussed further below.

1.8.3 *M.tb* possesses pili- a host attachment factor

The exact mechanism of how these clusters of bacilli form in the lung is unclear. However, the expression of pili may serve to anchor bacilli onto host tissues and has been shown to contribute to biofilm formation in Gram positive bacteria (Mandlik, Swierczynski et al. 2008). Pili are adherence factors that were shown, *in vitro,* to attach *M.tb* bacilli to host extracellular lamin, while serum derived from TB infected individuals contained IgG that could recognise and bind to these pili, suggesting they or a pili associated antigen is produced during infection (Alteri, Xicohtencatl-Cortes et al. 2007).

1.8.4 *M.tb* requires polyketide synthase 1 for biofilm formation

The polyketide synthase (PKS) 15/1 is required by *M.tb* to synthesise phenolic glycolipid (PGL). PGL is a lipid with immunomodulatory properties found in some pathogenic strains of *M.tb* that contributes to lipid diversity in the mycobacterial cell wall (Constant, Perez et al. 2002). PKS 15/1 is a multi-domain enzyme complex composed of PKS 1 and PKS 15. PKS 1 and PKS 15 possess five and one domains respectively that each have discreet enzymatic action that contribute to the synthesis of PGL (Chopra and Gokhale 2009). In order to form a functional PKS 15/1 enzyme complex, both PKS 1 and PKS 15 genes must be transcribed as a single Open Reading Frame (ORF). It has been demonstrated that certain *M.tb* strains possess a frameshift mutation that leads to a nonsense mutation, and can no longer produce PGL. Importantly, the strain most commonly used for TB research, *M. tuberculosis* H37Rv, does not produce GPL as PKS 1/15 is not transcribed as single ORF (Constant, Perez et al. 2002). The generation of a transposon library of H37Rv-derived mutant strains showed a significant reduction in their ability to form pellicle-biofilms when disruption of the *Pks1* locus occurred. Complementation of this *pks1* locus at a heterologous site in the genome re-established pellicle- biofilm formation, suggesting that PKS1 plays a role

in synthesis of molecules other than GPL required for biofilm maturation. The authors speculate that PKS1 may function alone or in complex with other enzyme(s) to generate lipids that contribute to ECM formation or clustering of bacilli (Pang, Layre et al. 2012).

1.8.5 *M.tb* quorum sensing

Mycobacterium species are members of the Actinobacteria, which is the largest phylum in the domain Bacteria, and is composed of 342 genera. Of these, only nine have known quorum sensing, including mycobacteria (Polkade, Mantri et al. 2016). Quorum sensing is cell to cell communication that is dependent on cell density for the regulation of specific genes and is associated with the induction of a range of pathways such as synthesis of virulence products, exopolysaccharide production and importantly biofilm production in numerous bacterial strains (Barber, Tang et al. 1997), (Beck von Bodman and Farrand 1995), (Li and Tian 2012). While quorum sensing has been well characterised in numerous Gram positive and Gram negative bacteria, it is unclear exactly what role quorum sensing plays in *M.tb* growth, virulence and biofilm formation. Bioinformatics analysis of the genome of *M.tb* H37Rv identified seven genes encoding LuxR family proteins, which have been shown to respond to auto-inducer (AI) molecules secreted by bacteria that initiate quorum sensing but experimental evidence for the role of these genes in *M.tb* is lacking (Patankar and Gonzalez 2009). LuxR binds AI, and together can recognise and bind to DNA promoter elements called *lux-boxes*, which leads to the activation of gene transcription. LuxR-AI will also bind to LuxI, a protein required for AI synthesis and feedback regulation of quorum sensing (Fuqua and Greenberg 2002). Importantly, LuxR was shown to regulate cell wall composition and virulence in *M. avium* subsp. *paratuberculosis,* a pathogen of ruminants such as cattle (Alonso-Hearn, Eckstein et al. 2010), (Thorel, Krichevsky et al. 1990). In *M.tb* however, only LuxR genes were identified with no AI synthesis genes found, suggesting that if LuxR dependent quorum sensing in *M.tb* occurs, the AI and mechanism has yet to be identified (Alonso-Hearn, Eckstein et al. 2010).

Quorum sensing is a variable process across bacterial species and can occur through a number of biochemical pathways, such as LuxR or through cell to cell signalling using second messenger molecules (Miller and Bassler 2001). C-d-GMP is one such second messenger implicated in quorum sensing bacteria that is also found in mycobacteria (Sharma, Petchiappan et al. 2014). Levels of c-di-GMP vary within the bacterial cell in response to extra and intracellular stimuli and directly contribute to a variety of bacterial

phenotypes such as cell motility, replication, virulence and crucially biofilm formation (Romling, Galperin et al. 2013).

Interestingly, a multiple domain enzyme MSDGC-1 was shown to be crucial for both synthesis and degradation of c-di-GMP in *M. smegmatis* and deletion of this gene severely impacted bacterial survival under nutrient starvation (Bharati, Sharma et al. 2012). The ortholog of this gene in *M.tb* is rv1354c, and when inserted into a MSDGC-1 gene knockout of *M. smegmatis* can restore cell survival under nutrient stress, highlighting the role c-di-GMP plays in mycobacterial survival under environmental stress. MSDGC-1 locates to the inner cell membrane of *M. smegmatis* at the poles of the cell, and altering MSDGC-1 levels leads to different cell surface phenotypes such as changes in cell length and colony formation (Sharma, Prakash et al. 2014). Building on this c-di-GMP induced cell wall variation, a transcriptional activator LtmA, which directly binds c-di-GMP for activity, was shown to alter lipid metabolism genes in *M. smegmatis* leading to reduced permeability of the cell wall and distinct changes to colony morphology (Li and He 2012). The role of quorum sensing in pathogenic mycobacteria remains unclear, but this experimental evidence in *M. smegmatis* suggests that c-di-GMP plays a role in reduced cell wall permeability and, potentially, in biofilm formation through cell wall remodelling and altered colony formation *in vitro* (Sharma, Petchiappan et al. 2014).

1.9 *In vitro* biofilm models of TB

In vitro cultures of mycobacteria exhibit spontaneous formation of macroscopic cellular clusters or structures at the air-interface of liquid media when they are not dispersed through the addition of a detergent, (such as polysorbate 80; Tween 80). These aggregates are referred to as pellicles (Dalton, Uy et al. 2016). Traditionally, mycobacterial are grown in media containing Tween 80 to generate planktonic homogenous suspensions of bacilli (Dubos and Middlebrook 1948). Use of planktonic mycobacterial cultures has numerous advantages, such as facilitating CFU enumeration, accurate dilution of cultures, homogenous exposure to drugs, and uniform multiplicity of infection (MOI) in pathogen-host interaction studies. There are however, disadvantages to using detergent-exposed planktonic cultures since these do not mimic *in vivo* conditions. Generation of various microenvironments within an aggregate of mycobacteria could generate conditions that induce stress-tolerant phenotypes of bacilli that could have implications for antimicrobial drug tolerance (Islam, Richards et al. 2012). Importantly, detergent-free aggregates, or biofilms, of

mycobacteria have been shown to harbour antimicrobial drug-tolerant bacilli. Ojha *et al* cultured *M. bovis* and *M.tb* in a thin layer of detergent-free Sauton's Modified Media, a specified mycobacterial liquid media in petri dishes sealed with parafilm for five weeks and incubated at 37°C. Interestingly, unsealed petri dish cultures failed to cultivate the dense biofilms at the liquid air interface that occurred in sealed petri dishes. The authors optimised their biofilm model in tightly sealed polystyrene bottles with 10% of the total volume Sauton's Modified Media for a three-week incubation followed by a two-week incubation at 37°C, with the bottle lids loosely closed to allow gaseous exchange. GC/MS analysis of the headspace of these bottles containing *M.tb* biofilms showed an increase in CO_2 and a decrease in O_2, when compared to *M.tb* cultured in bottles that had been vented for five weeks with no biofilm formation. This suggests that a headspace: media ratio of 9:1 and limited gaseous exchange with the atmosphere is required for biofilm formation. The authors noted that they were unsuccessful in identifying volatile gases that may have been generated during biofilm incubation. Treatment of these biofilms with up to 100X MIC isoniazid showed ~10% of biofilm bacilli survived, as determined by CFU/mL enumeration of biofilms that were homogenised with glass beads in the presence of Tween 80. When biofilms were treated directly with rifampicin, a bi-phasic kill curve was observed.; a >1000-fold reduction in cell viability was observed by day 3, but no further reduction in viability was seen with extended treatment times, suggesting the presence of a subpopulation of persister cells that exhibited INH and RIF antimicrobial drug tolerance as a result of growth within a biofilm (Ojha, Baughn et al. 2008).

The role biofilms play in generating antimicrobial drug tolerant sub-populations was investigated further by Trivedi *et al*, (Trivedi, Mavi et al. 2016), who found that thiol-reductive stress (through addition of dithiothreitol) to log-phase aerobic cultures led to an increase in culture biomass that was not due to cell aggregation, replication or increases in cellular size or shape, suggesting formation of an extracellular matrix (ECM). Biofilm-like mass accumulated at the liquid-air interface of shaking culture vessels. Dithiothreitol-treated biofilms exhibited antimicrobial drug tolerance to isoniazid, rifampicin and ethambutol treatment when measured using CFU counts and crystal violet assays, and none of these front-line drugs could disrupt mature biofilms. Interestingly there was only a slight decrease in bacterial metabolism, with NAD^+/NADH, $NADP^+$/NADPH and ATP/ADP ratios similar to planktonic cultures suggesting that bacilli within these biofilms were metabolically active. Transcriptional profiling of these biofilms showed that 284 genes were differentially expressed; overall, a shutdown of DNA, RNA and protein synthesis pathways was observed suggesting a

decrease in bacterial replication and division. Several pathways were up regulated, including carbohydrate and lipid metabolism, nucleotide synthesis, respiration and the tricarboxylic acid cycle (TCA). This transcriptional profiling suggests that bacilli residing within the biofilm are metabolically active but not necessarily dividing (Trivedi, Mavi et al. 2016).

1.10 Background and aims

Mounting evidence suggests that there are drug-tolerant sub-populations of *M.tb* in the human lung that are refractory to the sterilising action of standard chemotherapy. Targeting these sub-populations of drug tolerant "persister" bacilli likely explains the extended standard treatment length of six months for tuberculosis. Several *in vitro* models have been developed that induce drug tolerance, however few models have investigated whether the natural propensity of mycobacteria to grow as cords in clumps, as a biofilm, creates a source of drug tolerant bacilli. The main aim of this thesis was to optimise a novel low-shear, mycobacterial biofilm model and to characterise the impact of biofilm formation on mycobacterial drug tolerance, transcriptome and pathogen-host interactions. The specific aims are detailed below.

Chapter 3: Optimisation of the Rotary Cell Culture System (RCCS) for low shear, biofilm culture of *M. bovis* BCG

The aim of this chapter was to develop a low-shear Rotary Cell Culture System (RCCS) that would facilitate *in vitro* biofilm formation using *M. bovis* BCG as a model organism for *M.tb*. Culture conditions were optimised and Kinyoun staining and scanning electron microscopy used to describe biofilm formation.

Chapter 4: Antimicrobial drug tolerance of RCCS-derived cultures

The aim of this chapter was to characterise biofilm-derived bacilli in terms of growth state and in response to antimicrobial drug exposure using measures of viability. Two approaches were taken for antimicrobial susceptibility testing (AST); AST using routinely prescribed antimycobacterial drugs isoniazid, rifampicin, streptomycin or metronidazole and AST using novel antimycobacterial compounds isolated from sub-tropical plants from Brazil.

Chapter 5: Transcriptional profiling of RCCS-derived cultures

This chapter aimed to use unbiased genome-wide transcriptional profiling to characterise the impact of biofilm formation on the metabolic and respiratory state of bacilli. To identify up- and down-regulated genes that contribute to the antimicrobial

drug tolerant phenotype observed in RCCS-derived biofilms compared to control cultures. Mycobacterial mRNA was hybridised to tiling microarrays to define the transcriptome of RCCS-derived biofilm and control cultures.

Chapter 6: Pathogen-Host Interactions of RCCS-derived cultures

The work in this chapter assayed the response of macrophage-like human THP-1 cells to stimulation with RCCS-derived biofilm and control supernatants to investigate divergent host-pathogen interactions. A THP-1 human macrophage-like cell supernatant stimulation screen was developed, measuring cell viability and TNFα and IL-1β release.

Chapter 7: The role of a novel mismatch repair system in *M.tb*

This chapter begins to link concepts of mycobacterial drug tolerance and drug resistance. A non-canonical mismatch repair nuclease, NucS, was shown to maintain low rates of spontaneous mutation in mycobacteria. When this gene was deleted in *M. smegmatis* drug resistance rates significantly increased, (Castaneda-Garcia, Prieto et al. 2017). A *nucS* null mutant was constructed in *M.tb* H37Rv with our collaborators. The aim of this chapter was to define the spontaneous drug resistance pattern of this nuclease-deficient *M.tb* strain compared to wild type *M.tb.*

Chapter 2: Materials and Methods

2.1 Media and buffers

A number of media and reagents were used continuously throughout this PhD and are summarised in Tables 2.1 and 2.2 below.

Media	Composition
Middlebrook 7H9 Broth	1.88 g Middlebrook 7H9[a]; 360 mL dH_2O; 200 µL Tween 80[b]; 40 mL albumin, dextrose, catalase solution (ADC)
Middlebrook 7H10 Agar	7.6 g Middlebrook 7H10[a]; 360 mL dH_2O; 2 mL glycerol[c]; 40 mL oleic acid, albumin, dextrose, catalase solution (OADC)
ADC	50 g bovine albumin fraction V[b]; 20 g dextrose[b]; 0.04 g catalase[b]; 8.5 g sodium chloride[b]; up to 1 L dH_2O
OADC	50 g bovine albumin fraction V; 20 g dextrose; 0.04 g catalase; 8.5 g sodium chloride; 0.5 g oleic acid$_b$; up to 1 L dH_2O
Sauton's Modified Media	0.5 g potassium phosphate (monobasic)[b]; 0.5 g magnesium sulphate[b]; 4.0 g L-asparagine[b]; 0.05 g ferric ammonium citrate[b]; 2.0 g citric acid[b]; 75.6 g glycerol; 100 µL 1% zinc sulphate; up to 1L dH_2O
Luria Bertani Broth (LB)	10 g tryptone[d]; 5 g yeast extract[b]; 5 g NaCl[b]; up to 1 L of dH_2O
Luria Bertani Agar (LA)	10 g tryptone; 5 g yeast extract; 5 g NaCl; 15 g bacteriological agar[d]; up to 1 L of dH_2O

Table 2.1: Commonly used media

Reagents were purchased from: [a]Becton Dickinson, Oxford, UK; [b]Sigma Aldrich, Dorset, UK; [c]Fisher Scientific, East Grinstead, UK; [d]Oxoid, Basingstoke, UK

Buffers and Solutions	Composition
Phosphate Buffered Saline (PBS)	0.01 M phosphate buffer; 0.0027 M potassium chloride; 0.137 M sodium chloride
50X TAE	242 g Tris-base; 57.1 mL glacial acetic acid; 100 mL 0.5 M sodium EDTA; up to 1 L of dH2O
10X TBE	121.1 g Tris-base; 61.8 g Boric acid; 7.4 g sodium EDTA; up to 1 L dH2O
10X TE	100 mL Tris-HCl pH 7.5; 20 mL 0.5 M sodium EDTA pH 8.0; up to 1 L dH2O
5M GTC	295.4 g guanidine thiocyanate; 2.5 g N-lauroyl-sarcosine; 12.5 mL 1 M sodium citrate; 5 mL Tween 80; β-mercaptoethanol up to 500 mL dH2O
4M GTC	236.3 g guanidine thiocyanate; 2.5 g N-lauroyl-sarcosine; 12.5 mL 1 M sodium citrate; 5 mL Tween 80; β-mercaptoethanol up to 500 mL dH2O

Table 2.2: Commonly used buffers

Reagents were purchased from: [a]Becton Dickinson, Oxford, UK; [b]Sigma Aldrich, Dorset, UK; [c]Fisher Scientific, East Grinstead, UK; [d]Oxoid, Basingstoke, UK

2.2 Bacterial strains and growth conditions

2.2.1 *M. bovis* BCG, *M. tuberculosis* growth conditions

Mycobacterium bovis BCG (*M. bovis* BCG) and *M. tuberculosis* H37Rv (*M.tb*), Public Health England culture collection numbers NCTC 5692 and NCTC 7416 respectively, were reconstituted from 15% glycerol frozen stocks stored under liquid nitrogen by passaging in Middlesbrook 7H9 broth (Becton Dickinson GmbH) plus 0.05% v/v Tween 80 (Sigma Aldrich, Dorset, UK) enriched with 10% v/v ADC (7H9 + ADC, Tween 80 broth) (Becton Dickinson GmbH, Oxford, UK), Table 2.1. This enriched 7H9 media is referred to as "7H9 broth" throughout this thesis. Liquid cultures were incubated statically at 37°C and 1 mL of culture passaged into 10 mL 7H9 + ADC, Tween 80 broth every seven days. Optical density (O.D.) of liquid cultures was measured using single use 1 cm cuvettes and a spectrophotometer with absorbance of 600 nm.

2.2.2 *M. bovis* BCG, *M. tuberculosis* growth curves

M. bovis BCG and *M.tb* H37Rv growth curves were conducted in a 250 mL Erlenmeyer flask (Corning, London, UK) containing 50 mL 7H9 + ADC, Tween 80 broth at 37°C, 180 RPM. This was inoculated with 1 mL 7 day old *M. bovis* BCG or *M.tb* H37Rv that had been maintained as in section 2.2.1. The $O.D._{600nm}$ was monitored in in 24 hour segments up to 30 days.

2.2.2.1. *M. bovis* BCG, *M. tuberculosis* viable count determination

A serial dilution plate method was used to determine Colony Forming Units per mL (CFU/mL) of *M. bovis* BCG and *M.tb*. 100 µL of a liquid culture was added to 900 µL PBS (10^{-1} dilution) and vortexed for ten seconds to ensure homogeneity. 100 µL of this 1 x 10^{-1} dilution was then pipetted into 900 µL PBS (10^{-2} dilution) and vortexed for ten seconds. Each dilution was subsequently further diluted in PBS until bacterial cultures were diluted to 10^{-8}. 150 µL of each dilution was drop pipetted onto one half of a Middlebrook 7H10 enriched with OADC agar plate, Table 2.1, allowed to dry, sealed in Ziploc bags and incubated at 37°C in a static incubator for four weeks.

Plates selected for CFU/mL calculations were in the dilution range that yielded individual, well-isolated colonies per dilution plated. CFU/mL was calculated using the following formula:

$$\frac{CFU}{mL} = \frac{\#\ Colonies\ x\ Dilution\ Factor}{Vol\ Plated\ in\ mL}$$

2.2.3 *Escherichia coli* culture conditions

Neb-5 alpha competent *Escherichia coli* (genotype: fhuA2 Δ(argF-lacZ)U169 phoA glnV44 Φ80 Δ(lacZ)M15 gyrA96 recA1 relA1 endA1 thi-1 hsdR17 (New England Biolabs, Ipswich, UK) were employed for plasmid transformations. *E. coli* were cultured in Luria Bertani broth for liquid media and LA agar for solid biomass growth, Table 2.1. Liquid cultures were grown at 225 RPM, 37°C overnight and agar cultures were incubated overnight at 37°C. Both liquid and solid media were supplemented with 50 µg/mL kanamycin sulphate (Sigma Aldrich, Dorset, UK).

2.3 Bacterial growth plotting

Bacterial growth was graphed using Microsoft Excel 2013 and GraphPad 6 with O.D.600nm, CFU/mL and time used to plot growth.

2.4 The Rotary Cell Culture System

2.4.1 Inoculation of the Rotary Cell Culture System (RCCS)

All work using *M. bovis* BCG was performed aseptically in a Class II cabinet in a Category Level 2 laboratory. All 10 mL rotary bioreactor vessels (Synthecon, Houston, USA) were equilibrated with sterile PBS (Sigma Aldrich, Dorset, UK) overnight before inoculation with *M. bovis* BCG and incubated in a humidified atmosphere at 37°C. To prepare the RCCS inoculum, a frozen 15% v/v glycerol stock of *M. bovis* BCG was thawed at room temperature and added to 10 mL 7H9 Tween 80 broth and incubated for seven days. Next, 1 mL of this culture was subsequently passaged into 10 mL 7H9 broth and incubated for seven days. 1 mL of this culture was passaged into 10 mL Sauton's Modified Media with Tween 80 and incubated for seven days. This culture was then diluted to an O.D.600 nm of 0.05- 0.06 (3×10^5 cells/ mL) with Sauton's Modified Media no Tween 80 to a final volume of 100 mL. This cell suspension was added to each of the four 10 mL RCCS vessels via the fill port using a 20 mL syringe while simultaneously removing any air bubbles with a 20 mL syringe from the opposing exit port. Fill port valves were closed and swabbed cleaned with 70%. The four RCCS vessels were incubated at 37°C in a humidified incubator at 15 RPM for two rotating vessels, with two vessels remaining stationary. RCCS vessels were inspected daily for the presence of air bubbles which were removed and air bubble volume replaced with

Sauton's Modified Media no Tween using sterile 5 mL syringes, swabbed with 70% ethanol, vessel port caps replaced and sealed and returned to incubation on the RCCS. RPM was adjusted as required to reduce biofilm contact with vessel walls. Media was replaced equally across all four vessels. Cell clusters in the RCCS were harvested on day 21 of incubation. The RCCS system is detailed further in section 3.2.

2.4.2 Harvesting of the RCCS

Rotating vessels contained biofilms, while control cultures were RCCS vessels that were kept stationary during incubation. Vessels were removed from the RCCS, exterior wiped with 70% ethanol and sample port cap removed. 10 mL vessel cultures were removed from vessels using 25 mL pipettes and were immediately transferred to 50 mL sterile Falcon tubes. Rotating or stationary vessels were not pooled, with each vessel acting as a biological replicate. All downstream applications for vessel cultures were performed immediately after harvesting, with RNA extraction performed first to prevent transcriptional profiles being altered due to harvesting process, Figure 2.1.

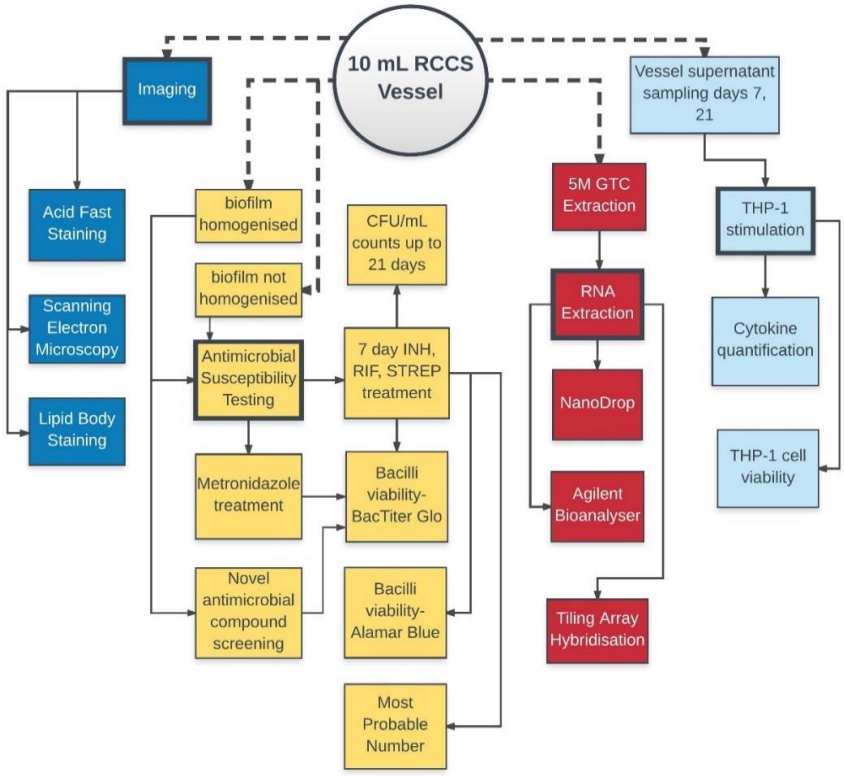

Figure 2.1: Flow chart summary of the techniques applied in this thesis to investigate mycobacterial biofilm growth in the RCCS

Core methods are colour-coded according to results chapters. Dark blue: Optimisation of the RCCS for low-shear, biofilm culture of the RCCS (chapter 3); Yellow: Antimicrobial drug tolerance of RCCS-derived cultures (chapter 4); Red: Transcriptional profiling of RCCS-derived cultures (chapter 5); Blue: Pathogen-host interactions of RCCS-derived cultures (chapter 6).

2.4.2.1 Biofilm homogenisation

Rotating RCCS vessel biofilms or stationary RCCS vessel control cultures were transferred to sterile 50 mL sterile Falcon tubes. Then, samples were homogenised using a sterile 10 mL syringe and a 25 gauge (0.5 x 25 mm) needle. Cultures were syringed ten times with the full culture volume syringed each time, to ensure a single cell suspension was achieved. Section 4.2.2.1 details how a single cell suspension was shown to be generated.

2.4.3 Supernatant sampling

RCCS biofilm and control vessel supernatants were sampled on days 7, 14 and 21 of an RCCS run, as well as a static 10 mL Sauton's no Tween culture in a 30 mL Universal tube that was inoculated with the RCCS inoculum. A 1 mL vessel medium aliquot was removed from each vessel with a 2 mL syringe, and 1 mL Sauton's no Tween medium added back in with a 2 mL syringe, ensuring no air bubbles were introduced to the vessel. 1 mL aliquots were also taken from the static 30 mL Universal tube in with a 2 mL syringe, and 1 mL Sauton's no Tween added back in. Each 1 mL aliquot was transferred to a 0.2 µM filter column, centrifuged 15,871 g for 3 minutes and filtrate stored at -80°C, figure 2.2.

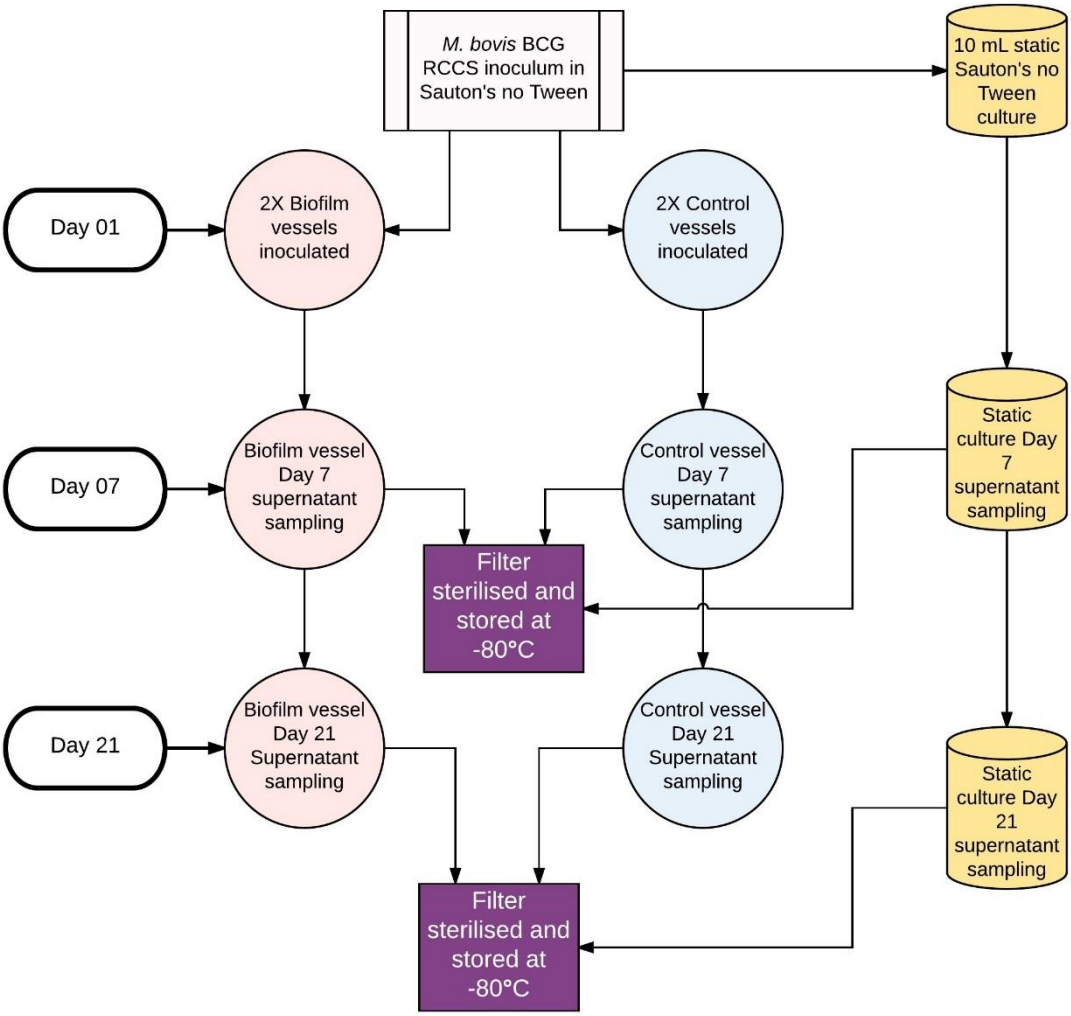

Figure 2.2: Flow chart summary of supernatant collection used for THP-1 cell stimulation experiments

A single *M. bovis* BCG Sauton's no Tween 80 suspension was used to inoculate an RCCS run as described in Materials and Methods 2.4.3, but was also used to inoculate one static 10 mL culture in a 30 mL Universal tube. Supernatants were sampled at days 7 and 21 for three RCCS runs; RCCS #9, RCCS #10, RCCS #11.

2.5 Antimicrobial Drug Susceptibility Testing (AST)

2.5.1 Antimicrobial drug stock preparation

Master stocks (10 mg/mL) of antimicrobial drugs were prepared by adding 100 mg of an antimicrobial drug to a 10 mL volumetric flask and made up to volume with an appropriate solvent (dH_2O for isoniazid, ethambutol, streptomycin and metronidazole and DMSO for rifampicin). This was mixed well on a vortex mixer and filtered through a 0.22 µm syringe filter into sterile 1.5 mL Eppendorf tubes. Master stocks were prepared for each antibiotic, and stored at -20°C. These were disposed of after six months' shelf life. Working stocks were freshly prepared aseptically by diluting master stocks with media and were single use only.

2.5.2 AST liquid culture method for determining the Minimum Inhibitory Concentration (MIC) for *M. Bovis* BCG

MICs for each antimicrobial were established using a microbroth dilution method in sterile 96 well microtiter plates. Wells adjacent to the outside of the microtiter plate were subject to greatest volume loss during incubation and were not used. Therefore, 200 µL dH_2O were added to these wells so as to minimise moisture loss during incubation. 500 µg/mL of each antimicrobial were prepared in 7H9 broth and diluted two-fold (500-0.98 µg/mL) with 7H9 broth in 100 µL per well in a 96 well microtiter plate in duplicate or triplicate. These were inoculated with 100 µL log-phase *M. bovis* BCG per well that had been adjusted to an $O.D._{600nm}$ of 0.05- 0.06 (3×10^5 CFU/mL) with 7H9 broth. A growth curve of *M. bovis* BCG is shown in figure 3.6. The final test antimicrobial concentrations post inoculation were 250- 0.49 µg/mL. 96 well microtiter plates were mixed using a microtiter plate shaker, sealed in Ziploc bags and incubated for seven days statically at 37°C. Appropriate positive (inoculated 7H9 broth, no antimicrobial), negative (un-inoculated 7H9 broth, no antimicrobial) and carrier (un-inoculated 7H9 broth, with antimicrobials) controls were carried out for all AST experiments. Viability was measured using Alamar Blue and BacTiter Glo cell viability assays, viable counts and Broth Culture Assay (BCA).

2.5.3 AST Method for antimicrobial drug tolerance of RCCS-derived cultures

A two-fold serial microbroth dilution method was not used for AST of RCCS-derived cultures. Instead, required antimicrobial drug concentrations (e.g. 0-3.0 µg/mL) were prepared by diluting working stocks in 7H9 broth in 1.5 mL Eppendorf tubes for each

individual concentration. RCCS-derived cultures were treated with these antimicrobial drugs in a microtiter plate as above in section 2.4.2.

2.5.4 AST solid media method for determining the MIC for *M. tuberculosis*

Middlebrook 7H10 agar plates were formulated as per Table 2.1 with one drug concentration as required (Materials and Methods section 2.5.1) added while agar was still molten. This was mixed well and poured into sterile agar plates and allowed to set. Each antibiotic 7H10 agar plate was inoculated with 1 x 10^8 CFU/mL log phase *M.tb,* and incubated for four weeks at 37°C. The lowest concentration of antimicrobial drug where there was no visible growth was taken as the MIC.

2.6 Bacterial cell viability assays

2.6.1 Viability assays

Mycobacterial cell viability was assessed by Alamar Blue® Cell Viability Assay (ThermoFisher Scientific, Loughborough, UK) and BacTiter Glo® Luminescent Bacterial Viability Assay (Promega, Southampton, UK).

For the Alamar Blue method, the reagent was added to a final concentration of 10% v/v of the culture volume and incubated at 37°C for 24 hours. Fluorescence was measured at excitation 530/25 nm, emission 590/35 nm in a Synergy HT plate reader. For BacTiter Glo, bacterial cultures were transferred to a white opaque 96 well microtiter plate and an equal volume of BacTiter Glo added, homogenised by pipetting and incubated at room temperature for 10 min. Luminescence was measured in a Synergy HT plate reader.

2.6.2 Broth Culture Assay

The contents of wells selected for Broth Culture Assay (BCA) from 96 well microtiter plates were centrifuged at 9,390 g for two minutes in a benchtop centrifuge, antimicrobial supernatants removed by pipetting and re-suspended in their original volumes using 7H9 ADC, Tween 80 broth. 10 µL of these cultures were serially diluted 10^{-1} to 10^{-6} in 7H9 ADC, Tween 80 broth in 96 well microtiter plates and incubated for 21 days. After 21 days incubation, wells were mixed thoroughly by pipetting and absorbance measured at wavelength 630 nm; wells with positive growth will have increased absorbance at this wavelength. 10 µL of all wells were spotted onto 7H10

agar plates to confirm mycobacterial growth for wells identified as positive growth using absorbance.

2.7 RNA extraction, analyses and hybridisation

2.7.1 Mycobacterial cell extraction from cultures

Mycobacteria were recovered for RNA extraction based on a guanidine thiocyanate (GTC) extraction method Monahan, 2001. Four volumes of 5 M GTC solution were added to the mycobacterial liquid culture and mixed well by inversion (40 mL 5M GTC to 10 mL *M.tb* culture for RCCS vessels). 25 mL aliquots of the culture: GTC mixtures were then centrifuged in 30 mL Universal tubes at 1,620 g for 30 minutes. The supernatant was removed and the bacterial pellets re-suspended and combined in approximately 10 mL spent GTC using plastic sterile pipettes to combine the bacterial pellets. Each Universal tube was then washed with 2-3 mL 5 M GTC solution to ensure all bacilli were recovered. These combined re-suspended pellets were then centrifuged in 30 mL Universal tubes at 1,620 g for 20 minutes. Each sample was re-suspended in 1 mL Trizol (Invitrogen, Paisley, UK) and stored at -70°C until RNA extraction was required.

2.7.2 Mycobacterial RNA extraction

One mL mycobacterial aliquots suspended in Trizol were thawed on ice, transferred to ribolyser tubes containing 0.1 mm silica beads and were then physically disrupted for 45 seconds using a tissue homogeniser set at a speed of 6.5 ms^{-1} (MP Bio, Santa Ana, CA, USA). Mycobacterial homogenates were incubated for 10 minutes at room temperature. Next, 200 µL of chloroform was added to each suspension. The tubes were inverted and vortexed for 30 seconds to re-suspend beads, and subsequently incubated at room temperature for 10 minutes to allow partitioning of the aqueous (top layer) and phenolic (coloured bottom layer) phases. Partitioned suspensions were then centrifuged at 15,871 g at 4°C for 15 minutes. Aqueous phases were then transferred to sterile RNase free 1.5 mL Eppendorf tubes using a P200 pipette and equal volumes of chloroform added. Tubes were inverted and vortexed for 30 seconds, incubated at room temperature for 10 minutes followed by centrifugation at 15,871 g at 4°C for 15 minutes. Aqueous phases were transferred directly to columns from a mirVana RNA isolation kit and total RNA isolated according to manufacturers' instructions. An

additional 80% v/v ethanol wash step for 1 minute at 9,390 RPM was performed to remove salts before eluting total cellular RNA in 25 µL 95°C RNase free dH2O.

Extracted total RNA was treated with DNase I (Primer Design, Southampton, UK) at 30°C for 15 minutes to degrade genomic DNA followed by a five minute 50°C incubation to denature DNase I. RNA concentrations were quantified using a NanoDrop (ThermoFisher Scientific, Loughborough, UK) with RNA integrity and the size distribution of RNA analysed using the Agilent 2100 Bioanalyser NanoChip system (Agilent, Edinburgh, UK). Finally, isolated DNase treated RNA was stored at -70°C until hybridisation to tiling arrays was required.

2.7.3 RNA hybridisation

2.7.3.1 RNA labelling for hybridisation

RNA samples to be hybridised to tiling arrays were thawed on ice and a non-enzymatic Cy3 fluorescent dye labelling kit (Kreatech, USA) was used to label RNA directly without RNA template amplification. Then, 2 µg of total RNA per sample was labelled following manufacturers' instructions.

2.7.3.2 RNA fragmentation

RNA samples were fragmented using Agilent fragmentation kit (Agilent, USA). 1 µL of each labelled, fragmented RNA sample was quantified for RNA labelled CY3 and RNA using a NanoDrop (ThermoFisher Scientific, Loughborough, UK).

2.7.3.3 Tiling array design

Tiling arrays were custom designed Agilent arrays (ArrayExpress accession A-BUGS-47) with 180,000 60-mer oligonucleotides evenly tiled across the whole *M.tb* H37Rv genome. These tiling arrays were designed by Bacterial Microarray Group at St George's, University of London (BµG@S).

2.7.3.4 RNA hybridisation

For this procedure, 20 µL of 2 µg labelled RNA was prepared for tiling array hybridisation according to Table 2.3. 100 µL of each hybridisation solution was pipetted onto one gasket well in a "drag and drop" manner ensuring no solution came into contact with gasket well walls. This was repeated for each hybridisation solution with four gasket arrays per gasket array slide. A tiling array slide (with four corresponding

tiling arrays per slide) was placed onto a gasket slide, secured in place using tiling array cassettes and incubated overnight at 65°C, 20RPM.

Reagent	Volume Added	Supplier	Address
Cy3 labelled RNA	20 µL	Kreatech	Amsterdam, Netherlands
Blocking Agent	27.5 µL	Kreatech	Amsterdam, Netherlands
2X Hybridisation Buffer	55 µL	Agilent	California, USA
dH_2O	7.5 µL	Sigma Aldrich	Dorset, UK

Table 2.3: RNA hybridisation reagents and concentrations

Reagents, volumes and suppliers of RNA hybridisation reagents.

2.7.3.5 Quantification of RNA hybridisation

The hybridised arrays were scanned at 2 micron resolution on an Agilent G2505C Microarray Scanner and data files exported as Tagged Image File Format (TIFF) files. The TIFF images were extracted using Agilent Feature Extraction Software (version 11.5.1.1) and analysed using GeneSpring 12.6 (Agilent Technologies). Tiling array data were normalised to the 75th percentile of all genes detected to be present on each array. Genes were identified as differentially expressed using moderated t-tests (p-value <0.05 with Benjamini and Hochberg multiple testing correction), and fold change >2.

2.8 Molecular Biology

2.8.1 Colony preparation for Polymerase Chain Reaction (PCR)

Selected *E. coli* colony biomass was removed with a sterile loop and added to 200 µL sterile dH_2O in a 1.5 mL microcentrifuge tube and incubated in a 99°C heating block for 10 minutes to kill and lyse cells. Lysed cell suspensions were centrifuged in a bench top centrifuge for 9,390 g for two minutes. The supernatant being used for PCR.

M.tb colony biomass was removed with a sterile loop and added to 500 µL dH_2O in screw-cap 2 mL microcentrifuge tubes. Snap lid microcentrifuge tubes are not suitable for the sustained boiling required to kill *M.tb* due to potential leakage of bacilli into the water bath. Tubes containing the cell suspension were transferred to a suitable

microcentrifuge rack and taped down to hold tubes in place. Tubes were placed in a boiling water bath for 45 minutes to heat kill bacilli, then centrifuged at 9,390 g for two minutes with the supernatant used for PCR.

2.8.2 Polymerase Chain Reaction (PCR)

PCR reactions were performed in a final volume of 12.5 µL in 0.2 mL thin walled PCR tubes (StarLab, Milton Keynes, UK) using reagent concentrations detailed in Table 2.4. PCR reactions were incubated at 98°C for two minutes followed by 30 cycles of 98°C for 30 seconds, 43°C- 55°C depending on melting temperature of primer pairs for 30 seconds and 72°C for 15 seconds with a final extension of 5 minutes at 72°C. PCR amplification was carried out in a Veriti 96-well thermal cycler (Life Technologies, Paisley, UK).

Reagent	[Stock]	[Final]	Supplier	Address
iProof High Fidelity DNA Polymerase	2 U/µL	0.25 U	BioRad	Hemel Hempstead, UK
iProof High Fidelity Buffer	5X	1X	BioRad	Hemel Hempstead, UK
MgCl2 Salt Solution	50 mM	1.5 mM	BioRad	Hemel Hempstead, UK
DMSO (PCR grade)	1	4-6 %	BioRad	Hemel Hempstead, UK
dNTPs	2 mM	200 µM	BioRad	Hemel Hempstead, UK
Forward Primer	10 µM	0.7 µM	Eurofins Genomics	Ebersberg, DE
Reverse Primer	10 µM	0.7 µM	Eurofins Genomics	Ebersberg, DE
Molecular Grade Water	N/A	as required	BioRad	Hemel Hempstead, UK
DNA Template	N/A	as required	various	Various

Table 2.4: Reagents and concentrations used for Polymerase Chain Reaction (PCR)

iProof High Fidelity DNA polymerase was used for all PCR experiments. DMSO was added to all reactions to enhance template DNA denaturation.

2.8.2.1 Agarose Gel Electrophoresis

Agarose gels were prepared at 1% w/v using high specification agarose (Web Scientific, Crewe, UK) and 1x TAE buffer to visualise PCR and DNA digestion products. 10,000X Gel Red (Biotium, CA, USA) was added to molten 1% w/v agarose, homogenised and poured into a gel electrophoresis rig and allowed to set. Hyperladder I (Bioline, London, UK) was used as a molecular marker of DNA band size. Gels were run at 120 V for 30-60 minutes, depending on expected DNA product size. All gel images were imaged in a UV transilluminator (GeneFlash, Syngene Bio Imaging, Cambridge, UK).

2.8.3 Transformation of *E. coli*

Chemically competent *E. coli* were prepared using the $CaCl_2$ method (Dagert and Ehrlich 1979). 5 mL pre-warmed LB broth in a 50 mL Falcon tube was inoculated with a single colony of *E. coli,* and incubated overnight at 37°C, 200 RPM. 2 mL of this overnight culture was added into 198 mL LB broth (i.e. 1/100 dilution) in a 250 mL Erlenmeyer flask and incubated at 37°C, 225 RPM. Once this culture reached an $O.D._{600nm}$ of 0.4 (which corresponds to early log phase) (Cohen, Chang et al. 1972), it was divided into four 50 mL single use tubes and centrifuged at 845 g for 10 minutes at 4°C to harvest *E. coli*. The cells were kept on ice for the remainder of the protocol. All pipettes, solutions and tubes were pre-chilled and cells kept on ice at all times so as not to reduce transformation efficiency of cells. The supernatants were carefully decanted without disturbing the cell pellets. Each pellet then was re-suspended in 1 mL ice-cold 100 mM $CaCl_2$. The four pellets were pooled and made up to a final volume of 10 mL $CaCl_2$ and stored on ice for 30 minutes. This cell suspension was then centrifuged for 845 g for 10 minutes at 4°C. Supernatant was carefully decanted and pellet re-suspended in 1 mL ice-cold 100 mM $CaCl_2$ and 15% (v/v) glycerol. This cell suspension was then aliquoted at a volume of 50 µL into pre-chilled 0.5 mL microcentrifuge tubes and immediately stored at -80°C.

2.8.4 Plasmid extraction

Pre-warmed 5 mL LB broth + 25 µg/mL kanamycin was inoculated with a single colony that had been confirmed by colony PCR to be a putative plasmid transformant and incubated at 37°C, 225 RPM for 5 hours. 100µl of this culture was then sub-cultured into 5 mL LB + 25µg/mL kanamycin overnight at 37°C, 225 RPM. This overnight culture was then centrifuged for three minutes at 1,500 g, 20°C and cell pellet used for plasmid

extraction using a GeneJet plasmid extraction mini-prep kit (ThermoFisher Scientific, Loughborough, UK) according to the manufacturers' instructions.

2.8.5 Plasmid drop dialysis

A 25 mm diameter Type-VS dialysis membrane (Millipore, UK) was floated onto 100 mL dH_2O in a glass beaker for 10 minutes to allow the filter to wet completely. The entire plasmid volume was pipetted onto the centre of the filter, beaker sealed with parafilm and left to stand for four hours. Dialysed plasmid was recovered by pipetting with a 10 µL pipette and recovered into a 1.5 mL Eppendorf tube and stored at -20°C.

2.8.6 Electroporation of *M. tuberculosis*

50 mL 7H9 broth, Tween 80 *M.tb* H37Rv culture was grown to log phase and 2M glycine added to a final volume of 1.5% v/v and incubated for 16-24 h. Section 3.2.1 details *M.tb* H37Rv growth curves. The *M.tb*-glycine culture were centrifuged at 845 g for 10 minutes to pellet cells and washed with 10 mL 10% glycerol followed by a 5 mL 10% glycerol wash. The cell pellet was re-suspended in 1 mL 10% glycerol and 0.2 – 5 µg of plasmid to be electroporated added to 0.2 mL of *M.tb* in 10% glycerol, mixed well, and transferred to a 0.2 cm electrode gap electroporation cuvette. Cells were electroporated with a single pulse of 2.5 kV, 25 µF and 1000 Ω. Electroporated cells were transferred immediately to 10 mL 7H9 broth, and incubated for 16 hours at 37°C. Cells were harvested at 845 g for 10 minutes, re-suspended in 1 mL 7H9 broth, serially diluted in sterile PBS and plated out onto 7H10 agar enriched with OADC containing an appropriate antibiotic and incubated for four weeks at 37°C.

2.9 Imaging

2.9.1 Kinyoun Staining of Mycobacterial cells

The Kinyoun stain works on a similar principle to the Acid Fast staining procedure but is advantageous in that the Kinyoun stain does not require heating to colourise acid fast bacilli. Staining for acid fast bacilli was performed using a specific Kinyoun staining kit and protocol (Becton Dickinson GmbH, Oxford, UK). Slides were heat fixed using a low heat 95% IMS flame prior to staining and allowed to further dry overnight. Slides placed on a staining rack were flooded with TB Carbol fuschin KF for four minutes then washed gently with dH_2O. Slides were decolourised for 3-5 seconds, washed gently again with dH_2O then counter stained with TB Brilliant Green K for 30 seconds. Slides were washed gently with dH_2O and left to dry overnight in a 37°C incubator before being imaged at 40X using an Axiovert 40CFL light microscope (Zeiss, Cambridge, UK). Images were captured using Axiovision SE64 software, version 4.9.1.

2.9.2 Scanning Electron Microscopy (SEM)

100% glutaraldehyde (Sigma Aldrich, Dorset, UK) was added to RCCS-derived biofilm and control cultures to a final volume of 10% v/v to fix samples for SEM. Critical point drying (CPD) was performed by submerging samples in porous sample pots in increasing concentrations of 50-100% ethanol to dehydrate samples. Sample pots were then transferred to a pressure chamber and liquid CO_2 was added to fill the chamber. This was vented to remove any remaining ethanol and re-filled with CO_2, incubated for 1 hour, warmed to 34°C and gas slowly vented. Samples were not coated. Samples were imaged using a Leo s420 Stereoscan electron microscope.

2.9.3 Lipid body staining

Samples for lipid body staining were first Kinyoun stained, as described above. LipidTox stain (Life Technologies, Warrington, UK) was applied to the heat-fixed bacterial smear and incubated in the dark for 2 hours at 37°C, stain removed to waste and washed gently in dH_2O and allowed to air dry. Slides were flooded with Auramine O and incubated at room temperature for 15 minutes. Auramine O (Sigma Aldrich, Dorset, UK) was prepared by dissolving 0.1 g Auramine O in 10 mL 95% v/v HPLC grade ethanol (Fluka, Maidstone, UK) and mixed with 90 mL phenol (Sigma Aldrich, Dorset, UK) solution (3 g phenol dissolved in 87 mL dH_2O). Auramine O was removed to waste and rinsed gently in dH_2O, slides flooded with acid-alcohol and incubated at room temperature for fifteen minutes. Acid Alcohol was prepared by adding 0.5 mL

concentrated hydrochloric acid to 70% v/v HPLC ethanol. Slides were rinsed in dH_2O and stained for 1 minute with 0.5% potassium permanganate solution. Slides were rinsed with dH_2O and allowed to air dry. Slides were mounted in 10% v/v glycerol in PBS cover slip applied and edges sealed with clear nail varnish. Slides were protected from light until imaged at excitation D460/50x, emission D550/50m for Auramine O and excitation ET560/40x and emission ET630/75m for LipidTox using a Nikon Eclipse TE2000-U Light-Fluorescence Microscope.

2.10 THP-1 cell line and culture conditions

THP-1 cell line is a human monocytic cell line derived from a male patient with acute monocytic leukaemia (Tsuchiya, Yamabe et al. 1980). THP-1 cells were obtained from the European Collection of Authenticated Cell Cultures (ECACC), reference number 88081201. They were routinely cultured in RPMI 1640 medium supplemented with 10% v/v final conc. heat inactivated foetal calf serum (FCS) (Invitrogen, Paisley, UK) and L-glutamine 2 mM final conc. (GLU) (Invitrogen, Paisley, UK). This enriched media is referred to as RPMI +FCS + L-GLU throughout this thesis. Media was supplemented with 100X penicillin-streptomycin solution (ThermoFisher Scientific, Loughborough, UK), except for THP-1 cell infections with *M. bovis* BCG *or M. tuberculosis*. Media was pre-warmed at 37°C before passaging culture to media every three days at a ratio of 1:5. Cells were incubated at 37°C in a 5% CO_2 humidified incubator.

2.10.1 Preparation of THP-1 frozen stocks

THP-1 frozen cell stocks were prepared using a “Mr Frosty” freezing container (ThermoFisher Scientific, Loughborough, UK) for cryopreservation that allows a slow steady rate of cooling of cells of -1°C/min when placed at -80°C. THP-1 cells cultured past eight passages were not used to make frozen THP-1 cell stocks. 250 mL isopropyl alcohol (Fluka, Maidstone, UK) was added to the fill chamber of the Mr Frosty (Nalgene, NY, USA) and stored at 4°C to cool chamber. Cell counts of cultures to be banked were performed using a haemocytometer to determine cells per mL, with 2 x 10^6 cells per mL required for frozen stocks. THP1 cell cultures were centrifuged at 160 g for 10 minutes, the supernatant was decanted and the cell pellet carefully re-suspended in 90% FCS and 10% dimethyl sulfoxide (DMSO) (Sigma Aldrich, Dorset, UK) to a cell density of 2 x 10^6 cells per mL. 1 mL aliquots in 1.5 mL cryovials were transferred to the Mr Frosty, placed at 4°C for fifteen minutes and then stored at -80°C overnight.

Following this, the THP-1 cell stocks were removed from -80°C and transferred to -150°C for long-term storage.

2.10.2 THP-1 cell differentiation

Four-day-old THP-1 cell cultures were centrifuged at 160 g for 10 minutes, supernatant removed and cell pellet re-suspended in 1 mL RPMI + FCS + GLU. THP-1 cells were counted using a haemocytometer and light microscope and adjusted with RPMI + FCS + GLU at a cell density of 1 x 10^6 cells per mL. 2 mM phorbol 12-myristate 13-acetate (PMA) (Sigma Aldrich, Dorset, UK) was added to a final concentration of 20 ng/mL and 100 µL aliquoted to each well of a 96 well microtiter plate. Cells were incubated for 24 h, media removed by pipetting and cells washed twice with 200 µL Tissue Culture-grade PBS to remove residual PMA. 200 µL RPMI + FCS + GLU was added to wells and incubated for 48 h to allow further cellular differentiation.

2.10.3 THP-1 cell viability

THP-1 cell viability was quantified using CellTiter Blue (Promega, Southampton, UK). Assay reagent was added to a final concentration of 10% v/v and incubated for 2 hours. Fluorescence was measured at excitation 530/25 nm and emission 590/35 nm in a Synergy HT plate reader.

2.11 Enzyme-Linked Immunosorbent Assay (ELISA)

Stimulated THP-1 supernatants were stored at -80°C and thawed shortly before ELISAs were performed. Cytokines were quantified in 96 well ELISA plates (ThermoFisher Scientific, Loughborough, UK).

2.11.1 IL-1β ELISA

ELISA plates were coated with 2 µg/mL primary antibody diluted in bicarbonate coating buffer and incubated overnight at 4°C. ELISA plates were washed once with wash buffer then blocked with 2% Bovine Serum Albumin (BSA) for 1 h at room temperature rocking at 25 RPM. ELISA plates were washed with wash buffer three times. Samples were diluted appropriately with 0.5% BSA in PBS, and a standard curve was generated by three fold dilutions of 10 pg/mL to 0.0137 pg/mL. 50 µL of samples and standards were added to ELISA plates in triplicate and incubated for 2 h at room temperature rocking at 25 RPM. ELISA plates were washed three times, 50 µL secondary antibody added to all wells and incubated for 1 h at room temperature rocking at 25 RPM. ELISA

plates were washed three times and 50 µL streptavidin horse radish peroxidase (HRP) added to all wells and incubated for 1 h at room temperature rocking at 25 RPM. ELISA plates were washed six times, 50 µL of the HRP substrate tetramethylbenzidine (TMB) microwell peroxidase solution (KPL, Gaithersburg, MD) was added to all wells and monitored until the fourth standard (0.37 pg/mL) becomes visible. 50 µL stop buffer was added to all wells, and absorbance measured at 450 nm in a Synergy HT plate reader.

2.11.2 TNF-α ELISA

ELISA plates were coated with 4 µg/mL primary antibody diluted in PBS pH 7.4 and incubated overnight at 4°C. ELISA plates were washed three times with wash buffer then blocked with 1% Bovine Serum Albumin (BSA) diluted in PBS pH 7.4 for 1 h at room temperature rocking at 25 RPM. ELISA plates were washed three times. Samples were diluted appropriately with 1% BSA in PBS pH 7.4, and a standard curve was generated by two-fold dilutions of 1000 pg/mL to 15.6 µg/mL. 50 µL of samples and standards in triplicate were added to ELISA plates and incubated for 2 h at room temperature rocking at 25 RPM. ELISA plates were washed six times, 50 µL secondary antibody added to all wells and incubated for 2 h at room temperature rocking at 25 RPM. ELISA plates were washed six times and 50 µL streptavidin horse radish peroxidase (HRP) added to all wells and incubated for 30 min at room temperature rocking at 25 RPM. ELISA plates were washed six times, 50 µL of the HRP substrate tetramethylbenzidine (TMB) microwell peroxidase solution (KPL, Gaithersburg, MD) was added to all wells and incubated for 20-30 min at room temperature rocking at 25 RPM. After this final incubation, 50 µL stop solution was added to all wells, and absorbance measured at 450 nm in a Synergy HT plate reader with wavelength correction of 540 nm.

2.12 Statistical analysis

All statistical analysis were performed in GraphPad 6. T-tests were used to compare the means of single test groups to single control groups. If multiple comparisons were required, a one-way ANOVA was performed with a post-test to compare the means of each possible pair of samples. For transcriptional profiling, Benjamini-Hochberg multiple testing correction was applied to p values derived from t-tests between probe signatures.

Chapter 3: Optimisation of the Rotary Cell Culture System (RCCS) for low shear, biofilm culture of *M. bovis* BCG

3.1 Overview

Several *in vitro* models have been developed to investigate antimicrobial tolerance in *Mycobacterium tuberculosis*. The Wayne Model reasoned that hypoxic conditions across a TB granuloma would induce differential metabolic states in bacilli present in the lesion that were dependent on the amount of O2 present. Two metabolic states were identified in this model, NRP1 and NRP2, that exhibited differential responses to isoniazid and metronidazole that was dependent on the extent of anaerobic metabolism present (Wayne and Hayes 1996). This study demonstrated eloquently how the drug tolerance phenotype of *M.tb* depended on the O_2 gradient of their environment, as INH was most efficacious against actively growing bacilli, while MTZ only targeted anaerobic bacilli.

Variation in O_2 saturation was shown *in vitro* to induce a differential antimicrobial response in *M.tb* (Wayne and Hayes 1996). Although hypoxia is often present within a tuberculous granuloma (Duque-Correa, Kuhl et al. 2014), other environmental factors such as nutrient starvation have also been shown to induce drug tolerance in *M.tb*. Betts *et al* (Betts, Lukey et al. 2002) modelled nutrient starvation in *M.tb* by re-suspending log phase cultures in phosphate buffered saline (PBS) for six weeks and treating these cultures with INH and MTZ. Nutrient-starved cultures showed increased tolerance to INH compared to log phase controls, however MTZ had no effect on either nutrient starved or log phase control cultures. The latter is expected, as MTZ requires an anaerobic environment to be effective against bacteria.

Both the Wayne model and Nutrient Starvation model result in varying degrees of antimicrobial tolerance through hypoxia and nutrient starvation respectively. This shows how antimicrobial tolerance in mycobacteria can be induced by more than one environmental stress, suggesting that a number of environmental factors, alone or in combination, within the tuberculous lung could be responsible for generating sub-populations of *M.tb* tolerant to chemotherapy. Few models however have investigated the role of mycobacterial biofilm formation in the context of antimicrobial phenotypes.

Some species of mycobacteria exhibit a propensity to grow in long rope or cord-like structures that leads to progressive cell aggregation and biofilm formation through a

process known as cording (Caceres, Vilaplana et al. 2013). While strains such as *M.tb* and *M. bovis* BCG readily exhibit this cording phenomenon when cultured *in vitro*, the role of cording and subsequent biofilm formation *in vivo* in the pathogenesis of human TB is less clear. During the 1930s, a clinical isolate of *M.tb* named H37 was serially passaged on various media types to differentiate this *M.tb* H37 isolate into an avirulent variant now designated H37Ra and a variant that retained its virulence, designated H37Rv (Steenken, Oatway et al. 1934). Interestingly, the avirulent variant displayed an altered colony morphology to H37Rv and failed to exhibit cording that was normally seen in the original *M.tb* H37 strain and H37Rv variant (Middlebrook, Dubos et al. 1947). Various groups in the following decades have investigated the effects of this H37Ra variant *in vivo* and demonstrated that the variant lacking a cording phenotype had decreased virulence in rabbit, guinea pig (Steenken, Oatway et al. 1934) and mouse (Larson and Wicht 1964) animal models, yet could still infect macrophages but failed to replicate within this intracellular environment (McDonough, Kress et al. 1993).

During the 1950s, Hubert Bloch and colleagues (Noll, Bloch et al. 1956) identified a membrane associated lipid called “cord factor” that was later identified as trehalose 6,6′-dimycolate (TDM). TDM was subsequently found to play a wide and varied role in the pathogenesis of *M.tb*; it is found in virulent but not avirulent strains of *M.tb* and is directly responsible for cording morphology (Bloch 1955); it enhances disease severity in both acute and chronic mouse models of TB (Bloch and Noll 1955) and removal of TDM from bacilli in *M.tb* abrogated their capability to survive within macrophages (Indrigo, Hunter et al. 2002). Meanwhile, Georges Canetti built upon the *in vivo* data obtained in animal models by providing direct evidence of *M.tb* cording in human sputa through micrographs, stating that “the caseum was full of colonies of bacilli” (Canetti 1955). Mitchison and Jindani (Jindani, Dore et al. 2003) investigated the sterilising activities of TB chemotherapy through enumeration of serial colony counts from patient sputa from day 0 (treatment naive) through 14 days of drug therapy. Reduction in bacillary load decreased sharply until day four, then continued to decline at a much slower rate. This bi-phasic kill curve suggested that *M.tb* present in the human lung during an active infection consisted of sub-populations that had varied phenotypic antimicrobial tolerance; it has now been established that INH has a bactericidal effect on rapidly growing, metabolically active bacilli killing rapidly in the first few days of treatment and a bacteriostatic effect on slow metabolising, non-dividing bacilli (Yamori, Ichiyama et al. 1992), (Ahmad, Klinkenberg et al. 2009). It is these latter antimicrobial tolerant or “persister”-like sub-populations of bacilli present in an active pulmonary TB

infection that are likely responsible for the long (six month) chemotherapy regimen required to effectively treat active TB (Mitchison 2004).

The aim of this chapter was to develop and optimise a novel culture method for *Mycobacterium bovis* BCG to mimic biofilm-like growth in the tuberculous human lung using a low shear *in vitro* culture model, the Rotary Cell Culture System (RCCS). Optimisation of this model will facilitate characterisation of antimicrobial responses of biofilm derived-bacilli, transcriptomics and pathogen-host interaction studies.

3.2 The Rotary Cell Culture System

The Rotary Cell Culture System (RCCS) was originally developed by the National Aeronautics and Space Administration (NASA) to investigate the *in vitro* effects of low-shear microgravity on human tissues, but has been repurposed for various tissue culture studies over the past 25 years (Gardner and Herbst-Kralovetz 2016). Viral and bacterial pathogen-host studies have been conducted using low shear culturing (Crabbe, Liu et al. 2017; Higginson, Galen et al. 2016; Gardner and Herbst-Kralovetz 2016) as well as a plethora of human tissue remodelling projects (Crabbe, Liu et al. 2015; Teo, Mantalaris et al. 2014). The RCCS has not been applied to mycobacterial culture prior to this thesis.

The RCCS consists of a central vertical support with four motors that facilitate the attachment of up to four RCCS 10 mL bioreactor vessels. Attached vessels' RPMs can be individually adjusted from zero to 15 RPM through a central control interface, Figure 3.1. The vertical support can be placed in an incubator while the central control interface remains external to the RCCS due to a two-metre connection cable. Single use bioreactor vessels, Figure 3.2, are transparent acrylic vessels with a semi-permeable membrane on the back that facilitate diffusion of gases such as O_2 and CO_2 between vessel cultures and the incubator atmosphere. A low-shear environment is generated when vessels are inoculated with media and bacilli at a specific RPM, Figure 3.3. Turbulence is minimised through removal of air bubbles, while bacilli are kept in suspension, or "freefall", as the rotation of the vessel counteracts the drag force of gravity via centrifugal and Coriolis forces (Hammond and Hammond 2001).

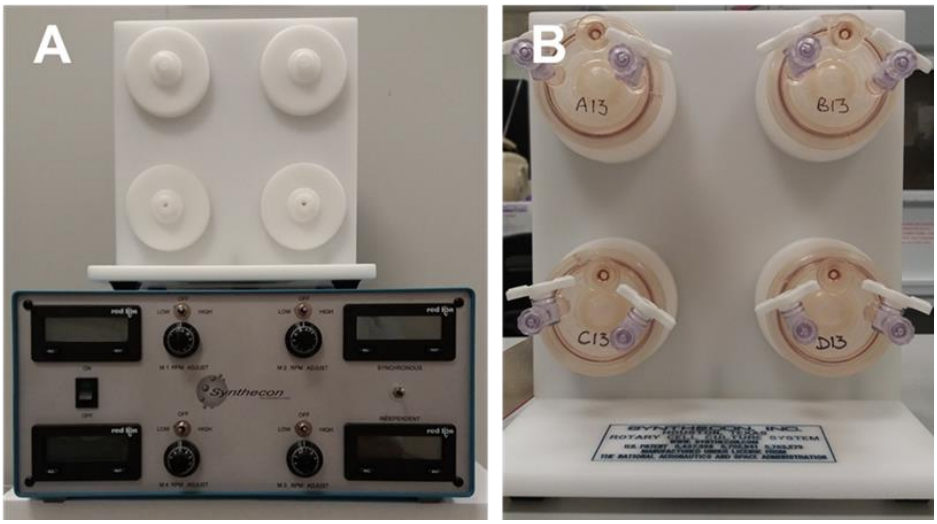

Figure 3.1: The Rotary Cell Culture System (RCCS)

(A) RCCS vertical support placed on top of the central control interface that controls the four motors' RPM independently of each other. Four screens display the tachometer value for each vessel; (B) The RCCS vertical support with four single use 10 mL bioreactor vessels attached.

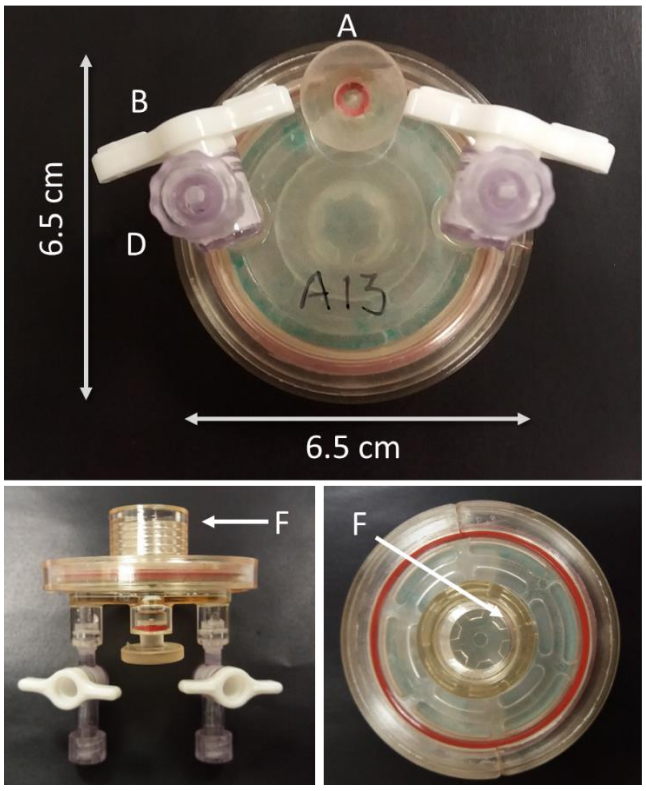

Figure 3.2: A 10 mL RCCS vessel

(A) Large outlet port for harvesting cultures; (B) In port butterfly valve; (C) Out port butterfly valve; (D) In port valve for addition of media; (E) Out port valve for removal of air bubbles; (F) RCCS attachment point. The semi-permeable membrane is visible when the reverse of the vessel is viewed.

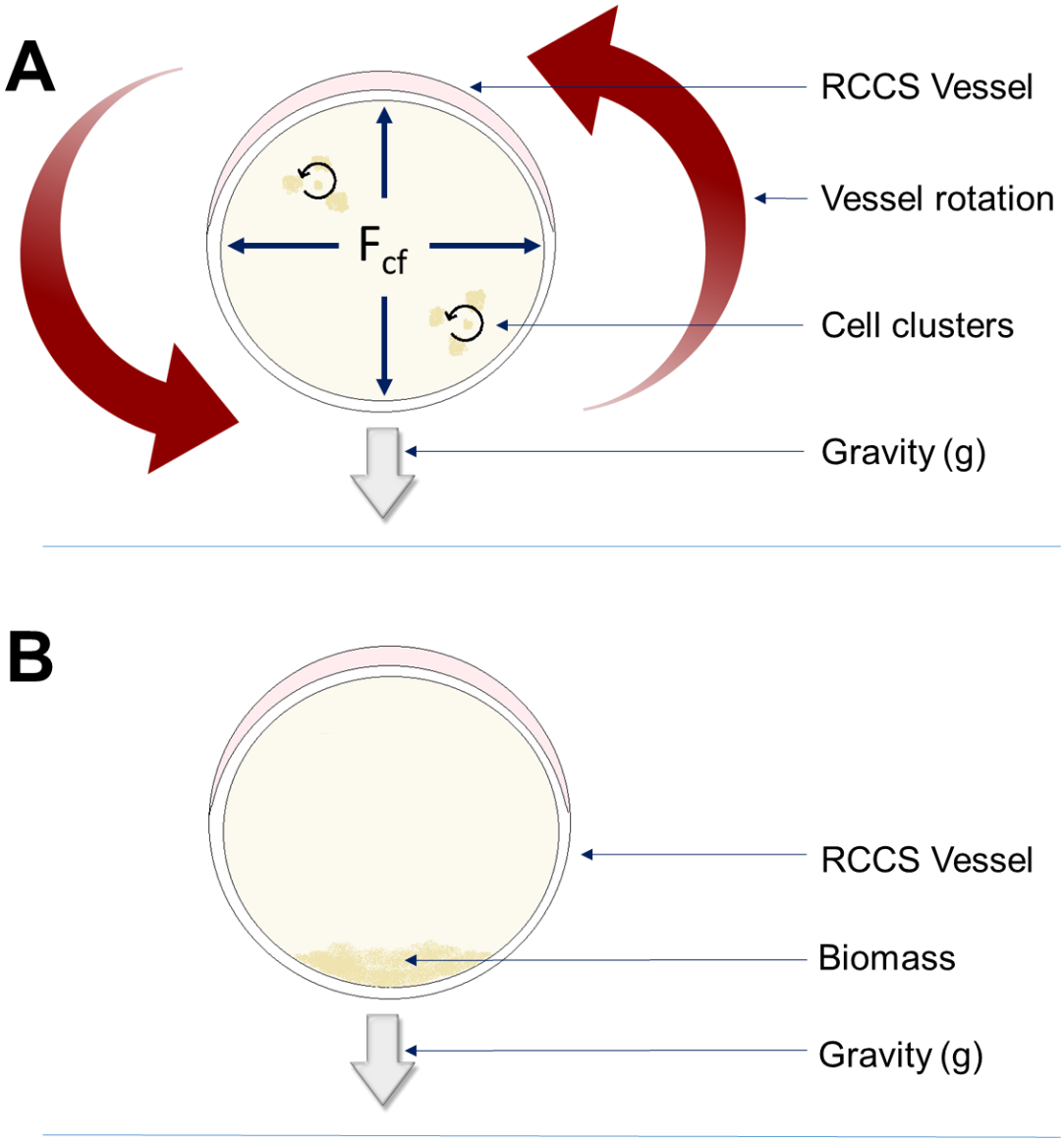

Figure 3.3: Biomass accumulation in the RCCS

(A) In a rotating vessel biofilms are formed over 21 days through *M. bovis* BCG clumping into cell clusters that are held in suspension through control of rotating vessels' RPM. F_{cf} denotes centrifugal force due to rotation. (B) In a non-rotating vessel *M. bovis* BCG biomass accumulates in the base of the stationary vessel over the course of 21 days.

3.2.1 Strain Selection for RCCS inoculation

M. bovis BCG was selected for culture in the RCCS due to a number of experimental and biosafety considerations compared to virulent *M. tuberculosis*, discussed below.

3.2.1.1 *M. bovis* BCG and *M. tuberculosis* are both slow growing mycobacteria

Both *M. bovis* BCG and *M.tb* are slow growing mycobacteria with their doubling times established experimentally in static 7H9 broth aerobic cultures as 22.3 hours and 25.6 hours respectively (Materials and Methods section 2.2.2.). Figures 3.4 and 3.5 show growth curves of *M. bovis* BCG and *M.tb* H37Rv measured by $O.D._{600nm}$ and colony forming units (CFU). Figures 3.6 and 3.7 show exponential phase growth parameters of *M. bovis* BCG and *M.tb* H37Rv, including doubling time. Bacterial growth in batch culture requires several environmental requisites; (i) a viable inoculum capable of replication, (ii) absence of growth inhibitors, (iii) appropriate culture conditions such as temperature, (iv) nutrients required to facilitate biomass synthesis, and (v) an energy source (Prescott 2005). If these conditions are met, then it is expected that biomass will experience a logarithmic growth phase where biomass doubles during a specified time interval known as doubling time, or T_d. The basic measure of this exponential growth is the "specific growth rate", or μ. μ must first be calculated to establish the T_d of bacterial strains in exponential growth.

The growth parameters μ and T_d were calculated for *M. bovis* BCG and for *M. tuberculosis* H37Rv, Figures 3.6 and 3.7. Values were derived from exponential growth between a starting $O.D._{600\ nm}$ value (X_0) and another $O.D._{600\ nm}$ value (X) that is still within exponential growth. Taking the time (T) between these two data points and factoring in natural log for exponential growth, the specific growth rate μ can be calculated using the following formula:

$$\mu = \frac{\ln\left(\frac{X}{X0}\right)}{t}$$

Formula 1

Calculation of the specific growth rate constant (μ) of a logarithmic bacterial population.

The bacterial population has doubled when $X = 2X_0$. Using μ calculated from formula 1, the doubling time (T_d) can be quantified using formula 2:

$$td = \frac{ln2}{\mu}$$

Formula 2

Calculation of the doubling time (T_d) of a logarithmic bacterial population.

As ln of 2 is a constant and will not change in value, Formula 2 can be written as:

$$Td = \frac{0.693}{\mu}$$

Formula 3

Calculation of the doubling time (T_d) of a logarithmic bacterial population.

Similar growth kinetics of *M. bovis* BCG and *M. tuberculosis* is important if *M. bovis* BCG is to be a representative biofilm model for *M.tb.* This enables minimal re-optimisation of inoculation procedure, incubation conditions, media replacement and length of incubation for future use with *M. tuberculosis*.

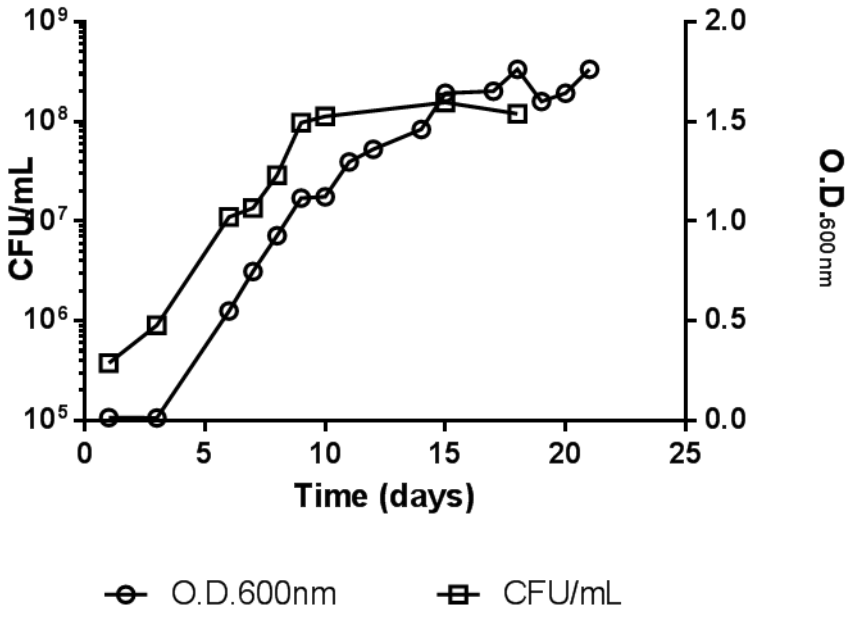

Figure 3.4: Growth curve of *Mycobacterium bovis* BCG

Growth was measured by CFU/mL (square) and O.D.600nm (circle) of 50 mL cultures in vented 250 mL Erlenmeyer flasks incubated statically up to 21 days. An n=1 was used for this growth curve.

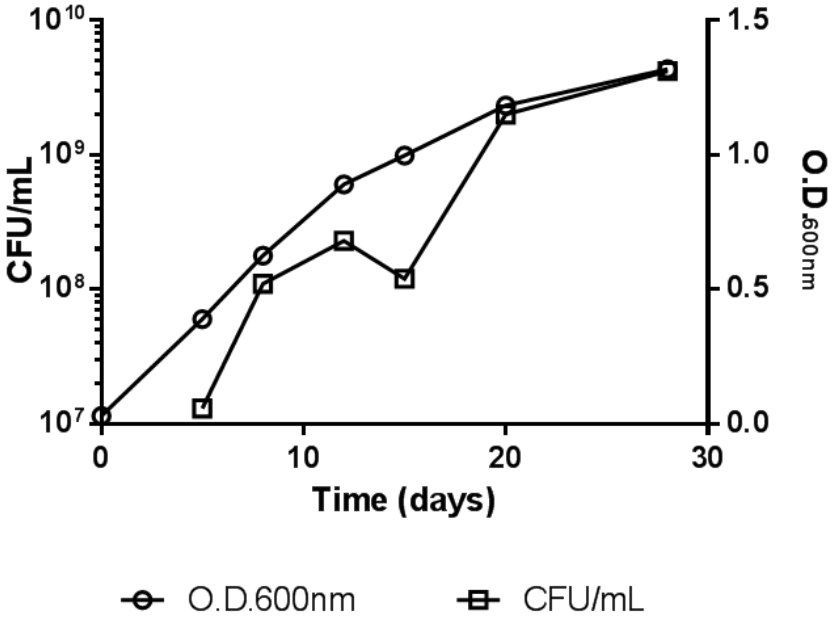

Figure 3.5: Growth curve of *Mycobacterium tuberculosis* H37Rv

Growth was measured by CFU/mL (square) and O.D.600nm (circle) of 50 mL cultures in vented 250 mL Erlenmeyer flasks incubated statically up to 21 days. An n=1 was used for this growth curve.

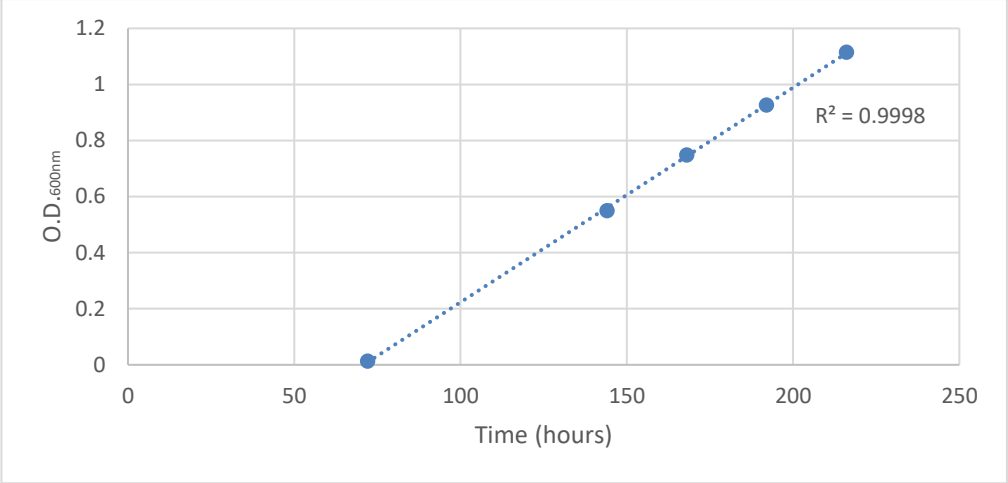

M. bovis BCG growth parameters						
X_0	X	t (hours)	X/X_0	$\ln(X/X_0)$	μ (hours)	T_d (hours)
0.013	1.150	144	88.46	4.480	0.030	22.3

Figure 3.6: Growth parameters of *M. bovis* BCG

Exponential growth curve of a static aerobic culture (n=1) of *M. bovis* BCG in 7H9 broth was used to calculate growth parameters including doubling time (T_d) of 22.3 hours.

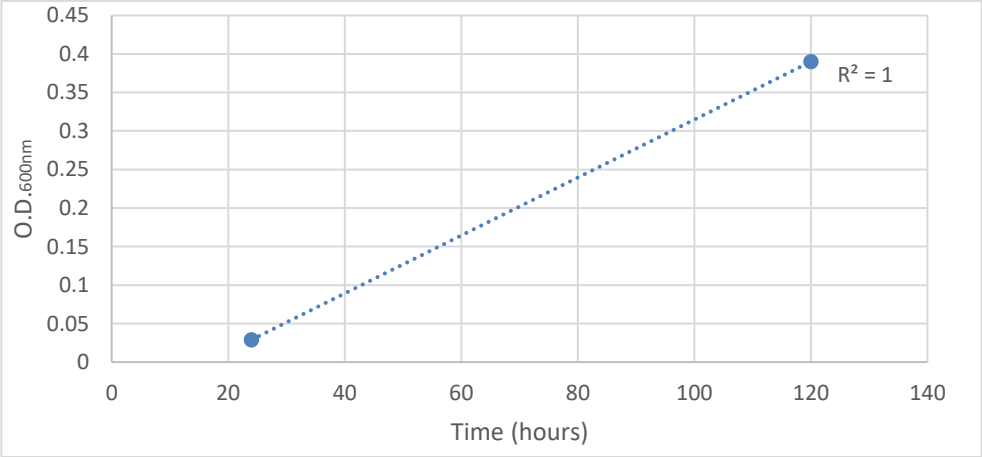

M. tuberculosis H37Rv growth parameters						
X_0	X	t (hours)	X/X_0	$\ln(X/X_0)$	μ (hours)	T_d (hours)
0.029	0.390	96	13.45	2.600	0.027	25.6

Figure 3.7: Growth parameters of *M.tb*

Exponential growth curve of a static aerobic culture (n=1) of *M. tuberculosis* H37Rv in 7H9 broth was used to calculate growth parameters including doubling time (T_d) of 25.6 hours.

3.2.1.2 *M. bovis* BCG and *M. tuberculosis* exhibit similar drug sensitivities

Both strains exhibit similar sensitivity to key drugs including isoniazid (INH), rifampicin (RIF), ethambutol (EMBU) and aminoglycosides such as streptomycin (STREP). Table 3.1. These values were taken from the literature and were established using a microbroth dilution method (Hurdle, Lee et al. 2008). This is the same AST methods used in this thesis as described in Materials and Methods section 2.5.

Antimicrobial	**Minimum Inhibitory Concentration [µg/mL]**	
	M. bovis BCG Pasteur	*M. tuberculosis* H37Rv
Isoniazid	0.05	0.024
Rifampicin	0.012	0.024
Ethambutol	0.8	0.8

Table 3.1: Minimum Inhibitory Concentrations of antimicrobial drugs for *M. bovis* BCG and *M. tuberculosis*

MIC values were established for both strains using a liquid microbroth dilution method with bacterial growth judged visually. MIC values taken from (Hurdle, Lee et al. 2008).

Similar antimicrobial drug susceptibility for *M. bovis* BCG compared to *M. tuberculosis* H37Rv was important, as RCCS-derived cultures will be tested with clinically relevant antimicrobial drugs used to treat tuberculosis.

3.2.1.3 *M. bovis* BCG and *M. tuberculosis* share high genomic and proteomic similarity

Both strains are members of the *Mycobacterium tuberculosis* complex (MTBC) and as such share high genome and proteome similarities. The *Mycobacterium tuberculosis* complex (MTBC) is a group of slow growing mycobacterial species that are closely related at the DNA sequence level that cause TB in humans or other mammals and includes *M. tuberculosis*, *M. bovis* and *M. bovis* BCG (Brosch, Gordon et al. 2002; Cousins, Bastida et al. 2003; Kubica, Rusch-Gerdes et al. 2003). *M. bovis* BCG however rarely causes disease, e.g. where individuals possess IL-12 or TNF-α production disorders that increase their susceptibility to mycobacterial infections (Nalepa, Strach et al. 2011). Both *M. bovis* BCG and *M. tuberculosis* H37Rv share

99.9% of their genome (Brosch, Gordon et al. 2007). Key differences between these strains have led to a loss of virulence in *M. bovis* BCG, such as the deletion of the virulence factor ESX-1 secretion system (Harboe, Oettinger et al. 1996) and attenuation of the PhoP/PhoR two component transcription regulator system that is required for intracellular replication of bacilli (Martin, Williams et al. 2006).

3.2.1.4 *M bovis* BCG is avirulent

One of the main advantages of using *M. bovis* BCG for culture in the RCCS is that this strain can only rarely cause disease and even then would require a genetic predisposition or an immune-compromising condition. It is the live, attenuated vaccine strain that is used to vaccinate over 100 million neonates annually (Harris, Dodd et al. 2016). For this reason, laboratory research can be carried out in a Biosafety Laboratory 2 facility with appropriate risk assessments and occupational health screening, whereas *M. tuberculosis* H37Rv research requires a Biosafety Level 3 facility as it is a virulent air-borne pathogen. The RCCS requires unrestricted access to a humidified incubator environment to allow for gaseous exchange; incubation of an *M.tb* RCCS in a BSL3 laboratory would require the RCCS to be placed in secondary containment that could impact on this gaseous exchange and access to a balanced humidified atmosphere.

3.2.2 Incubation conditions

The RCCS was incubated in a static incubator at 37°C that was kept humidified with an open source of water in the base of the incubator. The incubator was only opened when necessary to inspect the RCCS so as to maintain incubator humidity at a constant rate; due to the semi-permeable membrane of each vessel high transpiration rates of the media might occur if the incubator environment was not kept humidified. This could lead to volume loss and the generation of air bubbles, that could act as destructive shear forces on biofilms. No other organisms were incubated in the same incubator to reduce potential sources of contamination.

3.2.3 Media Selection

Dubos broth is a commonly used liquid media for mycobacterial culture, however this medium is specifically designed to disperse bacilli within culture, which would be inhibitory to biofilm formation in the RCCS and thus was discounted as a potential medium. 7H9 broth is a complex, nutrient-rich media specifically developed for mycobacteria. 7H9 broth is a powder that is reconstituted with distilled water and Tween 80 to prevent clumping of bacilli, autoclaved and albumin, dextrose and catalase (ADC) added after sterilisation. As it is a pre-formulated powder, it is not possible to omit specific components of 7H9 broth such as pyridoxine, biotin, or any of the large number of inorganic salts present, Table 3.2. Therefore, Sauton's Modified Media, a minimal media formulated component by component in the laboratory, was selected for the RCCS model, Table 3.3. This medium is more adaptable than 7H9 broth for a number of reasons; each individual component of this minimal media can be omitted entirely or added in increased ratios to other components; the carbon source can be easily modified based on experimental requirements, e.g. selecting cholesterol instead of glycerol; the pH of Sauton's Modified Media can also be adjusted to a more acidic or basic pH as required; Sauton's Modified Media does not require addition of exogenous protein such as albumin that could ameliorate biofilm formation or interfere with downstream RCCS supernatant experiments and L-asparagine is a key nitrogen source for *M.tb* virulence *in vivo* and is present in Sauton's Modified Media but not 7H9 broth (Gouzy, Larrouy-Maumus et al. 2014). Previous research by Ojha et al. has shown that iron is required for biofilm formation in *M. smegmatis*, and Sauton's Modified Media contains iron in the form of ferric ammonium sulphate (Ojha and Hatfull 2007). Sauton's Modified Media, pH 7.2 was selected as the media for culturing *Mycobacterium bovis* BCG in the RCCS using glycerol as a carbon source. Importantly, Tween 80, used to reduce clumping in mycobacterial cultures, was omitted from the RCCS enabling biofilm formation in the absence of detergent.

7H9 broth	*Component*	*Amount required*
Requisite components	Ammonium Sulphate	0.5 g
	L-Glutamic Acid	0.5 g
	Sodium Citrate	0.1 g
	Pyridoxine	1.0 mg
	Biotin	0.5mg
	Disodium Phosphate	2.5 g
	Monopotassium Phosphate	1.0 g
	Ferric Ammonium Citrate	0.04 g
	Magnesium Sulphate	0.05 g
	Calcium Chloride	0.5 mg
	Zinc Sulphate	1.0 mg
	Copper Sulphate	1.0 mg
	Sodium Chloride	8.5 g
Optional components	Albumin (Bovine Fraction V)	50.0 g
	Dextrose	20.0 g
	Catalase	0.03 g
	Glycerol	400 µL

Table 3.2: 7H9 broth composition

The composition of pre-formulated 7H9 broth (Becton Dickinson) when made up to 1 L with distilled water. Requisite components are present in 7H9 broth powder. Optional components are not present in 7H9 broth, with Tween 80 or glycerol added before autoclaving and ADC added after autoclaving media.

Sauton's Modified Media	*Component*	*Amount required*
Optional components	Potassium Phosphate (monobasic)	0.5 g
	Magnesium Sulphate	0.5 g
	L-Asparagine	4.0 g
	Ferric Ammonium Citrate	0.05 g
	Citric Acid	2.0 g
	Glycerol	60 mL
	1% Zinc Sulphate Solution	100 µL
	10 M NaOH	to pH 7.2

Table 3.3: Sauton's Modified Media composition

The composition of Sauton's Modified Media when made up to 1 L with distilled water. Individual components can be altered or omitted from Sauton's Modified Media as required.

3.3 Inoculation of the RCCS

3.3.1 Vessel Preparation

Four vessels were incubated over night with sterile PBS to equilibrate before addition of media. Insufficient equilibration with PBS would lead to rapid media evaporation within the first two days through the semi-permeable membranes. Two vessels were rotated (labelled “A” and “B”) for biofilm formation and two vessels were left static, acting as controls (labelled “C” and “D”). The number added after each letter corresponds to the RCCS run, e.g. A1 is a rotating vessel from the first RCCS run; C5 is a control vessel from the fifth RCCS run. This nomenclature is maintained throughout this thesis. Thirteen RCCS runs were performed in total.

3.3.2 Inoculum Selection and preparation

Three different inoculation trains (sequence of cultures before inoculating the RCCS) were tested before a standard operating procedure was selected, Figure 3.8.

1. 1 mL *M. bovis* BCG glycerol frozen stocks (containing 10^7 CFU/mL) was diluted with 100 mL Sauton’s Modified Media no Tween to yield 10^5 cells and used to immediately inoculate the RCCS directly, Figure 3.8A. A lag phase of at least 12 days was observed before visible biomass started to form in the RCCS.

2. 1 mL *M. bovis* BCG glycerol frozen stock was passaged into 10 mL 7H9 broth + ADC, Tween 80 for 7 days, then diluted with 100 mL Sauton’s modified media no Tween and used to inoculate the RCCS, Figure 3.8B. Again, a lag phase of at least 10 days was observed before visible biomass started to form in the RCCS.

3. This inoculum train was repeated but with an additional passage into 10 mL Sauton’s Modified Media no Tween after the 7H9 broth + ADC, Tween 80 passage, Figure 3.8C. Biomass could be observed to grow in the RCCS before or at day six. However, cells may not have been distributed equally between RCCS vessels; since the final passage into 10 mL Sauton’s Modified Media did not contain Tween 80 the culture contained bacilli in a clumped and corded state that could not be easily adjusted for $O.D._{600nm}$. The inoculum train optimised to inoculate the RCCS was 1 mL glycerol frozen stock of *M. bovis* BCG passaged for 7 days in two passages in 7H9 broth, followed by two consecutive passages in Sauton’s Modified Media + 0.05% Tween. Finally, this culture of *M. bovis* BCG was diluted to 100 mL volume with Sauton’s

Modified Media no Tween to an $O.D._{600nm}$ of 0.05-0.06 (corresponding to $3x10^5$ CFU/mL, Figure 3.4). This was used to directly inoculate RCCS vessels so that each vessel had $3x10^6$ *M. bovis* BCG total per 10 mL media added, Figure 3.9.

An inoculum containing 100X more *M. bovis* BCG was also used to inoculate the RCCS to investigate if a higher inoculum facilitated biofilm formation with less incubation time. $3x10^7$ CFU/mL bacilli or $3x10^8$ bacilli per total vessel volume was used to inoculate the RCCS as per Figure 3.9. Growth was monitored visually to assess bacterial growth and biofilm formation. By day 14 of incubation, no biofilms had formed in suspension as rotating vessels were dense with *M. bovis* BCG, and bacilli had adhered to the walls of the vessel. Following this failed RCCS, 10^5 CFU/mL (or 10^6 CFU per total vessel volume) was used for all further RCCS runs.

3.3.3 Media Replacement

Vessels were inspected daily for the presence of air bubbles that could physically shear biofilms that were forming. Sauton's Modified Media no Tween 80 was added to vessels to remove bubbles if present. When removing air bubbles, media was added to the rotating (biofilm) and control (stationary) vessels in equal volumes to prevent nutrient imbalance across duplicate vessels.

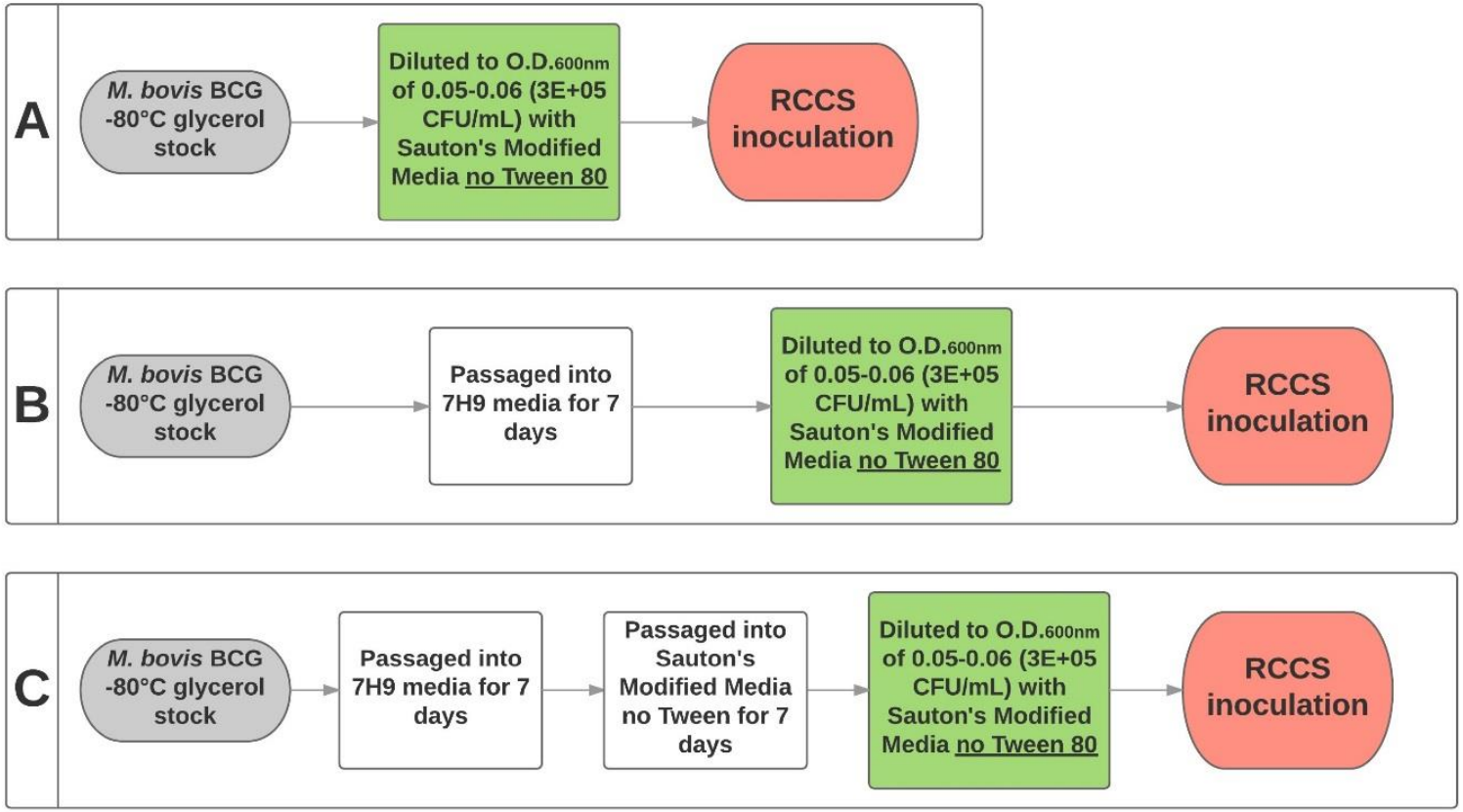

Figure 3.8: Optimisation of inoculum trains for the RCCS

(A) glycerol stock diluted with Sauton's Modified Media no Tween 80; (B) one 7 day passage in 7H9 ADC broth before dilution with Sauton's Modified Media no Tween; (C) one 7 day passage in Sauton's Modified Media no Tween 80 after 7H9 ADC broth passage. All cultures were incubated statically at 37°C.

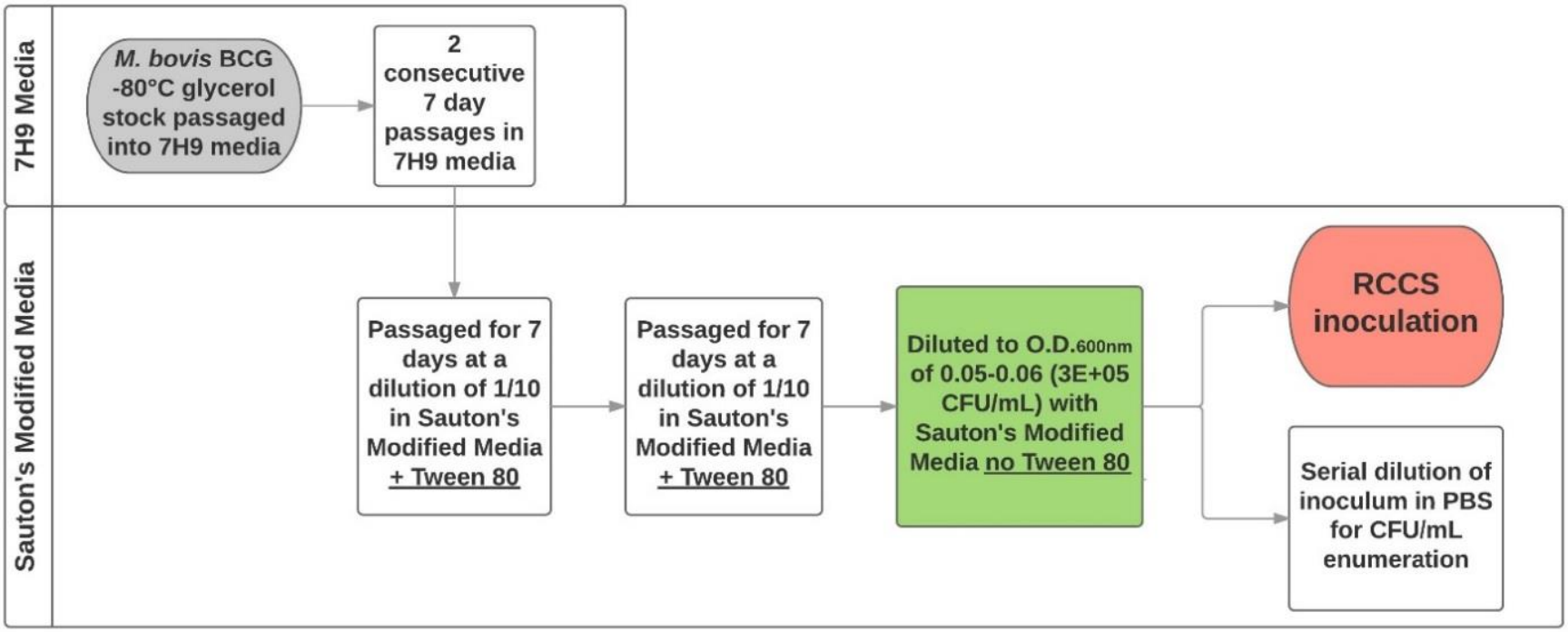

Figure 3.9: Final inoculum train for the RCCS

7H9 ADC broth and Sauton's Modified Media + Tween 80 contained 0.05% v/v Tween 80. All cultures were incubated statically at 37°C.

3.3.4 RCCS Rotation Speed

Control vessels were kept stationary throughout. Biofilm vessels' RPM were assessed daily with rotation speeds ranging from zero to 15 RPM. Rotating vessels were rotated at 15 RPM initially and decreased in accordance with biofilm formation to keep the cell clusters in suspension. Reduction of the RPM was necessary to balance the centrifugal force exerted by rotating vessels on biofilms, which would force clusters to the rim of the vessel, exposing them to potentially destructive shear forces.

Daily monitoring of the RCCS was crucial to clean biofilm formation. Although biofilms always formed using this model, Figure 3.10, there were instances where this process did not occur as expected. For example, one vessel formed a ring-like structure, Figure 3.11A, and on another occasion cells fragmented into many smaller clusters despite the RPM being adjusted in an attempt to correct this, Figure 3.11B.

To view an MP4 video file of the RCCS after 21 days' incubation, please view "RCCS video 3.1", attached to the back cover of this thesis.

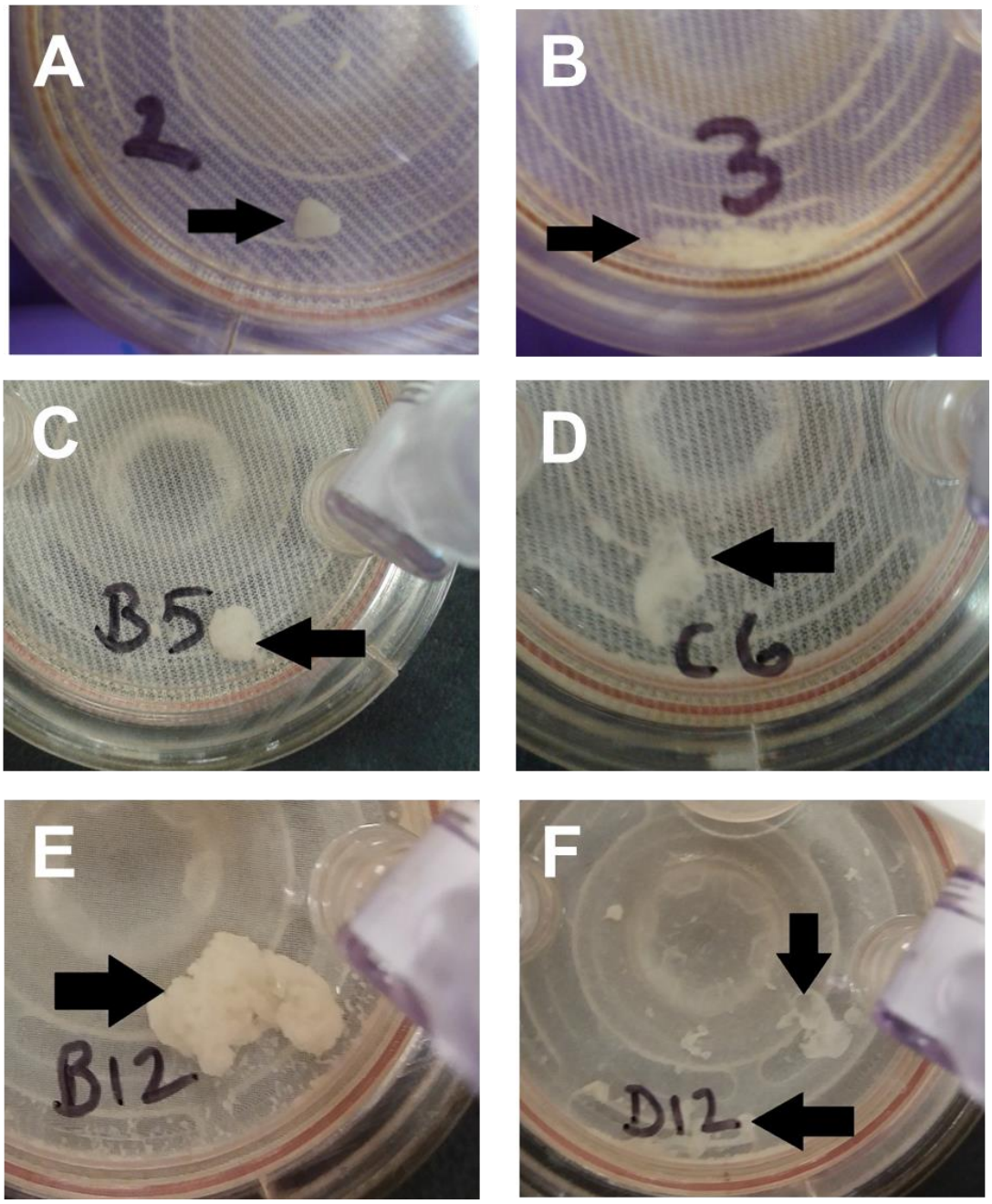

Figure 3.10: Representative images of *M. bovis* BCG biofilm and control growth in the RCCS over 21 days

Day 7 (A) biofilm formation or (B) control cultures; day 14 (C) biofilm formation or (D) control cultures; day 21 (E) biofilm formation (F) or control cultures. Control vessels (B, D, F) were agitated briefly for the purposes of imaging as biomass settled on the bottom of the vessel.

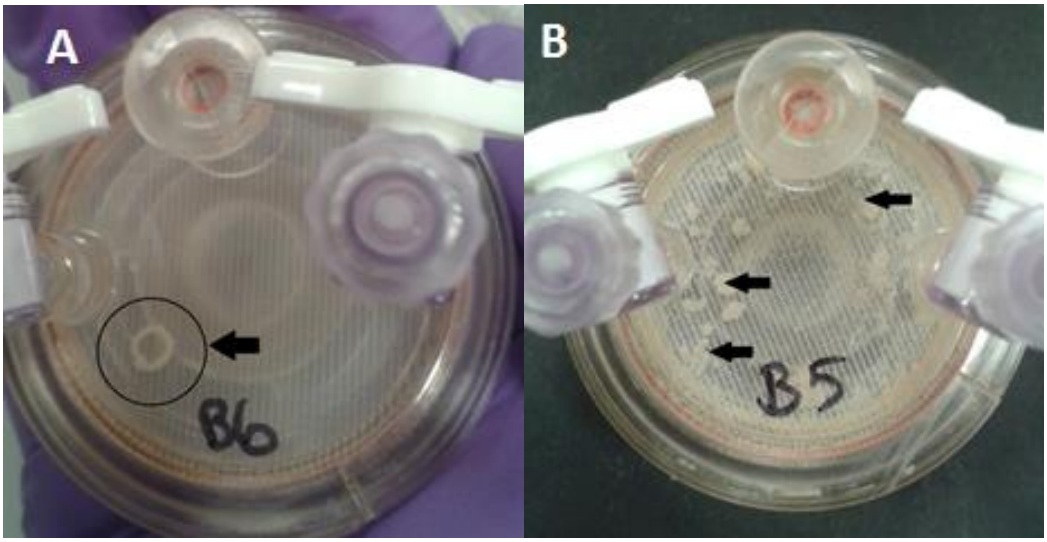

Figure 3.11: Unusual structures observed during rotation of the RCCS with *M. bovis* BCG

(A) a ring-like structure formed by day 5 in a rotating vessel (circled and highlighted with a black arrow); (B) a larger biofilm disaggregated into smaller cell clusters at day 15 with several of these highlighted by black arrows.

3.4 Harvesting of the RCCS

Cultures were removed from vessels using a 25 mL pipette through aperture of 1 cm in diameter that facilitates biofilm extraction without excessive shearing. Samples of all RCCS vessels harvested were plated onto LA agar, Blood Agar and Sabouraud agar plates and incubated at 37°C for up to five days to rule out bacterial and fungal contamination; Kinyoun staining was used to verify mycobacterial cultures (Materials and Methods section 2.9.1). 13 RCCS runs (26 biofilm and 26 control vessels; 52 vessels in total) were carried out during the course of this PhD with only one vessel identified as contaminated, Figure 3.12. In this instance, confluent bacterial growth was seen to grow on LA agar and Blood Agar after 48 hours incubation at 37°C degrees but the contaminant was not identified further.

The mycobacterial biofilm phenotype was characterised in comparison to static vessel growth using multiple techniques, Figure 2.1. It was not possible to conduct all methods simultaneously for every vessel due to the relatively small (<10 mL) volume of bacilli harvested.

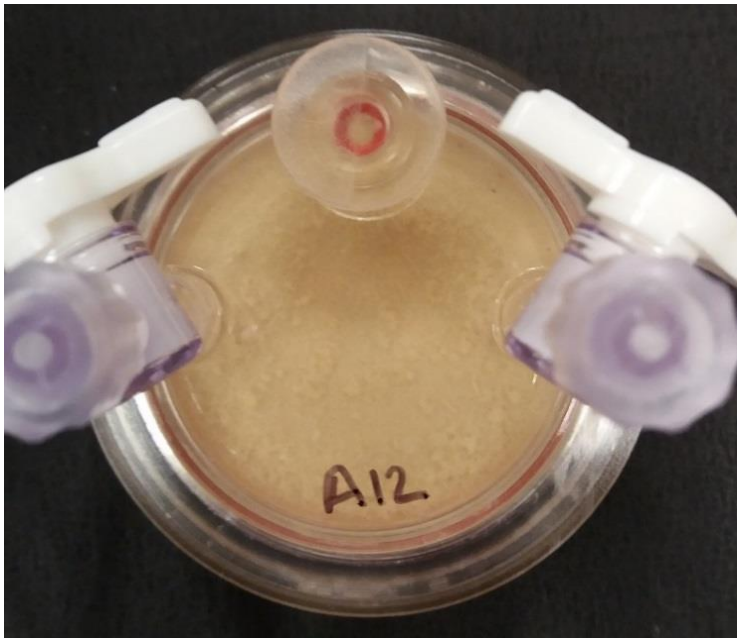

Figure 3.12: Contamination of a RCCS vessel after 21 days incubation

Image of a contaminated RCCS vessel. The LA agar-positive and Blood Agar positive contaminant. Contaminant was not identified.

3.4.1 Imaging of *M. bovis* BCG derived from the RCCS

3.4.1.1 Kinyoun Staining

The Kinyoun stain procedure comprises of a primary carbol fuschin dye that stains all cells red (Materials and Methods section 2.9.1). An acid alcohol wash removes this red dye from Gram negative and positive bacteria, but mycobacteria are resistant to this wash step and retain the red dye (mycobacteria are known as “acid-fast”). A secondary stain of Brilliant Green stains other cells green. The Kinyoun stain differs from the Ziehl Neelson stain in that heating is not required during the staining procedure.

Extensive corded structures were evident after 21 days incubation in biofilm-derived samples compared to control cultures, where single bacilli or small clumps were observed, Figure 3.13. These images represent the largest corded structures that were detectable after staining- it is likely that larger clusters of cells did not survive the washes and staining steps intact. Both biofilm and control cultures retained their acid-fastness after 21 days incubation in the RCCS.

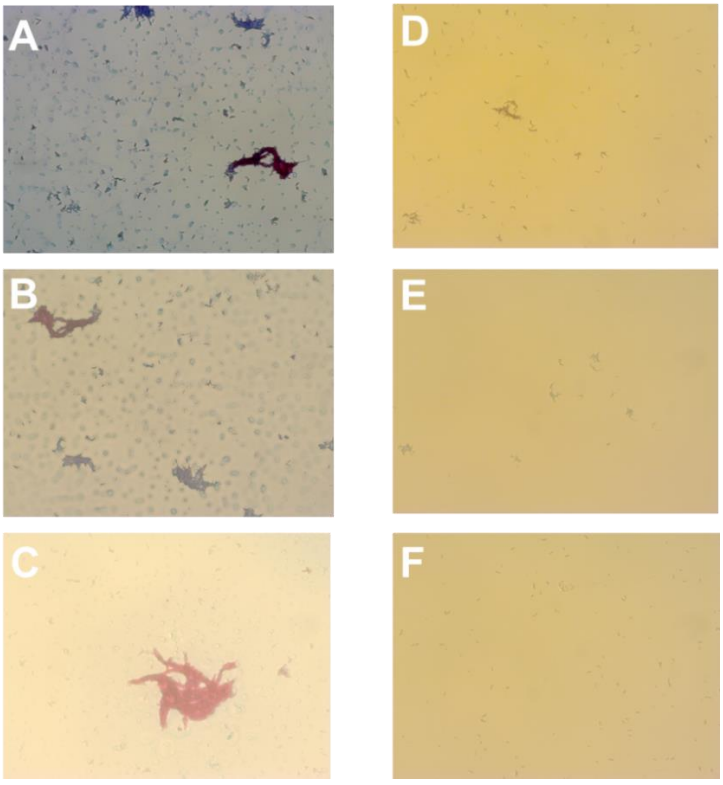

Figure 3.13: Kinyoun staining of *M. bovis* BCG biofilm and control cultures after 21 days’ culture in the RCCS

Non-homogenised biofilm (replicates A, B, C) and non-syringed control (replicates D, E, F) cultures after harvesting from the RCCS. Magnification of 40X, light microscope.

3.4.1.2 Scanning Electron Microscopy (SEM)

Scanning Electron Microscopy (SEM) allows detailed imaging of the topography and composition of a sample. SEM was conducted on RCCS-derived biofilm and control cultures after 21 days incubation in duplicate (Materials and Methods section 2.9.2).

Cluster derived cells were observed to have a complex convoluted surface area compared to the static controls, which appear as relatively flat surfaces. Biofilm-like clumps of bacteria presented as an uneven pockmarked surface where a greater extent of extracellular matrix was also apparent, Figure 3.14 C, D.

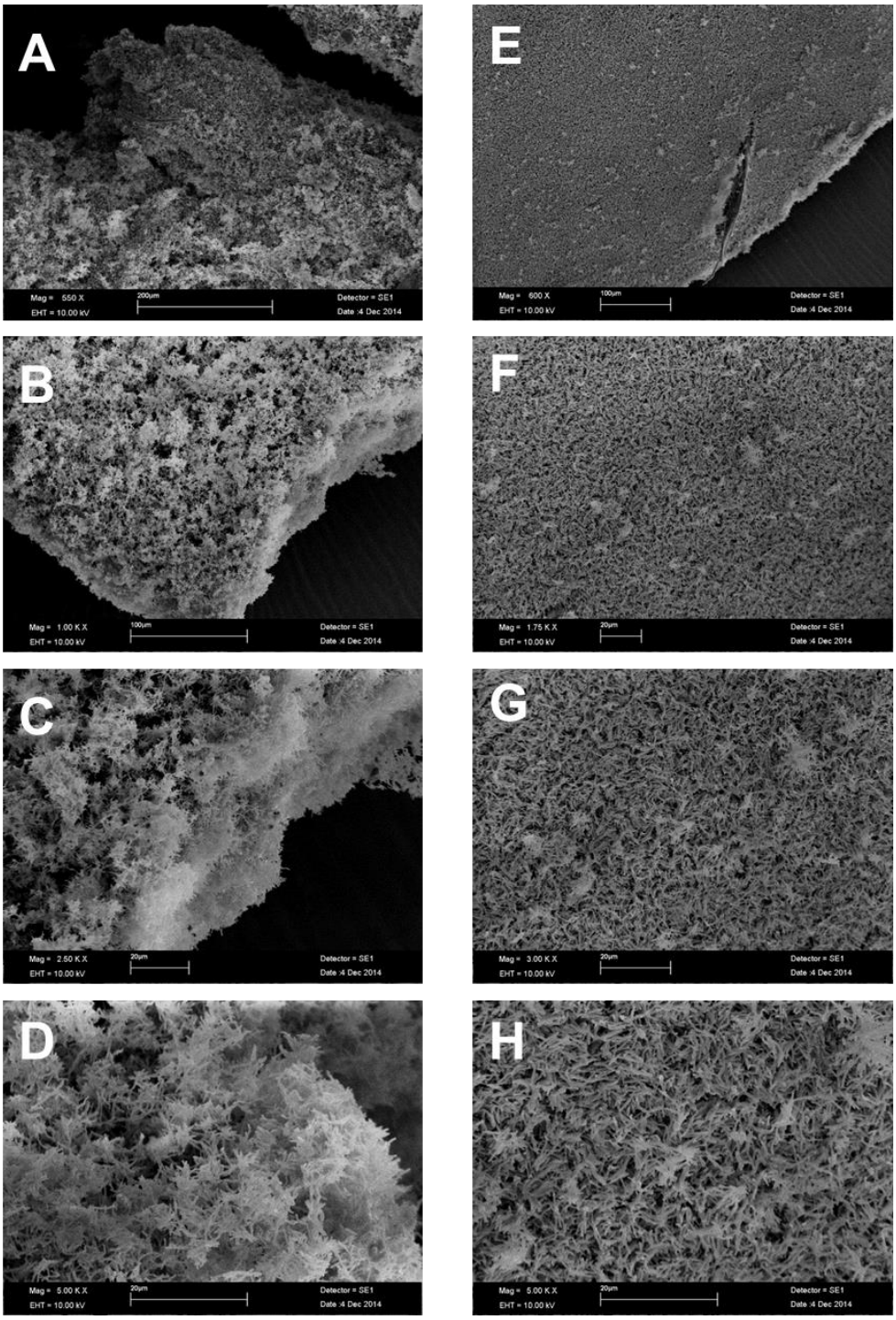

Figure 3.14: SEM images of biofilm (A, B, C, D) and control (E, F, G, H) cultures after 21 days incubation in the RCCS

Magnification and scale bar in µM are inset in each image legend. Biofilm or control cultures were not needle homogenised before imaging. Magnifications A (550X), B (1000X), C (2500X), D (5000X), E (600X), F (1750X), G (3000X), H (5000X)

3.4.1.3 Lipid body staining

Lipid body staining is a fluorescent dual stain that facilitates the visualisation of intracellular lipid bodies (Materials and Methods section 2.9.3). RCCS biofilm and control-derived bacilli taken from the RCCS at days 7, 14 and 21 were lipid body stained. It was not possible to visualise lipid bodies in either biofilm or control derived bacilli. Lipid body staining was repeated but with 7 day old *M. smegmatis*, an organism known to contain profuse lipid bodies at this stage of growth (Personal correspondence with Dr Natalie Garton). It was not possible to visualise lipid bodies, suggesting that the issue was technical- either operator error or an issue with reagents. RCCS biofilm and control samples were stored at -70°C to be stained for lipid bodies at a later date at the University of Leicester with Dr Natalie Garton. It was not possible to perform this staining before the submission of this thesis.

3.5 Oxygen tension in the RCCS

The aim of this RCCS model was to create a system where mycobacterial biofilm-like growth could be characterised without restricting key environmental parameters such as gaseous exchange or carbon source. The RCCS bioreactor vessels are acrylic vessels with a liquid silicone elastomer on the posterior side of the vessel that is 8 microns thick. This type of silicone elastomer has one of the highest gas permeabilisation rates among rubberlike materials. Gases such as O_2 and CO_2 freely diffuse through this silicone elastomer (Zhang 2006). The direction of gaseous exchange is driven by the concentration gradient of gases on both sides of the material. Gases move through the material via free volume “holes” that form due to the high flexibility of the silicon-oxygen side chain of the silicone molecules; low intermolecular forces are observed in silicone elastomers and these together with unhindered single bonds that form the silicone backbone allow for a high degree of movement (Polmanteer 1981). Both the diffusivity of the silicone elastomer and mobility of gas molecules through free volume holes increase with temperature. The 37°C temperature of the incubator housing the RCCS should favour gaseous exchange from within the vessel to the incubator atmosphere (Barbier 1955). The permeability of this RCCS vessel membrane was tested by Synthecon, Ltd who supply the vessels. Nitrogen was bubbled through cell culture media to displace all dissolved O_2, added to an RCCS vessel and O_2 measured using an oxygen probe. The initial O_2 reading was 0%. After 1 hour, it was 20% corresponding with

atmospheric O_2 levels (personal correspondence with Synthecon Ltd). This would suggest that the RCCS bioreactor vessel facilitates gaseous exchange so that cultures do not become anaerobic, as may be the case in extended incubation of static cultures. In order to establish the broad O_2 tension range of the RCCS when culturing *M. bovis* BCG Methylene Blue (MB) was added to RCCS bioreactor vessels on day 16 of incubation and examined on day 21. MB should decolourise from blue to colourless in line with oxygen consumption, with complete decolourisation indicative of hypoxia (Tan, Sequeira et al. 2010).

3.5.1 Methylene Blue

Methylene Blue (MB) is a thiazine dye that is often used as an indicator of O_2 tension of a bacterial culture (Wayne and Hayes 1996; Murugasu-Oei and Dick 2000; Tan, Sequeira et al. 2010). It remains blue in colour when in oxidising or O_2 rich environments *e.g.* log-phase aerobic cultures, but decolourises in accordance with a decrease in O_2 or reducing environments, such as in the Wayne Model of hypoxia. The aim of adding MB to the RCCS was to establish if MB decolourisation would occur or not, *i.e.* was the interior of an RCCS vessel truly aerobic. Although the majority of the literature judge decolourisation visually, MB decolourisation was quantified using absorbance at 670 nm to remove subjectivity of scoring results.

3.5.1.1 Methylene Blue is stable at 37°C for up to 28 days

MB was serially diluted in 7H9 + ADC, Tween 80 broth and incubated without inoculation for up to four weeks, Figure 3.15. 1 mL samples of 7H9 broth (0, 1, 4 and 50 µg/mL) were taken at days 1, 8, 14, 21, 28 and absorbance quantified at 670 nm. There was little variation in the absorbance readings of each MB concentration over 28 days, suggesting that MB is stable when incubated for sustained periods of time at 37°C, Figure 3.16.

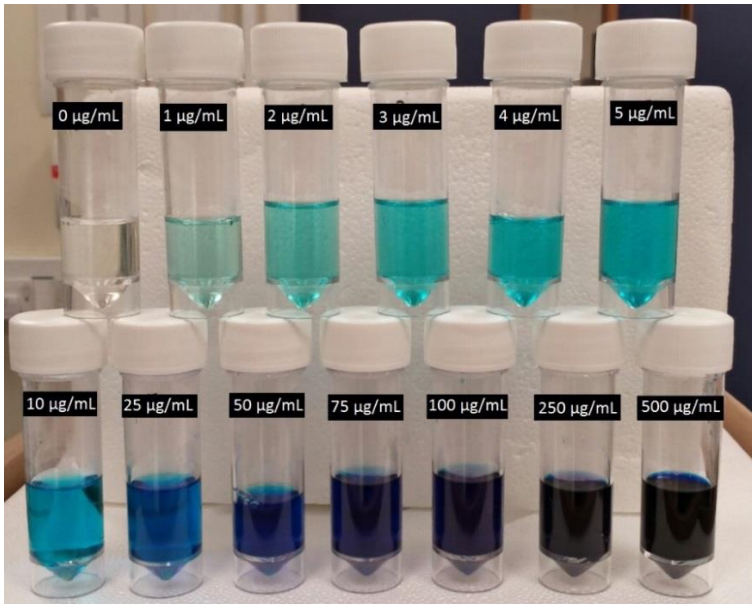

Figure 3.15: Dilution series of Methylene Blue in 7H9-ADC broth, Tween 80 at 37°C

Methylene Blue was diluted from a10 mg/mL stock in 7H9-ADC broth to establish stability and working concentration.

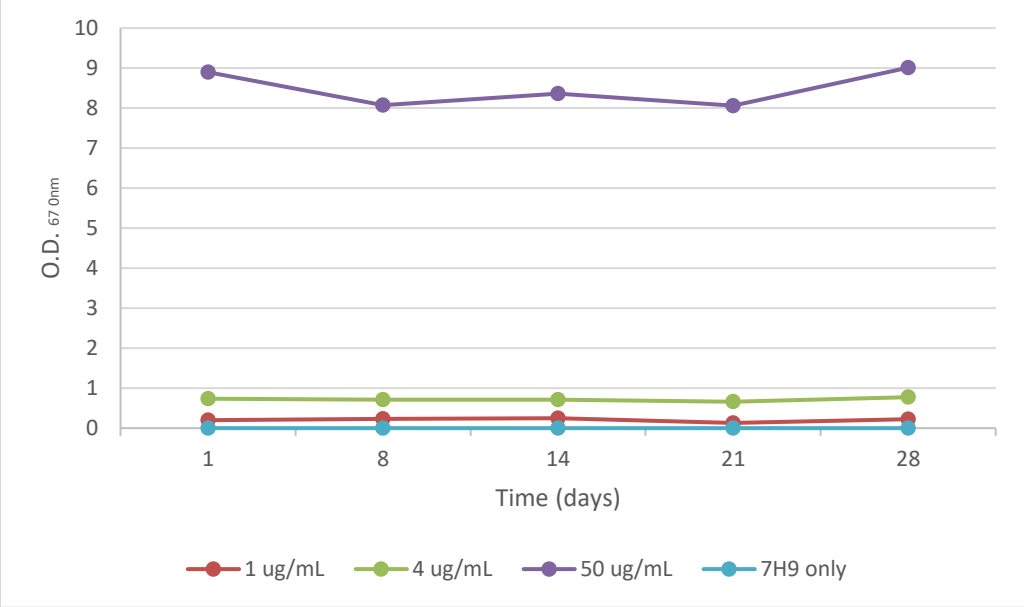

Figure 3.16: MB is stable after 28 days incubation at 37°C incubation in the absence of inoculation

The absorbance of MB at concentrations of 0, 1, 4, 50 µg/mL was measured at 670 nm. Each data point is a single O.D. reading from one experiment (n=1).

3.5.1.2 Methylene Blue working concentration is 2 µg/mL

MB exerts an antimicrobial effect on mycobacteria. It was necessary to establish what concentration of MB would be permissive for growth yet still be quantifiable at 670 nm. 2 and 25 µg/mL MB were inoculated with *M. bovis* BCG and incubated at 37 °C with daily mixing to ensure adequate exposure. MB working stocks were prepared in 7H9-ADC broth and so carrier controls were not performed as this would be the same as the 0 µg/mL control culture. Viable counting was performed at day 1 and 7, Figures 3.17, 3.18. There was a two-log reduction in bacilli cultured with 25 µg/mL MB compared to control culture (0 µg/mL). There was no reduction in cell survival at 2 µg/mL MB treated cultures compared to control culture (0 µg/mL). In addition, 1 mL samples were centrifuged to pellet bacilli. The bacterial pellet from 2 µg/mL MB was a creamy, off-white colour as is expected for pelleted *M. bovis* BCG. The bacterial pellet however for 25 µg/mL was shown to be stained blue, Figure 3.19. 2 µg/mL was used in future experiments as the working concentration for *M. bovis* BCG. The Wayne Model used 1.5 µg/mL of MB; this is quite dilute and difficult to judge by eye, which is why increased concentrations of MB were screened. In addition, many publications have not stated how much MB they have added to cultures so MB toxicity was established experimentally.

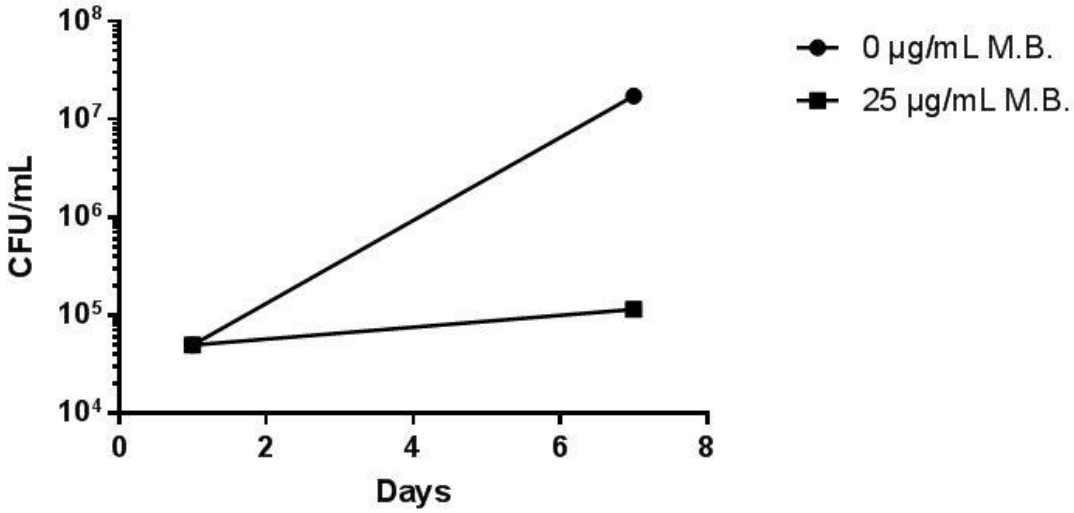

Figure 3.17: *M. bovis* BCG Survival after 7 day treatment with 25 µg/mL MB

The CFU/mL counts were taken at days 1 and 7. A two-log difference was observed between untreated and treated cultures. Data points are n=1.

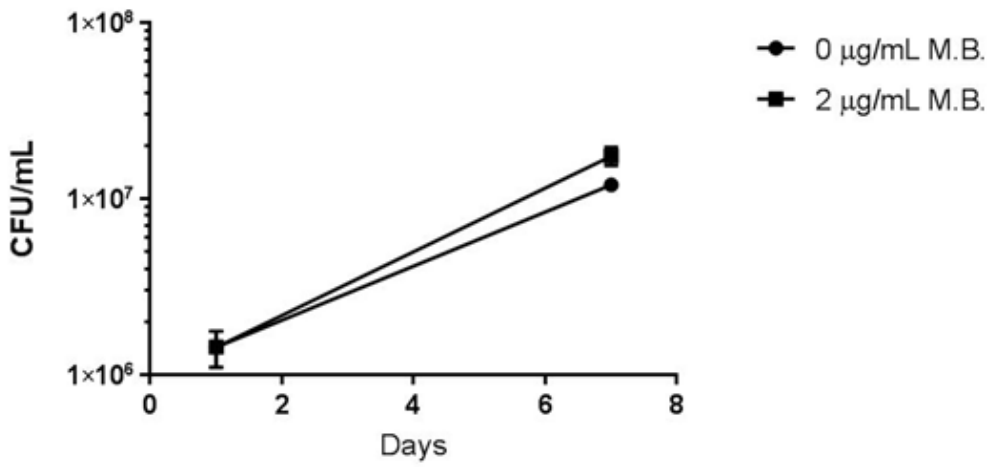

Figure 3.18: *M. bovis* BCG Survival after 7 day treatment with 2 µg/mL MB

CFU/mL counts were taken at days 1 and 7 of 0 and 2 µg/mL MB. Data points are n=1.

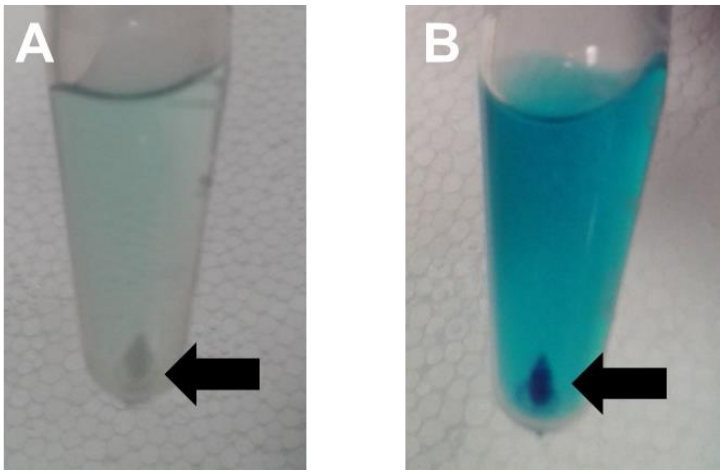

Figure 3.19: *M. bovis* BCG cell pellets after treatment with 2 µg/mL and 25 µg/mL Methylene Blue

M. bovis BCG cultures were treated with A: 2 µg/mL MB and B: 25 µg/mL MB for seven days. 1 mL aliquots were centrifuged and cell pellets imaged, highlighted with black arrows.

3.5.1.3 Methylene Blue decolourises in rotating and stationary RCCS vessels

1 mL of 20 µg/mL MB (to yield a final concentration of 2 µg/mL) was added to a rotating and a control RCCS vessel on day 16 of an RCCS run and incubated for 5 days. The rotating mycobacterial biofilm clusters stained with MB, while the stationary control cultures did not, Figure 3.20. Supernatants of both vessels were sampled and absorbance at 670 nm quantified. MB decolourised in both rotating and control vessels after five days incubation, Figure 3.21.

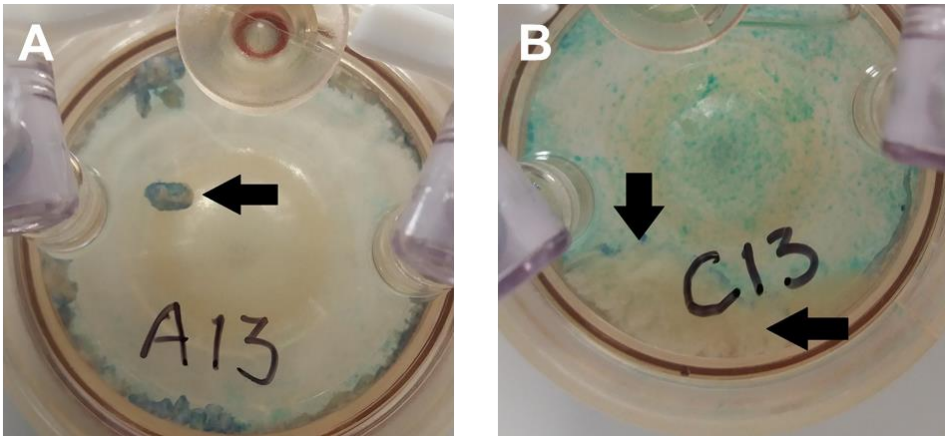

Figure 3.20: *M. bovis* BCG after five days' incubation with 2 µg/mL MB

A: Rotating vessel after 21 days total incubation time in the RCCS. MB stained biofilm highlighted by the black arrow. B: Stationary vessel after 21 days total incubation time in the RCCS. Biomass is highlighted by black arrows; no evidence of staining by MB

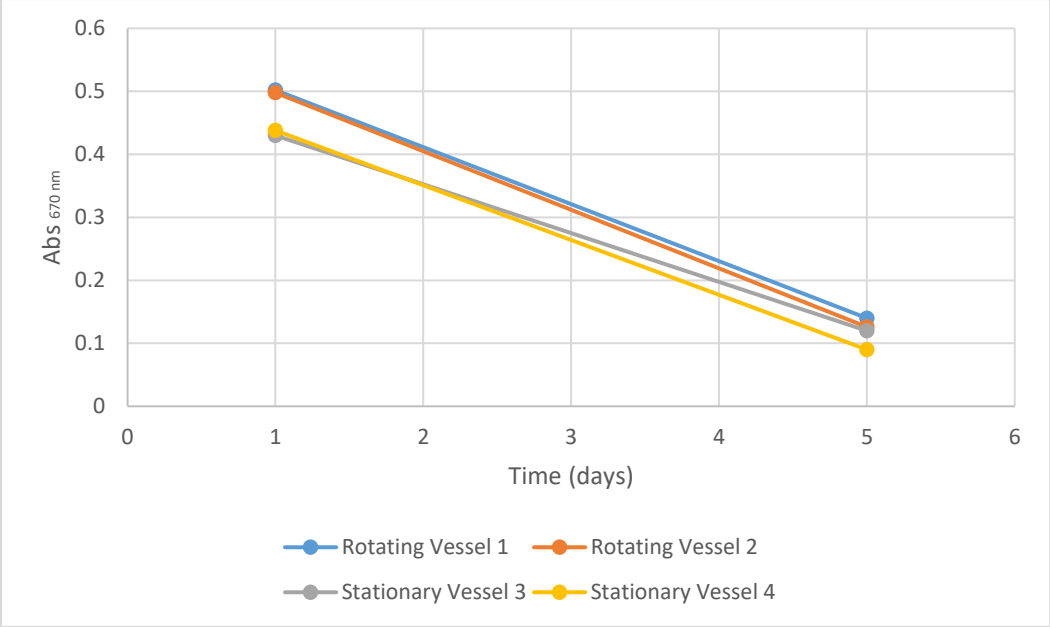

Figure 3.21: Absorbance of supernatants from rotating and stationary vessels after five days' incubation with 2 µg/mL MB

The Absorbance of supernatants from four RCCS vessels (two rotating; two stationary) measured at 670 nm at day 1 and day 7. Decolourisation was observed in all four vessels.

3.5.1.4 Methylene Blue decolourises in vented and sealed static cultures

In order to address the MB decolourisation observed in the RCCS vessels, Sauton's no Tween media (supplemented with 2 µg/mL MB) were prepared in 30 mL Universal tubes leaving no head space between media and tube cap. These cultures were mixed well by inversion 3X weekly and were either vented by loosening the cap or kept tightly sealed. Cultures were inoculated with *M. bovis* BCG or not. Absorbance was measured at 670 nm on day 1 and day 21 after incubation at 37°C. The hypothesis for this experiment was that vented cultures should not decolourise, as a constant supply of oxygen was available, while tightly sealed cultures should decolourise as actively respiring bacilli will diminish the O_2 present in the media. There was no decolourisation of culture media in the absence of bacilli whether vented or tightly sealed, as expected. However, MB decolourised in both vented and sealed cultures, Figures 3.22, 3.23.

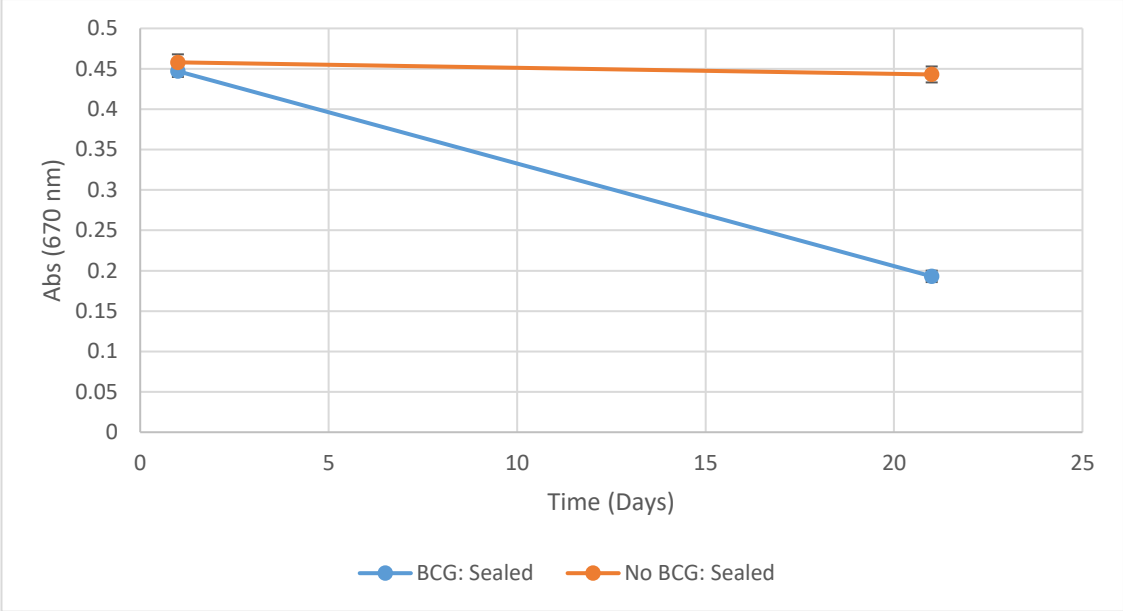

Figure 3.22: Absorbance of sealed 30 mL Universal tube cultures with no headspace after five day incubation with 2 µg/mL MB

The Absorbance of supernatants from 30 mL Universal cultures with *M. bovis* BCG (blue) or without *M. bovis* BCG (red). Each data point is the mean of n=2 ± SDEV

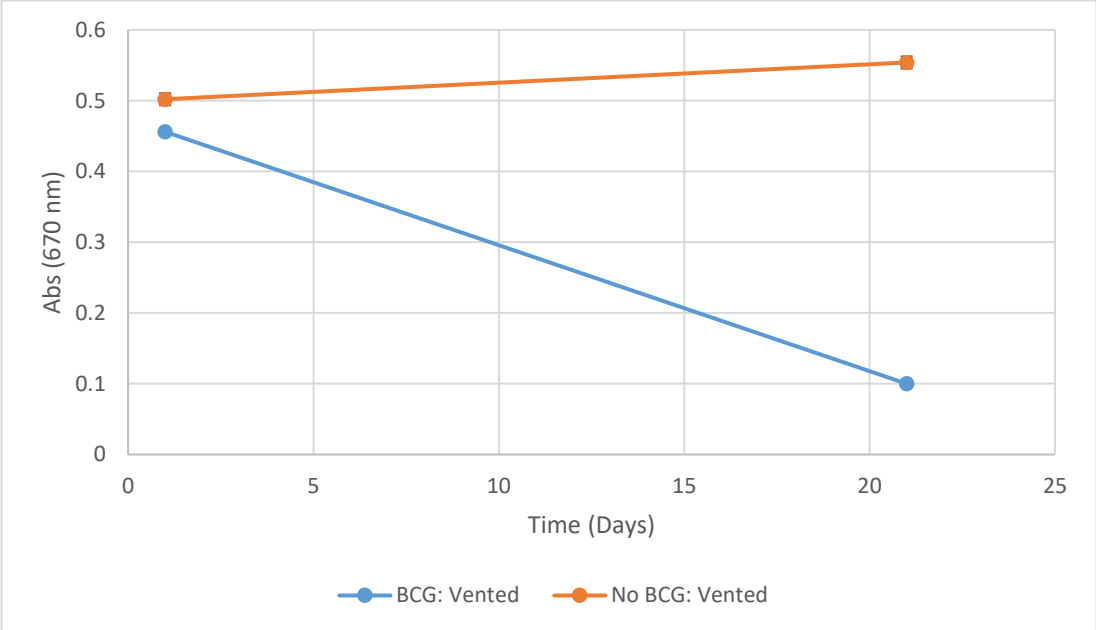

Figure 3.24: Absorbance of vented 30 mL Universal tube cultures with no headspace after five day incubation with 2 µg/mL MB

The Absorbance of supernatants from 30 mL Universal cultures with *M. bovis* BCG (blue) or without *M. bovis* BCG (red). Each data point is the mean of n=2 ± SDEV

3.6 Discussion

This chapter describes the optimisation of a low shear biofilm model of *M. bovis* BCG. Macroscopic examination of the RCCS biofilms showed a large cluster of bacilli adhered together that is not surface attached, but rather free-floating through the action of vessel rotation. Kinyoun staining of these biofilms and controls show that these biofilms are clusters of acid-fast bacilli. SEM revealed the complexity of the biofilm macrostructure, with bacilli located in convoluted structures encased with extracellular material that seemed to form a matrix.

The RCCS model has several advantages as a model of antimicrobial tolerance compared to other models. The low shear environment facilitates maximum cell clump interactions through RMP adjustment. Media, antimicrobials or other reagents such as MB can be added as required without disrupting biofilm formation. Gaseous exchange is facilitated though posterior silicone membrane that would not be possible when using traditional sealed plastic ware vessels. Vessels can be removed from the RCCS for examination or air bubble removal with minimal biofilm disruption. Biofilms in the RCCS form without attachment to a solid artificial medium, allowing greater surface area exposure to media, and finally bacterial clumping may be observed without severely limiting environmental factors necessary for logarithmic growth.

Despite the advantages of the RCCS as a biofilm model, it is not without its limitations. Even though *M. bovis* BCG and *M. tuberculosis* H37Rv are both slow growing mycobacteria and exhibit a high similarity at the genome and proteome level, *M. bovis* BCG is not a clinically relevant infectious strain. Several key genomic deletions occurred in *M. bovis* BCG when originally isolated with Region of Difference 1 (RD1) being of note. RD1 is associated with the loss of the protein secretion system, ESX1 which is comprised of ESAT-6 and CFP-10. ESAT-6 is a key early-secreted antigen that is associated with lowered innate immune responses to infection with TB though NF-kB inaction via TLR2 signalling (Pathak, Basu et al. 2007). CFP-10 is also a secreted antigen that contributes to *M.tb* virulence. CFP-10 forms a 1:1 heterodimer with ESAT-6 and it is the C-terminal of CFP-10 that is required for binding to macrophage and monocyte cells to exert ESAT-6 activity (Meher, Bal et al. 2006). The loss of these key secreted antigens is likely to impact pathogen host-interaction studies performed using supernatants or bacilli derived from the RCCS, for example in macrophage stimulation experiments. *M. bovis* BCG and *M. tuberculosis* H37Rv are both sensitive to isoniazid, rifampicin, streptomycin and ethambutol but *M. bovis* BCG is not sensitive to pyrazinamide (PYZ), a key front line drug in treating active *M.*

tuberculosis infection. PYZ is not efficacious against *M. bovis* BCG as this strain does not exhibit pyrazinamidase activity nor does it exhibit PYZ uptake into the cell. This highlights a limitation of *M. bovis* BCG as a model organism for *M. tuberculosis* that must be considered when developing *in vitro* models of TB, screening of novel antimicrobial compounds and elucidating genetic mechanisms of TB drug responses. Even though they share high sequence similarity, the difference between their genomes can translate to drug screening where novel compounds may be identified as ineffective against *M. bovis* BCG but could potentially target *M.tb.*

The use of methylene blue (MB) to determine likely respiratory status of bacilli in this model was not successful. Both vented and sealed cultures decolourised in the presence of bacilli indicating that *M. bovis* BCG may have metabolised MB to colourless regardless of O_2 tension. Bacilli, particularly from the biofilm model, stained with MB. This may suggest that an extracellular matrix (ECM) is present on biofilm surfaces that could provide a binding target for MB. SEM showed that biofilm clusters of bacteria appear to contain large deposits of an ECM-like substance, Figure 3.15. Mycobacterial biofilms have been shown to have an accumulation of extracellular DNA (eDNA) (Trivedi, Mavi et al. 2016) and free mycolic acids in their ECM (Ojha, Baughn et al. 2008). MB is a non-fluorescent dye that binds ionically to DNA (Stockert, Blazquez-Castro et al. 2014). The blue intensity of MB stained biofilms may also have been further enhanced by the presence of free mycolic acids in the ECM as the lower the pH of the substrate MB is bound to the more the intense the blue colour would be. In contrast, control cultures with no ECM would be able to metabolise MB from blue to colourless (Gibson, Sood et al. 2009). Bacilli treated with toxic levels of MB (25 µg/mL) stain blue, which is likely because killed bacilli cannot decolourise MB. Bacilli treated with a non-toxic MB concentration of 2 µg/mL remain unstained as the viable cells possess the metabolic activity to decolourise MB, Figure 3.20.

This raises the question, are the bacilli present on the exterior of these biofilm clusters dead or non-viable cells that do not possess the metabolic activity to convert MB to colourless? This is unlikely, as these exterior bacilli have access to nutrients and O_2 in the media. Therefore the staining pattern of MB suggests that an ECM forms in the biofilm model preventing MB access to bacilli; it is well documented how biofilm ECMs protect their cells from exogenous chemicals, such as drugs (Davies 2003), (Stewart 2003).

Chapter 4: Antimicrobial drug tolerance of RCCS-derived cultures

4.1 Overview

Antimicrobial drug resistance, well characterised in pathogenic bacteria, is identified as an increase in MIC for one or more antimicrobial drugs, rendering those antimicrobials as less efficacious or altogether ineffective (Pratt 2000). Antimicrobial drug resistance is genetically encoded through mutations to the bacterial chromosome or transfer of DNA between bacteria. Antimicrobial drug tolerance, however, has not been as well defined but is hypothesised to play critical roles in bacterial survival during chemotherapy and in the relapse of many bacterial infections such as those caused by *Chlamydia, Salmonella, Staphylococcus* and *Pseudomonas*, (Monack, Mueller et al. 2004; Palmer, Bankhead et al. 2009). In TB, it is hypothesised that subsets of bacilli arise during infection that are less responsive to chemotherapy (Jindani, Aber et al. 1980; Jindani, Dore et al. 2003). Antimicrobial drug tolerance, unlike antimicrobial resistance, is a non-heritable, phenotypic, transient state during which many antimicrobials may not be effective (Tudo, Laing et al. 2010). Antimicrobial drug tolerance does not arise through drug-resistance conferring mutations but rather through the expression of specific genes or a metabolic state that translates into a drug tolerant phenotype (Aldridge, Keren et al. 2014).

One approach to understanding the metabolic state and biological relevance of an *M.tb* model is to map the efficacy of first and second line anti-TB drugs against bacilli-derived from it. Previous *in vitro* biofilm models of *M.tb* identified sub-populations of bacilli that were drug tolerant (Ojha, Baughn et al. 2008; Trivedi, Mavi et al. 2016). Both of these models however treated biofilms directly with anti-TB drugs and did not generate planktonic suspensions of these biofilms before antimicrobial susceptibility testing. This chapter describes the antimicrobial susceptibility testing of homogenised (i.e. planktonic) and non-homogenised biofilms with isoniazid, rifampicin and streptomycin and the associated drug tolerance of biofilm-derived bacilli, and the use of RCCS-derived cultures as a screening tool for novel antimycobacterial compounds.

4.2 Results

4.2.1 Optimisation of cell viability assays

Two cell viability assays were optimised for quantifying bacillary survival post antimicrobial susceptibility testing (AST); BacTiter Glo ATP assay and Alamar Blue metabolic activity assay (Materials and Methods section 2.6.1).

4.2.1.1 BacTiter Glo ATP assay

The BacTiter Glo microbial cell viability assay (BTG assay) measures the amount of ATP as an estimate for the number of viable bacteria. A lysis buffer ruptures bacilli in culture allowing a luciferase enzyme to access released ATP. As a result a luminescence signal is generated that can be quantified using a 96 well microtiter plate reader, which is proportional to the number of viable bacteria.

The range of the BTG assay was tested; recombinant ATP (rATP) was serially diluted tenfold in 7H9 broth to yield a working range of rATP concentrations from 1 µM to 0.1 pM. The Relative Luminescence Units (RLU) was dose-dependent, Figure 4.1. 1 µM and 100 nM were saturated, and minimum rATP detectable was estimated to be 0.1 pM, giving this assay a range of at least 0.1 pM to 100nM rATP. No signal was generated from PBS only or 7H9 + ADC, Tween 80 broth only control wells.

Following this, a standard curve of *M. bovis* BCG was performed using the BTG assay. *M. bovis* BCG was cultured to log phase (approx.1.35 x 10^7 CFU/mL) (Materials and Methods section 2.2.1) was serially diluted (10^{-1} to 10^{-8}) in 7H9 + ADC, Tween 80 broth and cell viability quantified, Figure 4.2. The maximum limit of detection ($L.O.D._{max}$) was not reached with 10^{-1} dilution (1.35 x 10^6 CFU/mL). The maximum RLU obtained in Figure 4.1 before luminescence was saturated was 2.4 x 10^6 RLU for 10 nM rATP. In comparison, 1.35 x 10^6 CFU/mL generated 1.2 x 10^5 RLU. Based on the rATP standard curve, this is only 5.6% of the maximum RLU that can be detected with the BTG assay suggesting that luminescence saturation would be unlikely to occur with *M. bovis* BCG cultures; therefore bacterial cultures were not diluted before assaying with BTG. The minimum limit of detection ($L.O.D._{min}$) was not detected as RLU was still generated for the 10^{-8} serial dilution of *M. bovis* BCG, showing sensitivity for < 10 bacilli per well.

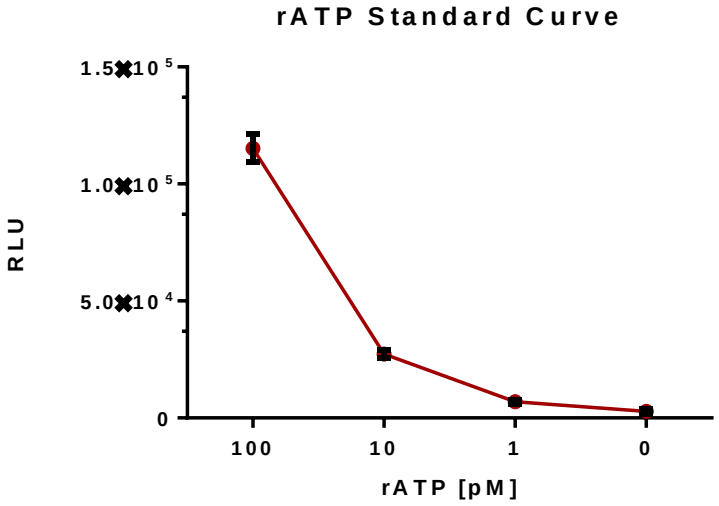

Figure 4.1: rATP standard curve for the BacTiter Glo ATP assay

Ten-fold serial diluted rATP quantified by BacTiter Glo ATP assay measured in Relative Luminescence Units (RLU). Each data point is the mean of three technical replicates ± SEM. 100,000, 10,000 and 1000 pM rATP are not plotted to show the rATP range that corresponds to the relevant microbiological range in Figure 4.2.

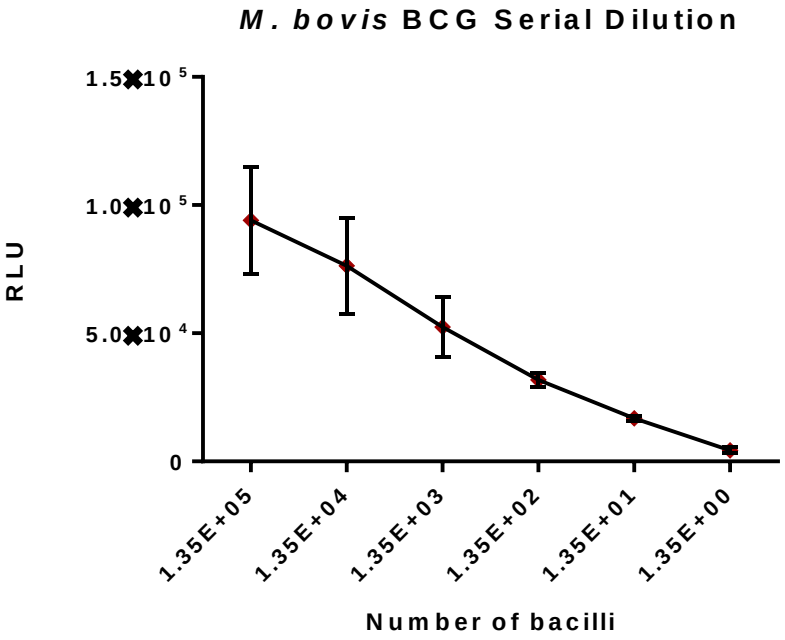

Figure 4.2: BacTiter Glo ATP assay Serial dilution of *M. bovis* BCG

Ten-fold serial diluted *M. bovis* BCG (from $1.35x10^5$ to $1.35x10^0$ bacilli) was quantified by BacTiter Glo ATP assay measured in Relative Luminescence Units (RLU). Each data point is the mean of two technical replicates ± SEM.

4.2.1.2 Alamar Blue Metabolic Activity Assay

Alamar Blue contains a blue redox dye, resazurin, that is taken up by viable cells and reduced to the pink metabolite resorufin via cellular NADH/NADPH dehydrogenases (Barnes and Spenney 1980). Cells that are no longer viable lose metabolic activity and can no longer convert resazurin to resorufin. The extent of this blue to pink resazurin-resorufin conversion correlates to metabolic activity of a culture and can be used to quantify cell viability.

Alamar Blue can be quantified using absorbance or fluorescence but is usually judged visually. For example with AST using a microbroth dilution method, wells that contain viable bacteria will change to a pink colour while wells containing dead bacteria will remain blue. The lowest concentration of antimicrobial drug in wells that remain blue is taken as the Minimum Inhibitory Concentration (MIC). MIC values of isoniazid, rifampicin and streptomycin were determined using this method.

Figure 4.3 shows INH AST of *M. bovis* BCG after 24 h incubation with Alamar Blue (Materials and Methods section 2.6.1). The MIC based on blue-pink is 0.78 µg/mL INH. The assay was also measured using a plate reader with absorbances at 490nm and 630nm, however no difference was observed in readings between any of the INH-treated wells or 7H9 +ADC, Tween 80 broth-only controls suggesting that absorbance was not sufficient to quantify in this system. Fluorescence was measured at excitation 530/25 and emission 590/35. Fluorescence measurement successfully differentiated between wells that were visually positive for growth and wells that were negative for growth, Figure 4.4. A clear breakpoint was demonstrated measuring Relative Fluorescence Units (RFU), so this method was adopted for all future assays. This provided a more robust assay than relying on user interpretation.

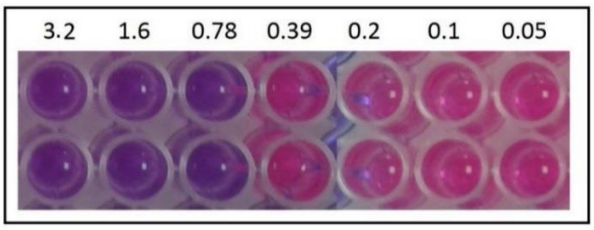

Figure 4.3: Alamar Blue assay of INH treated *M. bovis* BCG

M. bovis BCG was treated with two-fold serial dilutions of INH for seven days. Alamar Blue was added on day 7 and incubated for a further 24 hours before imaging. Concentrations are in µg/mL and in duplicate wells. INH MIC for this assay estimated to be 0.78 µg/mL.

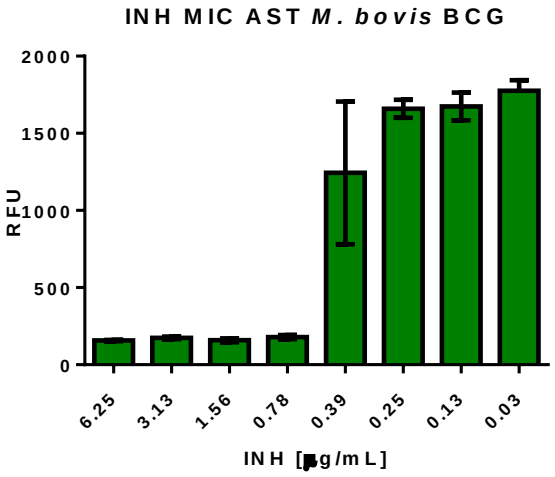

Figure 4.4: Alamar Blue assay of INH treated *M. bovis* BCG

M. bovis BCG was treated two-fold serial dilutions of INH for seven days. Alamar Blue was added on day 7 and incubated for a further 24 hours before assaying. Relative Fluorescence Units (RFU) were the mean of two technical replicates ± SEM. INH MIC for this assay by RFU is 0.78 µg/mL.

Control wells containing two-fold dilutions of 200- 0.01 µg/mL INH (no bacteria) were also assayed to determine fluorescence background caused by INH alone. 200 µg/mL was the only concentration that was fluorescent, and no fluorescence was detected for RIF or STREP at any concentration. Background fluorescence of 7H9 + ADC, Tween 80 broth was determined from the average of 10 wells as 500 RFU. All Alamar Blue data were corrected for 7H9 + ADC, Tween 80 broth background data in future experiments.

BTG and Alamar Blue MIC AST were also performed for RIF and STREP on log phase *M. bovis* BCG. Both assays yielded the same MIC for INH (0.78 µg/mL) and STREP (0.25 µg/mL) with the MIC for RIF determined as 0.025 µg/mL using BTG and 0.013 µg/mL using Alamar Blue, Table 4.1.

These two assays (Materials and Methods section 2.6.1), alongside viable counting on 7H10 plates ((Materials and Methods section 2.2.1), were used throughout this chapter to assay drug tolerance in biofilm-derived compared to control cultures.

Antimicrobial	Abbreviation	BacTiter Glo ATP Assay	Alamar Blue Metabolic Assay
Isoniazid	INH	0.78 µg/mL	0.78 µg/mL
Rifampicin	RIF	0.025 µg/mL	0.013 µg/mL
Streptomycin	STREP	0.25 µg/mL	0.25 µg/mL

Table 4.1: The Minimum Inhibitory Concentrations of isoniazid, rifampicin and streptomycin required to inhibit log phase 7H9 + ADC, Tween 80 broth *M. bovis* BCG growth by >95%.

Log phase *M. bovis* BCG was diluted to approximately 1 x 10^5 CFU/mL and treated with each antimicrobial drug for 7 days before assaying for cell viability using BacTiter Glo ATP assay and Alamar Blue metabolic assay.

4.2.2 Harvesting the RCCS for AST

RCCS 10 mL biofilm and control cultures were harvested as per Materials and Methods section 2.4.2, agitated gently by swirling in a sterile tube then the culture was divided into two equal volumes. One volume was needle homogenised to break up cell clusters into a single suspension, while the other was not (Materials and Methods section 2.4.2.1).

4.2.2.1 Biofilm homogenisation to generate planktonic cell suspensions

An effective needle homogenisation method was developed to generate planktonic suspensions of RCCS-derived biofilm and control cultures for antimicrobial susceptibility testing (AST). Cultures were syringed according to Methods section 2.4.2.1. Needle homogenised and non-homogenised cultures were serially diluted 10^{-1} to 10^{-7} in sterile PBS and viable counting performed. CFU/mL calculations from non-homogenised biofilm cultures were erratic compared to needle homogenised biofilm cultures with no decrease in non-homogenised CFU/mL in line with dilution. The majority of plate biomass from non-homogenised cultures grew as regions of partial confluence, whereas needle-homogenised biofilm bacilli showed well-isolated distinct colonies. Needle homogenisation had little impact on the viable counts of control cultures, suggesting that these were easily dispersed through preparation of their serial dilution for viable counting. Homogenised and non-homogenised biofilm and control cultures were also imaged with Kinyoun stain to directly observe disaggregation, Figure 4.5. Kinyoun staining showed that biofilm cell aggregates biofilm aggregates were broken down by needle homogenisation.

To test the effect of mycobacterial clumping on antimicrobial drug efficacy, needle homogenised and non-homogenised cultures were adjusted to an approximate equal $O.D._{600nm}$ with 7H9 +ADC, Tween 80 broth and exposed to 0 to 3.0 µg/mL (0.2 µg/mL increments) INH, RIF or STREP for seven days at 37°C (Materials and Methods section 2.5). Cell viability was measured using BacTiter Glo. The technical error between replicates was much lower for needle-homogenised cultures compared to non-homogenised cultures suggesting that cultures were sufficiently dispersed to allow adequate antimicrobial exposure to all bacilli, Figure 4.6. Interestingly, RIF kill curve profiles were not altered when biofilm cultures were needle homogenised or not. RCCS-derived control cultures were also tested in an identical manner, Figure

4.7. As expected, control cultures did not show erratic data points as observed for non-homogenised biofilm cultures in Figure 4.6.

Needle homogenisation and adjustment to equal $O.D._{600nm}$ of biofilm and control cultures was used throughout this thesis. On each occasion, the balancing of inoculum was measured by viable counting (Materials and Methods section 2.2.2.1) to define input into the AST assays and confirm that this is a robust method for adjusting inocula, Table 4.2.

AST inoculation		
RCCS #	**Biofilm**	**Control**
RCCS #3	5.71E+04	1.52E+05
RCCS #4	2.10E+06	5.81E+05
RCCS #5	3.38E+05	2.11E+05
RCCS #6	4.95E+05	3.60E+05
RCCS #9	1.60E+04	7.00E+03
RCCS #10	1.24E+03	2.60E+03
RCCS #11	2.90E+04	2.80E+04

Table 4.2: Summary Table of AST inoculums measured by viable counting

RCCS-derived biofilm and control cultures throughout this thesis were needle-homogenised and adjusted to an equal $O.D._{600nm}$ to balance inputs into AST assays. Values stated are CFU/mL from seven replicate runs.

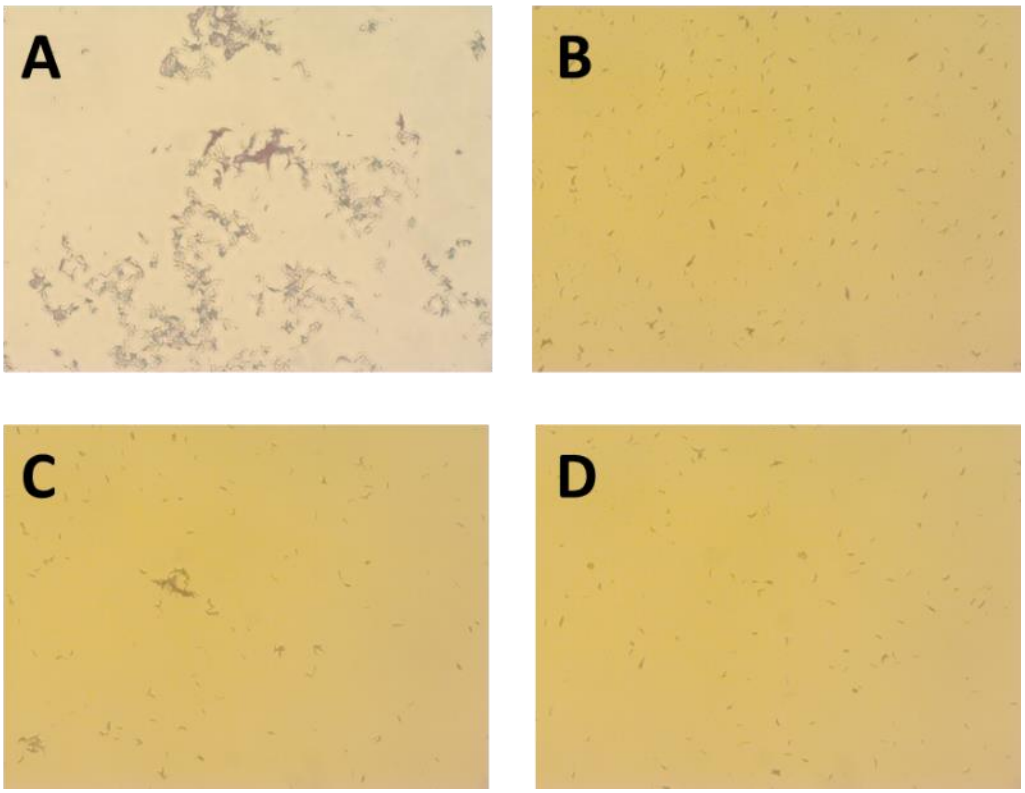

Figure 4.5: Needle homogenisation effectively homogenises RCCS-derived biofilms

A: Non-homogenised RCCS-derived biofilm culture; B: Homogenised RCCS-derived biofilm culture; C: Non-homogenised RCCS-derived control culture; D: Homogenised RCCS-derived control cultures. Kinyoun staining imaged at 40X

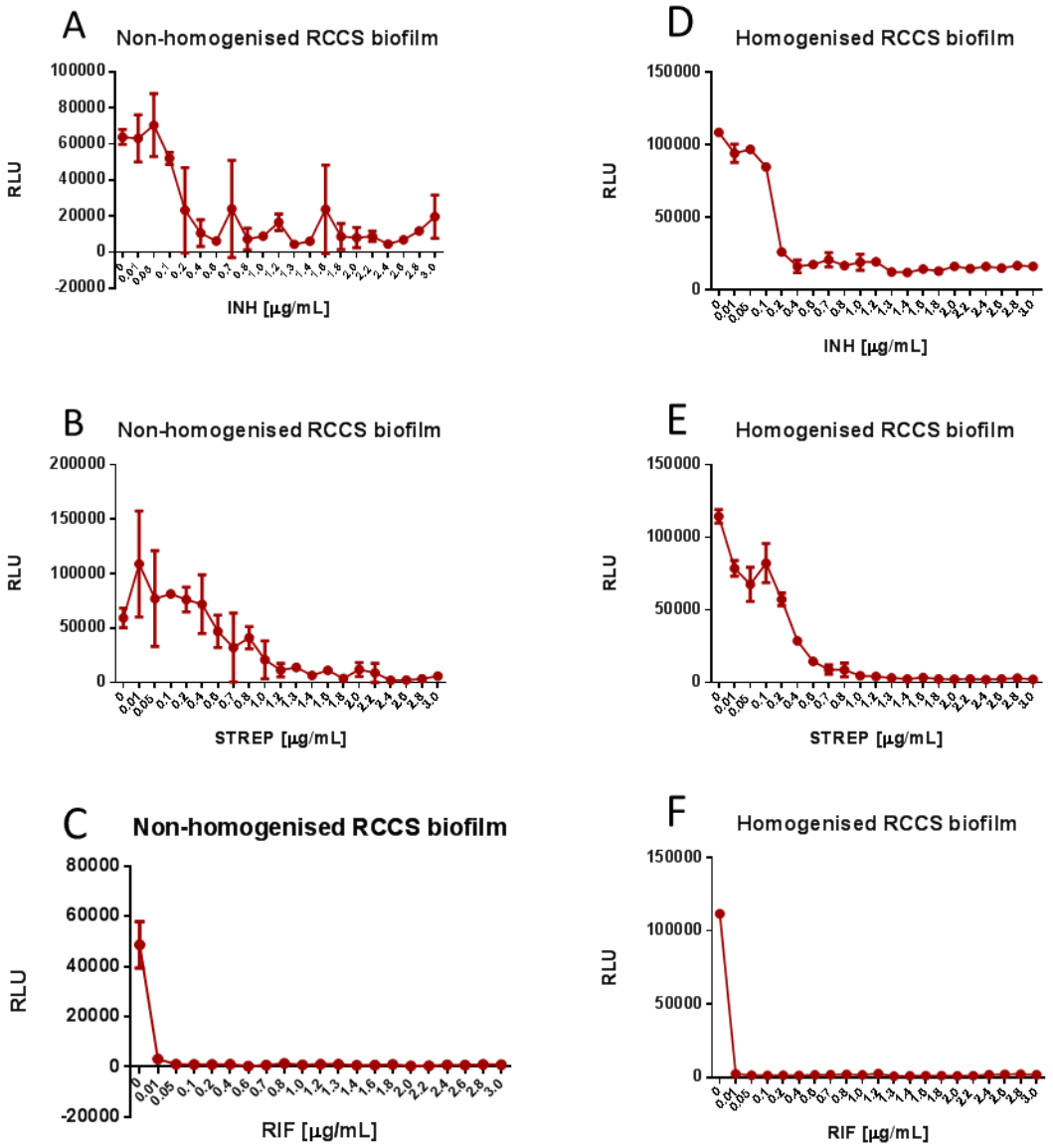

Figure 4.6: Needle homogenisation of RCCS-derived biofilms generates planktonic cell suspensions

Non-homogenised biofilm-derived cultures (A, B) treated with INH or STREP show erratic data points suggesting cultures are not planktonic. (D, E) Homogenisation of biofilm-derived cultures shows reduction of variability between replicate wells. Homogenisation did not alter RIF kill curves (C, F) of biofilm-derived cultures as the lowest dose of 0.01 µg/mL greatly reduced cell viability. Data points were the mean of two technical replicates ± SEM. Cell viability was measured in Relative Luminescence Units (RLU) by BTG.

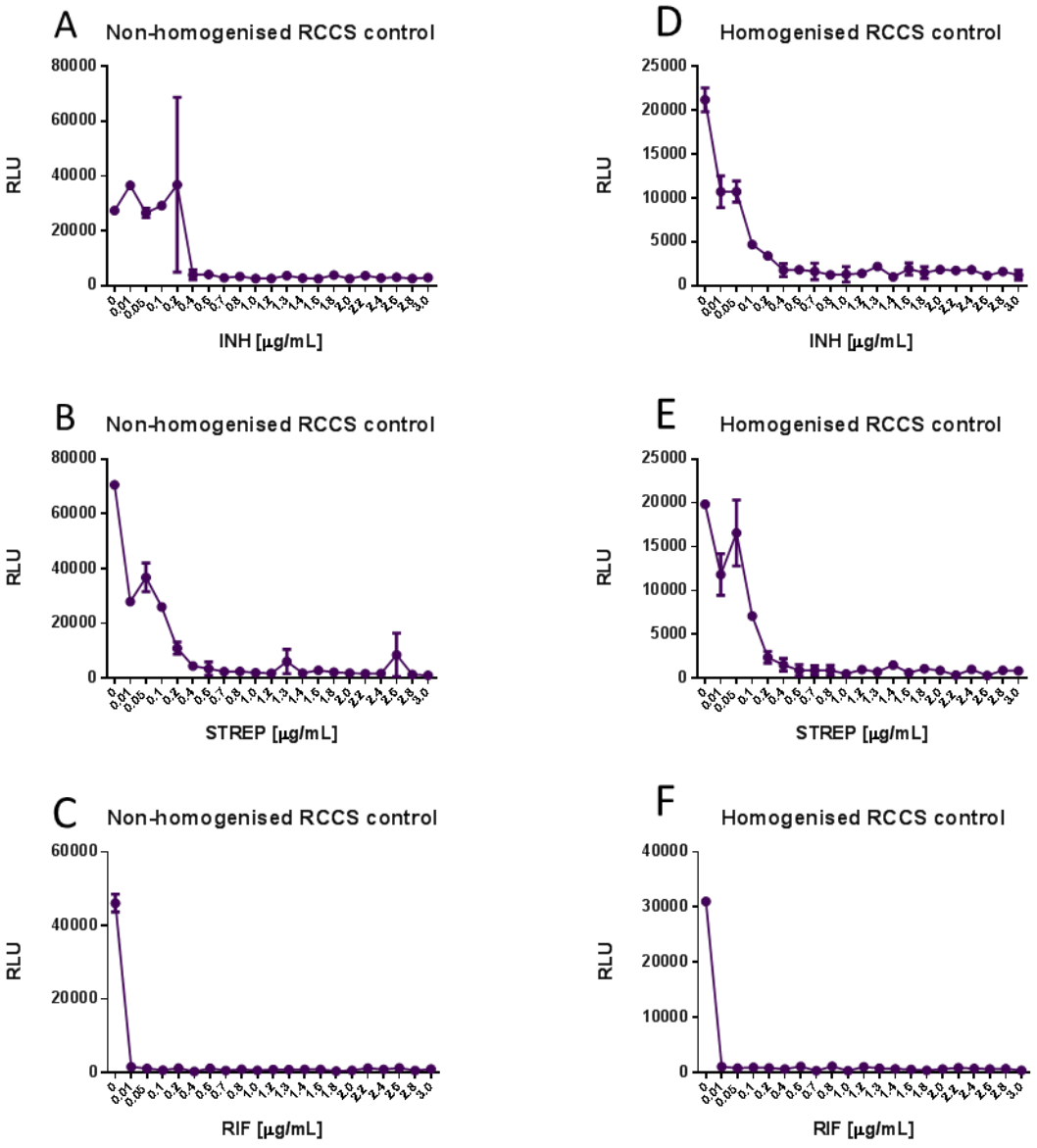

Figure 4.7: Needle homogenisation of RCCS-derived controls generated planktonic cell suspensions

The technical variation between control-derived cultures treated with INH or STREP did not differ whether needle homogenised or not. Homogenisation did not alter RIF kill curves of control cultures as the lowest dose of 0.01 µg/mL greatly reduced cell viability. Data points were the mean of two technical replicates ± SEM. Cell viability was measured in Relative Luminescence Units (RLU) by BTG.

4.2.2.2 Antimicrobial drug tolerance is induced in RCCS-derived biofilms

To determine whether mycobacteria derived from biofilms exhibited an antimicrobial drug tolerance phenotype, biofilms from rotating vessels and cultures from static vessels were harvested after 21 days incubation in the RCCS. Harvested cultures were needle-homogenised prior to AST as described above. 21-day old RCCS-derived biofilm and control-derived cultures were diluted with 7H9 + ADC, Tween 80 broth to an approximate $O.D._{600nm}$ of ~0.06, corresponding to approximately 1 x 10^5 CFU/mL. There was variability within this CFU calculation, as highlighted by the variation in Table 4.2. Diluted cultures were incubated for 7 days with a range of concentrations of INH, RIF or STREP. Cell survival was assessed using the BacTiter Glo ATP assay and the Alamar Blue metabolic activity assay. Three scenarios were postulated;

1) *Biofilm tolerance*. Biofilm-derived cultures have statistically significant (t-test P value <0.05) increased percent survival compared to control-derived cultures at one or more concentrations of antimicrobial drug;

2) *Control tolerance.* Control-derived cultures have statistically significant (t-test P value <0.05) increased percent survival compared to biofilm-derived cultures at one or more concentrations of antimicrobial drug;

3) *No tolerance.* There is no significant (t-test P value<0.05) difference in percent survival between biofilm and control-derived cultures at one or more concentration of antimicrobial drug.

AST was conducted on seven biological replicates of RCCS biofilm and control cultures (N=7); RCCS #3, #4, #5, #6, #9, #10, #11. RCCS #3 was the first RCCS to be used for AST and cell viability was quantified with BTG only. All subsequent AST of RCCS runs had their cell viability quantified with both BTG and Alamar Blue. This is reflected in the data presented in this chapter, where seven AST results are shown for BTG but only six AST results are shown for Alamar Blue.

AST Survival was calculated as a percentage of biofilm or control cultures after seven days in antimicrobial-free 7H9 ADC, Tween 80. Statistical significance testing to define “biofilm tolerance”, “control tolerance” or “no tolerance” was calculated using a two-tailed t-test on biofilm and control cultures at one concentration of antimicrobial drug.

4.2.2.2.1 Isoniazid tolerance is induced in RCCS-derived biofilms

Biofilm-derived cultures showed increased survival after seven days INH treatment compared to control cultures. Increased biofilm survival was statistically significant for 6 out of 7 RCCS INH AST for BTG and 5 out of 6 RCCS INH AST for Alamar Blue. The INH susceptibility testing profiles for RCCS-derived biofilm and control cultures are shown in Figure 4.8 (BTG data) and Figure 4.9 (Alamar Blue data), and are summarised in Table 4.3.

The results showing INH drug tolerance were reproducible and robust. The RCCS AST was repeated seven times independently, and antimicrobial activity was quantified with two assays with redundant measures of cell viability. In all but one RCCS run (RCCS #9), biofilm-derived cells survived INH exposure significantly better than controls, Table 4.3. There was some variation in the INH concentration where tolerance was observed. For example, RCCS #4 and #10 showed INH tolerance at the same concentration (0.8 µg/mL) when comparing BTG and Alamar Blue assays, Table 4.3. Conversely, BTG did not show INH tolerance for RCCS #9 biofilm-derived cultures, while Alamar Blue performed alongside BTG showed INH tolerance at 0.4 µg/mL with statistical significance of $p=0.0245$. INH tolerance was observed in only one RCCS-derived control culture, RCCS #5. This was only observed with Alamar Blue, Figure 4.9, where control tolerance is seen at 3 µg/mL. BTG does not detect this control tolerance, but does conflict with this Alamar Blue result, suggesting that there was biofilm tolerance at 0.2 µg/mL. These two discrepancies between these assays cannot be easily explained without technical error. Tolerance patterns varied between RCCS AST. Two general patterns were observed; INH tolerance was observed at one concentration with no tolerance at higher concentrations, such as Figure 4.8, RCCS #5, or tolerance was maintained throughout all concentrations tested, Figure 4.8, RCCS #10.

RCCS Run Number	BacTiter Glo ATP Assay					
	INH Tolerance					
	Tolerance phenotype	INH tested [µg/mL]	Highest [µg/mL] tolerance	Percent Survival (%)	Significance	No. of technical replicates
RCCS #3	Biofilm tolerance	0 - 2.40	2.40	Biofilm: 94.1 ± 0.1 Control: 0.15 ±0.1	**** (P= <0.0001)	2
RCCS #4	Biofilm tolerance	0 - 3.00	3.00	Biofilm: 13.7 ± 0.7 Control: 5.0 ± 1.6	* (P= 0.0395)	2
RCCS #5	Biofilm tolerance	0 - 3.00	0.20	Biofilm: 86.4 ± 5.7 Control 19.6 ± 1.4	** (P= 0.0076)	2
RCCS #6	Biofilm tolerance	0 - 3.00	0.20	Biofilm: 71.6 ± 0.8 Control: 7.8 ± 0.7	*** (P= 0.0003)	2
RCCS #9	No tolerance	0 - 0.800	no difference in percent survival	Biofilm: 8.7 ±0.16 Control: 12.4 ± 6.3 at 0.8 µg/mL	n/s	3
RCCS #10	Biofilm tolerance	0 - 0.800	0.80	Biofilm: 113.5 ± 8.7 Control: 17.1 ± 0.7	*** (P= 0.0004)	3
RCCS #11	Biofilm tolerance	0 - 0.800	0.80	Biofilm: 28.9 ± 5.1 Control: 12.6 ± 1.2	* (P= 0.0363)	3
RCCS Run Number	Alamar Blue Metabolic Assay					
	INH Tolerance					
	Tolerance phenotype	INH tested [µg/mL]	Highest [µg/mL] tolerance	Percent Survival (%)	Significance	No. of technical replicates
RCCS #3	ND	ND	ND	ND	ND	ND
RCCS #4	Biofilm tolerance	0 - 3.00	3.00	Biofilm: 30.8 ± 0.5 Control: 7.9 ± 0.06	*** (P= 0.0004)	2
RCCS #5	Control tolerance	0 - 3.00	3.00	Biofilm: 13.7 ± 0.3 Control: 28.4 ± 0.3	*** (P= 0.0008)	2
RCCS #6	Biofilm tolerance	0 - 3.00	2.80	Biofilm: 25.1 ± 0.6 Control: 7.4 ± 0.4	** (P= 0.0018)	2
RCCS #9	Biofilm tolerance	0 - 0.800	0.40	Biofilm: 84.0 ± 8.0 Control: 54.9 ± 2.3	* (P= 0.0245)	3
RCCS #10	Biofilm tolerance	0 - 0.800	0.80	Biofilm: 76.1 ± 2.4 Control: 59.7 ± 1.2	** (P= 0.0036)	3
RCCS #11	Biofilm tolerance	0 - 0.800	0.60	Biofilm: 54.5 ± 2.1 Control: 14.1 ± 0.4	**** (P= <0.0001)	3

Table 4.3: RCCS-derived biofilms exhibit isoniazid tolerance

INH tolerance was demonstrated for six out of seven RCCS biofilms using BacTiter Glo, and five out of six RCCS biofilms using Alamar Blue. Orange shows biofilm tolerance, blue shows control tolerance. ND= Not done. Significance using a two-tailed unpaired t-test between biofilm and control INH concentrations are marked using *= p<0.05, **= p<0.01, ***= p< 0.0001

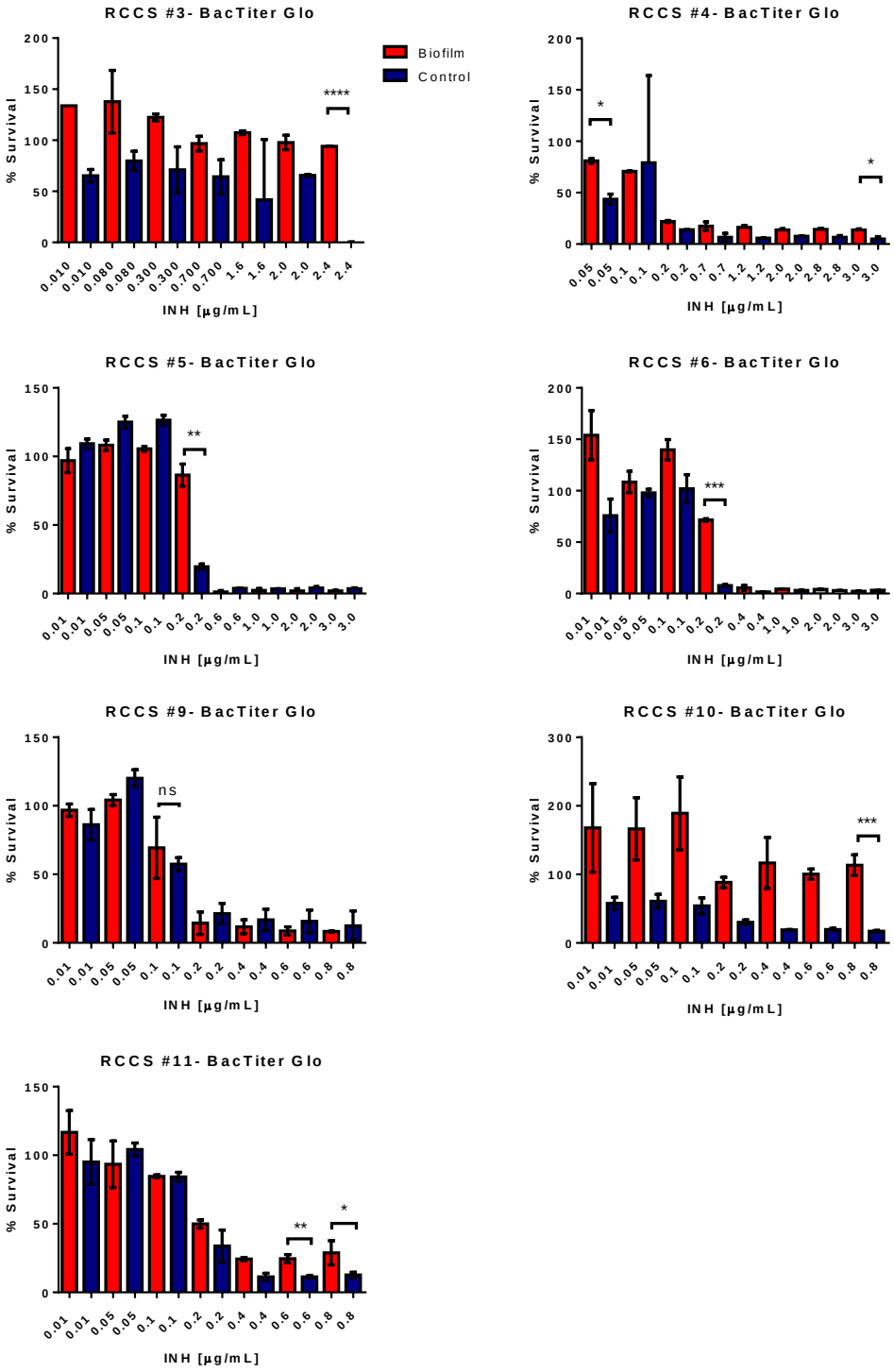

Figure 4.8: Survival of RCCS-derived biofilm and control bacilli after 7-day treatment with isoniazid using BacTiter Glo assay

Red: biofilm; Blue: control. Y-axis details percentage survival compared to drug-free biofilm or control growth; X-axis marks increasing concentration of INH. Statistical testing was applied at the highest concentration where tolerance was identified. NS = $p > 0.05$; * = $p \leq 0.05$; ** = $p \leq 0.01$; *** = $p \leq 0.001$; **** = $p \leq 0.0001$. Each data point is the mean of two technical replicates ± SEM for RCCS #3 #4, #5, #6 and the mean of three technical replicates ± SEM for RCCS #9, #10, #11.

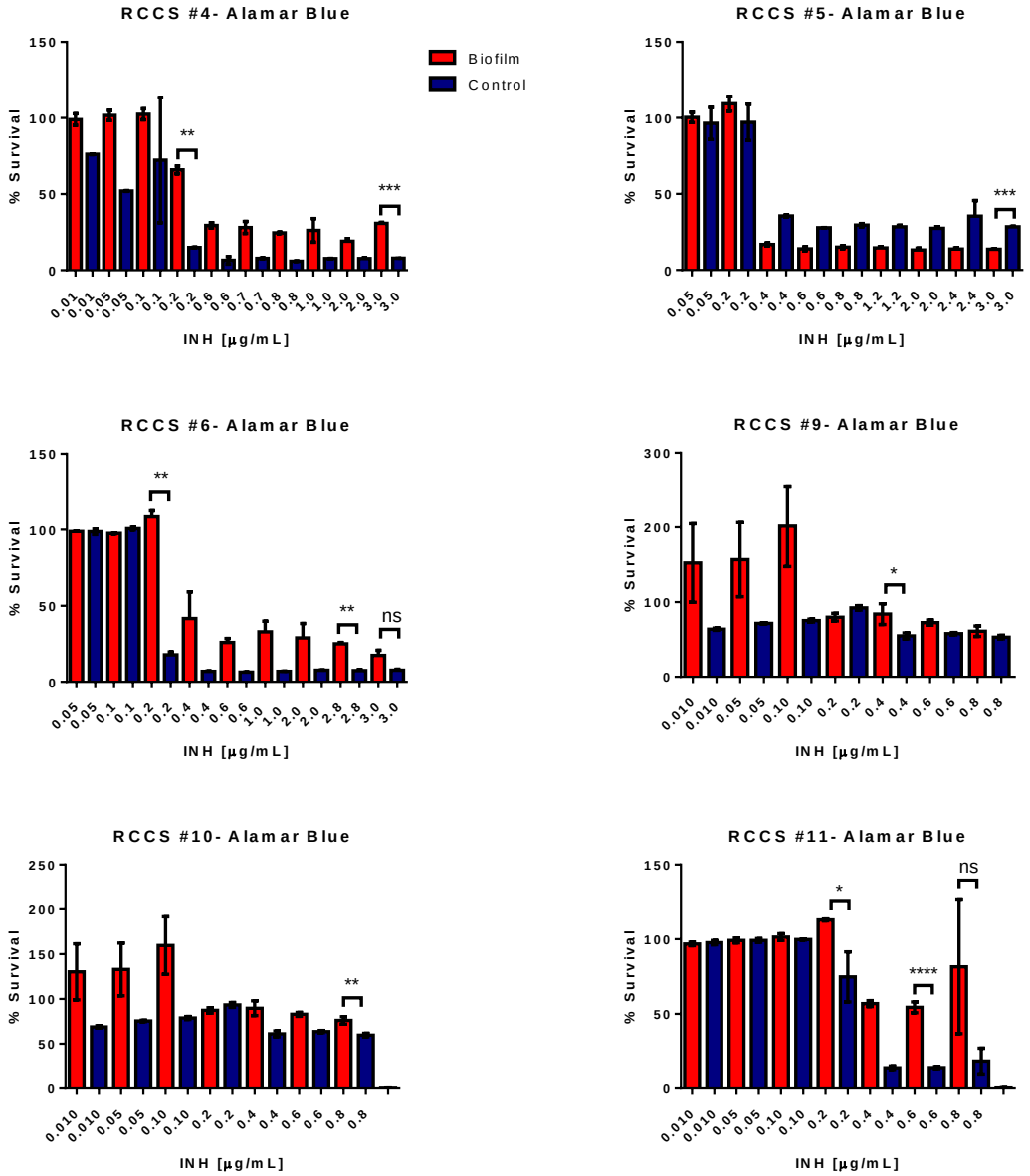

Figure 4.9: Survival of RCCS-derived biofilm and control bacilli after 7-day treatment with isoniazid using Alamar Blue assay

Red: biofilm; Blue: control. Y-axis details percentage survival compared to drug-free biofilm or control growth; X-axis marks increasing concentration of INH. Statistical testing was applied at the highest concentration where tolerance was identified. NS = $p > 0.05$; * = $p \leq 0.05$; ** = $p \leq 0.01$; *** = $p \leq 0.001$; **** = $p \leq 0.0001$. Each data point is the mean of two technical replicates ± SEM for RCCS #3 #4, #5, #6 and the mean of three technical replicates ± SEM for RCCS #9, #10, #11.

4.2.2.2.2 Rifampicin tolerance is assay specific

Out of seven RCCS runs, BTG identified three RCCS-derived biofilms that were RIF tolerant (RCCS #3, #10, #11), three RCCS-derived biofilms exhibited no RIF tolerance compared to controls (RCCS #4, #5, #9), and one RCCS-derived control culture showed RIF tolerance compared to biofilm (RCCS #6), Table 4.4. It is interesting to note that although statistical significance identified 3 RCCS-derived biofilms as RIF tolerant, the peak percent survival was low at 10.0%, 11.44% and 1.6% compared to RCCS-derived controls at 1.3%, 0.6% and 0.7% at 2.4, 0.2 and 0.1 µg/mL RIF respectively. Cell survival was >50% for many of the RCCS-derived biofilms treated with INH, by contrast the survival seen with RIF is much lower.

The control culture-derived from RCCS #6 was identified as RIF tolerant with 103.0% survival compared to biofilm bacilli from RCCS #6, which was only at 0.8% survival at 0.3 µg/mL RIF. This is likely due to technical error, as control bacilli do not exhibit any tolerance at the lower RIF concentration of 0.2 µg/mL.

The Alamar Blue assay identified two RCCS-derived biofilms as RIF tolerant (RCCS #5, #11) and 4 RCCS-derived control cultures that were tolerant to RIF (RCCS #4, #6, #9, #10), Table 4.4. Biofilm survival compared to control survival was 10.5% to 19.8%, 2.4% to 99.1%, 16.9% to 103.7% and 12.6% to 20.4% at RIF concentrations of 0.5, 0.3, 0.1 and 0.013 µg/mL respectively. BTG and Alamar Blue assays correlated only for RCCS #6; this RCCS-derived control culture was tolerant to RIF. Biofilm survival compared to control survival was 0.8% to 103.0% for BacTiter Glo and 2.4% to 99.1% for Alamar Blue. These results suggest that there is considerable variation in identifying RIF tolerance for RCCS-derived cultures between BTG and Alamar Blue assays, Figures 4.10 and 4.11.

RIF tolerance leading to high levels of mycobacterial survival following drug exposure was not consistently observed in RCCS-derived biofilm or control bacilli. The mode of action of RIF is distinct to INH, with INH targeting cell wall biosynthesis while RIF targets protein synthesis. INH has previously been shown to exert a bacteriostatic effect on non-replicating or slow metabolising bacteria, which could suggest the lower kill of INH compared to RIF.

RCCS Run Number	BacTiter Glo ATP Assay					
	RIF Tolerance					
	Tolerance phenotype	RIF tested [µg/mL]	Highest [µg/mL] tolerance	Percent Survival (%)	Significance	No. of technical replicates
RCCS #3	Biofilm tolerance	0 - 2.40	2.4	Biofilm: 10.0 ± 0.1 Control: 1.3 ± 0.01	**** (P= <0.0001)	2
RCCS #4	No tolerance	0 - 1.50	no difference in percent survival	Biofilm: 1.6 ± 0.1 Control: 1.4 ± 0.07 at 1.5 µg/mL	n/s	2
RCCS #5	No tolerance	0 - 1.50	no difference in percent survival	Biofilm: 1.0 ± 0.2 Control: 0.86 ± 0.2 at 1.5 µg/mL	n/s	2
RCCS #6	Control tolerance	0 - 3.00	0.3	Biofilm: 0.8 ± 0.1 Control: 103.0 ± 1.3	*** (P= 0.0002)	2
RCCS #9	No tolerance	0 - 0.1	no difference in percent survival	Biofilm: 1.7 ± 0.6 Control: 21.1 ± 14.4 at 0.1 µg/mL	n/s	2
RCCS #10	Biofilm tolerance	0 - 0.2	0.2	Biofilm: 11.44 ± 3.0 Control: 0.6 ± 0.06	* (P= <0.0228)	3
RCCS #11	Biofilm tolerance	0 - 0.2	0.1	Biofilm: 1.6 ± 0.14 Control: 0.7 ± 0.2	* (P= 0.0267)	3
RCCS Run Number	Alamar Blue Metabolic Assay					
	RIF Tolerance					
	Tolerance phenotype	RIF tested [µg/mL]	Highest [µg/mL] tolerance	Percent Survival (%)	Significance	No. of technical replicates
RCCS #3	ND	ND	ND	ND	ND	ND
RCCS #4	Control tolerance	0 - 1.50	0.5	Biofilm: 10.5 ± 0.21 Control: 19.8 ± 1.5	* (P= 0.0239)	2
RCCS #5	Biofilm tolerance	0 - 1.50	1.0	Biofilm: 3.5 ± 0.09 Control: 2.1 ± 0.3	* (P= 0.0450)	2
RCCS #6	Control tolerance	0 - 1.50	0.3	Biofilm: 2.4 ± 0.35 Control: 99.1 ± 2.3	*** (P= 0.0006)	2
RCCS #9	Control tolerance	0- 0.1	0.1	Biofilm: 16.9 ± 0.6 Control: 103.7 ± 8.6	** (P= 0.0098)	2
RCCS #10	Control tolerance	0 - 2.0	0.013	Biofilm: 12.6 ± 0.7 Control: 20.4 ± 0.75	** (P= 0.0015)	3
RCCS #11	Biofilm tolerance	0 - 0.2	0.2	Biofilm: 4.8 ± 0.12 Control: 3.46 ± 0.18	** (P= 0.0030)	3

Table 4.4: Rifampicin tolerance is assay specific

RIF tolerance was demonstrated for three out of seven RCCS biofilms using BacTiter Glo, and two out of six RCCS biofilms using Alamar Blue. Orange shows biofilm tolerance, blue shows control tolerance. ND= Not done Significance using a two-tailed unpaired t-test between biofilm and control RIF concentrations are marked using *= $p<0.05$, **= $p<0.01$, ***= $p< 0.0001$

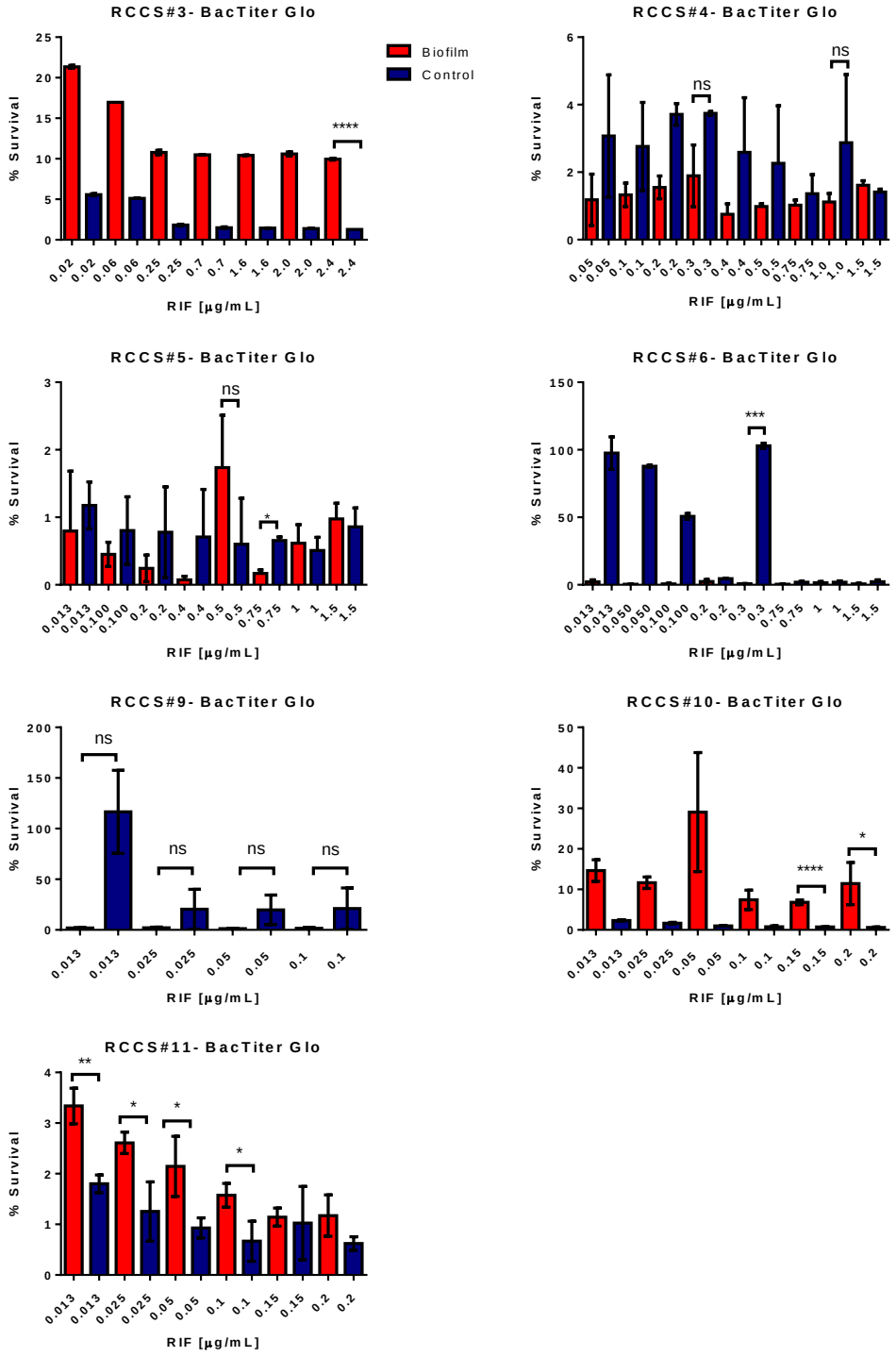

Figure 4.10: Survival of RCCS-derived biofilm and control bacilli after 7-day treatment with rifampicin using BacTiter Glo assay

Red: biofilm; Blue: control. Y-axis details percentage survival compared to drug-free biofilm or control growth; X-axis marks increasing concentration of RIF. Statistical testing was applied at the highest concentration where tolerance was identified. NS = $p > 0.05$; * = $p \leq 0.05$; ** = $p \leq 0.01$; *** = $p \leq 0.001$; **** = $p \leq 0.0001$. Each data point is the mean of two technical replicates ± SEM for RCCS #3 #4, #5, #6 and the mean of three technical replicates ± SEM for RCCS #9, #10, #11.

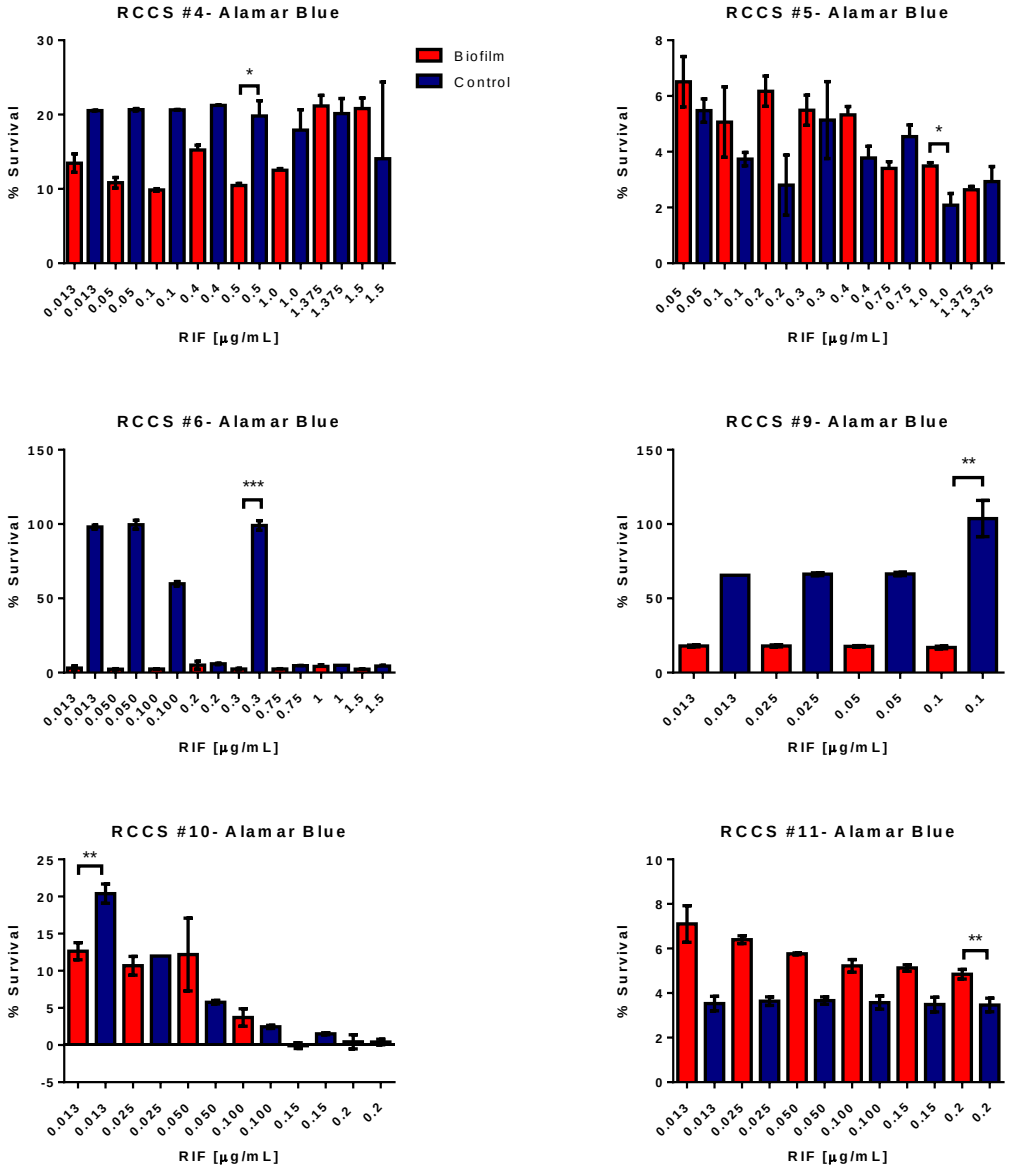

Figure 4.11: Survival of RCCS-derived biofilm and control bacilli after 7-day treatment with rifampicin using Alamar Blue assay

Red: biofilm; Blue: control. Y-axis details percentage survival compared to drug-free biofilm or control growth; X-axis marks increasing concentration of RIF. Statistical testing was applied at the highest concentration where tolerance was identified. NS = $p > 0.05$; * = $p \leq 0.05$; ** = $p \leq 0.01$; *** = $p \leq 0.001$; **** = $p \leq 0.0001$. Each data point is the mean of two technical replicates ± SEM for RCCS #4, #5, #6 and the mean of three technical replicates ± SEM for RCCS #9, #10, #11.

4.2.2.2.3 Streptomycin tolerance is induced in RCCS-derived biofilms

BacTiter Glo data identified five RCCS-derived biofilms as tolerant to STREP (RCCS #3, #4, #9, #10, #11), one RCCS-derived control culture was tolerant to STREP (RCCS #5) and in RCCS #6 no STREP tolerance was observed for either biofilm or control cultures, Table 4.5.

The Alamar Blue assay identified three RCCS-derived biofilm cultures were tolerant to STREP (RCCS #4, #10, #11) and there was no tolerance observed for either biofilm or control cultures in three RCCS runs (RCCS #5, #6, #9), Table 4.5.

Both assays showed biofilm tolerance to STREP from the same three RCCS runs (RCCS #3, #10, #11). Biofilm tolerance varied across the RCCS-derived biofilms with a trend of 2-4 fold increases in survival compared to control cultures. For RCCS #5, control-derived bacilli survival was 106.2% ± 1.0% compared to biofilm-derived bacilli survival of 83.91%± 2.9%. This survival was only at the lower concentration of 0.025 µg/mL, which is well below the STREP MIC of 0.25 µg/mL. Alamar Blue did not show any control-derived tolerance to STREP at this or any other concentration.

RCCS Run Number	BacTiter Glo ATP Assay Streptomycin Tolerance					
	Tolerance phenotype	STREP tested [µg/mL]	Highest [µg/mL] tolerance	Percent Survival (%)	Significance	No. of technical replicates
RCCS #3	Biofilm tolerance	0 - 2.40	2.4	Biofilm: 9.96 ± 0.07 Control: 0.1.3 ±0.005	**** (P= <0.0001)	2
RCCS #4	Biofilm tolerance	0 - 1.50	0.1	Biofilm: 51.63 ± 2.8 Control: 12.8 ± 2.6	** (P= 0.0094)	2
RCCS #5	Control tolerance	0 - 1.50	0.025	Biofilm: 83.91 ± 2.9 Control 106.2 ± 1.0	* (P= 0.0184)	2
RCCS #6	No tolerance	0 - 1.50	no difference in percent survival	Biofilm: 0.7 ± 0.48 Control: 0.32 ± 0.03 at 1.5	n/s	2
RCCS #9	Biofilm tolerance	0 - 0.300	0.025	Biofilm: 111.6 ± 2.4 Control: 90.91 ± 0.8	** (P= 0.0075)	3
RCCS #10	Biofilm tolerance	0 - 0.300	0.3	Biofilm: 87.7 ± 3.5 Control: 19.0 ± 1.8	**** (P= <0.0001)	3
RCCS #11	Biofilm tolerance	0 - 0.300	0.3	Biofilm: 27.2 ± 2.1 Control: 14.7 ± 0.8	** (P= 0.0050)	3
RCCS Run Number	Alamar Blue Metabolic Assay Streptomycin Tolerance					
	Tolerance phenotype	STREP tested [µg/mL]	Highest [µg/mL] tolerance	Percent Survival (%)	Significance	No. of technical replicates
RCCS #3	ND	ND	ND	ND	ND	ND
RCCS #4	Biofilm tolerance	0 - 1.50	0.1	Biofilm: 84.89 ± 6.4 Control: 19.52 ± 6.3	* (P= 0.0187)	2
RCCS #5	No tolerance	0 - 1.50	no difference in percent survival	Biofilm: 3.182 ± 0.04 Control: 10.14 ± 2.0 at 1.5 µg/mL	n/s	2
RCCS #6	No tolerance	0 - 1.50	no difference in percent survival	Biofilm: 4.48 ± 0.34 Control: 4.75 ± 0.25 at 1.5	n/s	2
RCCS #9	No tolerance	0 - 0.300	no difference in percent survival	Biofilm: 37.02 ± 7.1 Control: 40.45 ± 0.5 at 0.3 µg/mL	n/s	3
RCCS #10	Biofilm tolerance	0 - 0.300	0.3	Biofilm: 47.96 ± 3.57 Control: 29.53 ± 1.14	** (P= 0.0079)	3
RCCS #11	Biofilm tolerance	0 - 0.300	0.3	Biofilm: 33.24 ± 0.9 Control: 7.8 ± 0.4	**** (P= <0.0001)	3

Table 4.5: RCCS-derived biofilms exhibit streptomycin tolerance

STREP tolerance was demonstrated for five out of seven RCCS biofilms using BacTiter Glo, and three out of six RCCS biofilms using Alamar Blue assay. Orange shows biofilm tolerance, blue shows control tolerance. ND= Not done. Significance using a two-tailed unpaired t-test between biofilm and control STREP concentrations are marked using *= $p<0.05$, **= $p<0.01$, ***= $p< 0.0001$.

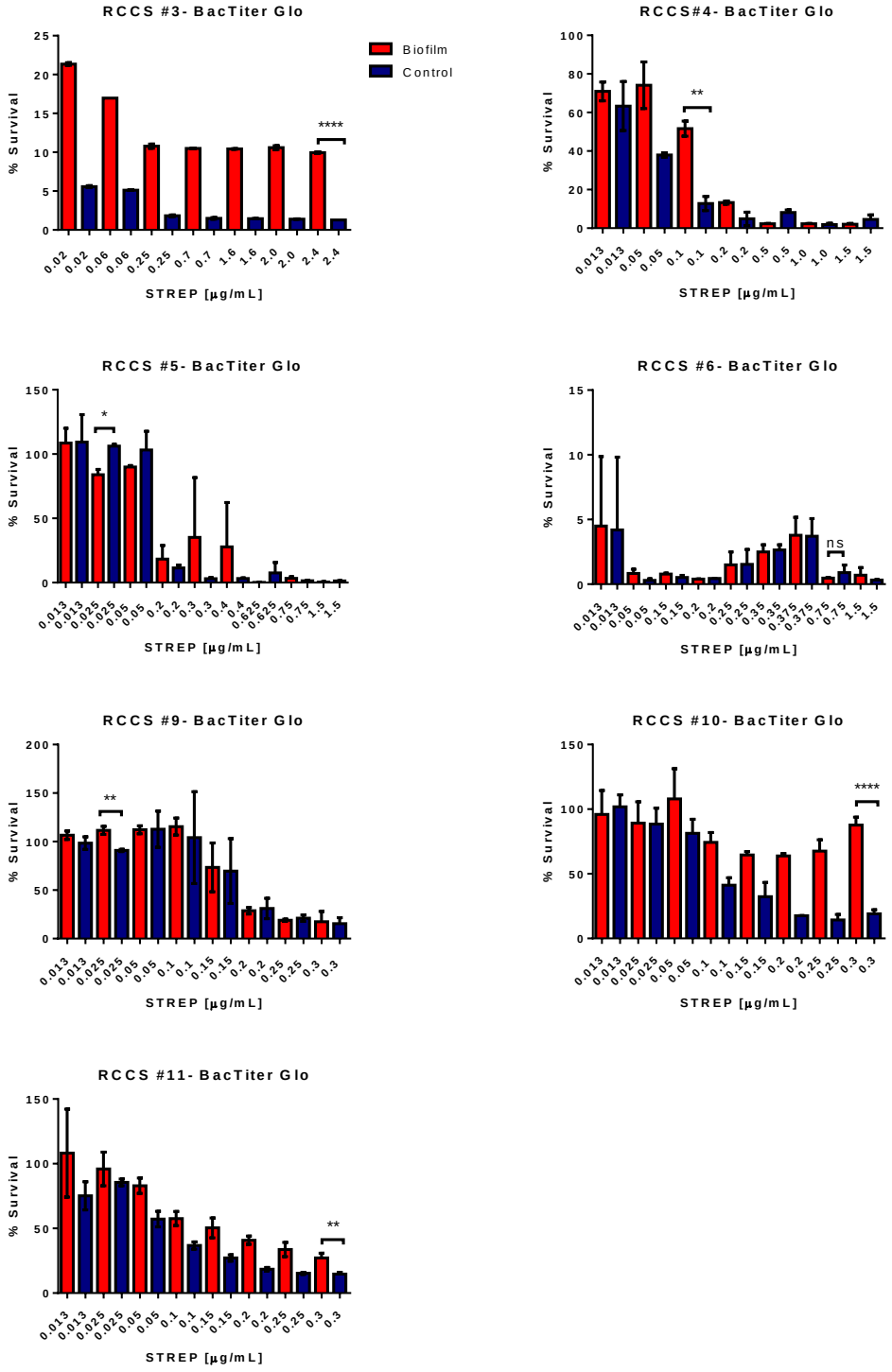

Figure 4.12: Survival of RCCS-derived biofilm and control bacilli after 7-day treatment with streptomycin using BacTiter Glo assay

Red: biofilm; Blue: control. Y-axis details percentage survival compared to drug-free biofilm or control growth; X-axis marks increasing concentration of INH. Statistical testing was applied at the highest concentration where tolerance was identified. NS = p > 0.05; * = p ≤0.05; ** = p ≤0.01; *** = p ≤0.001; **** = p ≤0.0001. Each data point is the mean of two technical replicates ± SEM for RCCS #3 #4, #5, #6 and the mean of three technical replicates ± SEM for RCCS #9, #10, #11.

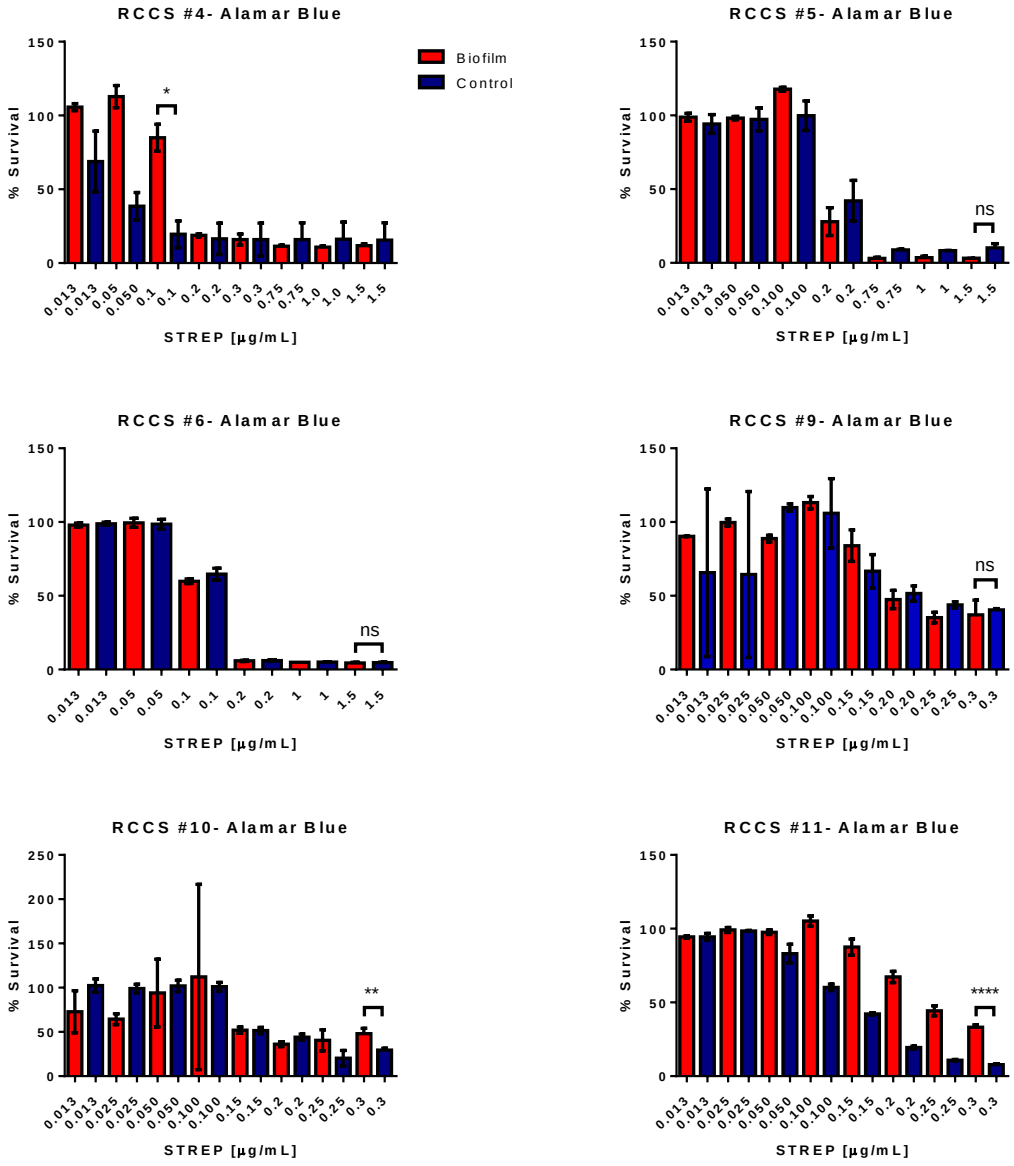

Figure 4.13: Survival of RCCS-derived biofilm and control bacilli after 7-day treatment with streptomycin using Alamar Blue assay

Red: biofilm; Blue: control. Y-axis details percentage survival compared to drug-free biofilm or control growth; X-axis marks increasing concentration of RIF. Statistical testing was applied at the highest concentration where tolerance was identified. NS = $p > 0.05$; * = $p \leq 0.05$; ** = $p \leq 0.01$; *** = $p \leq 0.001$; **** = $p \leq 0.0001$. Each data point is the mean of two technical replicates ± SEM for RCCS #4, #5, #6 and the mean of three technical replicates ± SEM for RCCS #9, #10, #11.

The tolerance profiles of all RCCS subjected to INH, RIF or STREP AST are summarised in Table 4.6.

RCCS Run Number	**BacTiter Glo**			**Alamar Blue**		
	INH Tolerance	**RIF Tolerance**	**STREP Tolerance**	**INH Tolerance**	**RIF Tolerance**	**STREP Tolerance**
	Column 1	*Column 2*	*Column 3*	*Column 4*	*Column 5*	*Column 6*
RCCS #3	Biofilm tolerance	Biofilm tolerance	Biofilm tolerance	ND	ND	ND
RCCS #4	Biofilm tolerance	No tolerance	Biofilm tolerance	Biofilm tolerance	Control tolerance	Biofilm tolerance
RCCS #5	Biofilm tolerance	No tolerance	Control tolerance	Control tolerance	Biofilm tolerance	No tolerance
RCCS #6	Biofilm tolerance	Control tolerance	No tolerance	Biofilm tolerance	Control tolerance	No tolerance
RCCS #9	No tolerance	No tolerance	Biofilm tolerance	Biofilm tolerance	Control tolerance	No tolerance
RCCS #10	Biofilm tolerance	Biofilm tolerance	Biofilm tolerance	Biofilm tolerance	Control tolerance	Biofilm tolerance
RCCS #11	Biofilm tolerance	Biofilm tolerance	Biofilm tolerance	Biofilm tolerance	Biofilm tolerance	Biofilm tolerance
Corresponding data Tables	Table 4.3	Table 4.4	Table 4.5	Table 4.3	Table 4.4	Table 4.5
Corresponding AST profiles	Figure 4.8	Figure 4.10	Figure 4.12	Figure 4.9	Figure 4.11	Figure 4.13

Table 4.6: Summary of all INH, RIF and STREP AST carried out on RCCS-derived biofilm and control cultures

Summary of all tolerance profiles of INH, RIF and STREP AST of RCCS-derived cultures. ND: Alamar Blue assay was not done. Red: Biofilm-derived cultures show a statistically significant increase in percent survival compared to control cultures; blue: Control-derived cultures show a statistically significant increase in percent survival compared to biofilm cultures; green: there is no statistically significant difference in biofilm cultures compared to control cultures.

4.2.2.2.4 Broth culture assay confirms antimicrobial drug tolerance

INH, RIF and STREP tolerance were observed for biofilm cultures compared to controls in AST of RCCS #11, Table 4.6. After antimicrobial 96 well microtiter plates were assayed for viability using BacTiter Glo and Alamar Blue, three technical replicate wells at a low and high antimicrobial concentrations were selected for broth culture assay, (BCA), Table 4.7. BCA was performed as per Materials and Methods section 2.6.2. BCA results are summarised in Table 4.10. Growth scoring was based on growth occurring for each triplicate well taken from INH, RIF or STREP 96 well microtiter plates. Positive growth in each triplicate is marked as "+", in two triplicates as "++" and in three triplicates as "+++".

0.6 µg/mL INH treated biofilm-derived bacilli grew when diluted to 10^{-4}, compared to control-derived bacilli, which only grew at 10^{-2} dilution correlating with cell viability assays that suggest RCCS #11 biofilm-derived cultures were INH tolerant.

There was no positive growth for biofilm or control-derived cultures that had been treated with RIF at either the low or the high dose. Although statistically significant growth was seen with RIF treated biofilm-derived cultures compared to controls, Table 4.7, the percentage survival for this biofilm culture was only 1.6% at 0.1 µg/mL for BTG and 4.8% at 0.2 µg/mL for Alamar Blue. It is likely that there were too few bacilli present for growth to occur even at a 1 in 10 dilution.

0.25 µg/mL STREP treated biofilm-derived bacilli grew when diluted to 10^{-5}, however only one of the triplicates grew at this dilution. All three triplicates grew when diluted to 10^{-4}. Control cells that had been treated at this concentration grew only until a dilution of 10^{-3} and only for two of the three triplicates selected for BCA, suggesting that RCCS #11 biofilm-derived culture was STREP tolerant.

RCCS #11	INH (0.8 µg/mL)	RIF (0.1 µg/mL)	STREP (0.3 µg/mL)
BacTiter Glo	Biofilm: 28.9 ± 5.1 Control: 12.6 ± 1.2	Biofilm: 1.6 ± 0.14 Control: 0.7 ± 0.2	Biofilm: 27.2 ± 2.1 Control: 14.7 ± 0.8
Alamar Blue	Biofilm: 54.5 ± 2.1 Control: 14.1 ± 0.4	Biofilm: 4.8 ± 0.12 Control: 3.46 ± 0.18	Biofilm: 33.24 ± 0.9 Control: 7.8 ± 0.4

Table 4.7: Antimicrobial drug tolerance in RCCS #11 defined by BacTiter Glo and Alamar Blue assay

INH, RIF and STREP antimicrobial drug tolerance was observed in RCCS #11-derived biofilm compared to control cultures. Values given as % survival compared to untreated biofilm or control cultures ± SEM

Antimicrobial	Concentrations selected for MPN	
INH	0.2 µg/mL	0.6 µg/mL
RIF	0.025 µg/mL	0.2 µg/mL
STREP	0.05 µg/mL	0.25 µg/mL

Table 4.8: Concentrations of RCCS #11 AST chosen for broth culture assay

One low and high concentration were selected for BCA. Each concentration had three technical wells that were centrifuged, supernatant pipetted to waste to remove antimicrobial, and re-suspended in their original volume in antimicrobial free 7H9 broth. Each bacilli from each well were centrifuged and re-suspended in 7H9 broth (10^{-1} to 10^{-6}) in 96 well microtiter plates and incubated for 21 days. Repeated in triplicate for each well.

Antimicrobial	Inoculum	[Antimicrobial]	10^{-1}	10^{-2}	10^{-3}	10^{-4}	10^{-5}	10^{-6}
INH	*Biofilm*	0.2 µg/mL	+++	+++	+++	+++	+++	+++
		0.6 µg/mL	+++	+++	+++	+++	-	-
	Control	0.2 µg/mL	+++	+++	+++	+++	+++	+++
		0.6 µg/mL	++	++	-	-	-	-
RIF	*Biofilm*	0.025 µg/mL	-	-	-	-	-	-
		0.2 µg/mL	-	-	-	-	-	-
	Control	0.025 µg/mL	-	-	-	-	-	-
		0.2 µg/mL	-	-	-	-	-	-
STREP	*Biofilm*	0.05 µg/mL	+++	+++	+++	+++	+++	+++
		0.25 µg/mL	+++	+++	+++	+++	+	-
	Control	0.05 µg/mL	+++	+++	+++	+++	+++	+++
		0.25 µg/mL	++	++	++	-	-	-

Table 4.9: Broth culture assay counts of RCCS-derived biofilm and control cultures

BCA of RCCS-derived biofilm and control cultures that had been treated with INH, RIF or STREP for seven days. Three replicate wells were selected for each concentration of antimicrobial drug and serially diluted 10^{-1} to 10^{-6} in 7H9 broth and incubated for 21 days. Positive culture was determined by absorbance at 630nm. Growth of each triplicate well corresponds to one “+”.

4.2.2.2.5 Antimicrobial drug tolerance is phenotypic

Figures 4.8 through to 4.13 demonstrate INH and STREP tolerance of biofilm-derived bacilli. In order to establish if this increased survival observed (summarised in Table 4.6) was phenotypic rather than genotypic, i.e. antimicrobial resistance, biofilm and control-derived bacilli were passaged in antimicrobial-free 7H9 broth three consecutive times immediately after harvesting from the RCCS. INH, RIF and STREP susceptibility testing was performed on these cultures as described in Methods section 2.5, Figures 4.14, 4.15 and 4.16. No significant difference was determined using t-test analysis in cell survival was observed for biofilm or control-derived bacilli after three consecutive passages in antimicrobial-free 7H9 broth when treated with INH, RIF or STREP. This suggested that the difference in survival observed in biofilm cultures from the RCCS, Table 4.7, was a phenotypic trait rather than the selection of spontaneous drug-resistance conferring mutations. If the difference in survival was actually genetically encoded antimicrobial resistance, then biofilm-derived cultures passaged in antimicrobial-free 7H9 broth should have shown increased survival compared to control cultures when treated with INH, RIF or STREP.

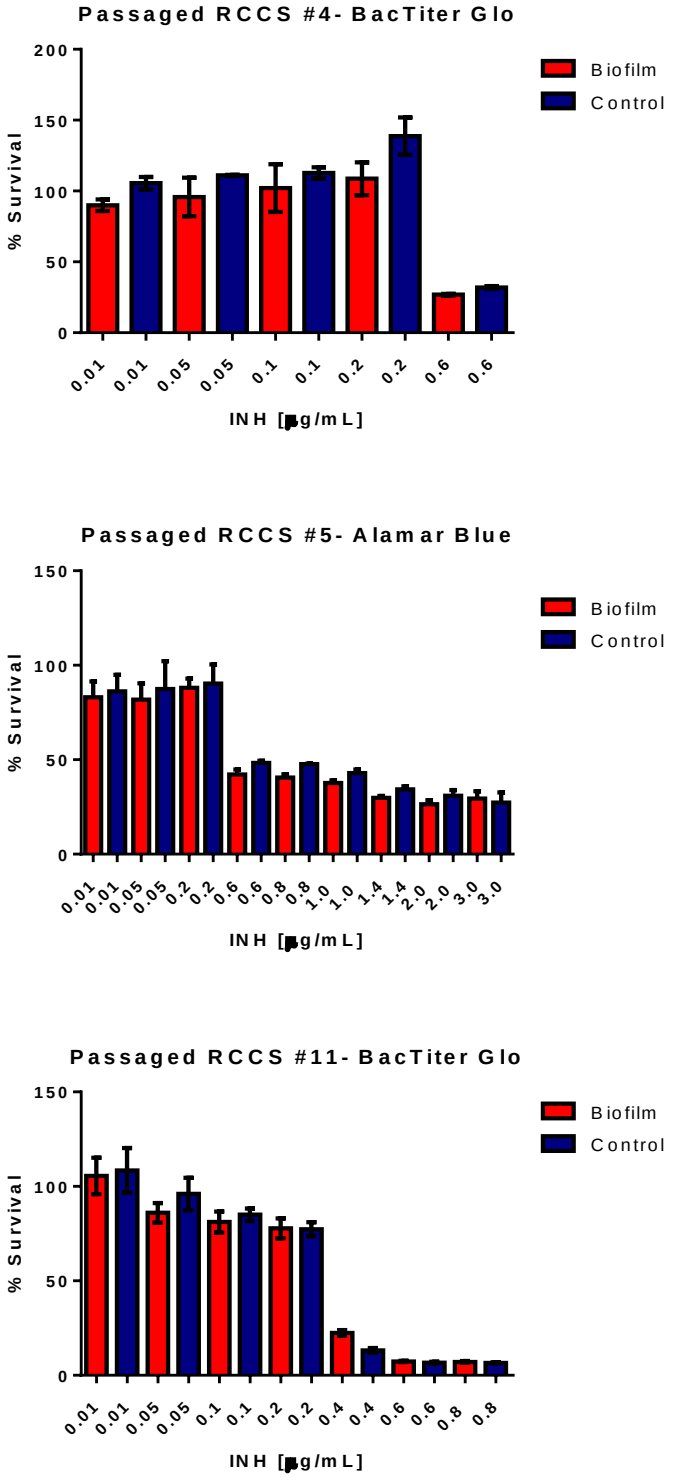

Figure 4.14: INH tolerance is phenotypic

RCCS-derived biofilm and control cultures were passaged in antimicrobial-free 7H9 broth and AST was performed with a range of INH concentrations. Percentage survival was calculated as a percentage of untreated biofilm or controls. No statistically significant difference in cell survival was identified between any of the biofilm or control. Cell viability was quantified using Alamar Blue or BacTiter Glo. Each data point is the mean of two technical replicates ± SEM

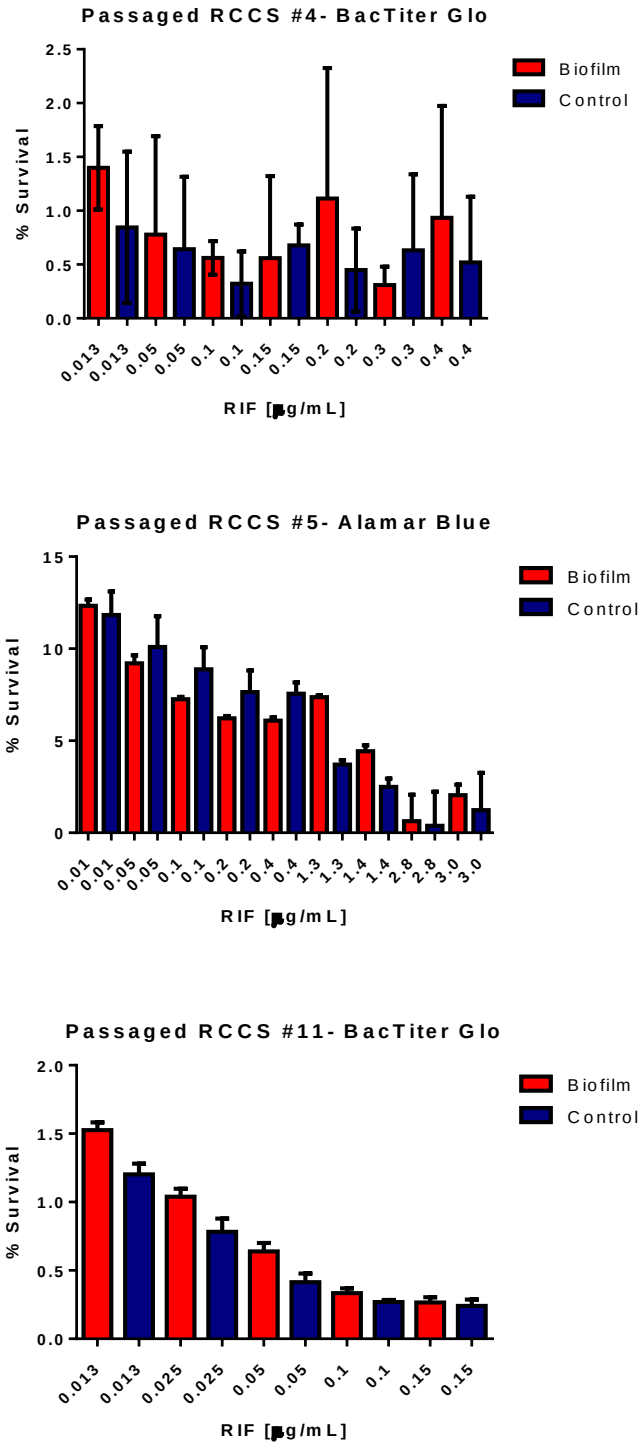

Figure 4.15: RIF tolerance is phenotypic

RCCS-derived biofilm and control cultures were passaged in antimicrobial-free 7H9 broth and AST performed with a range of RIF concentrations. Percentage survival was calculated as a percentage of untreated biofilm or controls. No statistically significant difference in cell survival was identified between any of the biofilm or control. Cell viability was quantified using Alamar Blue or BacTiter Glo. Each data point is the mean of two technical replicates ± SEM

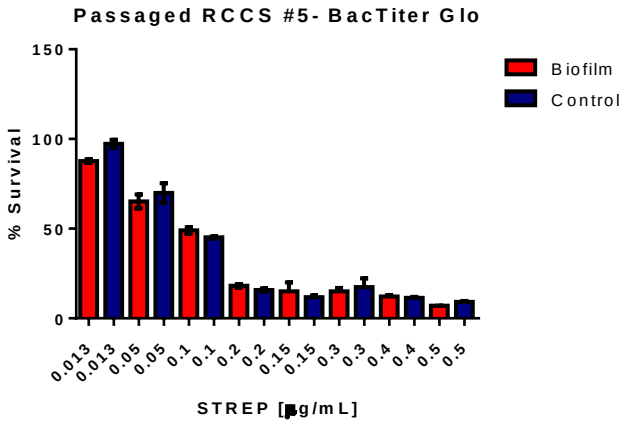

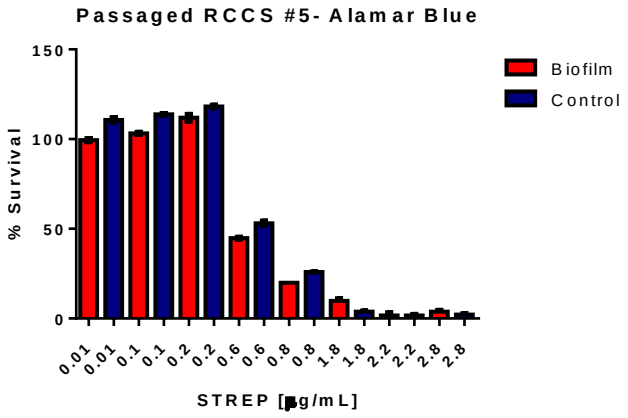

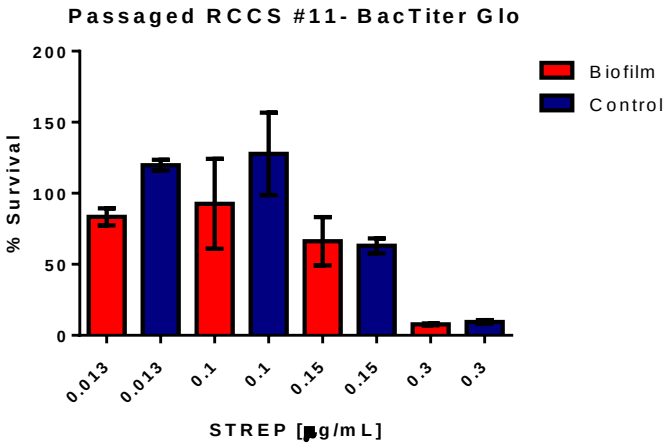

Figure 4.16: STREP tolerance is phenotypic

RCCS-derived biofilm and control cultures were passaged in antimicrobial-free 7H9 broth and AST was performed with a range of STREP concentrations. % survival was calculated as a percentage of untreated biofilm or controls. No statistically significant difference in cell survival was identified between any of the biofilm or control. Cell viability was quantified using Alamar Blue or BacTiter Glo. Each data point is the mean of two technical replicates ± SEM

4.2.2.2.6 Biofilm induced Antimicrobial drug tolerance is temporal

Antimicrobial tolerance profiles in Table 4.6 were generated after assaying cell survival post 7-day antimicrobial exposure. 7-day incubation was selected for antimicrobial treatment, as this is an arbitrary time point for slow-growing mycobacterial AST (Hall, Jude et al. 2011). Antimicrobial drug tolerance varied across RCCS runs, assays and antimicrobial selected. For instance, Alamar Blue showed STREP tolerance in three RCCS runs and no tolerance in another three RCCS runs. Antimicrobial drug tolerance is a phenotype and as such is temporal. In order to establish if the observed Antimicrobial drug tolerance in RCCS-derived biofilms is temporal and "no tolerance" shown in BacTiter Glo and Alamar Blue assays could be because a tolerance phenotype was no longer being transcribed at day 7, Antimicrobial drug tolerance was assayed for up to 14 days using CFU/mL.

4.2.2.2.7 Antimicrobial tolerance measured by viable counting

Research performed by Jindani *et al* showed a bi-phasic kill curve of *M.tb* from human sputa in response to INH treatment, Figure 1.6. This kill profile suggests the presence of an antimicrobial tolerant sub-population of *M.tb* that was identified through viable counting of *M.tb* on solid media. The antimicrobial tolerance profiles described in this chapter however were determined with BacTiter Glo and Alamar Blue, which are liquid based assays. In order to establish if this bi-phasic kill curve could be shown with biofilm-derived bacilli, RCCS #9 and RCCS #10 biofilm and control-derived cultures were treated with 2X MIC (1.56 µg/mL) INH or 2X (1.2 µg/mL) in 96 well microtiter plates and incubated for 14 days. Viable counting was performed every 1-3 days as per Methods section 2.2.2.1. The results of this are discussed below.

4.2.2.2.8 Viable counting did not demonstrate isoniazid tolerance

Viable counting did not show a bi-phasic kill curve, nor did biofilm-derived bacilli show INH tolerance compared to control bacilli, Figures 4.17, 4.18. Interestingly, RCCS #9 and RCCS #10 biofilm-derived cultures were INH tolerant based on percent survival with Alamar Blue and BTG at day seven for 1X MIC (0.8 µg/mL); this increase in biofilm survival at day seven is not reflected by CFU/mL at day seven, Figures 4.17, 4.18.

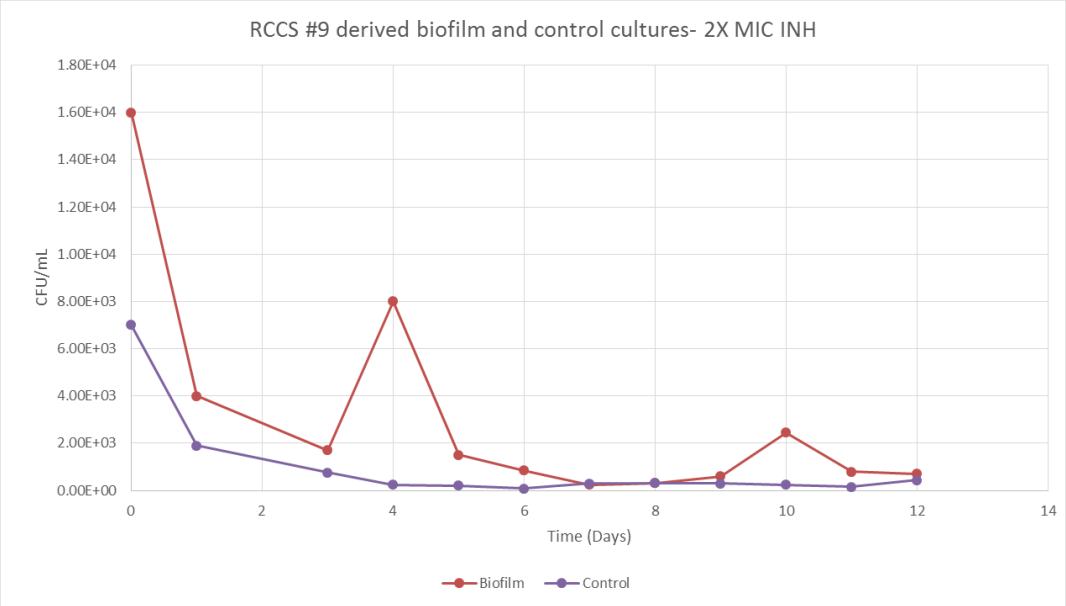

Figure 4.17: CFU/mL do not show INH tolerance in RCCS #9 biofilm-derived bacilli

CFU/mL counts were carried out every 1-3 days for biofilm and control-derived bacilli treated 2X MIC INH. Data points are the mean of two technical replicates ± SEM

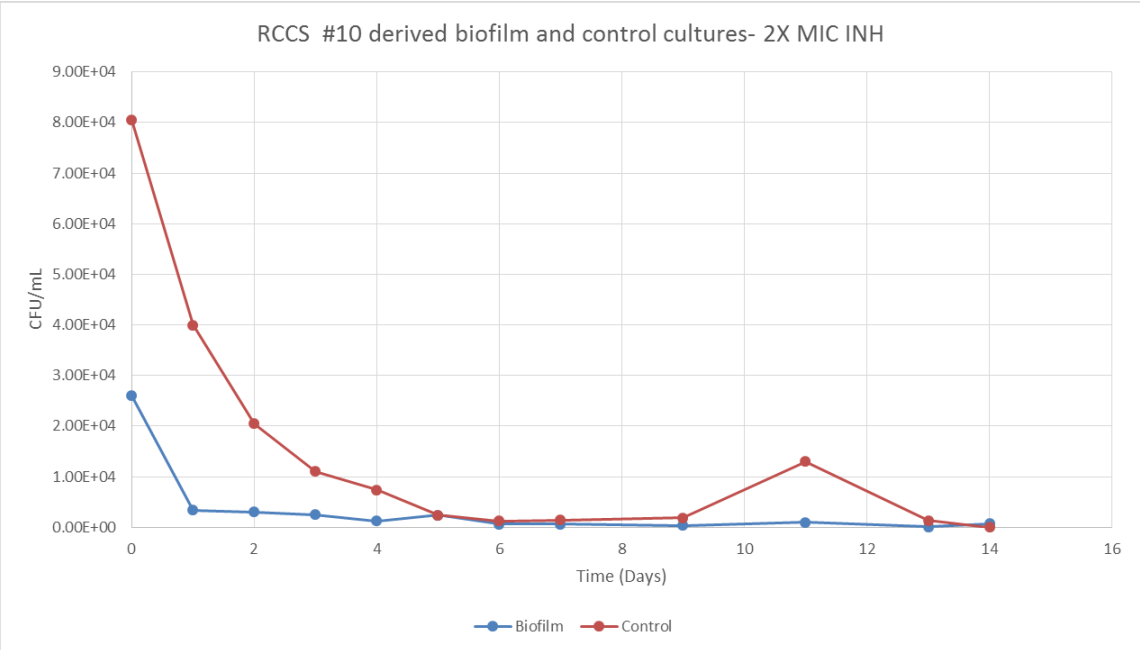

Figure 4.18: CFU/mL do not show INH tolerance in RCCS #10 biofilm-derived bacilli

CFU/mL counts were carried out every 1-3 days for biofilm and control-derived bacilli treated 2X MIC INH. Data points are the mean of two technical replicates ± SEM

4.2.2.2.9 Viable counting demonstrated STREP tolerance

Viable counting of biofilm-derived bacilli treated with 2X MIC STREP showed two distinct profiles for RCCS #9 and RCCS #10, Figures 4.19, 4.20.

RCCS #9 biofilm-derived bacilli showed a rapid increase in CFU/mL at day 3. The CFU/mL of biofilm-derived bacilli decreased over time, and reached a level comparable to control-derived bacilli at day 6. An increase in biofilm-derived bacilli was observed at day 7 but CFU/mL returned to control levels at day 8. This peak at day 7 could be due to a technical error, as day 7 colonies counted to calculate CFU/mL failed to grow when cultured in 7H9 broth supplemented with 2X MIC STREP.

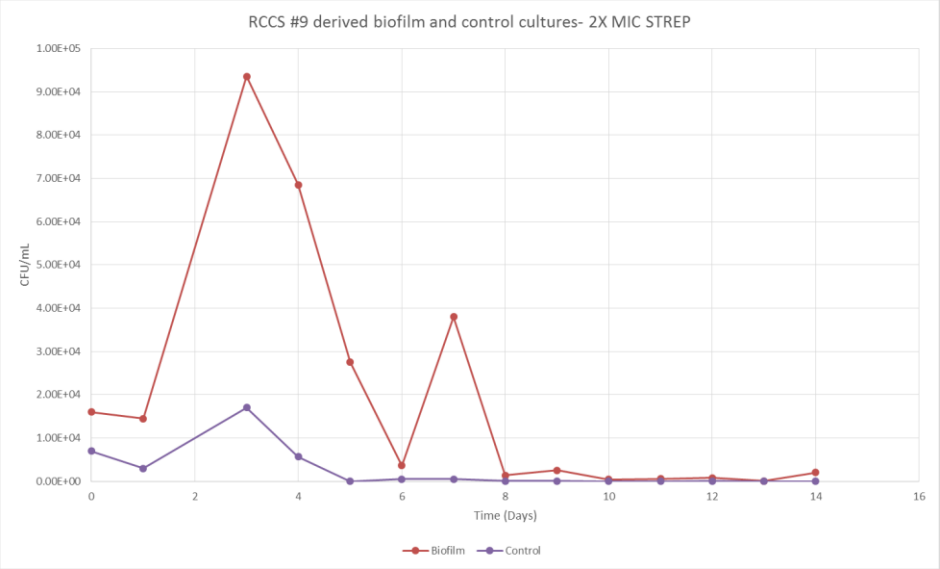

Figure 4.19: Streptomycin tolerance in biofilm-derived bacilli is temporal

Biofilm-derived bacilli were treated with 2X MIC STREP for up to 14 days and plated out onto antimicrobial free 7H10 agar plates with CFU/mL enumerated. Data shown are the mean of two technical replicates ± SEM of one biological replicate

RCCS #10 biofilm-derived bacilli did not show an increase in CFU/mL at day 3 as observed in Figure 4.20. Instead, viable counting showed that there was little reduction in biofilm-derived bacilli numbers in response to STREP over the first 3 days of exposure. By comparison, control-derived bacilli showed a rapid decrease in bacilli over the same period of STREP exposure. Both biofilm and control-derived bacilli reached comparable levels by day 4. Interestingly, there were no colonies for biofilm-derived bacilli at day 7, but BacTiter Glo suggested STREP tolerance for both RCCS #9 and RCCS 10, Table 4.6. These viable counting experiments show biofilm-derived bacilli have increased survival within the first six days of STREP exposure compared to control cultures.

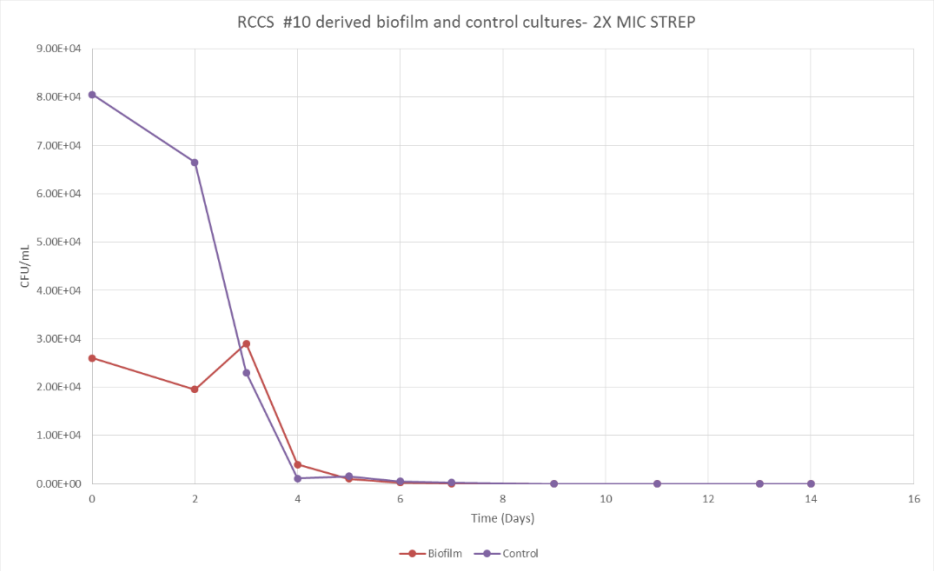

Figure 4.20: Streptomycin tolerance in biofilm-derived bacilli is temporal

Biofilm-derived bacilli were treated with 2X MIC STREP for up to 14 days and plated out onto antimicrobial free 7H10 agar plates with CFU/mL enumerated. Data shown are the mean of two technical replicates ± SEM

4.2.2.2.10 Viable counting demonstrates that antimicrobial drug tolerance is phenotypic

A phenotypic screen was designed to establish whether individual colonies counted for biofilm and control-derived cells (RCCS #9 and RCCS #10) survived INH and STREP treatment due to a tolerance phenotype, or spontaneous genetically encoded antimicrobial resistance mutations that could be selected due to antimicrobial exposure, Figure 4.21. In total, biomass from 1,064 colonies from solid media after INH and STREP exposure that formed Figures (4.17-4.20) were picked individually with sterile 10 µL pipette tips and inoculated into 96 well microtiter plates containing 10X MIC (7.8 µg/mL) INH or 10X MIC (6.0 µg/mL) STREP, alongside 7H9 broth (drug-free) controls to ensure colonies were viable. Alamar Blue was added to all wells after 14 days incubation, mixed well, incubated for a further 24 hours before quantifying fluorescence, Materials and Methods section 2.6.1. Wells were deemed to contain INH or STREP resistant colonies when the following condition was met:

$$Resistance = 10X\ INH, STREP\ fluor\ \geq\ corresponding\ drug - free 7H9\ fluor$$

No STREP resistant colonies were identified using this criterion. Four colonies that were treated with 10X INH (Figure 4.17) were defined as INH resistant. Two biofilm-derived colonies plated on day 1 and day 3, and two control-derived colonies plated on day 3. No other INH resistant mutants were identified at any other time point. Therefore, it was concluded that there were low levels of spontaneous antimicrobial resistant-encoding mutations and that the increase in biofilm-derived bacilli viable counts was due to a phenotype rather than genetically encoded antimicrobial resistance.

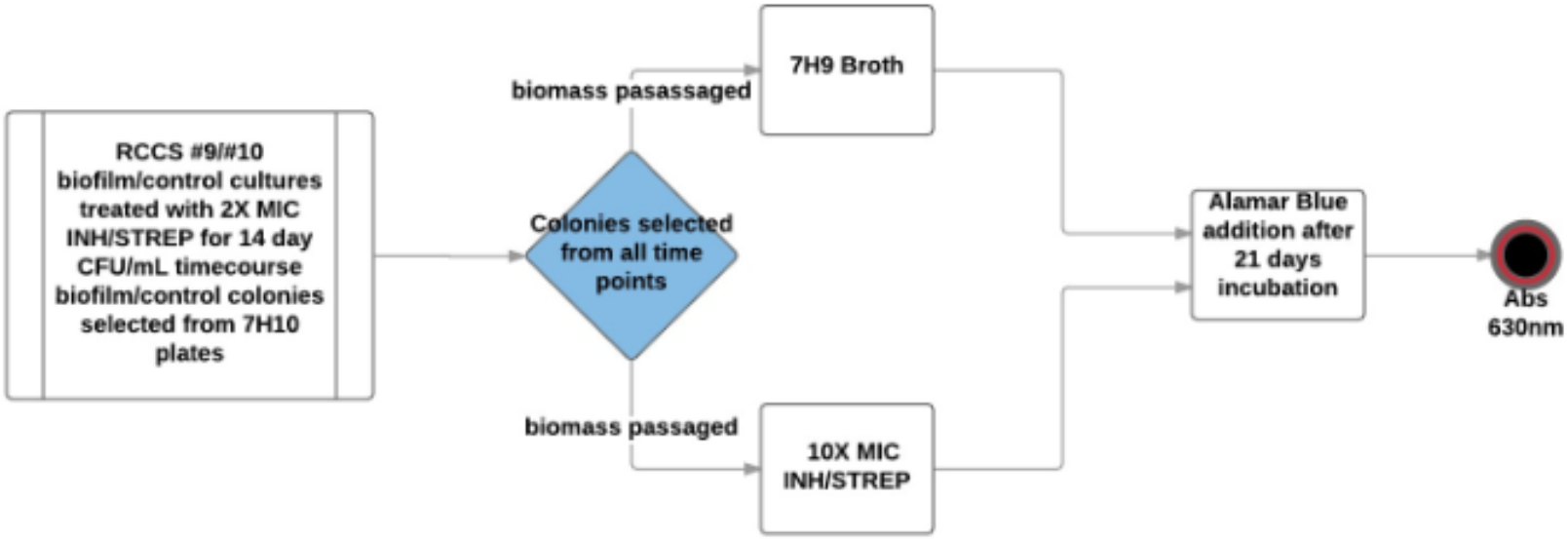

Figure 4.21: Phenotypic screen of single colonies from RCCS biofilm and control cultures exposed to 2X MIC INH or 2X MIC STREP

Colonies from viable count plates after exposure to 2X MIC (Figures 4.17-4.20) were passaged from 7H10 agar plates into 7H9 broth containing 10X MIC INH or 10X MIC STREP if treated before plating with 2X MIC STREP. Alamar Blue was added after 14 days incubation to define antimicrobial resistant mutants.

4.2.2.2.11 Metronidazole treatment of RCCS-derived cultures

Metronidazole (MTZ) is an imidazole pro-drug that requires a reductive environment to convert it to its active form. Once reduced to its active form, MTZ binds DNA covalently leading to inhibition of DNA replication and ultimately cell death (Edwards 1979). Because of the requirement for a reductive environment, MTZ typically only functions against anaerobic bacteria (Muller 1983). To probe the respiratory state of RCCS-derived bacilli, biofilm and control cultures were treated with MTZ for 7 days (Materials and Methods section 2.5) and cell viability measured using BTG (Materials and Methods section 2.6.1). As expected, no MIC could be established for MTZ when tested against an aerobic log phase culture of *M. bovis* BCG using a microbroth dilution method with cell viability quantified with BacTiter Glo, Figure 4.22. The most pronounced effect is 41% inhibition of growth with 250 µg/mL MTZ, which was the highest concentration of MTZ tested. Due to limited RCCS biomass, biofilm and control-derived cultures were tested using two concentrations of MTZ, 10 µg/mL and 1 µg/mL, Figure 4.23. These concentrations have been used in the literature for mycobacterial MTZ susceptibility testing (Betts, Lukey et al. 2002). There was no statistically significant difference between biofilm and control cultures at 10 µg/mL MTZ. There was a significant difference ($p=0.0069$) between biofilm and control-derived cultures at 1 µg/mL MTZ, Figure 4.23. Biofilm survival was 92.6% ± 6.6% compared to 120.9% ± 2.3% for control cultures. From these results it is unlikely that the majority of the bacterial population were respiring anaerobically, otherwise greater MTZ efficacy would have been observed, as seen when hypoxic *M. bovis* BCG-derived from the Wayne Model were treated with MTZ (Lim, Eleuterio et al. 1999).

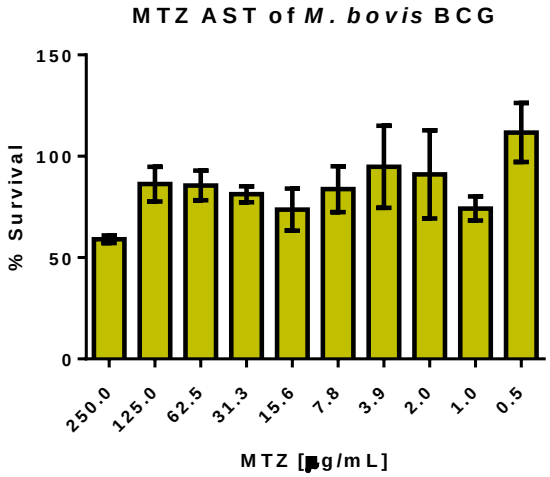

Figure 4.22: MTZ does not kill log phase *M. bovis* BCG

The BacTiter Glo assay was used to establish the MIC of MTZ on aerobic log phase cultured *M. bovis* BCG. As expected, no MIC could be calculated. Growth was reduced by 41% at the highest concentration of 250 µg/mL. MTZ % survival was determined as a percentage of untreated control cultures. Each data point is the mean of three technical replicates ± SEM.

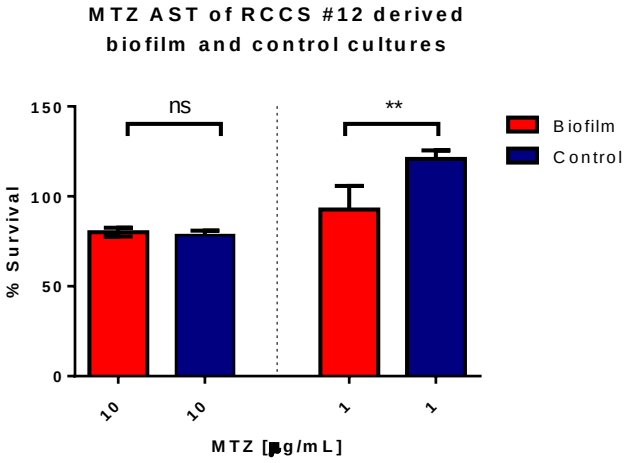

Figure 4.23: MTZ AST RCCS-derived biofilm and control cultures

RCCS biofilm and control-derived cultures were treated with 10 and 1 µg/mL MTZ for seven days and cell viability quantified with BacTiter Glo. Statistical analysis was performed using t-testing. NS (no significance) = $p > 0.05$; * = $p \leq 0.05$; ** = $p \leq 0.01$; *** = $p \leq 0.001$; **** = $p \leq 0.0001$. Each data point is the mean of four technical replicates ± SEM

4.2.2.2.12 Screening of novel antimicrobial compounds

Antimicrobial susceptibility testing (INH, RIF, STREP and MTZ) has been applied so far in this thesis to characterise the metabolic/respiratory state of bacilli in this RCCS biofilm model. To demonstrate the utility of this model for anti-mycobacterial drug discovery, RCCS-derived cultures were used to screen novel anti-mycobacterial compounds to establish their efficacy against bacilli that exhibit tolerance to clinically relevant TB antimicrobials. Sesquiterpenes are a chemical class that occur naturally in plants and insects. *Calea uniflora,* a flowering plant endemic to the Amazon rainforest, has been widely used in Brazilian folk medicine to treat a range of conditions, including bacterial infections. Research carried out by Dr Leticia Muraro Wildner at Brighton and Sussex Medical School in conjunction with Universidad Federale de Santa Catarina showed that a series of these compounds were efficacious against *M.tb in vitro*. Three compounds were identified to have most anti-mycobacterial activity in aerobic log phase conditions; compound A, compound B and compound C. These compounds were also tested in a Nutrient Starvation model of *M.tb* designed to induce an antimicrobial tolerant phenotype (Betts, Lukey et al. 2002). The efficacy of these three novel compounds was tested against RCCS-derived biofilm and control cultures using a microbroth dilution method detailed in section2.5.2. Interestingly, biofilm cultures showed statistically significant tolerance to all three compounds compared to control cultures, Figure 4.24.Compound B reduced control survival by 34% at 12.5 µg/mL, whereas biofilm-derived bacilli survival was not significantly reduced (by 65%) until 50 µg/mL. Importantly, compound B exposure actually increased biofilm derived bacilli survival by as much as 100% for 6.3 µg/mL. Drug C inhibited biofilm and control bacilli to same extent, with the exception of 50 µg/mL where biofilm-derived bacilli had statistically significant higher survival. Based on this experiment, the RCCS could play a role in screening of novel anti-mycobacterial compounds that could maintain efficacy against antimicrobial-tolerant populations.

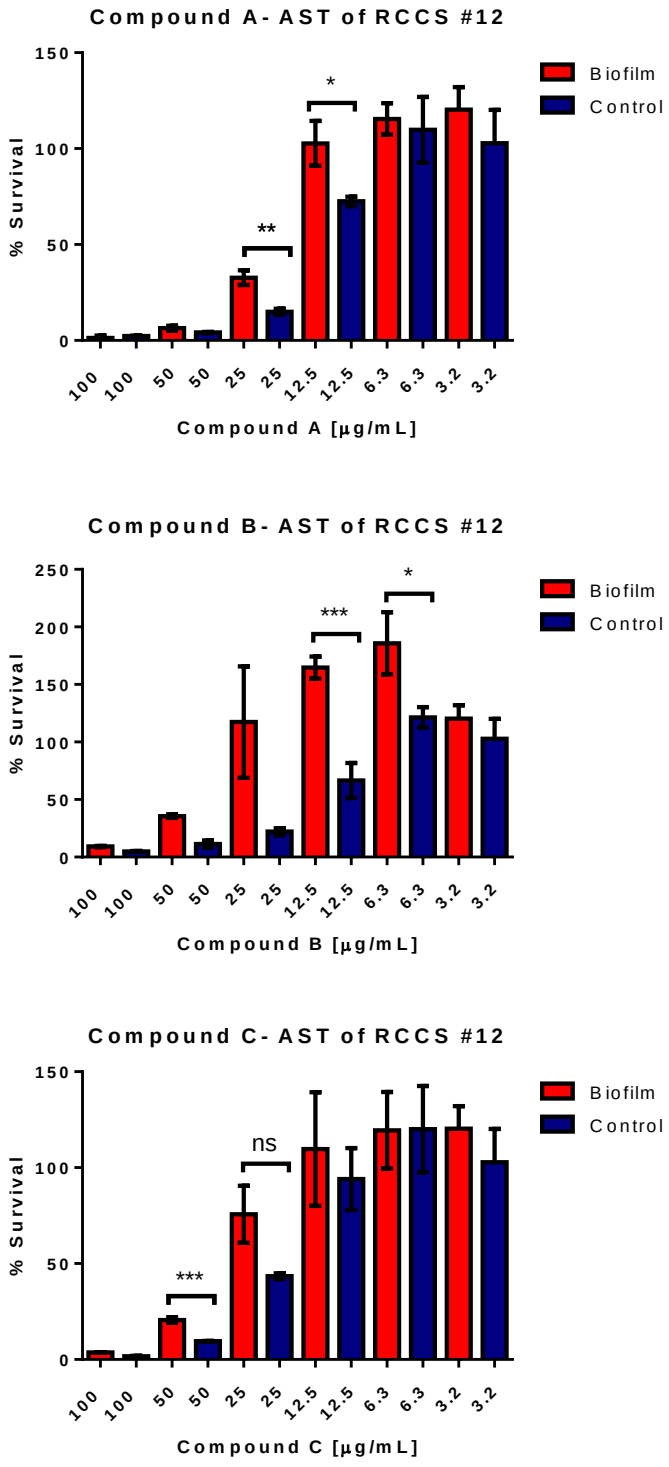

Figure 4.24: Biofilm-derived bacilli show tolerance to novel antimicrobial compounds

RCCS-derived biofilm and control cultures show antimicrobial tolerance to compound A, compound B and compound C. A microbroth dilution method was used to screen three novel antimycobacterial compounds on planktonic suspensions of RCCS-derived biofilm and control-derived cultures. Statistical analysis was performed using t-testing. NS (no significance) = $p > 0.05$; * = $p \leq 0.05$; ** = $p \leq 0.01$; *** = $p \leq 0.001$; **** = $p \leq 0.0001$. Each data point is the mean of three technical replicates ± SEM.

4.3 Discussion

Bacterial biofilms have been well documented to be recalcitrant to antimicrobial chemotherapy (Stewart 2015). The presence of an extracellular matrix (ECM) not only facilitates adhesion of biofilms to host tissues or medical devices (Limoli, Jones et al. 2015), but also affords physical protection to bacteria within the biofilm from environmental and chemical insults, such as antimicrobial exposure. As is evident from the limited efficacy of INH and STREP on non-homogenised biofilms, antimicrobials may fail to penetrate the mycobacterial clusters that grow in the RCCS system. Interestingly however, when biofilms are homogenised to planktonic suspensions and the physical features of biofilm growth removed, bacilli continue to exhibit antimicrobial drug tolerance up until day 7. As the physical barrier of mycobacterial clumping was no longer in place, antimicrobial drug tolerance was not caused by protection of bacilli by an extensive ECM or similar, but rather phenotype changes to bacilli that conferred drug tolerance to selected first and second line TB drugs.

Biofilm-derived bacilli were identified as antimicrobial drug tolerant if there was a statistically significant increase in mycobacterial survival compared to control cultures. Two assays were used to quantify this cell survival; BacTiter Glo for seven RCCS ASTs and Alamar Blue for six RCCS ASTs. Both assays correlated to varying extents on biofilm tolerance, control tolerance or no tolerance depending on the antimicrobial used. Biofilm tolerance was observed for both assays for four RCCS INH susceptibility testing; one RIF susceptibility testing and three STREP susceptibility testing. Despite both assays not correlating on all RCCS AST carried out, two assays were used for AST endpoint measurement for a number of reasons. Data would not be lost if assay issues invalidated data generated from one of the assays; descriptiveness of results would increase as BacTiter Glo details intracellular ATP and Alamar Blue is indicative of metabolic activity; artefactual data is reduced through analysing cell viability through two redundant mechanisms, e.g. signal generated from antimicrobials; both assays vary in specificity and sensitivity. As every RCCS run would yield at most ~10 mL of biofilm culture and ~10 mL of control culture after three weeks, reducing assay error was crucial, as the amount of technical replicates that could be inoculated for AST was limited. False positives could occur through contamination of a well, or not accounting for fluorescence of carrier controls. False negatives could occur when there is growth in a well but an assay fails to detect this. Employing two redundant assays to measure the same endpoint can greatly improve specificity and sensitivity, which reduce type I and type II errors respectively. Despite the advantages of both assays, BTG had a more dynamic range of RLU (0- 400,000) compared to the range of RFU from Alamar Blue (0-2000).

Because of this, BTG was more sensitive than Alamar Blue and could discriminate more effectively where there was relatively small variation between wells.

INH tolerance in biofilm-derived cells was observed using both BTG and Alamar Blue at day 7 of antimicrobial treatment- meaning that the phenotypic changes that occurred in the RCCS biofilm still influenced INH drug action as much as 7 days after resuspension of homogenised bacilli in media designed for logarithmic growth. This tolerance was not observed when using viability counts over a time course of 14 days. In active TB infection in the human lung treated with INH, a bi-phasic kill curve is seen when viable counts of sputa are carried out (Jindani, Aber et al. 1980). An initial rapid decline in bacilli that are actively metabolising and sensitive to INH is followed by a prolonged decrease in viable counts at a much slower rate, which is hypothesised to represent a slow growing or non-dividing sub-population. INH-tolerant biofilm-derived cells from the RCCS did not show this biphasic kill curve when re-suspended in fresh media containing INH. This biphasic kill curve may not have been observed using viable counting and RCCS-derived biofilm bacteria due to the mode of action of INH. INH primarily targets the mycobacterial cell wall. Dhar *et al* showed that *M. tuberculosis* cultures that were recovered onto 7H10 after exposure to a cell wall targeting drug have up to a 10 fold decrease in CFU/mL count due to the presence of Malachite Green (MG) in 7H10 (Gelman, McKinney et al. 2012) compared to MG free 7H10. MG is a broad spectrum antimicrobial added to 7H10 to prevent extra-experimental contamination during the four-week incubation required to culture slow growing mycobacteria. However, bacilli that have been exposed to a cell wall targeting antimicrobial such as INH are more susceptible to MG cytotoxicity. This is likely due to two mechanisms; increased membrane permeability allowing enhanced cell entry of MG (Banaei, Kincaid et al. 2009), (Bianco, Blanco et al. 2011) and MG generating reactive oxygen species (ROS) within the cell that may potentiate the ROS generated by INH (Panandiker, Maru et al. 1994). Because of this INH-MG synergistic toxicity, CFU counts may not be an appropriate cell viability measure in RCCS induced INH tolerance.

Alternatively, INH tolerant bacilli may not be viable on solid media. Mounting evidence suggests that a population of antimicrobial tolerant bacilli may exist as Viable but Non-Culturable (VBNC) within antimicrobial tolerant cultures, (Li, Mendis et al. 2014, Salina, Waddell et al. 2014), (Ramamurthy, Ghosh et al. 2014). These bacilli can grow in liquid culture, but cannot be cultured on solid media. This may lead to underestimation of the number of bacilli present if viable counting is used as the sole measure of antimicrobial efficacy. In order to ensure that these VBNC bacilli were being accounted for, AST was performed using liquid culture. A broth culture assay (BCA) was used to confirm that wells that were INH, RIF or STREP tolerant contained more bacilli, i.e. a BCA would

confirm the results from BTG and Alamar Blue. BCA confirmed that biofilm-derived bacilli had a two-log increased survival after 7-day treatment with INH compared to control cultures. BCA confirms STREP tolerance; one of the three replicate wells that had been treated with 0.25 µg/mL STREP for seven days was positive for growth at 10^{-6} dilution, while all three replicates grew at 10^{-4} dilution. Control-derived bacilli treated under the same conditions only grew until 10^{-3} dilution, suggesting at least a log difference in biofilm-derived bacilli survived STREP treatment compared to control-derived bacilli.

Two distinct STREP growth curves were observed for CFU/mL counts carried out for biofilm-derived bacilli. For RCCS #9, a 6-fold increase in CFU/mL by day three was observed that continued to decline until day 6. For RCCS #10, CFU/mL remained stable for the first three days of 2X MIC STREP treatment while control-derived bacilli showed a continued reduction in CFU/mL despite control cultures having a higher initial inoculum than biofilm-derived cultures. The mechanism of action of STREP is to inhibit protein synthesis through binding to the 16S subunit of the 30S bacterial ribosome, unlike INH, which is a cell wall inhibitor. As such, Malachite Green (MG) will not exert a synergistic antimicrobial effect on bacilli that have been exposed to STREP and CFU/mL can be enumerated on 7H10 agar plates.

RIF is a highly effective antimicrobial drug *in vitro* against *M. bovis* BCG, indicated by its low MIC value of 0.013 µg/mL and 0.025 µg/mL for BacTiter Glo and Alamar Blue respectively. RIF tolerance was observed for both biofilm and control cultures but without an obvious pattern. There was a much lower percent survival with RIF compared to INH and STREP, and RIF tolerance did not show high levels of bacilli surviving 7-day treatment with RIF. In conclusion, there is not enough evidence to suggest that biofilm-derived bacilli are tolerant to RIF.

AST of RCCS-derived cultures was designed to examine antimicrobial tolerance at day 7 after resuspension in fresh media, i.e. bacilli are entering a growth permissive state after a potentially non-permissive microenvironment of a biofilm. This is likely to mirror conditions *in vivo*, with resuscitation of bacilli occurring upon exposure to a new microenvironment that is nutrient rich, such as a caseating granuloma. Importantly, there have been two biofilm models of *M.tb* that showed drug-tolerance (Trivedi, Mavi et al. 2016). (Ojha, Baughn et al. 2008). However, both of these models conducted AST on whole biofilms with homogenisation to planktonic suspensions. The AST presented in this chapter was performed on planktonic bacilli derived from biofilms, and showed INH and STREP tolerance. This is important as it shows that biofilm associated antimicrobial tolerance is a phenotype, and that bacillary antimicrobial tolerance does not derive from physical protection from residing within a biofilm.

Two approaches were applied to understand whether reduced drug efficacy in this biofilm model of TB was due to the accumulation of spontaneous antimicrobial resistance-conferring mutations or a change in mycobacterial phenotype that induced antimicrobial drug tolerance. Firstly, biofilm and control-derived cultures were passaged three consecutive times into antimicrobial free 7H9 ADC, Tween 80 and INH, RIF and STREP AST conducted. No statistically significant difference in survival was observed for biofilm compared to control cultures, suggesting that antimicrobial resistance-conferring mutations did not accumulate in the RCCS system, and that differences in antimicrobial efficacy seen in AST in bacilli extracted from the system immediately were likely be due to phenotypic antimicrobial tolerance.

Secondly, 1,064 colonies from serial viable counts after drug treatment were passaged into 7H9 ADC, Tween 80 with/without 10X INH or 10X STREP to screen for spontaneous antimicrobial resistance. No STREP resistant colonies from either biofilm or control-derived STREP treated colonies were identified. Two biofilm-derived colonies were identified as INH resistant and two control-derived colonies were identified as INH resistant; suggesting that emergence of INH resistance is minimal and evenly distributed between biofilm and control cultures. INH resistant colonies were stored at -80°C for future PCR amplification and sequencing to confirm INH resistance.

RCCS vessels were specifically designed to facilitate gaseous exchange and maintain culture media as aerobic; however, Methylene Blue results were inconclusive as to the oxygen tension of biofilm and control cultures in RCCS vessels. A homogenously hypoxic culture of *M. tuberculosis*-derived from the Wayne Model exhibited a 99.8% reduction in recoverable CFU/mL when treated with 8 µg/mL MTZ for 8 days, showing the efficacy MTZ exerts on anaerobic mycobacteria (Wayne and Sramek 1994). MTZ requires an anaerobic environment to reduce its nitro side group, which is required for its cidal DNA damaging effects in bacteria. In RCCS-derived bacilli treated with 1 µg/mL MTZ, a statistically significant difference was found between biofilm-derived bacilli (92.6% ± 6.6%) compared to control-derived bacilli (120.9% ± 2.3%). MTZ AST of log phase, aerobically grown bacilli showed a reduction in cell survival at the same concentration (74.2% ± 3.4%), Figure 4.22. Despite a reduction of 7.4% in biofilm-derived bacilli, it is still considerably less than the 25.8% reduction observed for aerobic log phase *M. bovis* BCG. Both RCCS-derived biofilm and control cultures exhibit less MTZ induced toxicity than aerobic *M. bovis* BCG at 1 µg/mL MTZ, suggesting that RCCS-derived cultures are not respiring anaerobically.

Antimycobacterial drug development faces several bottlenecks. Rates of lead compound attrition within drug development pipelines remains high and with a lack of appropriate *in*

vitro models of drug tolerant mycobacterial sub-populations hypothesised to be the cause of long treatment times. As described above, RCCS biofilm-derived bacilli exhibit an Antimicrobial tolerance phenotype when exposed to INH and STREP. RCCS biofilm and control-derived bacilli were screened with three novel antimycobacterial compounds (compound A, compound B and compound C) in order to establish if the RCCS could be used to predict compound efficacy against antimicrobial tolerant bacilli.

Two-tailed unpaired t-tests were used to establish statistically significant differences in cell survival between RCCS-derived biofilm and control bacilli. Compound B shows a 66.5% survival in control bacilli at 12.5 µg/mL, while at the same concentration biofilm-derived bacilli have had a statistically significant (P=0.0007) increase in growth (164.6%); biofilm-derived cell survival does not decrease below 100% until treated with 50 µg/mL compound B.

Differences in biofilm and control-derived bacilli treated with compound A were less pronounced than compound B but still statistically significant. At 12.5 µg/mL compound A, biofilm-derived bacilli showed 107.6% ± 6.8% cell survival compared to 72.4% ± 1.4% for control-derived bacilli (P=0.0119). Biofilm-derived cell survival decreases to 32.8% ± 2.2% at 25 µg/mL compound A, a statistically significant (P=0.0094) two fold increase in cell survival compared to control-derived cell survival of 14.9% ± 1.2%.

Finally, compound C showed the least statistically significant biofilm-derived cell survival compared to control-derived cell survival out of all three compounds, suggesting that biofilm-derived bacilli were least tolerant to this compound. Higher doses of compound C were however required for efficacy and biofilm-derived bacilli showed tolerance at 50 µg/mL of 20.6% ± 0.8% compared to control-derived cell survival of 9.5% ± 0.1%. AST of RCCS-derived cultures with compounds A, B and C demonstrates the importance of incorporating antimicrobial tolerance in screening of novel compounds for the treatment of TB.

Antimicrobial tolerance induced in RCCS biofilm formation was characterised using INH, RIF, STREP and MTZ. Importantly, this antimicrobial tolerance was shown to be phenotypic and not encoded by antimicrobial resistance spontaneous mutations. The RCCS model has been adapted to screen three novel anti-TB compounds and showed biofilm-derived bacilli had least tolerance of compound C, suggesting that this candidate could be efficacious in targeting antimicrobial tolerant bacilli. RCCS-derived cultures were further characterised through transcriptional profiling and pathogen-host interactions, described in chapters 5 and 6.

Chapter 5: Transcriptional analyses of RCCS-derived biofilms

5.1 Overview

Completion of the *M.tb* genome sequence in 1998 (Cole, Brosch et al. 1998) facilitated the design of micro arrays containing probes for all annotated genes (Wilson, DeRisi et al. 1999). Since then, this technology has contributed significantly to tuberculosis research. Microarrays quantify the degree of hybridisation of fluorescently labelled mRNA (or cDNA) molecules to complementary DNA oligonucleotides bound to a support structure such as a glass slide. Tiling arrays are based on the same principle but the probes overlap with each other on either strand of DNA through the whole genome. This allows for greater in-depth interrogation of the bacterial transcriptome, measuring expression from both sense and antisense strands and intergenic regions (Mockler, Chan et al. 2005). The amount of fluorescence generated based on mRNA-DNA oligonucleotide hybridisation is quantified, and thus the amount of mRNA present estimated in relation to comparator samples. These Agilent microarrays used in this study were designed at the Bacterial Microarray Group at St Georges, University of London with short oligonucleotide (>100 mer) probes.

Transcriptional profiling of *M.tb* has been used to characterise and define bacterial physiology, metabolism and pathogen-host interactions in both *in vivo* and *in vitro* environments. The transcriptional profile of *M.tb* after INH treatment was one of the first microarray data sets to be published and examined *M.tb* drug responses (Wilson, DeRisi et al. 1999). INH selectively inhibits mycolic acid synthesis through targeting the enoyl acyl carrier protein reductase InhA; transcriptional profiling showed several genes were induced by INH that were associated with the drug's mode of action, including type II fatty acid synthase enzymes. A number of genes were also shown to be upregulated that were not within pathways known to be affected by INH but likely to be linked to INH induced toxicity, illustrating how micro arrays can identify novel drug-induced pathways or targets. Following on from drug responses, microarrays have been used to probe pathogen-host interactions. The transcriptional adaptation of *M.tb* within macrophages was characterised in 2003 by Schnappinger *et al* (Schnappinger, Ehrt et al. 2003). The study described a distinct transcriptional profile that was induced intracellularly and how *M.tb* altered gene expression to adapt to an intracellular environment. Upregulation of IFN-γ and nitric oxide induced *M.tb* stress response signatures along with a shift from aerobic to anaerobic metabolism and increased β-oxidation of fatty acids, which illustrated the plasticity of mycobacterial metabolism (Schnappinger, Ehrt et al. 2003). The role for transcriptional profiling in TB was expanded from investigating drug

responses and pathogen-host interactions to investigating the transcriptional state of *M.tb* in human sputa. Smear positive sputum samples were collected from the Gambia and transcriptional profiling performed using micro arrays (Garton, Waddell et al. 2008). DosR was the most upregulated regulon in sputum; additionally the induction of isocitrate lyase (*icl1*) and triacylglycerol synthase (*tgs1*) suggested a shift in metabolism towards lipid utilisation. Building upon this research, Honeyborne *et al* profiled the transcriptome of *M.tb* in sputa before and during standard drug therapy in fifteen patients (Honeyborne, McHugh et al. 2016). The study showed that the transcriptional profile at day 7 and day 14, by which time *M.tb* subpopulations were hypothesised to be drug tolerant (Jindani, Dore et al. 2003), was similar to sputa-derived bacilli before drug treatment started. This suggests that there is a pre-existing, drug-tolerant sub-population that is slow or non-replicating present in sputa (and by extension, the lung) before drug therapy commences.

The previous chapter detailed drug tolerance of biofilm-derived bacilli in response to treatment with INH, RIF and STREP. The aim of this chapter was to perform transcriptional profiling of RCCS-derived biofilms using tiling microarrays to identify genes that may be implicated in the development of the drug-tolerant phenotype observed in biofilm-derived bacilli.

5.2 Results

5.2.1 Selection criteria for the tiling microarray analysis

The transcriptional profiles of four conditions in triplicate biological replicates were analysed by tiling microarray: Sauton's no Tween log phase 7-day culture (n=3), Sauton's no Tween stationary phase 21-day incubation (n=3), RCCS-derived biofilm cultures after 21 days incubation and RCCS-derived controls (n=3) after 21 days incubation (Materials and Methods section 2.7). A total of 177,427 data points were generated for each tiling array corresponding to one biological replicate of each condition, with each data point representing an oligonucleotide probe tiling through the *M.tb* H37Rv genome sequence. Tiling arrays were normalised to the 75th percentile of each tiling arrays' total expression, allowing comparison of expression ratios between arrays. Box plots of the array normalised dataset is shown for Sauton's no Tween log phase/ stationary phase, RCCS-derived biofilms and RCCS-derived controls, Figure 5.1.

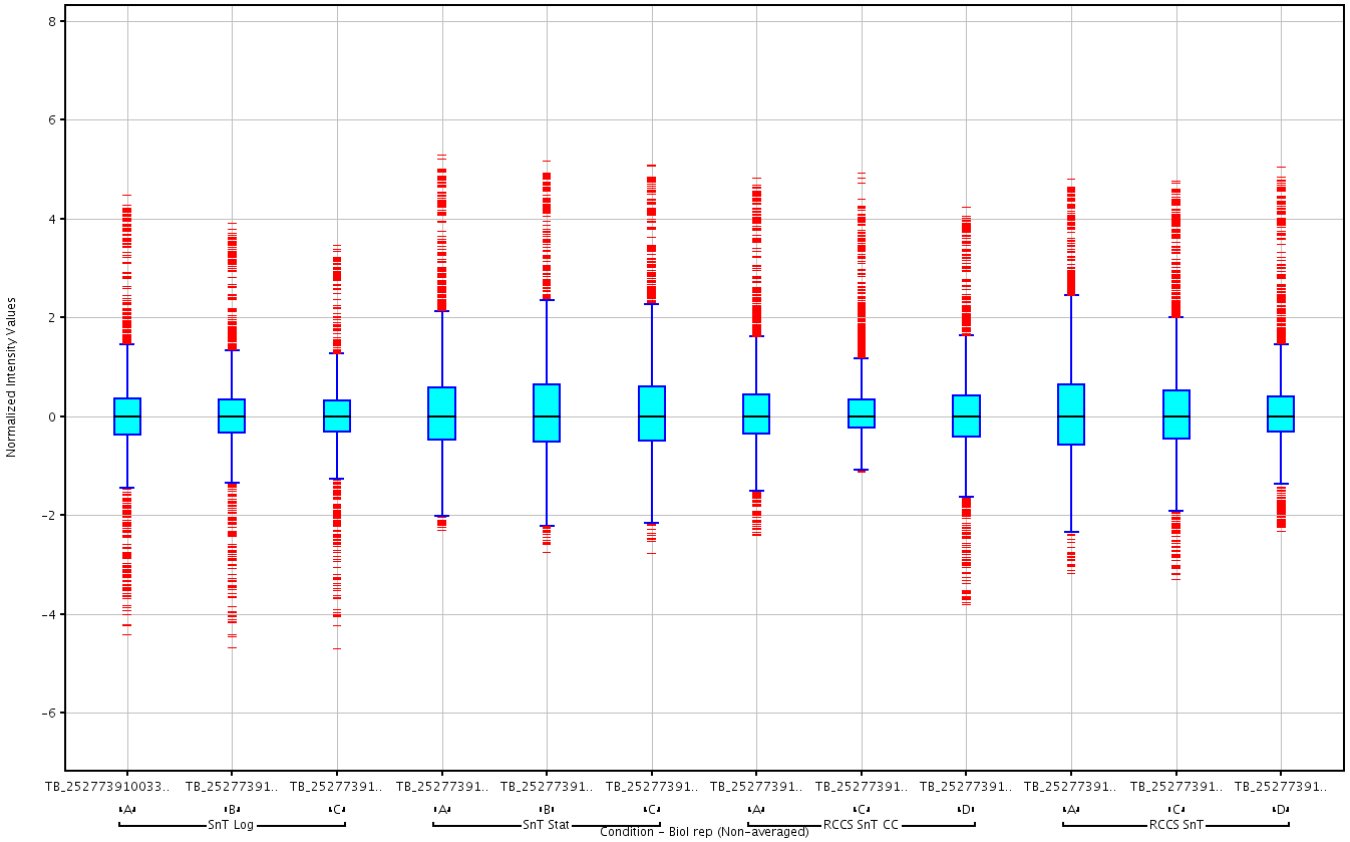

Figure 5.1: Normalisation of tiling array expression data

Tiling array expression data were normalised by dividing the tiling array expression data by the 75th percentile expression value of each array, allowing comparison between tiling arrays. The distribution of 177,247 probes per array are displayed as box plots. X-axis: A, B, C or D represent biological replicates of each condition. Four separate conditions are represented: SnT log: Sauton's no Tween log phase; SnT Stat: Sauton's no Tween stationary phase; RCCS SnT CC: Sauton's no Tween RCCS control vessel post 21 days' incubation; RCCS SnT: Sauton's no Tween RCCS biofilm vessels post 21 days' incubation. Y-axis: normalised intensity values.

Normalised tiling array data points (177,247 per array) were averaged per sense or anti-sense strands for each gene, intergenic regions or controls yielding 11,176 data points. The probe list was further filtered to remove control and intergenic probes, yielding 7,798 sense and anti-sense H37Rv genes. The sense gene probes were removed (since in this analysis alternative, antisense and small RNA expression from the alternative strand was not considered) to generate a final gene list of 3,986 H37Rv genes to analyse further. Principle component analysis (PCA) was performed on these 3,986 genes to examine the variation between biological replicates and conditions, Figure 5.2.

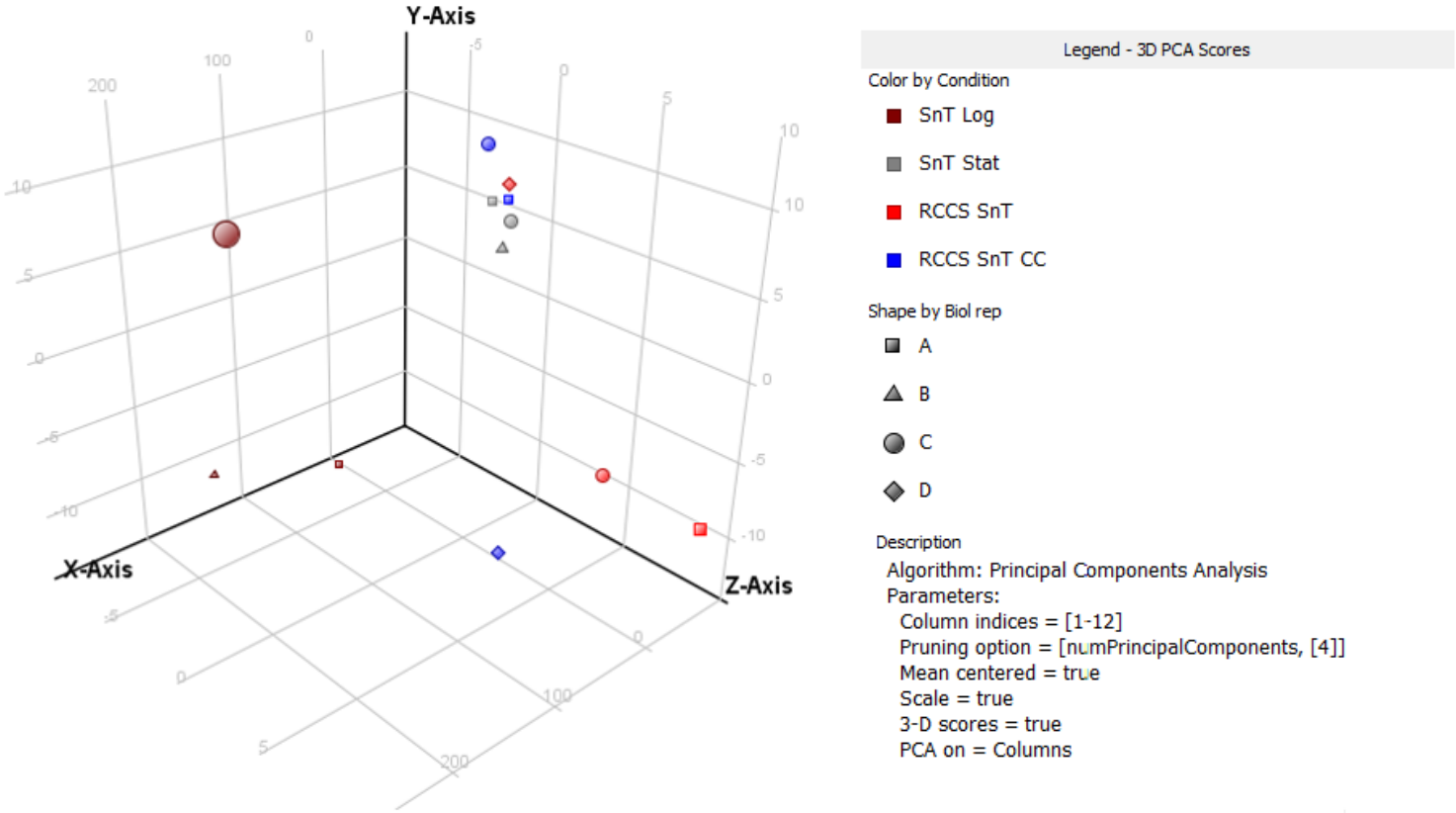

Figure 5.2: Principal component analysis plot of tiling array biological replicates

Biological replicates of Sauton's Modified Media no Tween 80 log phase, stationary phase, RCCS-derived biofilms and RCCS-derived controls after filtering to display 3,986 anti-sense genes. Conditions are represented by colours; brown: Sauton's no Tween log phase; grey: Sauton's no Tween stationary phase; red: RCCS-derived biofilms; RCCS-derived control cultures. Biological replicates are represented by shape; square: replicate A; triangle: replicate B; circle: replicate C; diamond: replicate D.

Hierarchical clustering was then performed on median-normalised gene profiles, generated by normalising the transcriptional profiles of each gene to the median expression of that gene across the dataset. Similar samples should cluster together. Four clusters were generated that show conditions cluster primarily together, with one RCCS biofilm and one RCCS control clustering with RCCS controls and log phase clusters respectively, Figure 5.3.

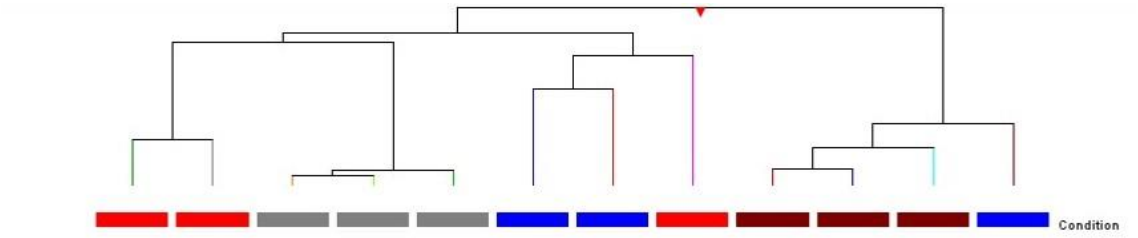

Figure 5.3: Hierarchical clustering of tiling array data

Dendrogram of the median normalised gene expression values from three replicate samples, displaying a separation of samples into four distinct clusters. Red: RCCS-derived biofilm cultures; blue: RCCS-derived control cultures; grey: Sauton's Modified Media no Tween 80 stationary phase; brown: Sauton's Modified Media no Tween 80 log phase.

A modified t-test with Benjamini-Hochberg multiple testing correction with p value ≤0.05 and a fold change of ≥2.0 was used to determine if genes significantly differed between RCCS-derived biofilms and Sauton's no Tween stationary phase. This comparison should identify genes involved in the adaptation to biofilm-like growth. A total of 96 significantly differentially expressed genes were identified between these two conditions, Figure 5.4. The microarray analysis pathway to identify and explore these genes is summarised in Figure 5.5.

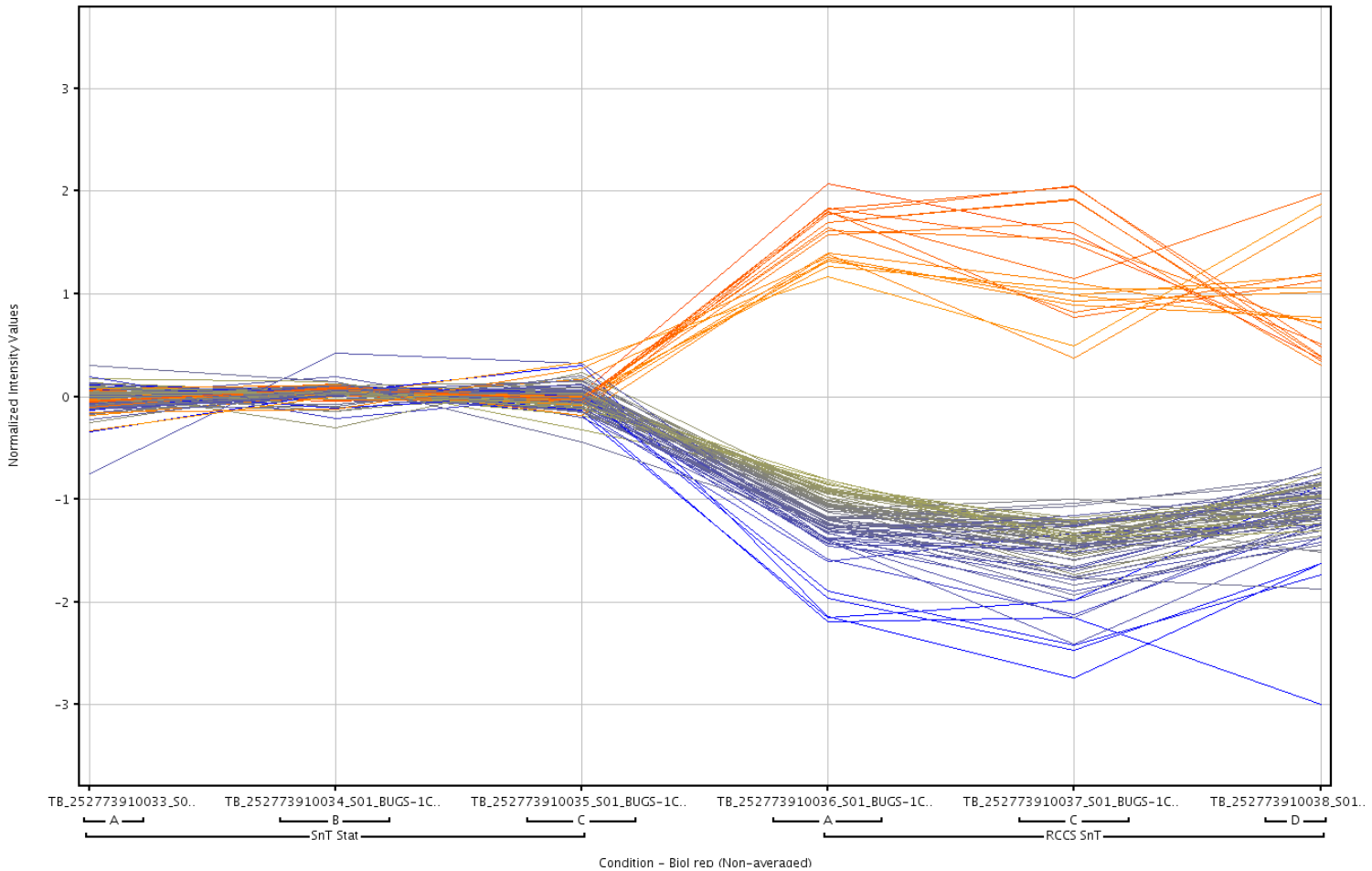

Figure 5.4: Line plot of significant differentially expressed genes in RCCS-derived biofilms compared to stationary phase bacilli

Line plot showing the expression of 96 significantly differentially expressed genes in each biological replicate of stationary phase bacilli and RCCS-derived biofilms. The dataset has been normalised to stationary phase for clarity. Red: genes upregulated in biofilms compared to stationary phase bacilli; blue: genes are downregulated in biofilm compared to stationary phase bacilli. X-axis: normalised intensity values; Y-axis: biological replicates from each condition.

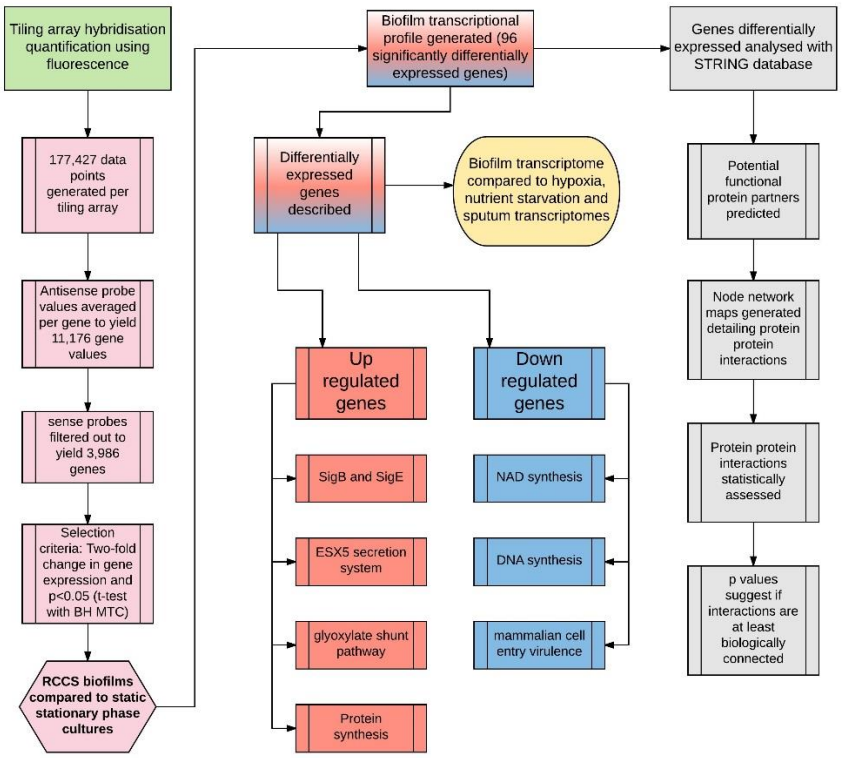

Figure 5.5: Summary of transcriptional profiling methodology

Differentially expressed genes in RCCS-derived biofilms were defined against stationary phase bacilli. BH MTC: Benjamini-Hochberg multiple comparison testing. Differentially expressed genes were then compared to the *M.tb* transcriptomes derived from models of hypoxia, nutrient starvation and from sputum. Predicted functional partners of differentially expressed genes were determined using STRING database analysis.

5.2.2 The transcriptional response to RCCS-derived biofilm growth in comparison to stationary phase cultures

M. bovis BCG mRNAs were hybridised to tiling arrays based on the *M.tb* H37Rv genome, so to verify the techniques applied here, it was necessary to first confirm that genes identified to be differentially expressed were indeed present in the *M. bovis* BCG genome. Gene sequences for the 96 differentially expressed genes were obtained from TubercuList (www.tuberculist.org) and a nucleotide BLAST search was performed on the genome sequence of *Mycobacterium bovis* BCG str. Pasteur 1173P2 using the U.S. National Library of Medicine online BLASTn suite. All differentially expressed genes were confirmed to be present in *M. bovis* BCG strain Pasteur with ≥99% sequence similarity to *M.tb* H37Rv. Protein-protein interactions (PPI) of genes that were differentially expressed were investigated using the Search Tool for the Retrieval of Interacting Genes/proteins (STRING) database. STRING analysis establishes both physical and

functional associations of proteins based on computational prediction and experimental data (Szklarczyk, Morris et al. 2017).

A total of 19 genes were upregulated and 77 genes downregulated in biofilm cultures compared to stationary phase bacilli. Genes were sorted by functional category using www.tuberculist.org, with seven “information pathways”, five “cell wall and cell processes”, three “intermediate metabolism and respiration”, three “conserved hypotheticals” and one “PE/PPE family” upregulated, Table 5.1. For downregulated genes, 77 genes were identified as downregulated, with 62 of these being identified as “possible” or “predicted” gene products. These 62 genes of unknown function were not analysed further. Six “virulence, detox and adaptation”, three intermediate metabolism and respiration”, two “cell wall processes”, two “information pathways” and two “PE/PPE families” were down regulated, Table 5.2.

Gene	Gene Name	Protein Function	Regulation	Fold Change	Functional Category	p Value
esxN	Rv1793	Putative ESAT-6 like protein EsxN (ESAT-6 like protein 5)	up	2.29	Cell wall and cell processes	0.0496
esxJ	Rv1038c	ESAT-6 like protein EsxJ (ESAT-6 like protein 2)	up	2.65	Cell wall and cell processes	0.0433
esxP	Rv2347c	Putative ESAT-6 like protein EsxP (ESAT-6 like protein 7)	up	2.51	Cell wall and cell processes	0.0420
esxW	Rv3620c	Putative ESAT-6 like protein EsxW (ESAT-6 like protein 10)	up	2.50	Cell wall and cell processes	0.0472
esxM	Rv1792	ESAT-6 like protein EsxM	up	2.73	Cell wall and cell processes	0.0337
sigB	Rv2710	RNA polymerase sigma factor SigB	up	2.36	Information pathways	0.0143
sigE	Rv1221	Alternative RNA polymerase sigma factor SigE	up	2.25	Information pathways	0 .0433
Rv0516c	Rv0516c	Possible anti-anti-sigma factor	up	2.33	Information pathways	0.0064
greA	Rv1080c	Probable transcription elongation factor GreA (transcript cleavage factor GreA)	up	3.12	Information pathways	0.0031
infA	Rv3462c	Probable translation initiation factor if-1 InfA	up	2.24	Information pathways	0.0027
rpsT	Rv2412	30S ribosomal protein S20 RpsT	up	2.11	Information pathways	0.0063
rpsL	Rv0682	30S ribosomal protein S12 RpsL	up	2.18	Information pathways	0.0024
icl1	Rv0467	Isocitrate lyase Icl (isocitrase) (isocitratase)	up	2.00	Intermediate metabolism and respiration	0.0061
Rv0097	Rv0097	Possible oxidoreductase	up	2.53	Intermediate metabolism and respiration	0.0494
Rv2451	Rv2451	Hypothetical proline and serine rich protein	up	2.02	Conserved hypotheticals	0.0078
Rv0100	Rv0100	Conserved hypothetical protein	up	2.43	Conserved hypotheticals	0.0276
cadI	Rv2641	Cadmium inducible protein CadI	up	2.27	Conserved hypotheticals	0.0496
PE19	Rv1791	PE family protein PE19	up	2.42	PE/PPE families	0.0126
hisE	Rv2122c	Phosphoribosyl-AMP pyrophosphatase HisE	up	2.15	Intermediate metabolism and respiration	0.0055

Table 5.1: Upregulated genes in RCCS derived biofilms

A total of 19 genes were upregulated in RCCS-derived biofilms compared to stationary phase cultures. Genes were identified as significantly upregulated when there was a fold change ≥2.00 and a p value ≤0.05, as determined by a modified t-test with Benjamini-Hochberg multiple testing correction. Gene name, Rv number, predicted protein function and functional categories for each gene as described in TubercuList are listed, based on Cole *et al* 1998 annotation. Adjusted p values after Benjamini-Hochberg multiple testing comparison are also detailed. Table is organised with genes grouped according to their functional category.

Gene	Gene Name	Protein Function	Regulation	Fold Change	Functional Category	p Value
mce1B	Rv0170	Mce-family protein Mce1B	down	2.43	Virulence, detox and adaptation	0.0027
mce3A	Rv1966	Mce-family protein Mce3A	down	2.55	Virulence, detox and adaptation	0.0024
mce3B	Rv1967	Mce-family protein Mce3B	down	2.62	Virulence, detox and adaptation	0.0031
mce3D	Rv1969	Mce-family protein Mce3D	down	2.85	Virulence, detox and adaptation	0.0034
mce3F	Rv1971	Mce-family protein Mce3F	down	2.15	Virulence, detox and adaptation	0.0056
mazE7	Rv2063	Antitoxin MazE7	down	2.20	Virulence, detox and adaptation	0.0039
ddn	Rv3547	Deazaflavin-dependent nitroreductase Ddn	down	2.11	Intermediate metabolism and respiration	0.0027
dfrA	Rv2763c	Dihydrofolate reductase DfrA (DHFR) (tetrahydrofolate dehydrogenase)	down	2.32	Intermediate metabolism and respiration	0.0031
nadE	Rv2438c	Glutamine-dependent NAD(+) synthetase NadE (NAD(+) synthase [glutamine-hydrolysing])	down	2.07	Intermediate metabolism and respiration	0.0030
nrdB	Rv0233	Ribonucleoside-diphosphate reductase (beta chain) NrdB (ribonucleotide reductase small chain)	down	2.02	Information pathways	0.0035
gltS	Rv2992c	Glutamyl-tRNA synthetase GltS (glutamate--tRNA ligase) (glutamyl-tRNA synthase) (GLURS)	down	2.16	Information pathways	0.0024
PE35	Rv3872	PE family-related protein PE35	down	4.50	PE/PPE families	0.0032
PPE59	Rv3429	PPE family protein PPE59	down	2.52	PE/PPE families	0.0025
esxE	Rv3904c	Putative ESAT-6 like protein EsxE (hypothetical alanine rich protein) (ESAT-6 like protein 12)	down	2.46	Cell wall and cell processes	0.0024
espK	Rv3879c	ESX-1 secretion-associated protein EspK. Alanine and proline rich protein.	down	2.31	Cell wall and cell processes	0.0027

Table 5.2: Downregulated genes in RCCS derived biofilms

A total of 15 genes were downregulated in RCCS-derived biofilms compared to stationary phase cultures. Genes were identified as significantly downregulated when there was a fold change ≥2.00 and a p value ≤0.05, as determined by a modified t-test with Benjamini-Hochberg multiple testing correction. Gene name, Rv number, predicted protein function and functional categories for each gene as described in TubercuList are listed, based on Cole *et al* 1998 annotation. Adjusted p values after Benjamini-Hochberg multiple testing comparison are also detailed. Table is organised with genes grouped according to their functional category.

5.2.3 The metabolic state of biofilm-derived bacilli

Of the 23 genes encoding subunits of the 30S bacterial ribosomal subunit, two were upregulated in biofilms (*rpsT* and *rpsL*), as well as a probable translation initiation factor *InfA*. This expression pattern of ribosomal associated genes suggests an increased demand for protein synthesis in biofilm-derived bacilli. Increased protein synthesis could be indicative of bacterial replication; however no genes associated with cell wall synthesis, such as fatty acid synthase (*fas*) enzymes were upregulated. Three genes were induced that were classed as “intermediate metabolism and respiration”; isocitrate lyase (*icl*), a key enzyme of the glyoxylate shunt pathway involved in β-oxidation of fatty acids, phosphoribosyl-AMP pyrophosphatase (*HisE*) involved in histidine synthesis and a possible oxidoreductase (Rv0097) that likely functions in metabolism. Dihydrofolate reductase (dfrA), involved in purine and pyrimidine synthesis, ribonucleoside-diphosphate reductase (ndrB), involved in DNA replication and NAD synthase (nadE), an essential enzyme in both *de novo* synthesis and salvage pathways for NAD (Rodionova, Schuster et al. 2014) were both repressed, suggesting a down regulation of DNA synthesis. These expression patterns suggest that biofilm derived bacilli are metabolically active with ongoing protein synthesis and β-oxidation of fatty acids but with reduced DNA and NAD synthesis.

5.2.4 Genes encoding ESAT6-like proteins are upregulated in RCCS-derived biofilms

A total of five ESAT-6 like proteins belonging to the ESX family were upregulated in RCS-derived biofilms, Table 5.1. Three were putative; esxN, esxP and esxW, while two were known to be ESAT-6 like proteins; esxJ and esxM. The associated ESX5 protein PE19 (2.42 FC) was also upregulated. Although *esx* genes are encoded by ESX5, *esx* genes can also be found outside of ESX loci. EsxN, esxM and PE19 are encoded within the ESX5 loci, while esxJ is encoded within a duplicated ESX5 region known as ESX5a (Shah, Cannon et al. 2015). These data suggests that the ESX5 secretion system is upregulated in RCCS-derived biofilms and could be transcribed as part as an ESX5 operon, Figure 5.6.

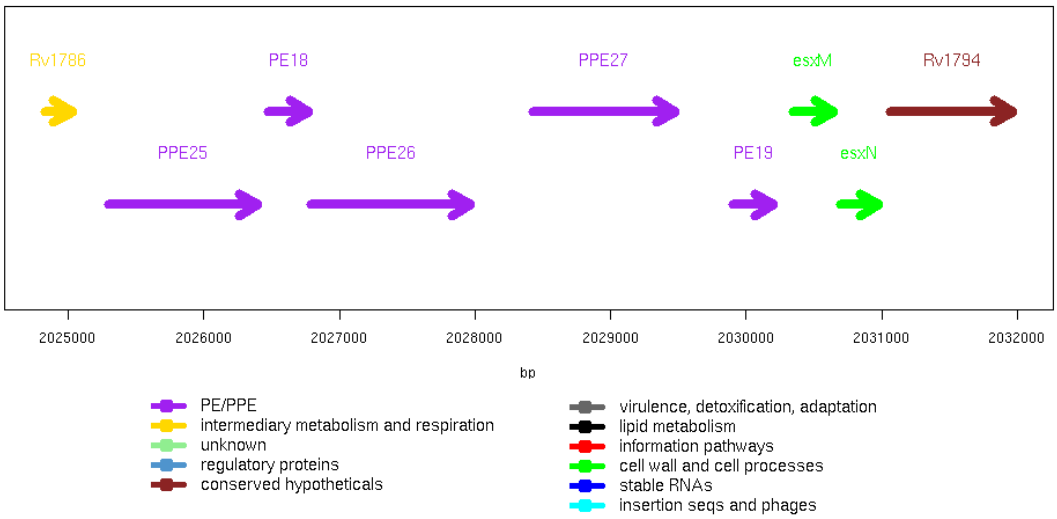

Figure 5.6: ESX5 loci of PE19, esxM and esxN

The ESX5 loci including *PE19*, *esxM* and *esxN* (Rv1791, Rv1792, and Rv1793) are encoded sequentially within the ESX5 operon. Image generated from TubercuList (TubercuList 2017)

In order to investigate the functional significance of these upregulated *Esx* proteins further STRING analyses of *EsxJ*, *EsxM*, *EsxN*, esxP and *EsxW* were performed (STRING 2017). Protein-Protein Interaction (PPI) analysis of each protein plus its predicted functional partners was conducted to assess if proteins have more interactions among themselves than would be expected for a random set of proteins of similar size, drawn from the genome. Such an enrichment is determined by a PPI p-value of ≤0.05, which indicates that the proteins are at least partially biologically connected as a group. Predicted functional partners of these Esx proteins are shown in Table 5.3. Only EsxJ and its predicted functional partners were assumed to be biologically connected based on significant PPI p-values. The EsxJ node network is shown in Figure 5.7.

Protein Name	Gene Name	Possible Functional Protein Partners	PPI p-value
esxJ	Rv1038c	ESAT-6 like protein ESXI; PPE family protein; PE family protein; truncated IS1560 transposase; transposase	0.0318
esxM	Rv1792	esxN; Specific chaperone for cognate PE/PPE proteins; PE family protein; hypothetical protein	0.213
esxN	Rv1793	Hypothetical protein; Specific chaperone for cognate PE/PPE proteins	0.5
esxP	Rc2347c	esxO; esxK; hypothetical protein	0.0522
esxW	Rv3620c	esxI; PPE family protein; PE family protein	0.157

Table 5.3: Possible functional partners of EsxJ, EsxM, EsxN, EsxP and EsxW

Possible functional partners of five Esx proteins upregulated in RCCS-derived biofilms were predicted using STRING analysis (STRING 2017). Only esxJ predicted functional partners were deemed to have statistically significant protein-protein interactions with a PPI p-value of 0.0318.

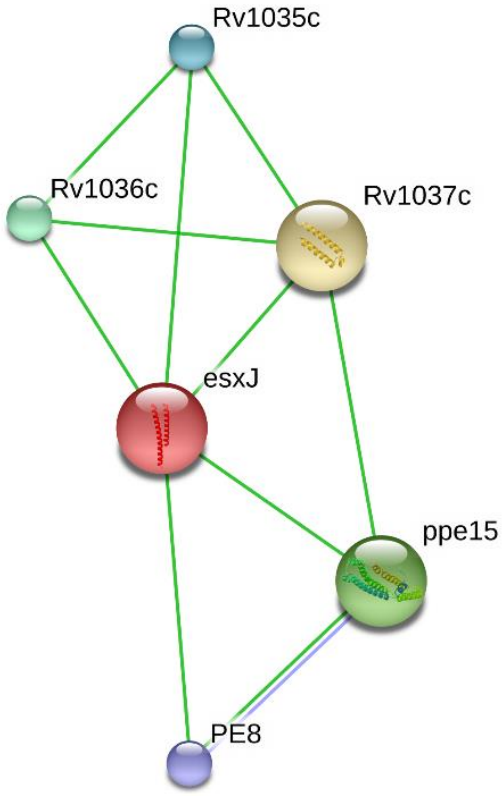

Figure 5.7: Predicted functional partners of EsxJ

The predicted functional partners of EsxJ were determined using STRING database analysis (STRING 2017). Green line: predicted interactions due to gene neighbourhood; blue line: predicted interactions due to protein homology; Rv1035c: Transposase; Rv1036c: Truncated transposase; Rv1037c: ESAT-6 like protein ESXI; ppe15: PPE family protein; PE8: PE family protein. PPI enrichment value of 0.0318 suggests these protein interactions are at least partially biologically connected and not due to random interactions.

5.2.5 Stress response sigma factors SigB and SigE are upregulated in RCCS-derived biofilms

A possible anti-anti sigma factor *rv0516c* and a probable elongation factor GreA were upregulated in biofilm growth versus stationary phase growth, as were the RNA polymerase alternative sigma factors SigB and SigE, Table 5.3. SigB and SigE are transcription initiation factors and are involved in a diverse range of DNA-protein interactions. To investigate if there was upregulation of STRING analysis highlights this complexity, Figure 5.8. Unsurprisingly the transcription initiation factor Sig B shows interactions with a range of DNA-dependent RNA polymerase subunits (rpoA, rpoB, rpoC, rpoZ). SigB also shows interactions with proteins involved in membrane transport, such as the glutamine transport proteins Rv0073 and Rv2564, and membrane-associated translocases SecA1, SecA2 and yYdC.

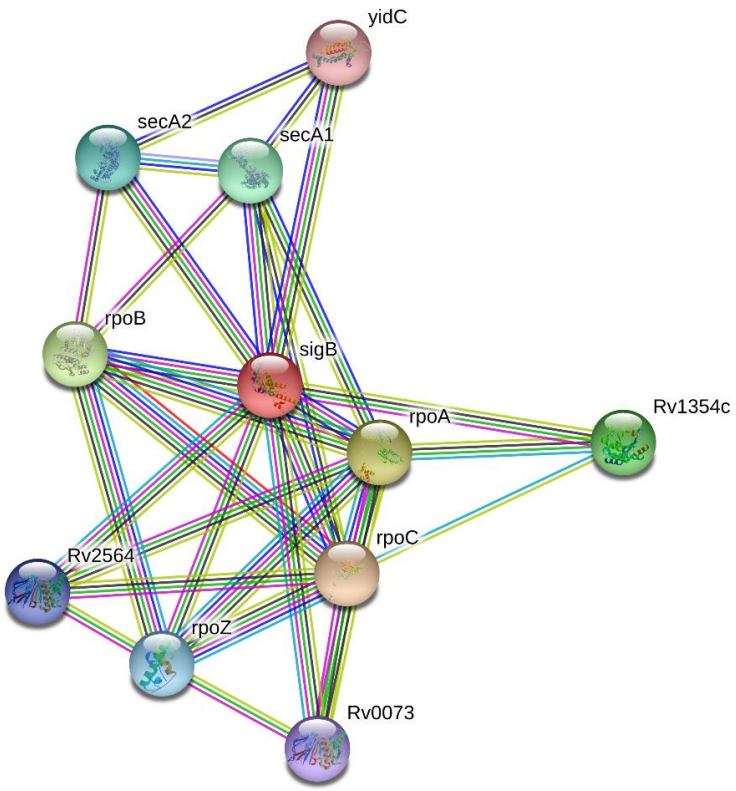

Figure 5.8: Predicted functional partners of SigB

The predicted functional partners of SigB were determined using STRING database analysis (STRING 2017). Green line: predicted interactions due to gene neighbourhood; blue line: predicted interactions due to protein homology; purple line: gene co-occurrence; red line: co-expression. PPI enrichment value of 0.0132 suggests these protein interactions are at least partially biologically connected and not due to random interactions.

SigE, an alternative transcription initiation factor, also shows a complex STRING network with many interactions, Figure 5.9. SigE interacts with DNA-dependent RNA polymerase proteins (rpoC and rpoD) as well as the fatty acid synthase fas. Interestingly, two protein-protein interactions are shown with rslA and rseA, two hypothetical proteins that are predicted to be anti-sigma factor factors which suggests these may be involved in SigE regulation. SigB is shown as a central node for protein-protein interactions with SigE-SigE is required for the full expression of SigB. Protein-protein interaction analysis however yielded a p value of 0.214, over the statistical cut-off of $p<0.05$. This suggests that the interactions generated here using the STRING database may not be biologically interactive. Rv1364c, rslA and rseA are hypothetical proteins, and their inclusion in STRING network maps reduces the statistical power of analysing protein-protein interactions, potentially masking real biologically relevant protein-protein interactions.

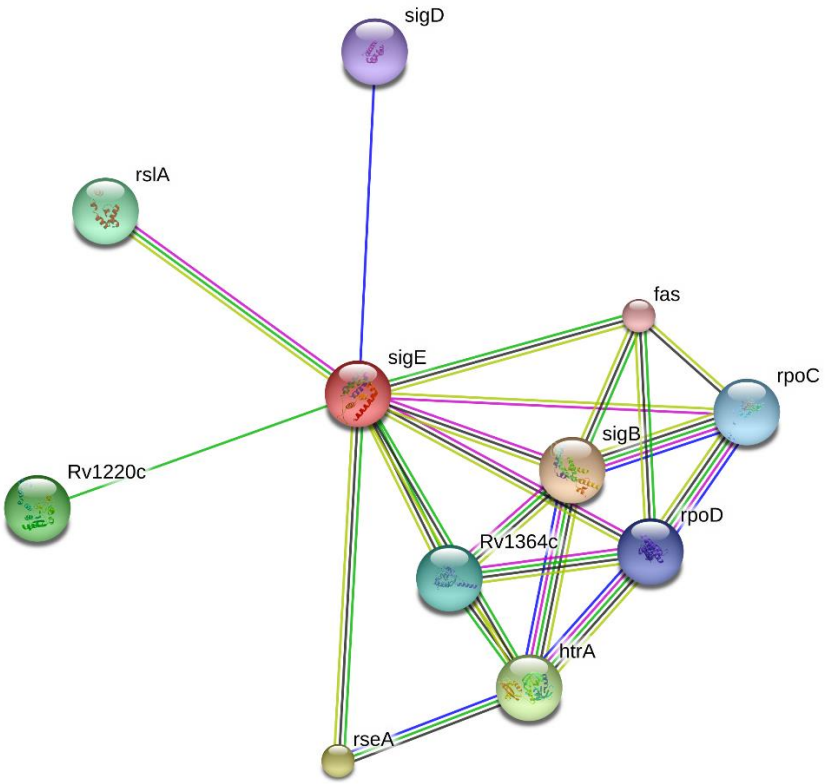

Figure 5.9: Predicted functional partners of SigE

The predicted functional partners of SigE were determined using STRING database analysis (STRING 2017). Green line: predicted interactions due to gene neighbourhood; blue line: predicted interactions due to protein homology; purple line: gene co-occurrence; red line: co-expression. PPI enrichment value of 0.214 suggests these protein interactions may not partially biologically connected and could be due to random interactions.

5.2.6 Isocitrate lyase is upregulated in RCCS-derived biofilms

Isocitrate lyase (*icl1*) functions in the glyoxylate shunt pathway to permit synthesis of glucose from acetate generated through β-oxidation of fatty acids. *Icl1* was upregulated 2.00 FC compared to stationary phase cultures. Unsurprisingly, STRING network analysis generated a protein-protein interaction map that focuses on the citric acid cycle and fatty acid metabolism, Figure 5.10. Fatty acid synthase (*fas*) and the associated fatty oxidation protein fadB map with aconitate hydratase, a catabolic enzyme involved in the degradation of short chain fatty acids via the citric acid cycle. Malate synthase (*glcB*) metabolises glyoxylate generated via ICL to form malate, which is further metabolised through the citric acid cycle.

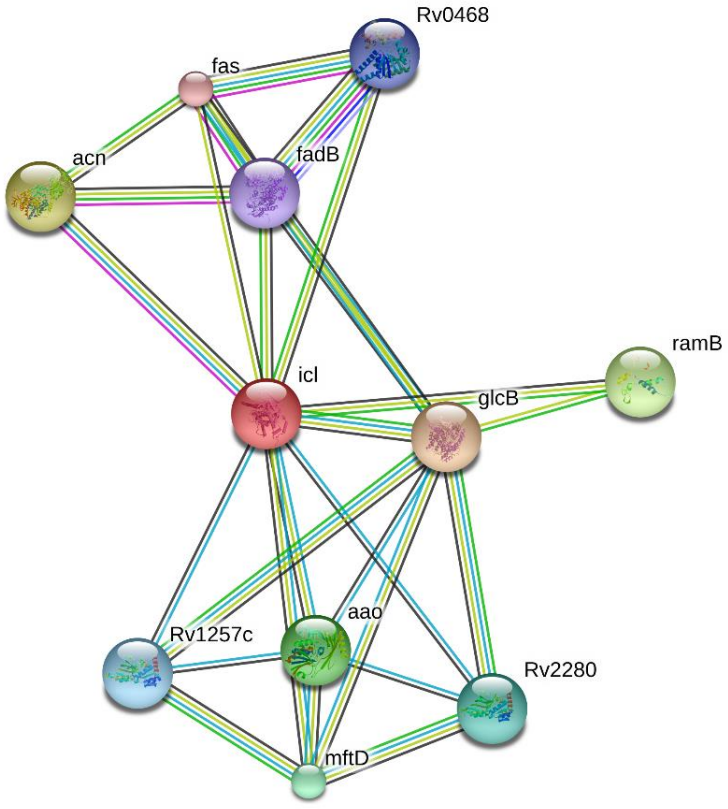

Figure 5.10: Predicted functional partners of isocitrate lyase

The predicted functional partners of isocitrate lyase were determined using STRING database analysis (STRING 2017). Green line: predicted interactions due to gene neighbourhood; blue line: predicted interactions due to protein homology; purple line: gene co-occurrence; red line: co-expression. *Fas*: fatty acid synthase; *ramB*: ICL transcriptional regulator; Rv0468, Rv2280: dehydrogenases; *acn*: aconitate hydratase; *glcB*: malate synthase; *mftD*: L-lactate dehydrogenase. PPI enrichment value of 0.0102 suggests these protein interactions are at least partially biologically connected and not due to random interactions.

5.2.7 The mammalian cell entry (MCE) protein family is down regulated in biofilms

Mammalian cell entry (*mce*) genes are secreted virulence factors that are organised into four operons, mce1-4 (de la Paz Santangelo, Klepp et al. 2009). Each operon consists of six *mce* genes (A-F), whose expression was first identified as important for bacterial entry into host cells (Zhang and Xie 2011). The specific functions of the *mce* operons remain elusive, especially as *mce* genes are known to function in virulence yet are also found in non-pathogenic mycobacteria (Haile, Caugant et al. 2002). *Mce1* encoded fadB5 has been shown to be involved in the catabolism of fatty acids (Dunphy, Senaratne et al. 2010), and structural analyses of Mce proteins suggest a role in membrane transport as they share protein structure homology to β-barrel containing porin proteins (Pajon, Yero et al. 2006). A total of five *mce* genes were significantly repressed in biofilms, *mce1B* and *mce3A, mce3B, mce3D* and *mce3F.* The *mce3* operon is shown in Figure 5.11.

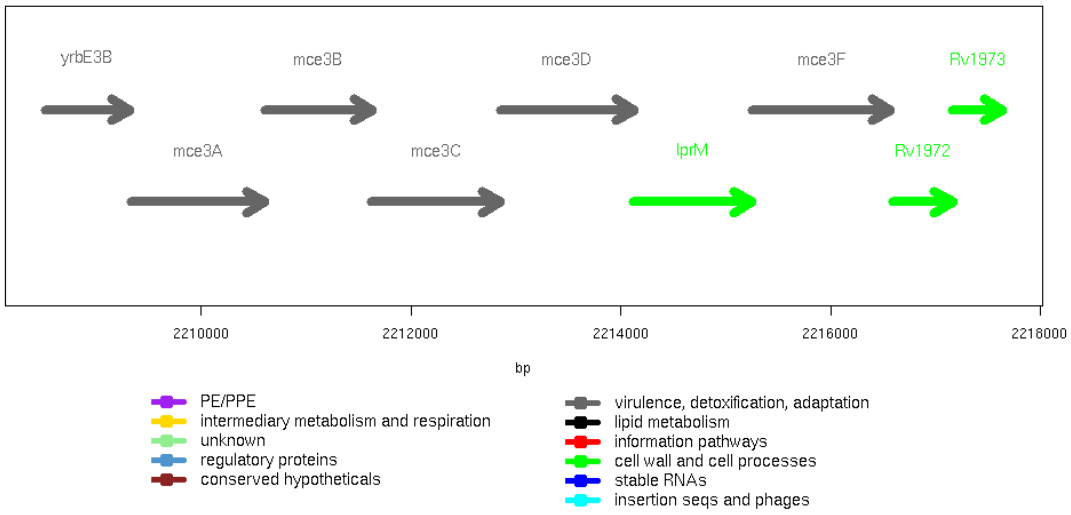

Figure 5.11: The *mce3* operon encodes *mce3A, mce3B, mce3D,* and *mce3F*

The *Mce3* loci *PE19*, *mce3A, mce3B, mce3D* and *mce3F* (Rv1966, Rv1967, Rv1969 and Rv1971) are encoded within the *mce3* operon. Image generated from TubercuList (TubercuList 2017)

Mce1B STRING analysis showed a significant complex network of protein-protein interactions (p value =4.88 x 10^{-15}) with genes from the *mce1* operon and hypothetical proteins, as well as the membrane proteins Rv0167 and Rv0168, Figure 5.12. These genes were shown to interact from experimental evidence, protein interaction algorithms and database predictions, generating this highly significant p-value. None of these genes however, were significantly differentially expressed in biofilm growth compared to stationary phase cultures.

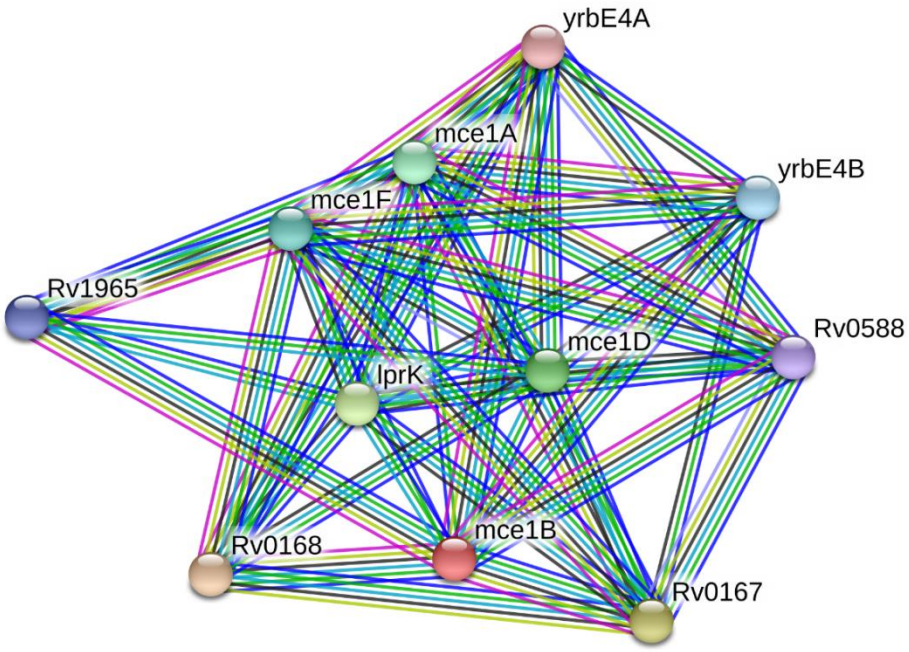

Figure 5.12: Predicted functional partners of mce1B

The predicted functional partners of mce1B were determined using STRING database analysis (STRING 2017). Green line: predicted interactions due to gene neighbourhood; blue line: predicted interactions due to protein homology; light blue line: interactions determined from experimental evidence; red line: proteins are co-expressed. Rv0167, Rv0168: membrane proteins; *yrbE4A*, *yrbE4B*, Rv1965: hypothetical proteins. PPI enrichment value of 4.88 x 10^{-15} suggests these protein interactions are at least partially biologically connected and not due to random interactions.

STRING analysis of *mce3A*, *mce3B*, *mce3D* and *mce3F* also showed complex interactions among proteins from the mce3 operon, along with interactions with hypothetical proteins, the membrane associated proteins Rv0164, Rv0165, Rv1972, Rv1973 and a lipoprotein *lprM*, Figure 5.13. The low p value (p value= 0.0) for protein-protein interactions suggests that the interactions between these mce proteins are significant and enriched. These four *mce3* genes downregulated in biofilm growth compared to stationary phase cultures are all present in this interaction map, suggesting that genes from the *mce3* operon may play a more significant role in biofilms than the one gene (*mce1B*) differentially expressed from the *mce1* operon,

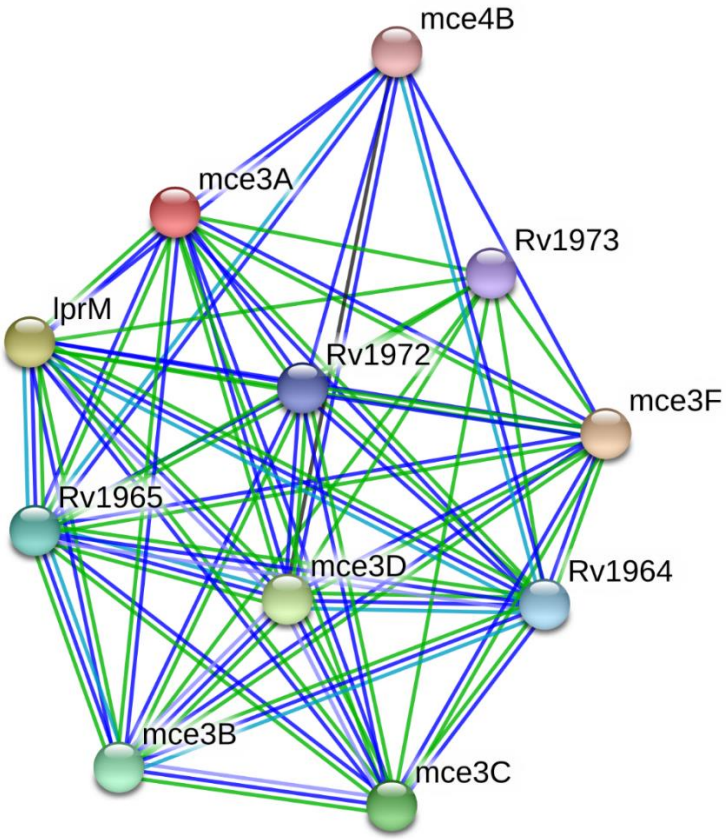

Figure 5.13: Predicted functional partners of mce3A, mce3B, mce3D, mce3F

The predicted functional partners of mce3A, mce3B, mce3D and mce3F were determined using STRING database analysis. Green line: predicted interactions due to gene neighbourhood; blue line: predicted interactions due to protein homology; pink line: interactions determined from experimental evidence; red line: proteins are co-expressed. Rv0164, Rv0165: membrane proteins; Rv1972, Rv1973: MCE membrane associated proteins. PPI enrichment value of 0.0 suggests these protein interactions are at least partially biologically connected and not due to random interactions.

5.2.8 The transcriptome of RCCS-derived biofilms does not correlate with the transcriptomes of hypoxia, nutrient starvation or *M.tb* from sputum

Hypergeometric probability testing was performed, with 19 statistically significant upregulated and 15 downregulated genes compared against 465 experimental, published and unpublished mRNA signature data sets maintained in the Waddell laboratory. The RCCS-derived biofilm transcriptome did not match any specific condition within these data sets with statistical significance ($p<0.05$). Four genes however were consistently identified across biofilm, hypoxia, nutrient starvation and *M.tb* derived from human sputum conditions, Table 5.4.

Gene Name	Rv number	Fold Change						
		RCCS Biofilm	Hypoxia	Nutrient Starvation	Sputum: pre-treatment	Sputum: Day 3 of treatment	Sputum: Day 7 of treatment	Sputum: Day 14 of treatment
Icl1	**Rv0467**	+2.00	+2.0	-	+2.81	+5.81	+3.08	+2.60
mce1B	**Rv0170**	-2.43	-1.9	-2.21	-2.91	-3.22	-3.47	-3.45
SigB	**Rv2710**	+2.36	-	+5.48	-17.6	-19.57	-22.63	-22.00
SigE	**Rv1221**	+2.25	-1.8	+5.87	-2.02	-2.15	-2.61	-2.90

Table 5.4: RCCS-derived *M. bovis* BCG biofilm gene expression compared to *M.tb*-derived from a range of conditions

Differentially expressed genes in RCCS-derived biofilms were compared to the transcriptomes of *M.tb* under hypoxia (Park, Guinn et al. 2003), nutrient starvation (Park, Guinn et al. 2003), *M.tb* derived from human sputum pre-treatment and *M.tb* derived from human sputum at days 3, 7 and 14 of treatment 27055815. Upregulation is shown by "+" and downregulation is shown by "-".

The biofilm transcriptional profile was compared to a hypoxia induced transcriptional profile of *M.tb* to establish if there were mRNA signatures common to both conditions, such as DosR operon induction (Park, Guinn et al. 2003). There was no induction of any of the DosR associated genes in RCCS-derived biofilms compared to stationary phase cultures. Isocitrate lyase (*icl1*) was the only gene found to be upregulated in both biofilms and hypoxia, with 2.0 FC induction of *icl* in both conditions. *Mce1B*, a virulence factor associated with mammalian cell entry, was the only gene repressed in both biofilms and hypoxia, with a 2.4 and 1.9 FC respectively.

Genes differentially expressed in RCCS-derived biofilms were compared to the transcriptional profile of *M.tb* after a 96 hour starvation period (Betts, Lukey et al. 2002).

Only three genes were upregulated in both conditions; *SigB*, *SigE* and a possible anti-sigma factor (rv0516), suggesting a general stress response is present in both biofilm-derived bacilli and nutrient starved cultures. *Icl1* is upregulated in biofilm cultures, but was not seen to be upregulated in nutrient starved cultures. The α-subunit of isocitrate lyase was however shown to be upregulated in nutrient starved cultures. Two genes were repressed in both transcriptomes- *mce1B* and glutamyl tRNA synthase (*gltS*). No mammalian cell entry (*mce*) genes were repressed in nutrient starved *M.tb*. In comparison, RCCS-derived biofilms four *mce3* genes were repressed in addition to *mce1B.*

The transcriptional profile of RCCS-derived biofilms was compared to the transcriptional profiles of *M.tb* derived from human sputa at days 0, 3, 7 and 14 of treatment (Honeyborne, McHugh et al. 2016). Overall, the biofilm transcriptional profile did not correlate with *M.tb* from human sputa at any day of treatment, including before drug therapy was initiated. Only two genes were upregulated in sputum at days 0, 3, 7 and 14 of treatment (in comparison to log phase bacilli) and in biofilms (compared to stationary phase bacilli); isocitrate lyase (*icl1*) and Rv2451, a hypothetical proline and serine rich protein. Both espK and mce1B were repressed in biofilms and in *M.tb* from human sputum at days 0, 3, 7 and 14 of treatment. Both of these are virulence factors, with the ESX1 secretion associated protein *espK* possibly acting as a chaperone for other ESX1 encoded proteins. There was no literature discussing the hypothetical protein Rv2451. In an attempt to further characterise Rv2451, a BLAST search of the amino acid FASTA sequence of Rv2451 was performed to search for orthologs of this protein in other bacterial species, including GC rich Gram positives. Only one other species possessed an ortholog with high sequence similarity (98%); the slow-growing *Mycobacterium tuberculosis* complex (MTBC) member *Mycobacterium canetti.* Following this, the secondary structure of this 132 amino acid protein was predicted using a protein homology/analogy recognition engine (Phyre 2). Phyre 2 was unsuccessful in generating a secondary structure, with only 9 out of 132 amino acids that could be modelled with a confidence of 35.2%. It was not possible to further detail Rv2451 within this thesis.

The gene expression patterns of genes relevant across these conditions are summarised in Table 5.4.

5.2.9 Differentially expressed genes are regulated by a diverse range of transcriptional regulators

Differentially expressed gene lists were entered into TB Genomes Database (TB Genomes Database 2017) to assess how these genes might be regulated. The TB

Genomes Database groups gene entries based on what regulatory proteins may be involved in their regulation based on data from ChIP-seq experiments (Galagan, Lyubetskaya et al. 2013). A comprehensive regulatory network of 50 transcription factors was generated by Galagan *et al* by combining ChIP-Seq, transcriptional profiling and metabolomics. Gene lists can be searched against this database to identify regulators that potentially regulate one or more genes entered.

Three search conditions were applied;

Search 1) regulator search for 19 upregulated genes,

Search 2) regulator search 15 downregulated genes searched,

Search 3) regulator search for 34 up and downregulated genes searched.

A total of 28 regulators were associated with combinations of upregulated genes. Lsr2 was the regulator associated with the most genes (10 genes), followed by Rv0081 with nine genes. PhoP was associated with four genes, Table 5.5.

Lsr2 was also the most associated regulator (10 out of 15 genes) with downregulated genes. Rv1776 was associated with six genes, five of which are *mce*-associated genes (*mce1B, mce3A, mce3B, mce3D, mce3F*). Interestingly, the two genes nrdB and mce1B were shown be associated with DosR, the regulatory component of the DosR response in mycobacteria, Table 5.6.

Finally, a total of 18 regulators were identified that could regulate both up and down regulated genes, including lsr2 (18 genes) and Rv0081 (12 genes). No novel regulators were identified that possible regulated up and downregulated genes that were not identified for up or downregulated genes alone.

Regulator	Gene	Gene Name	Protein Function	Functional Category
lsr2 (Rv3597c)	*Rv0097*	Rv0097	Possible oxidoreductase	Intermediate metabolism and respiration
	esxN	Rv1793	Putative ESAT-6 like protein EsxN (ESAT-6 like protein 5)	Cell wall and cell processes
	esxP	Rv2347c	Putative ESAT-6 like protein EsxP (ESAT-6 like protein 7)	Cell wall and cell processes
	esxW	Rv3620c	Putative ESAT-6 like protein EsxW (ESAT-6 like protein 10)	Cell wall and cell processes
	cadI	Rv2641	Cadmium inducible protein CadI	Conserved hypotheticals
	Rv0516c	Rv0516c	Possible anti-anti-sigma factor	Information pathways
	sigE	Rv1221	Alternative RNA polymerase sigma factor SigE	Information pathways
	rpsT	Rv2412	30S ribosomal protein S20 RpsT	Information pathways
	icl1	Rv0467	Isocitrate lyase Icl (isocitrase) (isocitratase)	Intermediate metabolism and respiration
	PE19	Rv1791	PE family protein PE19	PE/PPE families
Regulator	**Gene**	**Gene Name**	**Protein Function**	**Functional Category**
Rv0081	*Rv0097*	Rv0097	Possible oxidoreductase	Intermediate metabolism and respiration
	esxJ	Rv1038c	ESAT-6 like protein EsxJ (ESAT-6 like protein 2)	Cell wall and cell processes
	esxN	Rv1793	Putative ESAT-6 like protein EsxN (ESAT-6 like protein 5)	Cell wall and cell processes
	esxP	Rv2347c	Putative ESAT-6 like protein EsxP (ESAT-6 like protein 7)	Cell wall and cell processes
	esxW	Rv3620c	Putative ESAT-6 like protein EsxW (ESAT-6 like protein 10)	Cell wall and cell processes
	sigE	Rv1221	Alternative RNA polymerase sigma factor SigE	Information pathways
	rpsT	Rv2412	30S ribosomal protein S20 RpsT	Information pathways
	PE19	Rv1791	PE family protein PE19	PE/PPE families
Regulator	**Gene**	**Gene Name**	**Protein Function**	**Functional Category**
PhoP (Rv0757)	*esxJ*	Rv1038c	ESAT-6 like protein EsxJ (ESAT-6 like protein 2)	Cell wall and cell processes
	esxW	Rv3620c	Putative ESAT-6 like protein EsxW (ESAT-6 like protein 10)	Cell wall and cell processes
	sigB	Rv2710	RNA polymerase sigma factor SigB	Information pathways
	hisE	Rv2122c	Phosphoribosyl-AMP pyrophosphatase HisE	Intermediate metabolism and respiration

Table 5.5: Lsr2, Rv0081 and PhoP were predicted to associate with groups of upregulated genes in RCCS-derived biofilms

Hypergeometric analysis of upregulated genes in RCCS-derived biofilms using (TB Genomes Database 2017) to predict associated regulators.

Regulator	Gene	Gene Name	Protein Function	Functional Category
lsr2 (Rv3597c)	*mce1B*	Rv0170	Mce-family protein Mce1B	Virulence, detox and adaptation
	mce3A	Rv1966	Mce-family protein Mce3A	Virulence, detox and adaptation
	mce3B	Rv1967	Mce-family protein Mce3B	Virulence, detox and adaptation
	mce3D	Rv1969	Mce-family protein Mce3D	Virulence, detox and adaptation
	mce3F	Rv1971	Mce-family protein Mce3F	Virulence, detox and adaptation
	PPE59	Rv3429	PPE family protein PPE59	PE/PPE families
	ddn	Rv3547	Deazaflavin-dependent nitroreductase Ddn	Intermediate metabolism and respiration
	PE35	Rv3872	PE family-related protein PE35	PE/PPE families
Regulator	**Gene**	**Gene Name**	**Protein Function**	**Functional Category**
Rv1776c	*mce1B*	Rv0170	Mce-family protein Mce1B	Virulence, detox and adaptation
	mce3A	Rv1966	Mce-family protein Mce3A	Virulence, detox and adaptation
	mce3B	Rv1967	Mce-family protein Mce3B	Virulence, detox and adaptation
	mce3D	Rv1969	Mce-family protein Mce3D	Virulence, detox and adaptation
	mce3F	Rv1971	Mce-family protein Mce3F	Virulence, detox and adaptation
	mazE7	Rv2063	Antitoxin MazE7	Virulence, detox and adaptation
Regulator	**Gene**	**Gene Name**	**Protein Function**	**Functional Category**
DosR (Rv3133c)	*mce1B*	Rv0170	Mce-family protein Mce1B	Virulence, detox and adaptation
	nrdB	Rv0233	Ribonucleoside-diphosphate reductase (beta chain) NrdB (ribonucleotide reductase small chain)	Information pathways

Table 5.6: Lsr2, Rv1776c and DosR were predicted to associate with groups of downregulated genes in RCCS-derived biofilms

Hypergeometric analysis of upregulated genes in RCCS-derived biofilms using (TB Genomes Database 2017) to predict associated regulators.

5.3 Discussion

In order to define adaptations specific to biofilm growth, the transcriptional signature of RCCS-derived biofilms was compared to that of stationary phase bacilli. Both of these cultures were incubated for the same length of time (21 days), and in the same media type. A discreet list of genes was found to be significantly differentially expressed, with 19 genes upregulated and 77 genes downregulated. Of these 77 genes downregulated, 62 were of unknown function and were predicted or possible functional proteins. Because of this, they were removed from analysis, which left 15 genes of known function downregulated.

The significantly induced biofilm genes *esxJ*, *esxN* and *esxM* are secreted through the ESX-5 secretion system present in *M. bovis* BCG (Bottai, Di Luca et al. 2012), (Shah and Briken 2016). EsxJ, esxM, esxN and PE19 transcription are upregulated in RCCS-derived biofilms. Although not identified as significantly induced, the secreted ESX-5 virulence factors PE8 and PPE15 were identified by STRING analysis as predicted functional partners for esxJ. These data suggest that the ESX5 secretion system is active in RCCS-derived biofilms in comparison to stationary phase growth. The ESX5 secretion system is involved in the secretion of the PE/PPE proteins, and could potentially function in biofilm formation through secretion of components required for extracellular matrix formation (Shah and Briken 2016). Interestingly, only one ESX1 related gene, *espK*, was significantly differentially expressed. *EspK* is an ESX-1 secreted-associated protein that was downregulated 2.31 fold, and may function as a chaperone to other ESX1 related proteins (Mawuenyega, Forst et al. 2005). *M. bovis* BCG does not contain RD1, the genomic region found in *M. bovis* and *M.tb* where most ESX1 loci map to. As a result, it was not possible to investigate the role of ESX1 secretion systems in this biofilm model. However, these data do suggest that this biofilm model in *M. bovis* BCG and *M.tb* offers a novel approach to understanding the role of ESX systems in mycobacteria.

Four genes categorised by Cole *et al*, 1998 as “information pathways” were identified as upregulated (SigB, SigE, GreA and a possible anti-anti sigma factor Rv0561c) in biofilm growth. Transcription factors such as SigB and SigE exert global transcriptional control in response to changing environmental conditions and stress, and as such may play a significant role in adaptation to biofilm growth. SigB expression is induced at the transition of log phase to stationary phase, and both sigB and sigE are induced in response to environmental stresses including hypoxia and antibiotic exposure (Manganelli, Dubnau et al. 1999), (Hu and Coates 1999), (Pendzich, Maksymowicz-Mazur et al. 2004). We hypothesise that these factors are therefore induced in response to changes in nutrient or oxygen availability within the diverse microenvironments likely

to be generated within the RCCS biofilm. The principal mycobacterial sigma factor, SigA, was not differentially expressed in biofilms. Interestingly, the only genes that were upregulated in both biofilms and nutrient starved cultures were SigB, SigE and a possible anti-sigma factor Rv0561c, suggesting a transcriptional stress response to an environmental condition. Both SigB and SigE are important for the transcriptional regulation in response to environmental stressors and could play a role in the antimicrobial tolerance seen in both biofilm-derived bacilli and nutrient starved cultures.

Isocitrate lyase (*icl1*) is an essential enzyme for the generation of isocitrate and glyoxylate through the glyoxylate shunt pathway by shuttling malate from the citric acid cycle. It has been shown to be essential for infectivity and intracellular survival within macrophages, (Nandakumar, Nathan et al. 2014) and *icl1* null *M.tb* mutants are unable to maintain a persistent infection in mice (Honer Zu Bentrup, Miczak et al. 1999), (McKinney, Honer zu Bentrup et al. 2000). *Icl1* is also induced two-fold in a hypoxia model of *M.tb* (Park, Guinn et al. 2003), and is also up regulated in *M.tb* in sputum both before and during treatment (Honeyborne, McHugh et al. 2016). Importantly, induction of *icl1* has been shown to mediate broad antimicrobial tolerance. Although the mechanisms of how this occurs are not fully elucidated, it is possible ICL functions in antioxidant defence when exposed to antimicrobials (Munoz-Elias and McKinney 2005).

The transcriptional profile seen in RCCS-derived biofilms did not correlate with hypoxia or nutrient starvation models of mycobacterial drug tolerance. When compared to an *M.tb* hypoxia transcriptional profile, there was only one mRNA signature that was found in both conditions; a two-fold induction of ICL (Park, Guinn et al. 2003). When the biofilm transcriptional signature was compared to a nutrient starvation model transcriptional profile, there were some similarities in differential gene expression. Both SigB and SigE were upregulated; however, these are not nutrient starvation specific sigma factors and are induced under a range of environmental conditions. Transcriptional profiling did not correlate the biofilm transcriptional profile with that of a hypoxic or a nutrient starved condition as there was not a distinct repression of aerobic genes in biofilms. If this were the case, down regulation of the NADH dehydrogenase operon (*nuoA-M*) would have been expected, as this is the primary aerobic respiratory pathway in *M.tb* through oxidation of NADH to NAD+. Additionally, there was no evidence to suggest that any of the eight genes that encode ATP synthase (*atpA-H*) were downregulated compared to 21-day-old stationary cultures. Transcriptional profiling shows two 30S ribosomal sub units (RpsT and RpsL) were upregulated, along with a possible translation initiation factor (InfA) suggesting that protein synthesis was not inhibited in biofilm-derived bacilli. Previous evidence suggests that down regulation of mycobacterial translation apparatuses occurs in carbon limited environments and this was not observed (Betts,

Lukey et al. 2002). Following this, genes identified as up or downregulated in RCCS-derived biofilms were compared to the transcriptional profiles of *M.tb* derived from human sputum at days 0 (treatment naive), days 3, 7 and 14 (Honeyborne, McHugh et al. 2016). Only two of 19 genes up regulated in biofilms were found to be upregulated in sputum-derived bacilli; ICL and a conserved hypothetical proline and serine rich protein. A total of ten genes upregulated in biofilms were in fact downregulated at all time points in sputum. Of the 11 genes repressed in biofilms, two genes were found to be upregulated in sputum-derived *M.tb*, nadE and mce3D.

Entry to the mammalian host cell is a crucial step in the virulence of *M.tb.* Four operons encode mammalian cell entry (mce1-4) genes, five of which are repressed in biofilms (*mce1B*, *mce3A*, *mce3B*, *mce3D*, *mce3F*). *Mce* genes are found in both pathogenic and non-pathogenic bacteria- the presence of *mce* genes does not necessarily suggest virulence but rather virulence is dictated by their expression (Haile, Caugant et al. 2002). The exact function of these secreted mce proteins are not fully understood but interestingly, the mce operon is repressed in biofilm bacilli, suggesting a shift in the transcriptome away from that of host cell entry (Singh, Katoch et al. 2016), (Kumar, Bose et al. 2003).

Several enzymes were differentially expressed that affect antimicrobial efficacy in RCCS-derived biofilms. INH not only inhibits the enoyl acyl carrier protein InhA, but can also target a range of mycobacterial enzymes and processes (Slayden, Lee et al. 2000). Dihydrofolate reductase (*dfrA*) catalyses the reduction of dihydrofolate to tetrahydrofolate and is essential for purine and certain amino acid synthesis in *M.tb*; inhibition of this enzyme has been shown to cause cessation of DNA synthesis and ultimately cell death (Li, Sirawaraporn et al. 2000). DfrA has been shown to be a target for INH-NAD adducts that leads to inhibition of mycobacterial DNA synthesis (Argyrou, Vetting et al. 2006). RCCS-derived biofilms show a 2.3 fold reduction in activity which possibly suggest a reduction in DNA synthesis and cell replication, but this down regulation of dfrA may reduce INH toxicity through reducing target availability, contributing to the INH tolerant phenotype seen in biofilm-derived bacilli.

The enzyme deazaflavin-dependent nitroreductase (*ddn*) was repressed 2.1 fold in RCCSA-derived biofilms. Importantly, this enzyme is involved in the activation of bicyclic 4-nitroimidazole pro-drugs such as delamanid and pretomanid, two of the latest drugs developed to treat TB. *Ddn* converts pretomanid to three biologically active metabolites that exert a range of cidal effects in *M.tb*, most notably generation of reactive nitrogen radicals (Manjunatha, Boshoff et al. 2009). Pretomanid and delamanid susceptibility testing was not carried out using RCCS derived cultures- based on this transcriptional

profiling, it is feasible that biofilm-derived bacilli could exhibit drug tolerance towards both of these drugs due to down regulation of *ddn*.

M.tb possess genes to synthesise NAD *de novo* and to recycle NAD within the bacillus. NadE is a glutamine dependent NAD synthetase that functions in both pathways and as such is indispensable in *M.tb* (Boshoff, Xu et al. 2008). While no current anti-TB drugs target NadE, it has been investigated as a potential therapeutic target. Inhibition of NadE leads to rapid depletion of the free NAD pool within the bacillus, leading to a "global metabolic catastrophe" and subsequent cell death (Rodionova, Schuster et al. 2014). Importantly, NadE has been identified as an essential enzyme in both actively growing and non-replicating bacilli (Boshoff, Xu et al. 2008). It was however down regulated 2.1 fold in biofilm-derived bacilli. Similar to *dfrA* and *ddn*, it is important to consider the down regulation of potential therapeutic targets in the RCCS biofilm model when used for novel compound screening as a more predictive alternative to the standard of using log phase bacilli for novel compound screening.

Regulator redundancy was seen when predicted regulators were determined for up or downregulated genes using TB Genomes Database (TB Genomes Database 2017). The transcriptional regulator Lsr2 associates with upregulated esxW, esxP, esxN and PE19 while also associating with the repressed PPE59 and PE35. Lsr2 is a global transcription factor with a diverse range of targets; it is likely that there are more regulatory accessory proteins involved in this differential expression rather than just Lsr2. Interestingly, Lsr2 is required for disease pathology in the mouse lung and adaptation to hostile environments such as variation in O_2 and has been shown to induce various drug tolerance-associated genes in *M. smegmatis* such as efflux pumps (Bartek, Woolhiser et al. 2014; Colangeli, Helb et al. 2007). PhoP was also predicted to regulate *esxJ*, *esxW*, *SigE* and *HisE*. PhoP is part of a two-component system in conjunction with PhoR that are important for virulence and in particular the secretion of virulence proteins, such as esx proteins (Ryndak, Wang et al. 2008). Two genes (*mce1B* and *nrdB*) were shown to be associated with DevR, a regulator of the DosR dormancy operon. *Mce1B* is a mammalian cell entry virulence factor, while nrdB is a ribonucleoside-diphosphate reductase important in the DNA replication pathway. Downregulation of these genes could suggest a shift from a host cell invasion phenotype, with a reduction in cell division as measured by repression of DNA replication enzymes. This does not however suggest transcription of the DosR dormancy operon in biofilms. Only two genes were repressed that could be associated with DosR, and these could alternatively be associated with other regulators, such as Lsr2.

Overall, we identified 31 genes that were significantly differentially expressed in biofilm growth compared to 21-day stationary phase bacilli. These genes range in function from

ESX5 secretion system components to mammalian cell entry virulence factors. Protein synthesis is maintained, with a shift towards glyoxylate and β-oxidation metabolism. Upregulation of the ESX5 secretion system, crucial for virulence, is contrasted by downregulation of the mammalian cell entry (*mce*) genes suggesting biofilm cultures are maintaining protein synthesis accompanied by secretion of ESX5 associated virulence factors.

Single gene expression must be confirmed by qPCR to validate significantly differentially expressed genes, and for genes of interest Western blotting could be performed to identify proteins. Alternatively, our tiling microarray data could be re-analysed using a different comparator, such as log phase bacilli. Transcriptional profiling was performed using the Gene Spring software; the computer program Artemis could be used which would allow analysis of intergenic binding sites for mRNA.

Chapter 6: Pathogen Host Interactions of *M. bovis* BCG biofilms

6.1 Overview

The destructive pathology seen in the TB lung is primarily driven by the immune system through inflammation and granuloma formation (Ehlers and Schaible 2012). Alveolar macrophages possess a diverse range of cell surface receptors that allow them to identify and phagocytose invading bacteria as well as recognising and responding to host cell secreted cytokines and chemokines (Gordon, Pluddemann et al. 2014). *M.tb* has evolved strategies such as inhibition of phagolysosome maturation that allows bacilli to replicate within the macrophage (Deretic, Singh et al. 2006).

Alveolar macrophages secrete TNFα in response to infection through activation of their TLR2 surface receptor. TLR2 responds to a diverse range of mycobacterial PAMPs such as cell wall components, e.g. lipoarabinomannan (Jo, Yang et al. 2007). TNFα is critical in controlling infection through induction of apoptosis in infected macrophages that leads to restriction of mycobacterial growth, as well as modulating granuloma formation (Barnes et al, 1990). The role of TNFα in controlling active TB infection is highlighted with the use of TNFα suppressors to treat inflammatory conditions such as arthritis. These suppressants have been shown to induce the development of active TB infection in individuals with latent TB 20491796. Secretion of TNFα activates both infected and uninfected alveolar macrophages and enhances their antimicrobial activities against *M.tb* through secretion of additional cytokines, such as IL-1β (Moldoveanu, Otmishi et al. 2009; Zwerling, Behr et al. 2011). IL-1β is an important pro-inflammatory immune system mediator as it induces protective immunity in macrophages in response to mycobacterial infection through the upregulation of TNFα surface receptors and increased TNFα secretion from infected macrophages (Kleinnijenhuis, Joosten et al. 2009). Increased secretion of TNFα and IL-1β can induce a potent inflammatory response to infection that can lead to bacterial clearance and granuloma formation, while reduced levels of these cytokines can allow *M.tb* to replicate and colonise the lung and potentially disseminate throughout the body (Bourigault, Segueni et al. 2013).

The aims of this chapter were:

1. To establish if mycobacterial products generated through biofilm formation impact macrophage cell viability in comparison to control cultures;
2. To determine if mycobacterial biofilms induce altered macrophage TNFα and IL-1β secretion in comparison to control cultures.

6.2 Results

6.2.1 THP-1 macrophage culture model

THP-1 cells are a human monocytic cell line that can be differentiated into a macrophage-like cell through stimulation with phorbol-12-myristate-13-acetate (PMA) (Materials and Methods section 2.10). THP-1 cells were optimised for 96 well microtiter plate culture for stimulation with *M. bovis* BCG bacilli supernatants. THP-1 cells were differentiated with PMA and 1 x 10^3, 1 x 10^4 or 1 x 10^5 THP-1 cells added per well. 1 x 10^3 and 1 x 10^4 wells showed poor cell density, with attached cells only visible around the edge of the well. 1 x 10^5 wells showed more attached THP-1 cells in a confluent lawn throughout the well, Figure 6.1. Cell viability of 1 x 10^3, 1 x 10^4 and 1 x 10^5 differentiated THP-1 cells was quantified using the ATP assay CellTiter Glo. An ATP concentration dependent signal was observed with 1 x 10^3 and 1 x 10^4 cells per well compared to 1 x 10^5 cells per well, Figure 6.2, confirming microscopic observations and validating the CellTiter Glo assay that there was less ATP, and thus less cells in 1 x 10^3 and 1 x 10^4 cells per well. A THP-1 cell density of 1 x 10^5 cells per well was used for subsequent experiments.

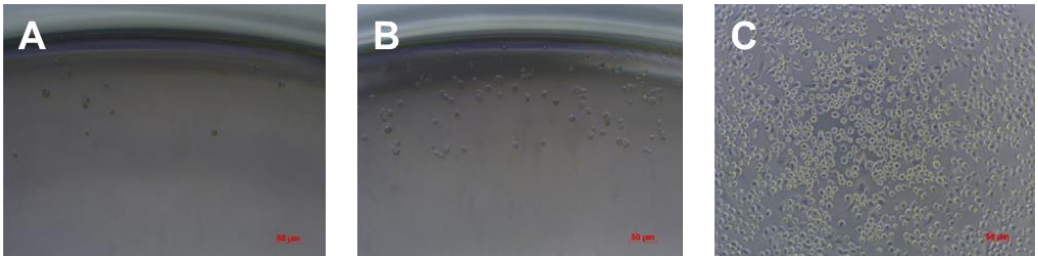

Figure 6.1: PMA differentiated THP-1 cells in 96 well microtiter plates

A: 1 x 10^3 cells per well; B: 1 x 10^4 cells per well; C: 1 x 10^5 cells per well. Differentiated THP-1 cells 48 h post treatment with PMA. Magnification 40X.

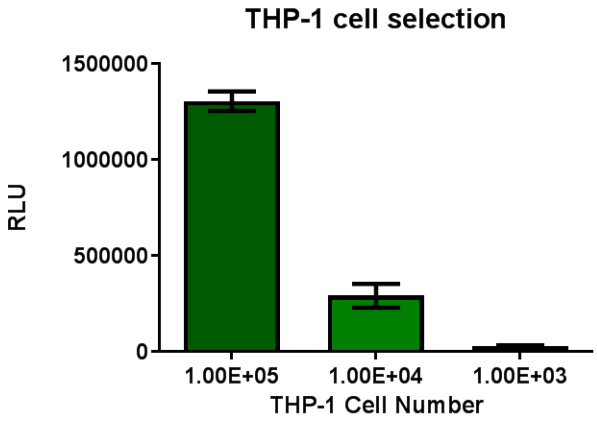

Figure 6.2: THP-1 cell numbers estimated using the CellTiter Glo assay

Differentiated THP-1 cells were assayed for cell viability using CellTiter Glo 48 h post differentiation with PMA at 1 x 10^3, 1 x 10^4 and 1 x 10^5 cells per well. Cell viability was measured in Relative Luminescence Units (RLU). Each data point is the mean of three technical replicates ± SEM.

6.2.1.1 Inter-well THP-1 cell number variation is minimal

Addition of PMA to a planktonic suspension of THP-1 cells induced cells to immediately start to attach to the vessel surface and pipette tips. In order to establish whether this introduced variation in cell number across wells that may influence results, six independent cultures of THP-1 cells were PMA-treated and aliquoted across eight microtiter plate wells (Materials and Methods section 2.10.2). Cell viability was quantified after 48 h with CellTiter Glo, Figure 6.3. The variation from the mean across each group of eight wells was <10%, and there was no statistically significant difference between the means of each independent culture when tested using ANOVA, suggesting that inter-well variation in the number of differentiated THP-1 cells is minimal and that this macrophage model is applicable to assaying THP-1 cytokine responses.

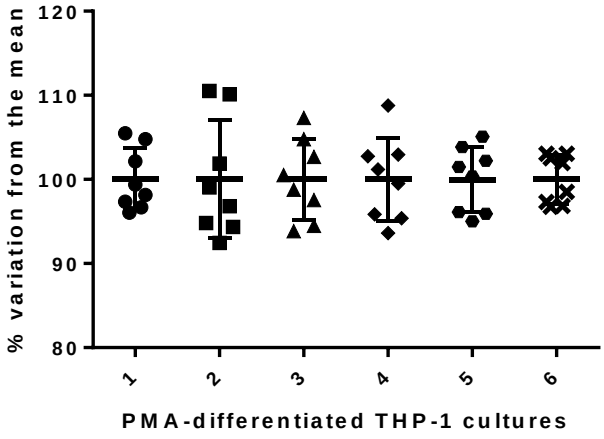

Figure 6.3: Inter well variation of PMA-treated THP-1 cells

Six THP-1 cell cultures were PMA-differentiated and pipetted into 10 wells per culture to determine inter-well variability. Each data point represents percentage variation from the mean for each of the ten wells per culture. Cell number was measured using the CellTiter Glo assay. No statistically significant differences were observed when tested using one-way ANOVA. The means ± SDEV of each independent cultures are shown.

6.2.2 Bacterial culture media is toxic to PMA-differentiated THP-1 cells

To establish media toxicity and to titrate the maximum concentration of bacterial supernatants that could be added to TLHP-1 cells without reducing cell viability PMA-differentiated THP-1 cells were treated with bacterial culture media (mycobacteria-free) diluted in RPMI media at concentrations of 10, 25 and 50% v/v. All bacterial culture media and PBS at 50% reduced THP-1 cell viability (Materials and Methods section 2.10.3), Figure 6.4. Sauton's Modified Media +/- Tween 80 had the most dramatic effect on cell viability at 50%, and Sauton's Modified Media no Tween 80 reduced cell viability at ≥25% v/v. Increasing v/v of all media tested reduced THP-1 cell survival, Figure 6.4. The Sauton's Modified Media no Tween 80 (used in the RCCS model) was toxic to PMA-differentiated THP-1 cells in a dose dependent manner.

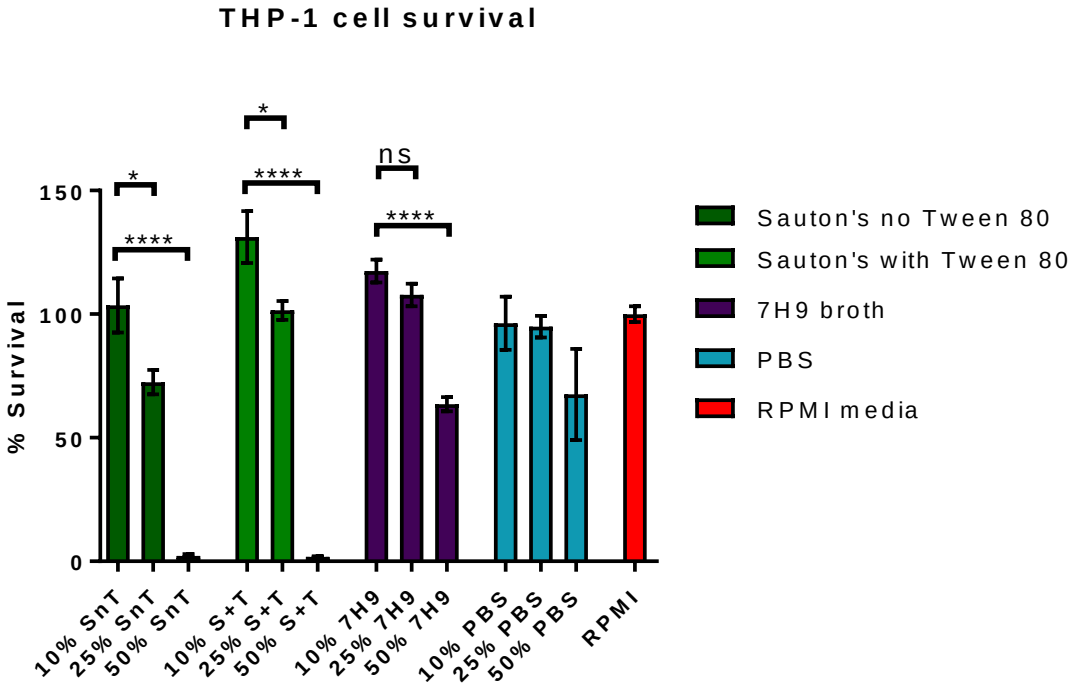

Figure 6.4: THP-1 cell survival after 24 h exposure to sterile bacterial culture media or PBS

PMA-differentiated THP-1 cells were treated with a range of sterile bacterial culture media or PBS for 24 h to establish media toxicity. Percentage is v/v of bacterial media diluted with THP-1 RPMI media. SnT; Sauton's Modified Media no Tween 80; S+T: Sauton's Modified Media plus Tween 80; 7H9: 7H9 + ADC, Tween 80 broth; PBS: Phosphate Buffered Saline; RPMI: THP-1 cell media 1640 RPMI + FCS + GLU. Each data point is the mean of three technical replicates + SEM relative to untreated THP-1 cells. Cell survival was assayed for using the CellTiter Glo assay.

6.2.3 Biofilm supernatants do not decrease THP-1 cell viability compared to control supernatants

RCCS-derived biofilm and control culture supernatants as well as static cultures of the initial RCCS inoculum were collected at days 7 and 21 (Materials and Methods section 2.4.3) . Supernatants were collected from three independent RCCS runs (n=3). Bacterial culture supernatants were diluted to 10% v/v with RPMI, as this dilution did not detrimentally affect THP-1 cell viability (Figure 6.4). PMA-differentiated THP-1 cells were stimulated for 24 h with 10% v/v sterile bacterial supernatants. THP-1 cells were also stimulated with IL-1β and TNFα producing toll-like receptor agonists LPS (TLR4) and PAM3 (TLR1/2) as well as 10% and 100% v/v Sauton's Modified Media no Tween and RPMI media only. Cell viability was quantified using CellTiter Glo ATP viability assay (Materials and Methods section 2.10.3). Analysis of variance (ANOVA) was used to assign statistical significance, comparing biofilm, control and stationary supernatants. There was no statistically significant effect on THP-1 cell viability after 24 h stimulation with biofilm, control or static culture derived supernatants, Figure 6.5. As expected, the only significant difference was 100% v/v Sauton's no Tween compared to all other data sets ($p>0.0001$ compared to all other conditions). This bacterial media reduced cell viability (>99%) at 100% v/v as previously established, Figure 6.4. THP-1 cell viability was not affected by 10% v/v sterile bacterial cell supernatants from any of the models suggesting that at this dilution; biofilm-derived supernatants were not more cytotoxic compared to control supernatants.

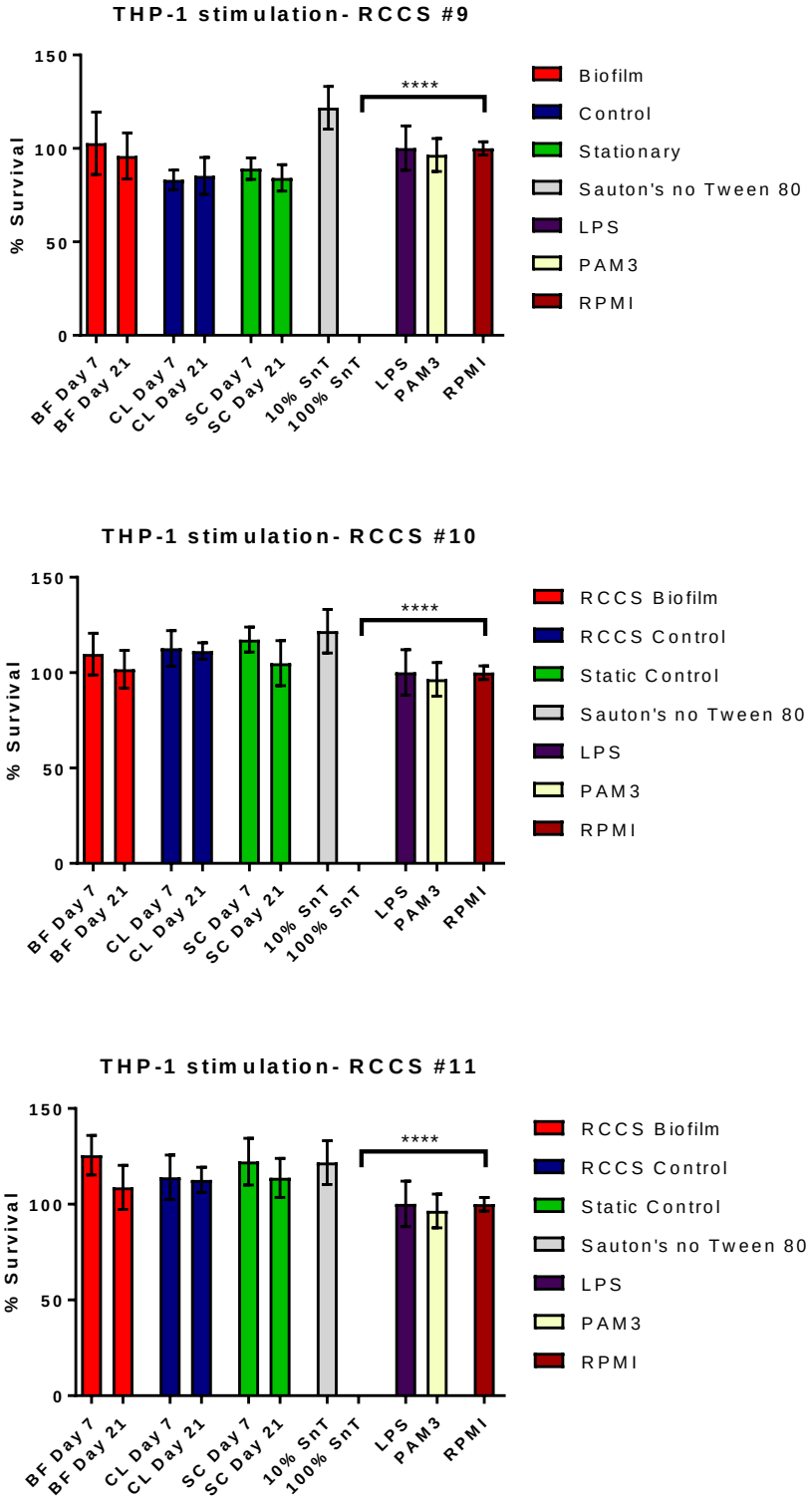

Figure 6.5: THP-1 cell survival after 24 h stimulation with sterile *M. bovis* BCG supernatants

PMA-differentiated THP-1 cells were stimulated with supernatants taken at days 7 and 21 from three RCCS runs (Biofilm, Control), RCCS #9, #10 and #11, and from a corresponding static culture (Stationary). BF: RCCS biofilm; CL: RCCS control; SC: stationary control culture; LPS: lipopolysaccharide; PAM3: Pam3CSK4; SnT: Sauton's Modified Media no Tween; RPMI: THP-1 cell culture media. Cell survival was determined using CellTiter Glo. Each data point is the mean of three technical replicates ± SEM relative to untreated THP-1 cells. Cell survival was assayed for using the CellTiter Glo assay.

6.2.4 RCCS-derived biofilm supernatants do not induce differential IL-1β release

There was no statistically significant difference in IL-1β production between RCCS-derived biofilm, control or static supernatants, Figure 6.6. THP-1 stimulation with day 21 RCCS supernatants did induce IL-1β production compared to RCCS day 7 supernatants for RCCS #9 and RCCS #11. The strongest IL-1β response was seen with 100% v/v Sauton's no Tween 80, followed by LPS exposure. 10% Sauton's no Tween 80 media alone control did not elicit IL-1β secretion, suggesting IL-1β detected was due to THP-1 cells responding to *M. bovis* BCG derived factors. IL-1β was quantified using an IL-1β specific ELISA (Materials and Methods section 2.11.1).

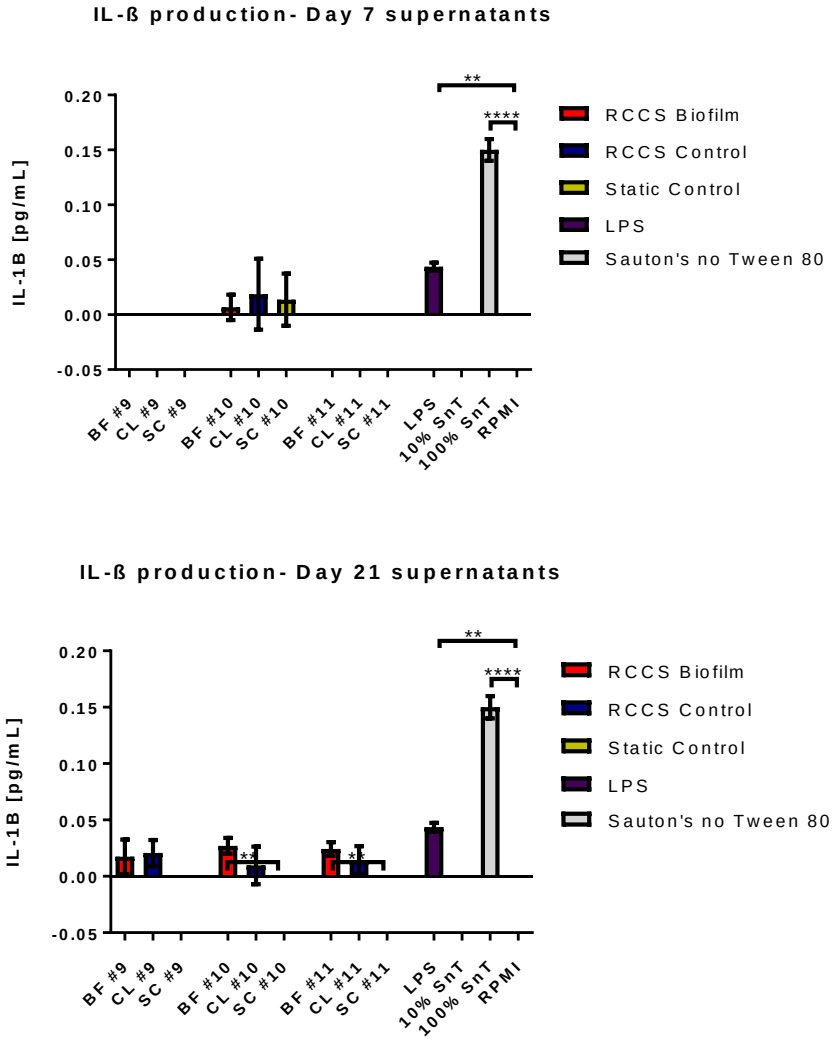

Figure 6.6: THP-1 cell IL-1β secretion after 24 h stimulation with *M. bovis* BCG derived supernatants

PMA differentiated THP-1 cells were stimulated with supernatants taken at days 7 and 21 from three RCCS runs (Biofilm, Control), RCCS #9, #10 and #11, and from a corresponding static culture (Stationary). BF: RCCS biofilm; CL: RCCS control; SC: stationary control culture; LPS: lipopolysaccharide; SnT: Sauton's Modified Media no Tween; RPMI: THP-1 cell culture media. IL-1β concentration was determined using an IL-1β ELISA. Each data point is the mean of three technical replicates ± SEM. Data were analysed using ANOVA.

6.2.5 Day 7 RCCS biofilm-derived supernatants do not induce TNFα secretion in comparison to control cultures

Sterile supernatants harvested at day 7 from RCCS #9, #10, #11 biofilm and control cultures induced low levels of TNFα secretion from THP-1 cells, although not as high as after LPS exposure. There was no statistically significant difference between biofilm and control cultures, Figure 6.7. Both 10% and 100% Sauton's no Tween 80 control did not induce TNFα secretion suggesting TNFα detected is due to THP-1 cells responding to *M. bovis* BCG derived factors. TNFα was quantified using a TNFα specific ELISA (Materials and Methods section 2.11.2).

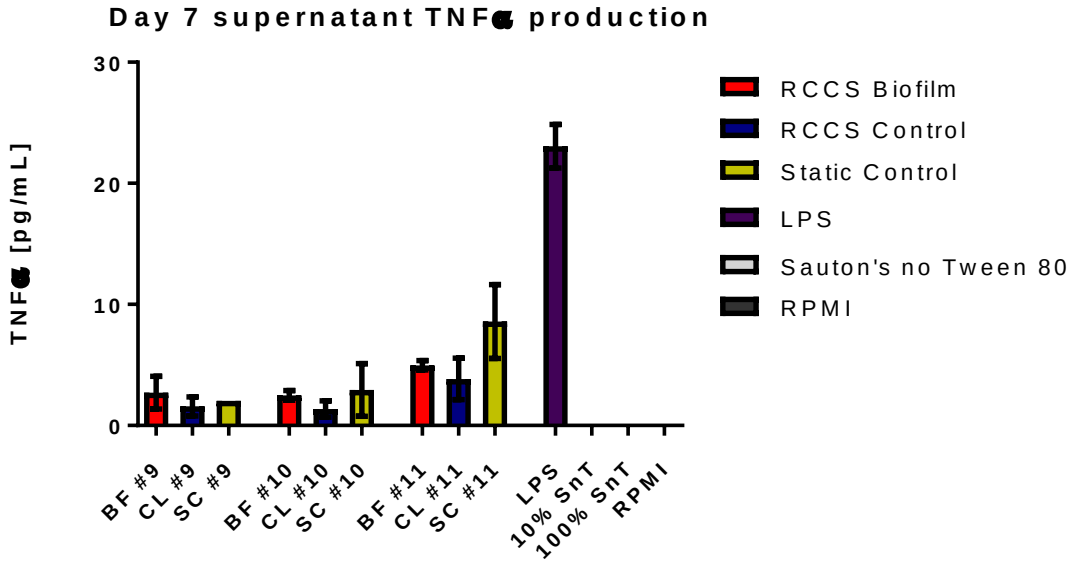

Figure 6.7: THP-1 cell TNFα secretion after 24 h stimulation with *M. bovis* BCG derived supernatants

PMA differentiated THP-1 cells were stimulated with supernatants taken at day 7 from three RCCS runs (Biofilm, Control), RCCS #9, #10 and #11, and from three corresponding static cultures (Stationary). BF: RCCS biofilm; CL: RCCS control; SC: stationary control culture; LPS: lipopolysaccharide [20 ng/mL]; SnT: Sauton's Modified Media no Tween; RPMI: THP-1 cell culture media. TNFα concentration was determined using a TNFα ELISA. Each data point is the mean of three technical replicates ± SEM. Data were analysed using ANOVA.

6.2.6 Day 21 RCCS biofilm-derived supernatants induce increased TNFα secretion

There was differential secretion of TNFα between RCCS biofilm and control culture supernatants harvested at day 21. Biofilm TNFα levels were increased compared to both RCCS control and static control cultures derived from RCCS #9, #10 and #11, Figure 6.8. One-way ANOVA analysis deemed this difference in TNFα secretion statistically significant in RCCS #10 and RCCS #11, with Confidence Intervals of 95%. TNFα was quantified using a TNFα specific ELISA (Materials and Methods section 2.11.2).

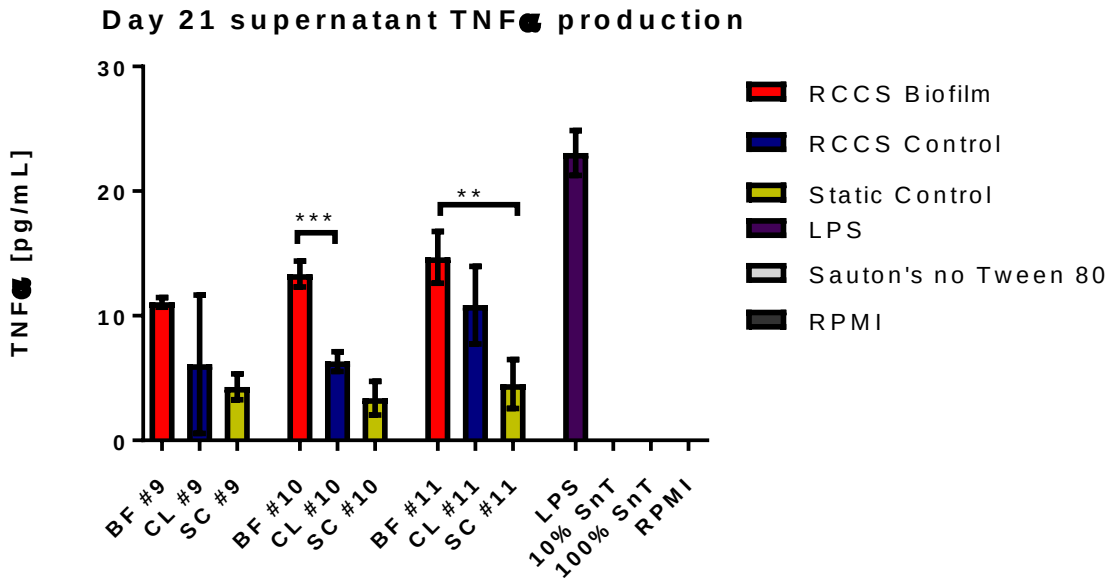

Figure 6.8: THP-1 cell TNFα secretion after 24 h stimulation with *M. bovis* BCG derived supernatants

PMA differentiated THP-1 cells were stimulated with supernatants taken at day 21 from three RCCS runs (Biofilm, Control), RCCS #9, #10 and #11, and from three corresponding static cultures (Stationary). BF: RCCS biofilm; CL: RCCS control; SC: stationary control culture; LPS: lipopolysaccharide; PAM3; SnT: Sauton's Modified Media no Tween; RPMI: THP-1 cell culture media. TNFα concentration was determined using a TNFα ELISA. Each data point is the mean of three technical replicates ± SEM. Data were analysed using ANOVA.

The three biological replicates (RCCS #9, #10, #11) were pooled for RCCS-derived biofilm, RCC-derived controls and static control cultures, Figure 6.9. Biofilm-derived supernatants induced a statistically significant induction of TNFα compared to either RCCS control or stationary control supernatants with 95% Confidence Intervals.

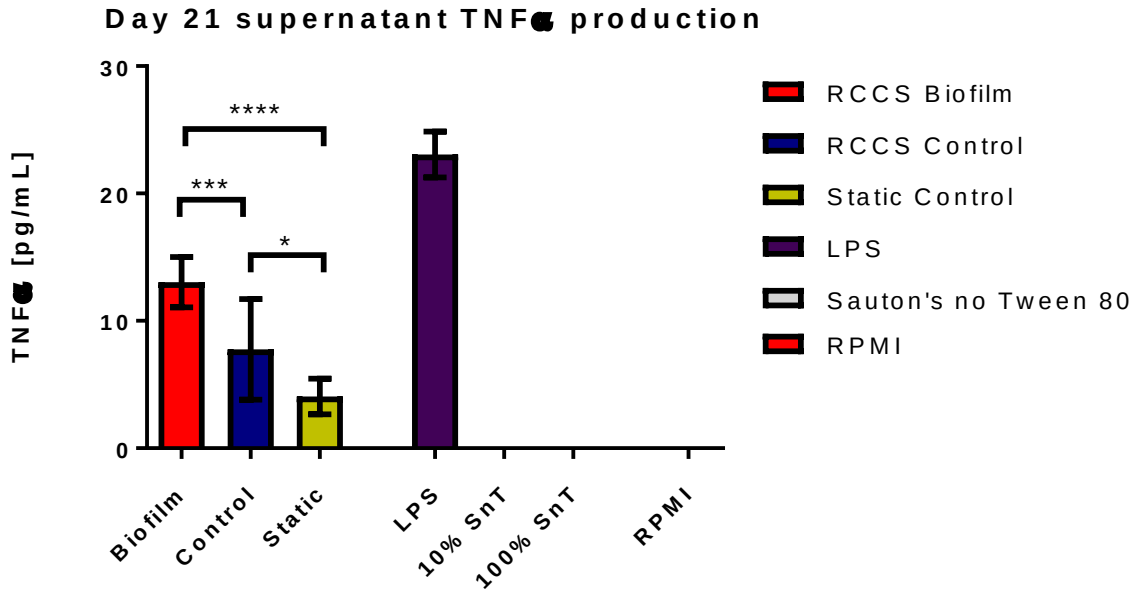

Figure 6.9: THP-1 cell TNFα secretion after 24 h stimulation with *M. bovis* BCG derived supernatants

PMA differentiated THP-1 cells were stimulated with supernatants taken at day 21 from three RCCS runs (Biofilm, Control), RCCS #9, #10 and #11, and from three corresponding static cultures (Stationary). BF: RCCS biofilm; CL: RCCS control; SC: stationary control culture; LPS: lipopolysaccharide; PAM3; SnT: Sauton's Modified Media no Tween; RPMI: THP-1 cell culture media TNFα concentration was determined using a TNFα ELISA. Each data point is the mean of three biological replicates ± SEM. Data were analysed using ANOVA.

6.3 Discussion

M. bovis BCG 10% v/v sterile culture supernatants were not cytotoxic to THP-1 cells after 24 h exposure; there was no statistically significant reduction of THP-1 cell viability when stimulated with supernatants. *M. bovis* BCG is attenuated, and as such has lost key secreted virulence factors such as ESAT6 and CFP10; these proteins are secreted antigens that form a heterodimer complex, and have been shown to be key to the virulence of *M.tb* (Meher, Bal et al. 2006). Addition of these purified proteins in single and combined amounts to THP-1 cells however did not show a reduction in cell viability (Seghatoleslam, Hemmati et al. 2016), suggesting that attenuation of *M. bovis* BCG does not reduce toxicity compared to *M.tb* culture supernatants.

Two cytokines were assayed for that are known to be important in TB infection; IL-1β and TNFα. Both cytokines were produced in response to LPS, showing that THP-1 cells were capable of cytokine production in response to the presence of bacterial products in this *in vitro* system, albeit at low levels of secretion for IL-1β. After 24 h, there was no statistically significant difference in IL-1β production for THP-1 cells stimulated with day 7 or day 21 cell supernatants. There was no statistically significant difference in TNFα production for THP1 cells stimulated with day 7 RCCS biofilm, RCCS control or static control supernatants. There was however, a statistically significant increase in TNFα production for THP-1 cells treated with day 21 RCCS supernatants compared to RCCS control and static control supernatants. It is likely that RCCS biofilm secreted PAMPs differ to RCCS and static control secreted PAMPs; these PAMPs are not sufficient to induce a differential IL-1β response but can induce increased TNFα production when harvested at day 21 from the RCCS. The extracellular matrix that hold clusters of bacilli together in a biofilm will likely increase in size as biofilms grow over 21 day's incubation and this ECM is a likely source of PAMPs. TNFα production was not significant with day 7 supernatants but was with day 21 supernatants; this suggests that maturation of RCCS biofilms is necessary to either allow secretion of certain pro-inflammatory PAMPs or that the concentration of secreted PAMPs must first accumulate past a threshold to induce TNFα production in THP-1 macrophages. Increased TNFα production suggests that biofilm secreted products, or the formation of an extracellular matrix in the RCCS model, differs to bacilli grown in standard culture conditions and may contribute to unrecognised inflammatory mechanisms in the lung.

There were limitations to these studies. The THP-1 cell line was selected for pathogen host interaction studies as these cells are a clonal population of human monocytes from a single donor, which reduces variability across experiments, and THP-1 cells are an established tissue culture model for mycobacterial research. This cell line however is immortalised and does not exactly represent an *in vivo* alveolar macrophage due to

altered cytokine secretion and receptor expression (Schildberger, Rossmanith et al. 2013). IL-1β secretion was very low in THP-1 cells stimulated with cell supernatants and LPS. LPS will induce pro-IL-1β accumulation intracellularly in the THP-1 macrophage but a second signalling step induced through caspase-1 activation is required to cleave pro-IL-1β to the secreted form, mature IL-1β (Bauernfeind, Horvath et al. 2009). LPS alone may not have been sufficient in this model to induce higher levels of IL-1β. As an alternative, blood could be collected from human donors, monocytes extracted and differentiated into *ex vivo* macrophages. This is likely to be more representative of an *in vivo* macrophage, although these cells show considerable diversity depending on the genetic background of the donor and as such, cytokine responses can vary. For the purposes of an initial screen reported here, the THP-1 cell line was deemed appropriate for initial cytotoxicity screening and cytokine response assays.

Bacterial supernatants had to be diluted with THP-1 cell RPMI media to 10% v/v before stimulation, as ≥25% v/v Sauton's no Tween was cytotoxic to cells. Dilution steps may have reduced the potency of these supernatants; bacterial PAMPs may not have been present in sufficient quantities to induce high levels of TNFα or IL-1β. IL-1β release was quantified for THP-1 cells treated with 100% Sauton's no Tween 80, which was cytotoxic to THP-1 cells. The mechanism of cell death induced by this media was not identified but it is likely THP-1 cell lysis released IL-1β as this cytokine is present intracellularly as pro-IL-1β (Lopez-Castejon and Brough 2011), while TNFα must first be synthesised in response to TLR activation hence why no TNFα was measured with Sauton's no Tween 80 induced cell death.

Previous studies have shown increased TNFα production in THP-1 cells in response to stimulation with non-tuberculous *Mycobacterium avium* biofilm supernatants (Rose and Bermudez 2014). This chapter demonstrates that biofilm supernatants derived from *M. bovis* BCG, a member of the Mycobacterium Tuberculosis Complex that cause TB in humans, can elicit pro-inflammatory cytokine production in this THP-1 macrophage model, which has not been shown to date.

Chapter 7: The role of a novel mismatch repair nuclease in *Mycobacterium tuberculosis*

7.1 Overview

Mismatch mutations occur when an incorrect nucleotide base is incorporated by DNA polymerase during DNA replication (Fukui 2010). Mismatch mutations may be repaired by the proofreading activity of DNA polymerase; however, alternative DNA repair systems also play an important role. Mismatched bases are recognised by a canonical mismatch repair system in most bacterial species that utilise MutS and MutL protein families to repair the DNA lesion. Actinobacteria however do not possess homologues for MutS or MutL although these protein families are near-ubiquitous throughout Gram-positive and Gram-negative bacteria (Sachadyn 2010), (Banasik and Sachadyn 2014). Despite the lack of a canonical mismatch MutS-MutL repair system, Actinobacteria exhibit similar mutation rates to species that do contain MutS-MutL mismatch repair (Kucukyildirim, Long et al. 2016). This suggests that Actinobacteria are likely to contain a previously un-discovered non-canonical mismatch repair system. Bioinformatic analyses identified a potential nuclease gene called nucS in Actinobacteria that resembled a nuclease in Archaea; the recent crystal structure of the archaeal NucS indicated that this nuclease was a component of a mismatch repair pathway (Nakae, Hijikata et al. 2016).

The Blasquez and Doherty laboratories together with the Waddell laboratory collaborated to investigate the potential role of NucS in an Actinobacteria non-canonical mismatch repair pathway in *M. smegmatis and Streptomyces coelicolor* (Castaneda-Garcia, Prieto et al. 2017). The study demonstrated that deletion of *nucS* significantly increased spontaneous mutation rates in Actinobacteria- measured through increased accumulation of antimicrobial drug resistance-conferring mutations to isoniazid and rifampicin. Rifampicin and streptomycin resistance increased 150-fold and 86-fold in *M. smegmatis* and 108-fold and 197-fold for *S. coelicolor* respectively. These hypermutable phenotypes could be rescued by complementation with the wildtype *nucS* gene. Bioinformatic analyses of approximately 1,600 clinical isolates of drug-resistant *M.tb* revealed nine single nucleotide polymorphisms in the *nucS* gene that may be clinically relevant to drug resistance. *M. smegmatis* was complemented with these nine alleles and mutation rates measured. Five alleles significantly increased mutation rates, suggesting the mutations in *nucS* might generate hypermutable isolates of *M.tb*. This chapter describes my work extending these findings in *M. smegmatis* and *S. coelicolor* to *M.tb*.

A *nucS* null strain of *M.tb* (*ΔnucS*) was generated with collaborators to investigate the role of *nucS* in *M.tb* H37Rv.

The aims of this chapter were two-fold:

i) To characterise spontaneous antimicrobial drug resistance in a *nucS* null *M.tb* H37Rv strain compared to wild type H37Rv *M.tb* using ethambutol, isoniazid, rifampicin and streptomycin;

ii) To complement the *nucS* null *M.tb* strain and *M.tb* H37Rv wildtype strain with an *M.tb* H37Rv wildtype *nucS* gene, a drug-sensitive *M.tb* clinical isolate *nucS* gene and a drug-resistant *M.tb* clinical isolate *nucS* gene for further characterisation.

7.2 Results

7.2.1 Minimum Inhibitory Concentration (MIC) determination of *M. tuberculosis* H37Rv

In order to detect spontaneous drug-resistant mutations, minimum inhibitory concentrations (MIC) of each drug were determined in a 7H10 agar plate-screening model (Materials and Methods section 2.5.4), Figure 7.1 shows the range of antibiotic concentrations tested. MIC values were estimated as 10 µg/mL ethambutol, 5 µg/mL isoniazid, 0.5 µg/mL rifampicin and 5 µg/mL streptomycin.

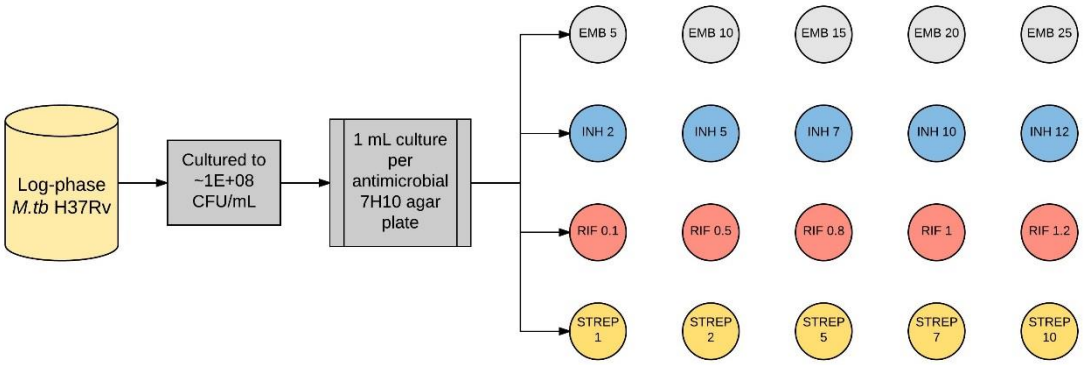

Figure 7.1: Minimum inhibitory concentration (MIC) determination of *M.tb* H37Rv

Log-phase 1 x 10^8 CFU/mL *M.tb* H37Rv was used to inoculate a range of concentrations of ethambutol (5, 10, 15, 20, 25 µg/mL), isoniazid (2, 5, 7, 10, 12 µg/mL), rifampicin (0.1, 0.5, 0.8, 1, 1.2 µg/mL) and streptomycin (1, 2, 5, 7, 10 µg/mL). The MICs estimated for this model are 10 µg/mL ethambutol, 5 µg/mL isoniazid, 0.5 µg/mL rifampicin and 5 µg/mL streptomycin.

7.2.2 The deletion of *nucS* in *M.tb* increases the emergence of antimicrobial drug resistant colonies compared to wildtype

Three biological replicates of *M.tb* H37Rv cultures (n=3) and three biological replicates of *M.tb* H37Rv *Δnuc* cultures (n=3) were grown aerobically to late log-phase, corresponding to an O.D. of 1.0 of approximately 1 x 10^8 CFU/mL. Cultures were centrifuged to pellet bacilli and were re-suspended in one-fifth the original volume, concentrating the CFU/mL five-fold. Agar MIC determination of three biological replicates of *M.tb* H37Rv cultures (n=3) and three biological replicates of *M.tb* H37Rv *Δnuc* cultures (n=3) was performed as per Materials and Methods section 2.5.4 but inocula were concentrated in one-fifth original volumes to increase likelihood of obtaining resistant colonies. This is summarised in Figure 7.2. Viable counts were performed to determine the CFU/mL of each inoculum (Materials and Methods section, 2.2.1) and the results are summarised in Table 7.1.

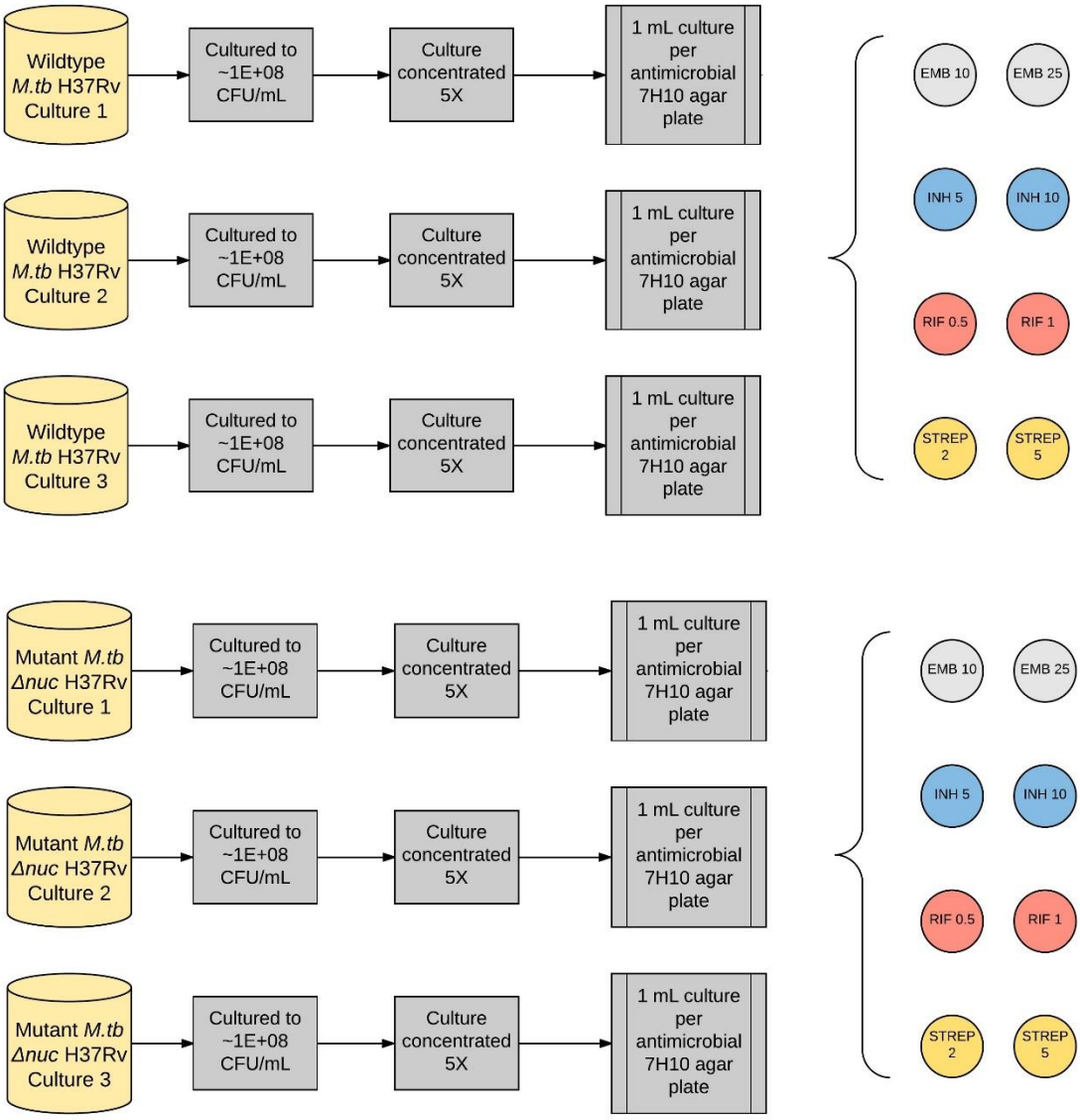

Figure 7.2: Concentrations of antimicrobial drugs used for the spontaneous mutation assays

Wildtype *M.tb* H37Rv and *M.tb Δnuc* mutant cultures were screened against EMB (10, 25 µg/mL), INH (5, 10 µg/mL), RIF (0.5, 1 µg/mL) and STREP (2, 5 µg/mL).

CFU/mL	*M.tb* H37Rv	*M.tb Δnuc*
Culture 1	8.15E+08	7.35E+08
Culture 2	9.55E+08	6.80E+08
Culture 3	4.13E+08	6.55E+08

Table 7.1: Number of *M.tb* H37Rv and *M.tb Δnuc* bacilli (CFU/mL) used for the spontaneous mutation assays

The CFU/mL of each inoculum was determined by viable counting.

These five-fold concentrated triplicate cultures were used to inoculate 7H10 agar plates prepared with two concentrations of each antimicrobial drug, Figure 7.2. The lower concentrations are the MICs determined from Figure 7.1. The higher concentration is at least two-fold this MIC value. Plates were inoculated with 1 mL of each culture and incubated for four weeks at 37°C before drug resistant colonies were counted.

Drug resistance-conferring mutation rates, as measured by the number of colonies on antimicrobial drug selection plates, were higher in the *M.tb Δnuc* mutant compared to wildtype *M.tb* H37Rv for ethambutol, isoniazid, rifampicin and streptomycin. There was variability across biological replicates however. The number of spontaneous drug-resistant mutants observed was dependent on the concentration of antimicrobial drug. Although a trend towards a greater frequency of drug-resistant mutations in the nucS null mutant was observed, no statistically significant difference was identified between wildtype and mutant by Mann-Whitney U test. Results are presented for each antimicrobial drug in the following sections.

7.2.2.1 Ethambutol (EMB)

No spontaneous drug-resistant mutants were isolated from wildtype *M.tb* H37Rv at 10 and 25 µg/mL EMB, while 27 spontaneous drug-resistant mutants were isolated from *M.tb Δnuc* at 10 µg/mL only, Table 7.2, Figure 7.3.

Ethambutol 10 µg/mL			**Ethambutol 25 µg/mL**		
CFU/mL	***M.tb* H37Rv**	***M.tb Δnuc***	**CFU/mL**	***M.tb H37Rv***	***M.tb Δnuc***
Culture #1	0	0	Culture #1	0	0
Culture #2	0	12	Culture #2	0	0
Culture #3	0	15	Culture #3	0	0

Table 7.2: EMB-resistant mutants identified from wildtype *M.tb* H37Rv and *M.tb Δnuc* cultures

A greater number of drug-resistant mutants were recovered from *M.tb Δnuc* compared to wildtype *M.tb* H37Rv at 10 µg/mL EMB. No colonies were observed at 25 µg/mL EMB for either strain. Columns indicate the number of single drug-resistant colonies on EMB 7H10 agar plates.

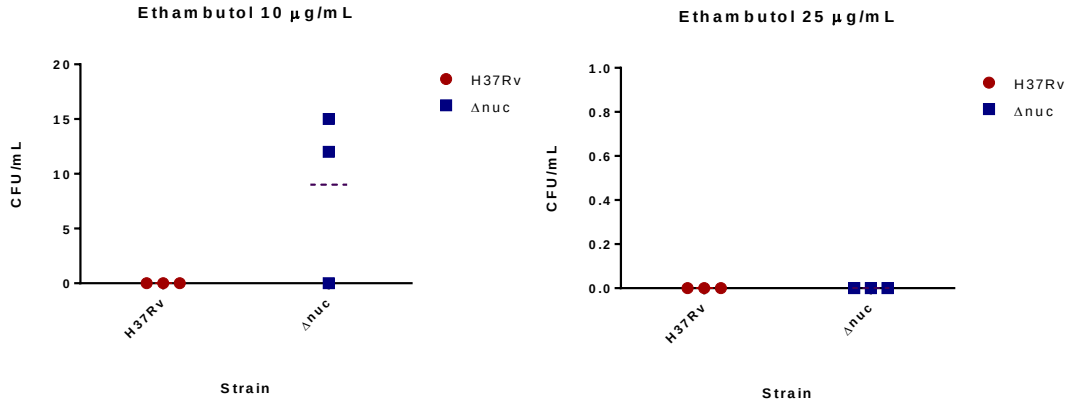

Figure 7.3: The number of EMB-resistant mutants identified from wildtype *M.tb* H37Rv and *M.tb* Δnuc cultures

The *M.tb Δnuc* mutant (blue) has increased drug resistance rates compared to wildtype *M.tb* H37Rv (red) at 10 µg/mL EMB. No growth was evident at 25 µg/mL EMB for either strain. The dotted line represents the mean of three biological replicates.

7.2.2.2 Isoniazid (INH)

Increased INH resistance was observed for two out of three triplicate *M.tb Δnuc* mutant cultures compared to wildtype *M.tb* H37Rv at 5 µg/mL INH. Only one *M.tb Δnuc* mutant culture showed increased drug resistance at the higher concentration of 10 µg/mL INH with 72 colonies compared to 14 colonies for one wildtype *M.tb* H37Rv culture, Table 7.3, Figure 7.4.

Isoniazid 5 µg/mL			**Isoniazid 10 µg/mL**		
CFU/mL	***M.tb* H37Rv**	***M.tb Δnuc***	**CFU/mL**	**M.tb H37Rv**	***M.tb Δnuc***
Culture #1	7	1	Culture #1	14	0
Culture #2	3	200	Culture #2	0	1
Culture #3	4	38	Culture #3	1	72

Table 7.3: CFU/mL of wildtype *M.tb* H37Rv and *M.tb Δnuc* mutant cultures post four-week INH exposure

The *M.tb Δnuc* mutant has increased drug resistance rates compared to wildtype *M.tb* H37Rv at 5 µg/mL INH. One out of the three triplicate *M.tb Δnuc* mutant cultures showed increased drug resistance at 10 µg/mL INH.

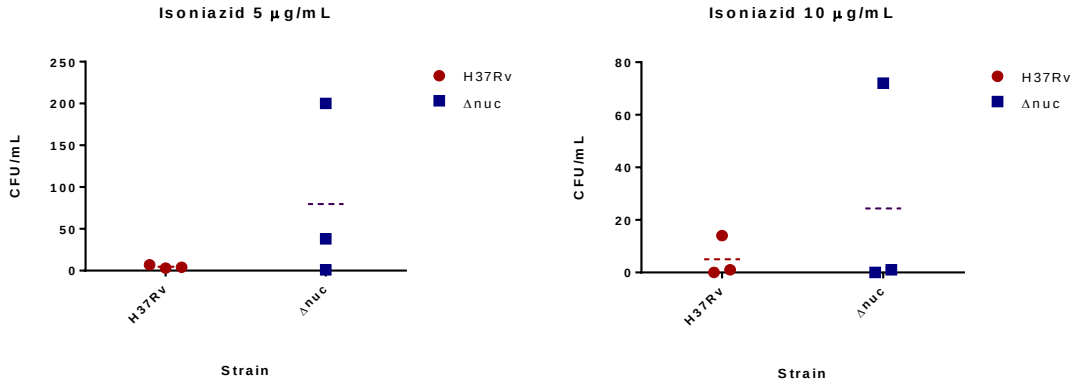

Figure 7.4: CFU/mL of wildtype *M.tb* H37Rv and *M.tb Δnuc* mutant cultures post four-week post INH exposure

The *M.tb Δnuc* mutant (blue) has increased drug resistance rates compared to wildtype *M.tb* H37Rv (red) at 5 µg/mL INH. One out of the three triplicate *M.tb Δnuc* mutant cultures showed increased drug resistance at 10 µg/mL INH. The mean of each three cultures is shown by a dotted line.

7.2.2.3 Rifampicin (RIF)

RIF resistance in the *M.tb Δnuc* mutant strain was less pronounced than INH resistance. No wildtype *M.tb* H37Rv colonies were observed for 0.5 or 1.0 µg/mL RIF, with 1, 4 and 16 colonies observed for the three triplicate *M.tb Δnuc* mutant cultures, Table 7.4, Figure 7.5.

Rifampicin 0.5 µg/mL			Rifampicin 1.0 µg/mL		
CFU/mL	***M.tb* H37Rv**	***M.tb Δnuc***	**CFU/mL**	***M.tb H37Rv***	***M.tb Δnuc***
Culture #1	0	4	Culture #1	0	0
Culture #2	0	16	Culture #2	0	0
Culture #3	0	1	Culture #3	0	0

Table 7.4: CFU/mL of wildtype *M.tb* H37Rv and *M.tb Δnuc* mutant cultures post four-week RIF exposure

The *M.tb Δnuc* mutant had marginally increased drug resistance rates compared to wildtype *M.tb* H37Rv at 0.5 µg/mL RIF. No colonies were recorded for either strain at 1.0 µg/mL RIF.

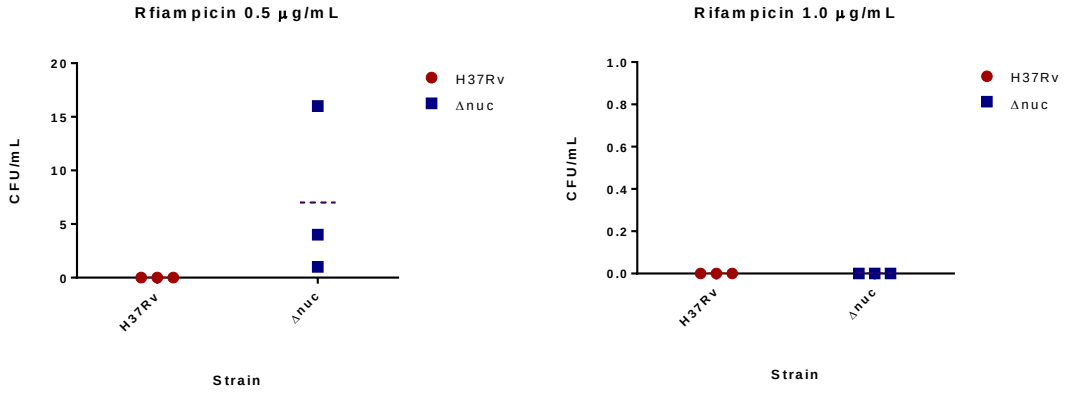

Figure 7.5: CFU/mL of wildtype *M.tb* H37Rv and *M.tb* Δnuc mutant cultures post four-week post RIF exposure

The *M.tb Δnuc* mutant has marginally increased drug resistance rates compared to wildtype *M.tb* H37Rv at 0.5 µg/mL RIF. No colonies were recorded for either strain at 1.0 µg/mL RIF. The mean of each three cultures is shown by a dotted line.

7.2.2.4 Streptomycin (STREP)

Increased drug resistance for the *M.tb Δnuc* mutant was most evident at 2 µg/mL STREP. 49, 250 and 98 colonies were recorded for the three triplicate *M.tb Δnuc* mutant cultures, whereas only 33 colonies were recorded for one of the three triplicate wildtype *M.tb* H37Rv cultures. No colonies were recorded for the remaining two triplicate wildtype *M.tb* 37Rv cultures, Table 7.5, Figure 7.6. At 5 µg/mL STREP There was a ten-fold increase in colonies for one of the three *M.tb Δnuc* mutant triplicate cultures compared to the highest colony count of one of the wildtype *M.tb* H37Rv cultures.

Streptomycin 2 µg/mL			**Streptomycin 5 µg/mL**		
CFU/mL	***M.tb* H37Rv**	***M.tb Δnuc***	**CFU/mL**	***M.tb* H37Rv**	***M.tb Δnuc***
Culture #1	33	49	Culture #1	1	1
Culture #2	0	250	Culture #2	12	110
Culture #3	0	98	Culture #3	1	0

Table 7.5: CFU/mL of wildtype *M.tb* H37Rv and *M.tb Δnuc* mutant cultures post four week STREP exposure

The *M.tb Δnuc* mutant had increased drug resistance rates compared to wildtype *M.tb* H37Rv at 2 µg/mL STREP. The *M.tb Δnuc* mutant had less pronounced drug resistance at the higher concentration of 5 µg/mL STREP, with one of three *M.tb Δnuc* mutant triplicate cultures showing drug resistance at ten-fold more CFUs than wildtype *M.tb* H37Rv.

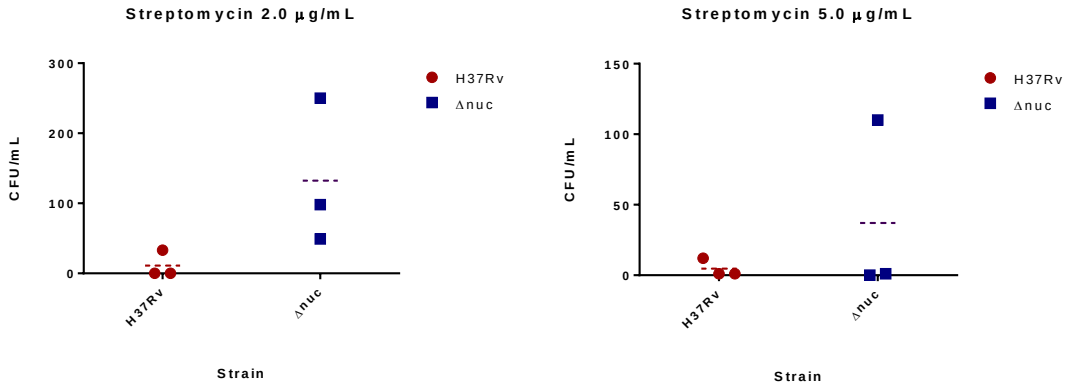

Figure 7.6: CFU/mL of wildtype *M.tb* H37Rv and *M.tb* Δnuc mutant cultures post four week STREP exposure

The *M.tb Δnuc* mutant had increased drug resistance rates compared to wildtype *M.tb* H37Rv at 2 µg/mL STREP. The *M.tb Δnuc* mutant had less pronounced drug resistance at the higher concentration of 5 µg/mL STREP, with one of three *Δnuc* mutant triplicate cultures showing drug resistance at ten-fold more CFUs than wildtype *M.tb* H37Rv. The mean of each three cultures is shown by a dotted line.

7.2.3 Complementation of *nuc* gene

The *M.tb Δnuc* mutant was complemented with one of three nuclease alleles;

1) Allele sequenced from a clinical, drug-sensitive TB strain (nuc^{sens});
2) *M.tb* H37Rv wildtype allele (nuc^{H37Rv})
3) Allele sequenced from a clinical MDR strain (nuc^{MDR}).

These nuc alleles were cloned into a pMV361 plasmid backbone with kanamycin (Kan) resistance selection and labelled as nuc^{sens}, nuc^{H37Rv} and nuc^{MDR} respectively. Wildtype *M.tb* H37Rv and *M.tb* Δ*nuc* mutant were complemented with each nucS allele. Figure 7.7 summarises the complementation experimental approach.

7.2.3.1 *M.tb* Δnuc mutant complementation strategy

pMV361 is a shuttle plasmid that possesses two origins of replication- one for *E. coli* and one for mycobacteria. It also possesses a kanamycin resistance cassette (KanR) for selection of cells transformed with the plasmid. pMV361 is an integrative vector that carries a site-specific integration system derived from the mycobacteriophage L5 that integrates at a single site in the *M.tb* chromosome, the *attb* site (Lee, Pascopella et al. 1991) removing the need for selection of single or double cross overs.

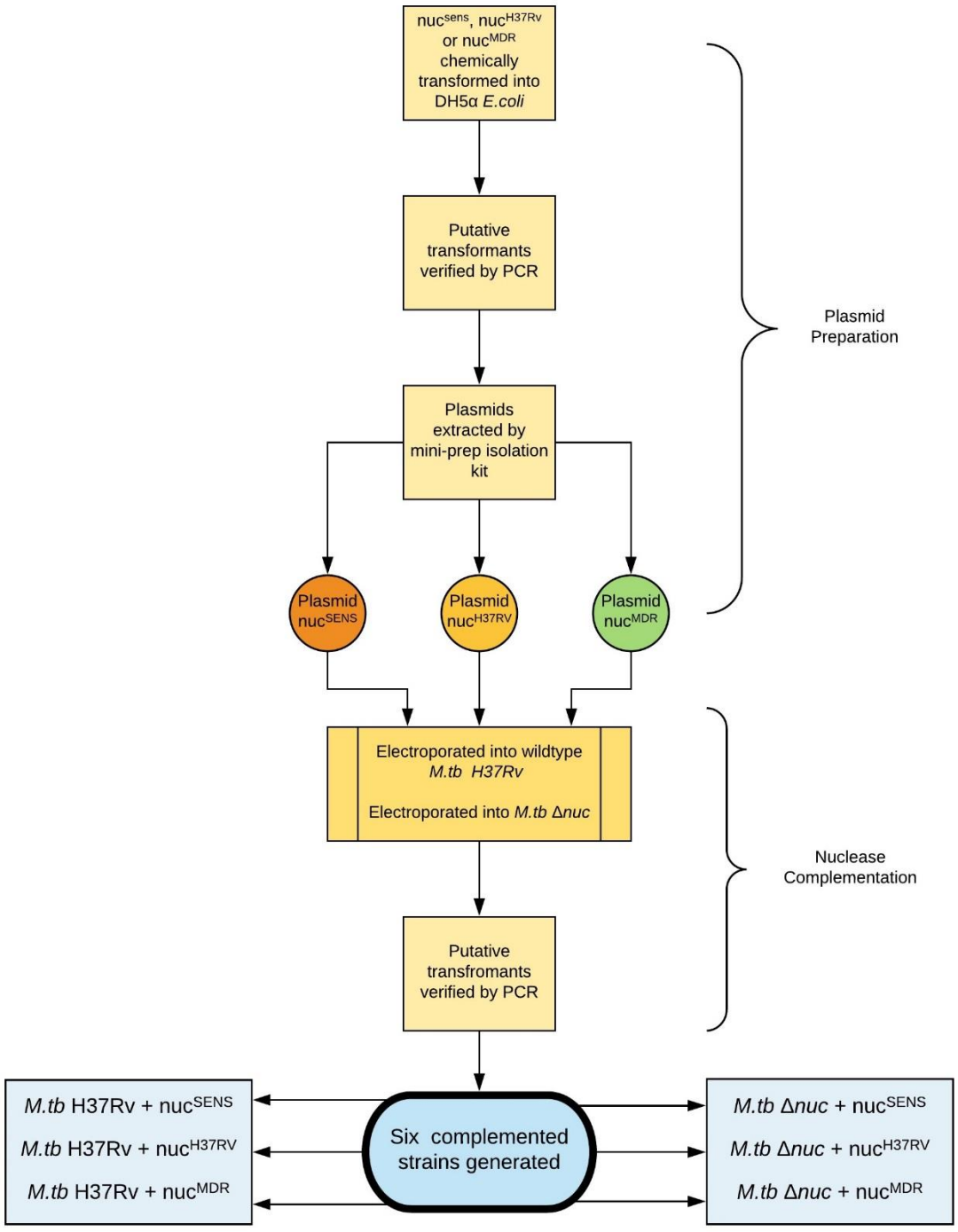

Figure 7.7: Flow chart of the experimental approach used to complement wildtype *M.tb* H37Rv and *M.tb Δnuc* with nucS alleles from clinical strains

Nuc^{sens} from a drug-sensitive *M.tb* clinical strain, nuc^{H37Rv} contains an H37Rv nuclease gene; nuc^{MDR} from a clinical multi-drug resistant strain.

7.2.3.2 Transformation of DH5α *E.coli*

DH5α *E.coli* were transformed with nuc^{sens}, nuc^{H37Rv} or nuc^{MDR} using a chemical transformation heat shock method and cultured onto LA agar supplemented with 20 µg/mL kanamycin (Kan). A forward and reverse primer pair (KmSeqF and KmSeqR) was used to PCR amplify the Kan resistance gene present in the pMV361 backbone to confirm plasmid presence in selected colonies. A gradient PCR was first performed using KmSeqF and KmSeqR primers with the control pMV361 plasmid (Kan resistance cassette present but no insert) to determine annealing temperatures of this primer pair, Figure 7.8.

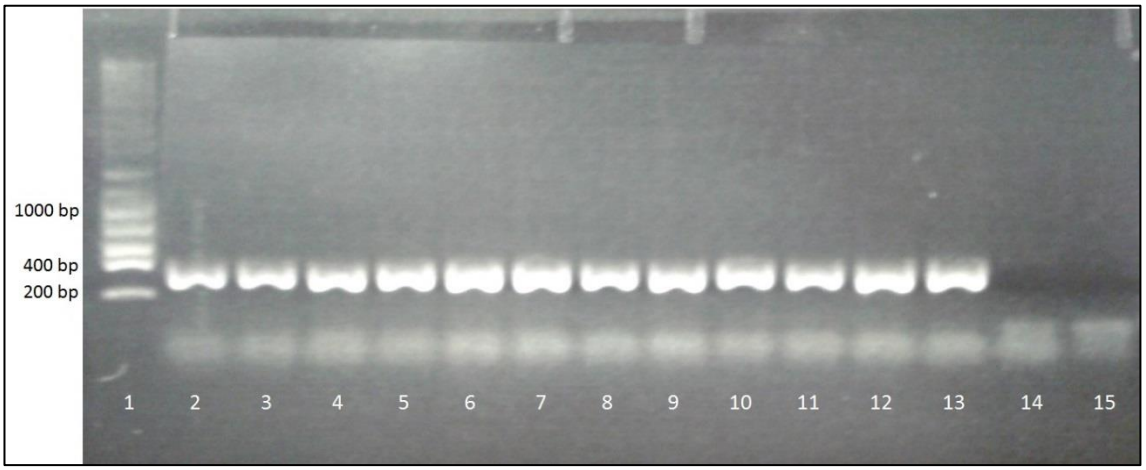

Figure 7.8: Gradient PCR of pMV361 plasmid to optimise the annealing temperature of KmSeqF and KmSeqR using a temperature gradient

Lane 1: Hyperladder I; Lanes 2-13: pMV361 plasmid amplified with an annealing temperature of 41.9°C to 53.0°C in approximately 1°C increments; Lane 14: negative control of pMV361at 44.8°C; Lane 15: negative control of pMV361at 53.0°C. Expected band size is 350 bp if KanR gene is present. PCR products present in lanes 2-13.

An annealing temperature of 46.6°C (lane 7, Figure 7.8) was selected for KmSeqF and KmSeqR primers. Putative transformants were PCR screened using KmSeqF and KmSeqR primers to amplify the KanR gene, Figure 7.9. Plasmid was isolated from PCR positive colonies and was drop dialysed to remove salts. These plasmids were used to complement wildtype *M.tb* H37Rv and *M.tb Δnuc* mutant by electroporation.

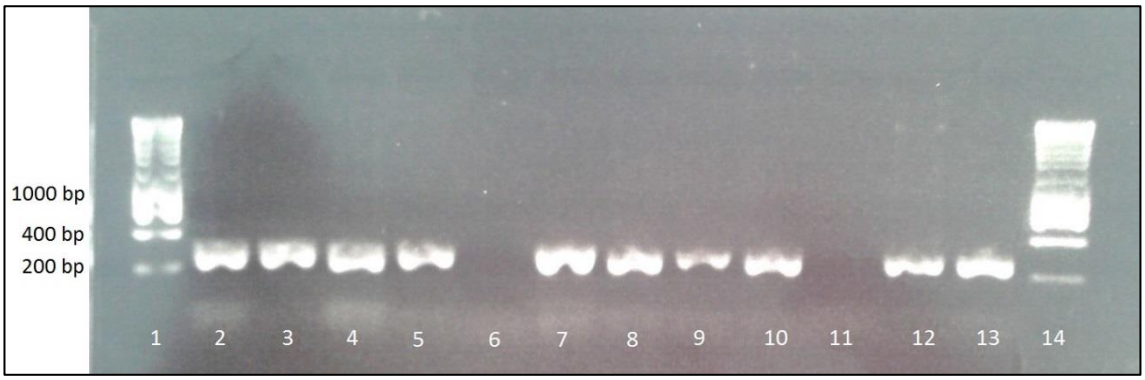

Figure 7.9: Colony PCR of kanamycin-resistant DH5α *E.coli* to confirm transformation

Lane 1: Hyperladder I; Lanes 2-4: colonies with nuc^{sens}; Lanes 5-7: colonies with nuc^{H37Rv}; Lanes 8-10: colonies with nuc^{MDR}; Lane 11: negative control; Lane 12: positive control purified pMV361 plasmid empty vector; Lane 13: positive control (purified plasmid nuc^{sens}); Lane 14: Hyperladder I. Expected band size is 350 bp if KanR gene is present. PCR products are present in lanes 2-5, 7-10 and 12, 13.

7.2.3.3 Electroporation of plasmids nuc^{sens}, nuc^{H37Rv} or nuc^{MDR} into wildtype *M.tb* H37Rv and *M.tb Δnuc* mutant

Plasmids nuc^{sens}, nuc^{H37Rv} or nuc^{MDR} were used as template DNA for positive controls, Figure 7.10. Plasmids nuc^{sens}, nuc^{H37Rv} or nuc^{MDR} were electroporated into wildtype *M.tb* H37Rv and the *M.tb Δnuc* null mutant. A primer pair, CompF and CompR, was designed to PCR amplify the nuclease gene from plasmids nuc^{sens}, nuc^{H37Rv} or nuc^{MDR}. Single putative transformants were picked from agar plates containing kanamycin as a selection and were heat killed and used as template DNA for PCR to check for plasmid insertion.

PCR amplification of nuclease alleles (using the primer pair CompF and CompR) were present in transformants from wildtype *M.tb* H37Rv complemented with nuc^{sens}, (Figure 7.11, lanes 2, 5), nuc^{H37Rv} (Figure 7.11, lane 13) and nuc^{MDR} (Figure 7.12, lanes 11, 14). CompF and CompR failed to amplify the nuclease allele of plasmids nuc^{sens}, nuc^{H37Rv} or nuc^{MDR} were transformed into *M.tb Δnuc* mutant strain, Figures 7.13, 7.14.

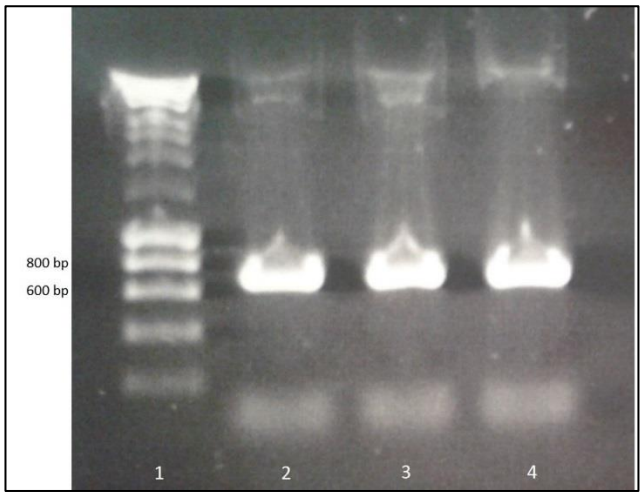

Figure 7.10: PCR of purified plasmid positive controls to confirm correct band size for primers CompF and CompR amplifying across the nuclease gene.

Lane 1: Hyperladder I; Lane 2: Nuc^{sens}; Lane 3: nuc^{H37Rv}; Lane 4: Nuc^{MDR}. Expected band size is 700 bp if a nuclease allele is present.

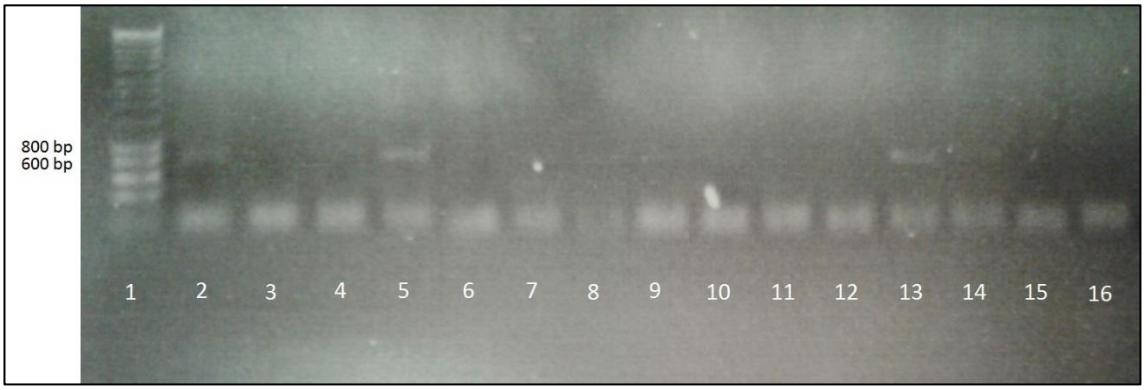

Figure 7.11: Colony PCR of wildtype *M.tb* H37Rv complemented with plasmids nuc^{sens} or nuc^{H37Rv} using primers CompF and CompR.

Lane 1: Hyperladder I; Lanes 2-9: *M.tb* H37Rv colonies complemented with nuc^{sens}; Lanes 10-16:*M.tb* H37Rv colonies complemented with nuc^{H37Rv}. Expected band size is 700 bp if nuc^{sens} or nuc^{H37Rv} is present. PCR products are present in lanes 2, 5, 13 and 14.

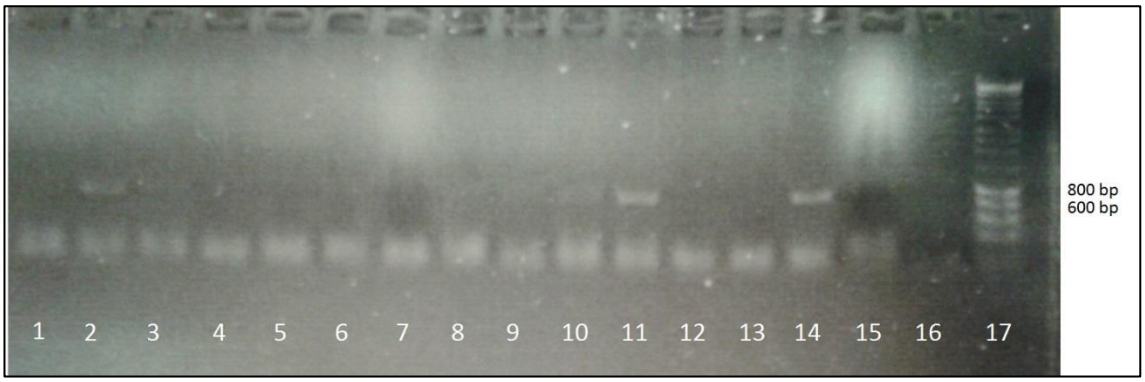

Figure 7.12: Colony PCR of H37Rv complemented with plasmids nuc^{H37Rv} or nuc^{MDR} using primers CompF and CompR.

Lanes 1-6: *M.tb* H37Rv colonies complemented with nuc^{H37Rv}; Lanes 7-15: *M.tb* H37Rv colonies complemented with nuc^{MDR}; Lane 16: negative control; Lane 17: Hyperladder I. Expected band size is 700 bp if nuc^{H37Rv} or nuc^{MDR} is present. PCR products are present in lanes 2, 3, 11 and 14.

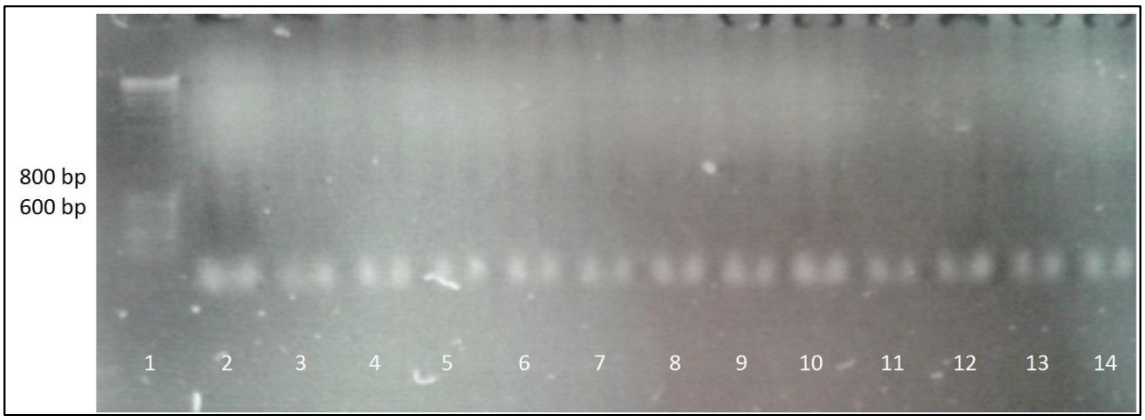

Figure 7.13: Colony PCR of *M.tb* Δnuc mutant complemented with plasmids nuc^{sens} or nuc^{H37Rv} using primers CompF and CompR

Lane 1: Hyperladder I; Lanes 2-9: *M.tb Δnuc* mutant complemented with nuc^{sens}; Lanes 10-14: *M.tb Δnuc* mutant complemented with nuc^{H37Rv}. Expected band size is 700 bp if nuc^{sens} or 02 is present. No PCR products were detectable.

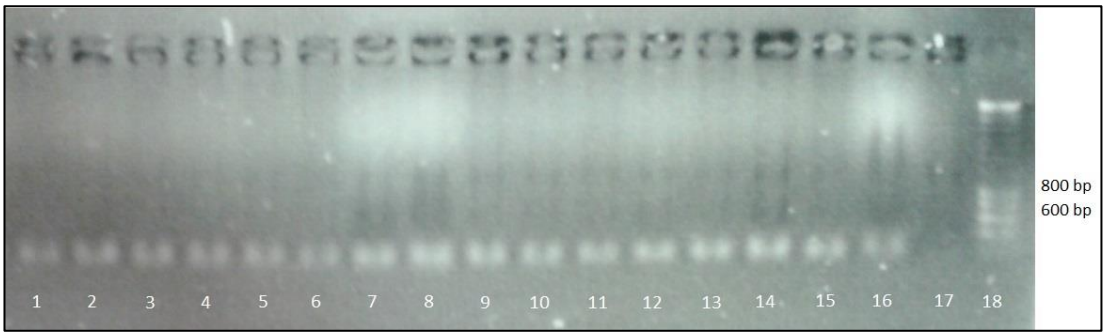

Figure 7.14: Colony PCR of *M.tb Δnuc* mutant complemented with plasmids nuc^{H37Rv} or nuc^{MDR} using primers CompF and CompR

Lanes 1-8: *M.tb Δnuc* mutant complemented with nuc^{H37Rv}; Lanes 9-16: *M.tb Δnuc* mutant complemented with nuc^{MDR}; Lane 17: negative control; Lane 18: Hyperladder I. Expected band size is 700 bp if plasmids 01 or 02 is present. No PCR products were detectable.

PCR amplification of the nuc^{sens}, nuc^{H37Rv} and nuc^{MDR} encoded nuclease alleles transformed into wildtype *M.tb* H37Rv was poor, with only 1-2 colonies containing nuc^{sens}, nuc^{H37Rv} or nuc^{MDR} . There was no PCR amplification for any putative nuc^{sens}, nuc^{H37Rv} and nuc^{MDR} transformants for the *M.tb Δnuc* mutant. This could be due to failure of PCR amplification to detect the vector-borne copy of nuc spontaneous kanamycin resistance mutants masking as transformants. To investigate this, PCR was repeated using the same colony template preparation but using the KmSeqF and KmSeqR primer pair to PCR amplify the pMV361 encoded Kan R gene. If nuc^{sens}, nuc^{H37Rv} and nuc^{MDR} were present in putative transformants a PCR product of 350 bp would be generated. Figure 7.15 shows PCR of the purified plasmids as positive controls using KmSeqF and KmSeqR to detect the KanR gene.

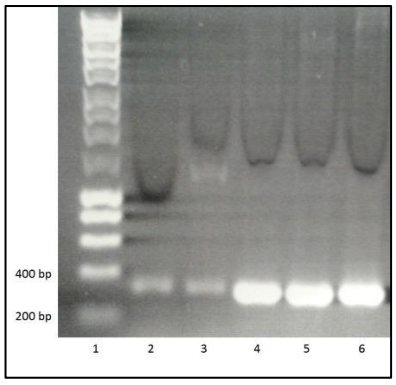

Figure 7.15: PCR amplification of purified positive control plasmids nuc^{sens}, nuc^{H37Rv} and nuc^{MDR} using KmSeqF and KmSeqR to detect the KanR gene.

Lane 1: Hyperladder I; Lane 2: *M.tb* H37Rv complemented with nuc^{sens}; Lane 3: *M.tb* Δnuc complemented with nuc^{sens}; Lane 4: purified nuc^{sens} used as template DNA; Lane 5: purified nuc^{H37Rv} used as template DNA; Lane 6: purified nuc^{MDR} used as template DNA. Expected band size is 350 bp if kanamycin resistance gene is present. PCR products were present in all lanes.

KanR PCR amplification was successful for all wildtype *M.tb* H37Rv and *M.tb Δnuc* mutant putative transformants of nuc^{sens}, nuc^{H37Rv} and nuc^{MDR}, Figures 7.16, 7.17. This successful PCR amplification suggests that CompF and CompR primers may not be compatible with this PCR.

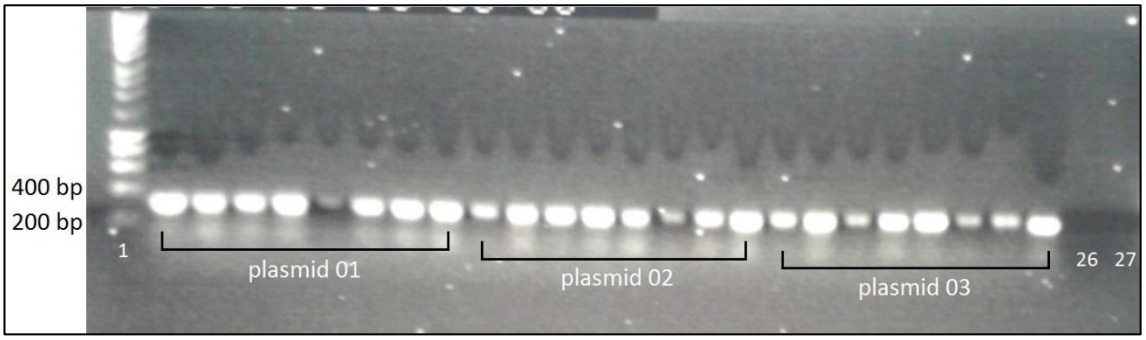

Figure 7.16: Colony PCR of *M.tb* H37Rv complemented with plasmids nuc^{sens}, nuc^{H37Rv} or nuc^{MDR} using primers KmSeqF and KmSeqR

Lane1: Hyperladder I; Lanes 2-9: *M.tb* H37Rv colonies complemented with nuc^{sens}; Lanes 10-17: *M.tb* H37Rv colonies complemented with nuc^{H37Rv}; Lanes 18-25*: M.tb* H37Rv complemented with nuc^{MDR}; Lane 26*: M.tb* H37Rv wildtype (no plasmid); Lane 27: negative control. Expected band size is 350 bp if PCR product if kanamycin resistance gene is present. PCR products were present for all colonies screened except for wildtype *M.tb* H37Rv.

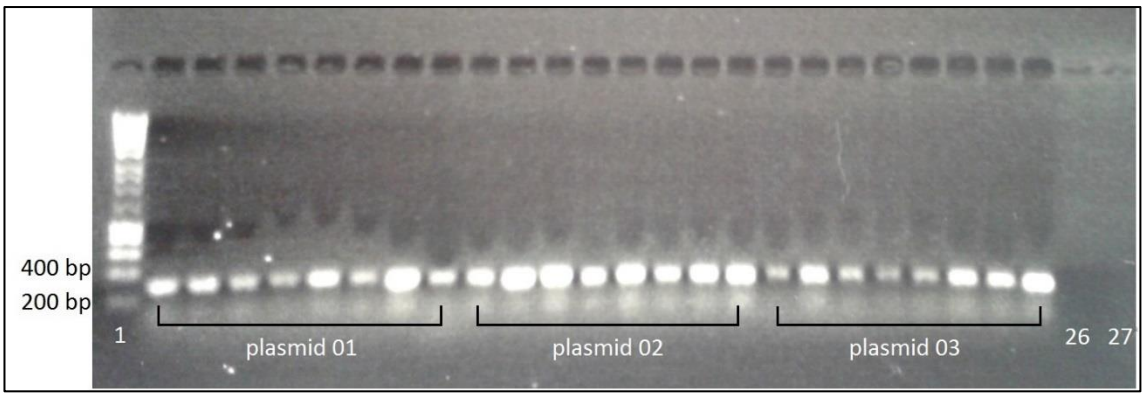

Figure 7.17: Colony PCR of *M.tb* Δnuc complemented with nuc^{sens}, nuc^{H37Rv} and nuc^{MDR} using primers KmSeqF and KmSeqR

Lane1: Hyperladder I; Lanes 2-9: *M.tb Δnuc* mutant colonies complemented with nuc^{sens}; Lanes 10-17: *M.tb Δnuc* mutant colonies complemented with nuc^{H37Rv}; Lanes 18-25 *M.tb Δnuc* mutant complemented with nuc^{MDR}; Lane 26: *M.tb Δnuc* (no plasmid); Lane 27: negative control. Expected band size is 350 bp if PCR product if kanamycin resistance gene is present. PCR products were present for all colonies screened except for non-complemented *M.tb Δnuc* mutant and negative control.

7.3 Discussion

MDR-TB and XDR-TB pose a serious threat to the eradication of TB; approximately half a million people are diagnosed with MDR-TB annually and require treatment times of up to two years, if treatment is feasible (World Health Organisation 2016). Drug resistance in *M.tb* develops from spontaneous chromosomal mutations in key drug targets (Ford, Shah et al. 2013). These mutations occur randomly within the genome, but require antibiotic treatment as a selection pressure to be propagated within a population (Davies and Davies 2010). Deletion of *nucS* in *M. smegmatis* and *S. coelicolor* significantly increased INH and RIF drug resistance rates (Castaneda-Garcia, Prieto et al. 2017); the effects of *nucS* deletion on *M.tb* drug resistance rates, however, are less clear. Deletion of *nucS* in *M. smegmatis* and *S. coelicolor* generated >100-fold increases in mutation rates (Castaneda-Garcia, Prieto et al. 2017). These rates were not seen in *M.tb Δnuc* detailed in this chapter. Mutation rate analysis of clinical isolates of *M.tb in vitro* showed that emergence of drug resistance varies substantially across lineages of *M.tb*; for instance Lineage 2 strains of *M.tb* are epidemiologically associated with increased rates of emerging drug resistance (Taype, Agapito et al. 2012). Polymorphisms in DNA replication, recombination and repair genes have been identified that may contribute to altered spontaneous mutation rates (Mestre, Luo et al. 2011). This inter-strain polymorphic variation in mutation rates may impact on drug resistance rates observed in *M.tb Δnuc*. The data generated in this chapter suggest that *nucS* deletion increases drug resistance emergence in the presence of inhibitory concentrations of EMB, INH, RIF and STREP compared to wildtype *M.tb* H37Rv although it was not statistically significant. These data were analysed using the non-parametric Mann-Whitney U test; three biological replicates were not sufficient to establish significance as no growth in wildtype *M.tb* H37Rv corresponds to a variance of zero, compared to the large variation seen across the three replicates for the *M.tb Δnuc* mutant. Spontaneous mutation assays should be repeated (N>3) to increase statistical power to define if deletion of *nucS* has a significant effect on drug resistance rates or not.

M.tb Δnuc and wildtype *M.tb* H37Rv were both complemented with three *nucS* alleles; *M.tb* H37Rv *nucS*, *M.tb* drug-sensitive clinical isolate *nucS* and drug-resistant *M.tb* clinical isolate *nucS*. Transformants were successfully isolated, however sequencing of insertions to verify complementation remains to be completed. It was not possible to assess the impact of this *nucS* complementation during this PhD but it was expected that the increased drug resistance rates observed in *M.tb Δnuc* mutant described in this chapter, would be abrogated to wildtype levels. Whole genome sequencing performed on *M.tb* H37Rv by collaborators after this thesis was submitted, showed a SNP in the wildtype *nuc* gene. This polymorphism could explain how deletion of the *nuc* gene did

not significantly increase mutation rates as measured through spontaneous drug resistant colonies exposed to INH, ETBU, RIF or STREP.

Recently, antimicrobial drug tolerance has been implicated in the emergence of drug resistance (Fonseca, Knight et al. 2015). Antimicrobial drug tolerance can confer an advantage over non-drug tolerant bacilli exposed to the same concentration of antimicrobial drug, allowing survival of bacilli until a drug resistant mutation develops (Ford, Shah et al. 2013). This suggests antimicrobial drug tolerance and resistance may not be mutually exclusive events, but rather that tolerance can facilitate drug resistance emergence. Levin-Reisman *et al.* investigated the role of tolerance in the development of drug resistance in *E. coli* (Levin-Reisman et al. 2017). Repeated β- lactam exposure led to *E. coli* acquiring mutations that increased their lag phase, allowing them to persist through antibiotic exposure. Using a mathematical population-genetics model they showed how the emergence of tolerance increases the probability that novel resistance mutations can spread through the population. Drug resistance was investigated in this chapter as emerging evidence shows that tolerance can lead to resistance and that these are not necessarily discrete biological events (Levin-Reisman et al. 2017; Fonseca, Knight et al. 2015). Deletion of the *nuc* nuclease did not statistically increase the rates of drug resistance, and further work is required to prove if it does or not. While this preliminary work in this chapter does not focus on cultures from the RCCS, future work would involve culturing this *nuc* mutant in the RCCS to investigate if a biofilm-induced tolerance phenotype would increase drug resistance mutations compared to the axenic log phase cultures tested in this chapter.

Chapter 8: General Discussion

8.1 Summary of findings

The aim of this study was to develop a novel *in vitro*, low-shear biofilm model of *M. bovis* BCG that would facilitate the investigation of drug tolerance in biofilm-derived bacilli. This study added to the body of knowledge of mycobacterial drug tolerance and is a novel, reproducible model. The RCCS biofilm model was optimised for biofilm formation, and biofilms were characterised using Kinyoun staining and scanning electron microscopy. Imaging showed biofilms had a complex, convoluted topography with a profuse extracellular matrix. Biofilm-derived bacilli showed isoniazid and streptomycin tolerance, up to 7 days after being inoculated into fresh media containing the antimicrobials. Previous biofilm studies have only exposed whole, intact mycobacterial biofilms to antimicrobials (Trivedi, Mavi et al. 2016) (Ojha, Baughn et al. 2008). Here we showed that homogenised, planktonic suspensions of biofilm-derived bacilli maintain drug tolerance. This significant finding suggests that antimicrobial tolerance is a phenotype or metabolic state of bacilli, rather than physical protection from antimicrobial exposure due to bacilli residing within a biofilm. Isoniazid and streptomycin tolerance was shown to be induced during biofilm formation, as biofilm-derived bacilli would no longer remain antimicrobial tolerant after being passaged in antimicrobial free media. The extent of antimicrobial tolerance generated within an RCCS-derived biofilm was probed further by evaluating three novel antimycobacterial compounds derived from a tropical plant used in local Brazilian folklore medicine. Biofilm-derived bacilli exhibited varying degrees of tolerance to these compounds, highlighting the role antimicrobial tolerance may play in evaluating efficacy of novel candidate antimycobacterial compounds. The RCCS biofilm model shows promise as a novel screening tool in antimicrobial drug development.

The transcriptome of RCCS-derived biofilms was defined compared to stationary phase bacilli to identify genes that may be involved in biofilm formation and antimicrobial tolerance. A total of 96 genes were differentially expressed, with 15 genes induced and 77 genes downregulated. Of the 77 genes repressed, 62 encoded proteins of unknown function and were filtered out from analysis. The ESX5 secretion system functions is present in all slow-growing mycobacteria and is required for the secretion of virulence factors, as well as functioning in the transport of cell envelope proteins necessary for nutrient uptake (Ates, Ummels et al. 2015). Isocitrate lyase was also upregulated, an enzyme that is essential for virulence within the host, as well as being implicated in antimicrobial tolerance through a potential isocitrate lyase-mediated anti-oxidant defence mechanism (Nandakumar, Nathan et al. 2014). SigB and SigE were both induced in RCCS-derived biofilms. Both of these genes encode for alternative sigma factors that

function in the bacillary response to environmental stresses. Interestingly, hypergeometric probability testing showed that the biofilm transcriptome did not correlate with an *in vitro* model of hypoxia or nutrient starvation, or with any one data set from a database of 465 experimental, published and unpublished mRNA signatures. When compared to the transcriptome of sputa-derived *M.tb* before and during standard chemotherapy for TB, only isocitrate lyase and the mammalian cell entry protein *mce1B* shared similar expression patterns (Honeyborne, McHugh et al. 2016). The lack of correlation with known transcription signatures suggests that gene expression in biofilm cultures is quite diverse compared to other known models of antimicrobial tolerance. The biofilm-derived transcriptome was compared to stationary phase bacilli as both of these conditions were cultured for the same length of time and in the same media. However, many other models of drug tolerance, including nutrient starvation and hypoxia, were compared against log phase bacilli (Betts, Lukey et al. 2002) (Park, Guinn et al. 2003). This could account for the low correlation between biofilm growth and other models of antimicrobial tolerance.

Pathogen-host interactions were investigated during the course of this thesis to establish if biofilm growth exerted differential immune responses compared to control culture supernatant. THP-1 macrophage cells were stimulated with biofilm or control supernatants and the production of TNFα and IL-1β produced in response was quantified with ELISA assays. There was no statistically significant induction of IL-1β between biofilm and control supernatants. Biofilm supernatants however, induced statistically significantly more TNFα from THP-1 cells than control cultures. Interestingly, this was only observed with supernatants taken from day 21; there was no difference in TNFα production when THP-1 cells are exposed to supernatants from day 7. This suggests that a mature mycobacterial biofilm is required to have a pro-inflammatory effect compared to control mycobacterial cultures. Mycobacterial biofilms may have an as yet undefined role in inflammation based on these data.

The final chapter in this thesis aimed to link antimicrobial tolerance and antimicrobial resistance. Previous research in our laboratory in conjunction with collaborators described a novel mismatch repair (MMR) pathway in mycobacteria (Castaneda-Garcia, Prieto et al. 2017). MMR had previously been unidentified, and our research showed that the nuclease *NucS* was required to maintain low levels of spontaneous mutation. When antimicrobials were introduced as a selection pressure to a *NucS Streptomyces coelicolor* or *M. smegmatis,* high rates of spontaneous antimicrobial resistant mutants were generated. In order to establish the effect of a *NucS* deletion in *M.tb*, a gene knockout was first generated and spontaneous antimicrobial resistance quantified, with viable counts as a measure of mutation. Antimicrobial resistant colonies were fewer than

predicted compared to *M. smegmatis* and there was no statistically significant difference between wildtype *M.tb* and an *M.tb NucS* null strain. This *M.tb NucS* null strain was then complemented with one of three *NucS* alleles that encoded for *NucS* derived from wildtype, multi-drug resistant *NucS* or clinical isolate drug-sensitive clinical isolate *NucS*. This complementation strategy was successfully achieved and complemented strains are awaiting further investigation through antimicrobial susceptibility testing.

8.2 General discussion

Historically, biofilm studies have not been performed with slow-growing mycobacteria despite their propensity to form corded structures *in vitro* and the potential role of biofilms *in vivo*. However, antimicrobial tolerance is now recognised as a significant obstacle in reducing standard drug regimen treatment times and in developing novel antimicrobial drugs for *M.tb.* Recent studies have begun to elucidate key regulatory and mechanistic aspects of biofilms and antimicrobial tolerance, such as generation of slow metabolising or non-dividing bacilli within a biofilm population (Trivedi, Mavi et al. 2016). The research presented in this thesis contributes to this field, adding antimicrobial tolerance data and the genes potentially involved in this process. Within the wider context of antimicrobial tolerance in pathogenic bacteria, tolerance and persistence, unlike resistance, are often ambiguously defined. Brauner and colleagues attempted to define these terms from their research on *E. coli.* Tolerance is the ability of a micro-organism to survive transient antibiotic exposure and applies to a whole population of cells, for instance a stationary phase culture that has reduced sensitivity to β-lactam antibiotics. Persistence however only applies to a sub-population of bacteria and are those cells that survive throughout antibiotic exposure (Brauner et al. 2016). They base these definitions on their previous research on the “tolerome”, which collectively are genes that accumulate mutations that induce tolerance. They showed that mutations in specific genes (such as tRNA synthetases) can increase the lag phase of *E. coli*, allowing them to “tolerate” ampicillin (Fridman et al. 2014). They suggest that tolerance is genetically encoded through mutations in genes in the tolerome as evidenced in *E. coli.* This genetic basis of antibiotic tolerance is in contrast to tolerance seen in mycobacteria, where it is an inducible phenotype rather than collective mutations in genes. *In vitro* models of hypoxia or nutrient starvation induces isoniazid and rifampicin tolerance (Wayne et al. 1996; Betts et al. 2002), while CFU counts of TB patient sputa show a bi-phasic kill curve in response to isoniazid, suggesting a sub-population are tolerant to isoniazid (Jindani et al. 1980). While it is possible that mutations in certain genes could induce tolerance as in *E. coli*, the literature discussed in this thesis together with the tolerance phenotype of biofilm-derived bacilli suggests that antibiotic tolerance in TB is an inducible phenotype rather

than a mutation derived phenotype. This is shown in chapter four, where passaging biofilm-derived bacilli in antimicrobial-free media rescues the antimicrobial tolerant phenotype. If mutations had been acquired that induced antimicrobial tolerance, it would be expected that tolerance would be seen in repeated antimicrobial susceptibility testing but this was not the case.

Global regulators have been shown to play a role in antimicrobial tolerance. The master regulator molecule ppGpp has been shown to be upregulated in *E. coli* and *Pseudomonas* persister cells. ppGpp controls global stress responses, and suggests that there may be a general mechanism of tolerance across different species of bacteria (Gerdes & Maisonneuve 2012). Interestingly, SigB and SigE was up-regulated in RCCS biofilm-derived bacilli, highlighting the role that stress response regulators may play in tolerance to antimicrobials in *M. bovis* BCG and likely *M.tb*. Since 2012 however, the literature on tolerance has expanded and it is likely that tolerance mechanisms involve specific pathways that induce tolerance to a specific antibiotic. Wakamoto *et al* investigated isoniazid tolerance in *M. smegmatis* using micro-fluidic culturing and time lapse fluorescence microscopy (Wakamoto et al 2013). They showed that expression of KatG, the catalase-peroxidase required for activation of isoniazid, is expressed stochastically in the bacterial population so that a sub-population of bacteria would survive isoniazid exposure as they would have low levels of KatG expression. Transcriptional analysis of RCCS-derived bacteria showed downregulation of deazaflavin-dependent nitroreductase (Ddn), which is required for the bio-activation of pretomanid, an antimycobacterial drug (Cellitti et al. 2012). Similar to the research published by Wakamoto and colleagues, downregulation of drug-activating enzymes is a mechanism of tolerance- although RCCS-derived bacilli were not tested with pretomanid. If biofilm-derived bacilli were, it is possible that they would exhibit pretomanid tolerance due to Ddn downregulation.

While the antimicrobial tolerance, transcriptional profile and pathogen-host interactions have been characterised for RCCS-derived biofilms, the specific role biofilms play in TB remains unclear. The RCCS required time intensive optimisation- inoculation, culture conditions and harvesting all required large amounts of trial and error approaches to reproducibly generate biofilms. Adapting the RCCS to generate biofilms using clinically relevant isolates or the laboratory strain *M.tb* H37Rv would prove challenging as this work would require CL3 containment, and these RCCS vessels are semi-permeable. This would be advantageous to do however, as transcriptional profiling showed the ESX5 secretion system was induced in RCCS biofilm-derived bacilli; in order to investigate the role of the ESX1 secretion system, *M.tb* would be required for biofilm formation as this

system is absent in *M. bovis* BCG. This highlights the caveat of using a model organism to investigate *M.tb.*

The research in this thesis shows how biofilm-like growth can induce an antimicrobial tolerant phenotype. Despite numerous *in vitro* models having being developed to characterise tolerance in mycobacteria, TB remains the number one cause of death globally due to an infectious agent (World Health Organisation, 2017). This highlights how the mechanisms of how TB persists through drug treatment are not fully understood and have not translated to a clinical cure. Development and characterisation of *in vitro* models of mycobacterial tolerance are needed to advance antibiotic development and screening of novel compounds to advance towards shortened treatment times and novel drugs for MDR and XDR TB. *In vitro* models can facilitate investigation of antimicrobial tolerance and contribute significantly to this growing body of literature. They are however not without limitations. Hypergeometric probability testing was performed to assess how the transcriptional signature of RCCS biofilm-derived bacilli compared to that of sputum-derived bacilli. Surprisingly there was little similarity in the transcriptional profile, highlighting that although the RCCS shows antimicrobial tolerance (as measured by cell viability with BTG and Alamar Blue) and antimicrobial tolerance is also seen in the human lung (when measured through CFU counts from sputa) (Jindani et al. 2003), there is still large variety between *in vitro* and *in vivo* transcriptional signatures. Despite this, development of *in vitro* drug tolerance models is crucial to understanding the physiology of this antimicrobial tolerance and would have far-reaching implications in the field of TB research. New *in vitro* models of antimicrobial tolerance are required to allow in–depth analysis of how antimicrobial tolerance develops, but would also contribute significantly to drug development. *In vitro* models that replicate the antimicrobial tolerance hypothesised to occur in the human lung could, in theory, predict the efficacy of novel antimycobacterial compounds against *in vivo M.tb* infections. This would drastically reduce novel compound attrition rates in the drug development process and screen out compounds that would not be efficacious enough at a much earlier stage. In this regard, a key finding in this thesis is that RCCS-derived biofilms can be used to screen novel antimycobacterial compounds. Data presented in this thesis showed that antimicrobial tolerance was induced for all three novel compounds screened, but to a lesser extent for compound C. This would suggest that compound A and compound B are likely to be ineffective if developed further into antimicrobial drugs to treat TB, although these are very preliminary data. The complexity of drug-*M.tb* interactions cannot be wholly defined within a defined set of assays used for compound activity, cell toxicity, etc. Through developing *in vitro* models that generate specific phenotypes (e.g. drug tolerance) that are replicative of what is seen clinically and isolated *in vivo*, drug development

procedures can be better informed as to what novel compounds show promise in treating TB and indeed what compounds should not be taken into lead candidate development.

The time limitations of this PhD prevented further characterisation of this biofilm model and associated tolerance phenotype. Extended AST with other antimicrobials would further characterise the spectrum of tolerance. In particular, pretomanid AST would show if Ddn downregulation induces pretomanid tolerance. Mean probable number experiments could identify what proportion of biofilm-derived bacilli are viable but non-culturable. Importantly, this has been performed for sputum-derived bacilli and identified an occult population of *M.tb* that were viable but non-culturable on solid media (Mukamalova et al. 2009). Whole genome sequencing (WGS) of biofilm and control derived bacilli from the before and after culturing in the RCCS would aid in further describing antimicrobial tolerance in mycobacteria. As previously discussed, a leading hypothesis in the development of tolerance in *E. coli* is the accumulation of mutations in genes collectively known as the tolerome. This thesis concludes that antimicrobial tolerance induced in the RCCS is phenotypic rather than genotypic. WGS would allow in depth analysis of any mutations accumulated during culturing in the RCCS and the role these mutations may play in tolerance to definitively state that this tolerance in biofilms is phenotypic.

8.3 Future work

One of the most striking results obtained in this study is that INH and STREP tolerance is induced through biofilm formation. Transcriptional profiling showed that 31 genes may be implicated in this phenotype and have been discussed in detail. These statistically significant differentially expressed genes will be verified by qPCR to confirm fold changes observed with tiling microarray analysis. We will consider comparing the RCCS-derived biofilm transcriptome to another control culture rather than stationary phase bacilli. This may facilitate higher hits for hypergeometric probability testing, as the biofilm mRNA signature would be normalised to a similar comparison as other datasets, i.e. log phase bacilli. Artemis software will be utilised to reanalyse tiling microarray data to interrogate the role of intergenic regions and small non-coding RNAs in biofilm formation.

Following screening of novel antimycobacterial compounds, a research visit was undertaken in April 2017 to meet with chemists at Universidade Federal de Santa Catarina, Brazil, to discuss screening of further compounds in the RCCS. A total of 56 compounds were obtained and will be screened in the RCCS to detect if bacilli are tolerant or not to these molecules.

Chapter 9: Bibliography

Abdallah, A. M., J. Bestebroer, N. D. Savage, K. de Punder, M. van Zon, L. Wilson, C. J. Korbee, A. M. van der Sar, T. H. Ottenhoff, N. N. van der Wel, W. Bitter and P. J. Peters (2011). "Mycobacterial secretion systems ESX-1 and ESX-5 play distinct roles in host cell death and inflammasome activation." J Immunol 187(9): 4744-4753.

Abdallah, A. M., N. D. Savage, M. van Zon, L. Wilson, C. M. Vandenbroucke-Grauls, N. N. van der Wel, T. H. Ottenhoff and W. Bitter (2008). "The ESX-5 secretion system of Mycobacterium marinum modulates the macrophage response." J Immunol 181(10): 7166-7175.

Adams, D. O. and T. A. Hamilton (1984). "The cell biology of macrophage activation." Annu Rev Immunol 2: 283-318.

Addison, N. O., S. Pfau, E. Koka, S. Y. Aboagye, G. Kpeli, G. Pluschke, D. Yeboah-Manu and T. Junghanss (2017). "Assessing and managing wounds of Buruli ulcer patients at the primary and secondary health care levels in Ghana." PLoS Negl Trop Dis 11(2): e0005331.

Aguirre-Blanco, A. M., P. T. Lukey, J. M. Cliff and H. M. Dockrell (2007). "Strain-dependent variation in Mycobacterium bovis BCG-induced human T-cell activation and gamma interferon production in vitro." Infect Immun 75(6): 3197-3201.

Ahmad, Z., L. G. Klinkenberg, M. L. Pinn, M. M. Fraig, C. A. Peloquin, W. R. Bishai, E. L. Nuermberger, J. H. Grosset and P. C. Karakousis (2009). "Biphasic kill curve of isoniazid reveals the presence of drug-tolerant, not drug-resistant, Mycobacterium tuberculosis in the guinea pig." J Infect Dis 200(7): 1136-1143.

Ai, J. W., Q. L. Ruan, Q. H. Liu and W. H. Zhang (2016). "Updates on the risk factors for latent tuberculosis reactivation and their managements." Emerg Microbes Infect 5: e10.

Akira, S., S. Uematsu and O. Takeuchi (2006). "Pathogen recognition and innate immunity." Cell 124(4): 783-801.

Al-Dhaheri, R. S. and L. J. Douglas (2008). "Absence of amphotericin B-tolerant persister cells in biofilms of some Candida species." Antimicrob Agents Chemother 52(5): 1884-1887.

Aldridge, B. B., I. Keren and S. M. Fortune (2014). "The Spectrum of Drug Susceptibility in Mycobacteria." Microbiol Spectr 2(5).

Alonso-Hearn, M., T. M. Eckstein, S. Sommer and L. E. Bermudez (2010). "A Mycobacterium avium subsp. paratuberculosis LuxR regulates cell envelope and virulence." Innate Immun 16(4): 235-247.

Alteri, C. J., J. Xicohtencatl-Cortes, S. Hess, G. Caballero-Olin, J. A. Giron and R. L. Friedman (2007). "Mycobacterium tuberculosis produces pili during human infection." Proc Natl Acad Sci U S A 104(12): 5145-5150.

Amato, S. M., C. H. Fazen, T. C. Henry, W. W. Mok, M. A. Orman, E. L. Sandvik, K. G. Volzing and M. P. Brynildsen (2014). "The role of metabolism in bacterial persistence." Front Microbiol 5: 70.

Andries, K., P. Verhasselt, J. Guillemont, H. W. Gohlmann, J. M. Neefs, H. Winkler, J. Van Gestel, P. Timmerman, M. Zhu, E. Lee, P. Williams, D. de Chaffoy, E. Huitric, S. Hoffner, E. Cambau, C. Truffot-Pernot, N. Lounis and V. Jarlier (2005). "A diarylquinoline

drug active on the ATP synthase of Mycobacterium tuberculosis." Science 307(5707): 223-227.

Aquinas, M. (1982). "Short-course therapy for tuberculosis." Drugs 24(2): 118-132.

Argyrou, A., M. W. Vetting, B. Aladegbami and J. S. Blanchard (2006). "Mycobacterium tuberculosis dihydrofolate reductase is a target for isoniazid." Nat Struct Mol Biol 13(5): 408-413.

Armstrong, J. A. and P. D. Hart (1971). "Response of cultured macrophages to Mycobacterium tuberculosis, with observations on fusion of lysosomes with phagosomes." J Exp Med 134(3 Pt 1): 713-740.

Ates, L. S., R. Ummels, S. Commandeur, R. van de Weerd, M. Sparrius, E. Weerdenburg, M. Alber, R. Kalscheuer, S. R. Piersma, A. M. Abdallah, M. Abd El Ghany, A. M. Abdel-Haleem, A. Pain, C. R. Jimenez, W. Bitter and E. N. Houben (2015). "Essential Role of the ESX-5 Secretion System in Outer Membrane Permeability of Pathogenic Mycobacteria." PLoS Genet 11(5): e1005190.

Banaei, N., E. Z. Kincaid, S. Y. Lin, E. Desmond, W. R. Jacobs, Jr. and J. D. Ernst (2009). "Lipoprotein processing is essential for resistance of Mycobacterium tuberculosis to malachite green." Antimicrob Agents Chemother 53(9): 3799-3802.

Banasik, M. and P. Sachadyn (2014). "Conserved motifs of MutL proteins." Mutat Res 769: 69-79.

Banerjee, A., E. Dubnau, A. Quemard, V. Balasubramanian, K. S. Um, T. Wilson, D. Collins, G. de Lisle and W. R. Jacobs, Jr. (1994). "inhA, a gene encoding a target for isoniazid and ethionamide in Mycobacterium tuberculosis." Science 263(5144): 227-230.

Bansal-Mutalik, R. and H. Nikaido (2014). "Mycobacterial outer membrane is a lipid bilayer and the inner membrane is unusually rich in diacyl phosphatidylinositol dimannosides." Proc Natl Acad Sci U S A 111(13): 4958-4963.

Barber, C. E., J. L. Tang, J. X. Feng, M. Q. Pan, T. J. Wilson, H. Slater, J. M. Dow, P. Williams and M. J. Daniels (1997). "A novel regulatory system required for pathogenicity of Xanthomonas campestris is mediated by a small diffusible signal molecule." Mol Microbiol 24(3): 555-566.

Barbier, J. (1955). Rubber Chemistry and Technology 28(514).

Barnes, S. and J. G. Spenney (1980). "Stoichiometry of the NADH-oxidoreductase reaction for dehydrogenase determinations." Clin Chim Acta 107(3): 149-154.

Barry, C. E., 3rd, H. I. Boshoff, V. Dartois, T. Dick, S. Ehrt, J. Flynn, D. Schnappinger, R. J. Wilkinson and D. Young (2009). "The spectrum of latent tuberculosis: rethinking the biology and intervention strategies." Nat Rev Microbiol 7(12): 845-855.

Barry, C. E., D. C. Crick and M. R. McNeil (2007). "Targeting the formation of the cell wall core of M. tuberculosis." Infect Disord Drug Targets 7(2): 182-202.

Bartek, I. L., R. Rutherford, V. Gruppo, R. A. Morton, R. P. Morris, M. R. Klein, K. C. Visconti, G. J. Ryan, G. K. Schoolnik, A. Lenaerts and M. I. Voskuil (2009). "The DosR regulon of M. tuberculosis and antibacterial tolerance." Tuberculosis (Edinb) 89(4): 310-316.

Bartek, I. L., L. K. Woolhiser, A. D. Baughn, R. J. Basaraba, W. R. Jacobs, Jr., A. J. Lenaerts and M. I. Voskuil (2014). "Mycobacterium tuberculosis Lsr2 is a global

transcriptional regulator required for adaptation to changing oxygen levels and virulence." MBio 5(3): e01106-01114.

Basha, S., N. Surendran and M. Pichichero (2014). "Immune responses in neonates." Expert Rev Clin Immunol 10(9): 1171-1184.

Basu Roy, R., N. Brandt, N. Moodie, M. Motlagh, K. Rasanathan, J. A. Seddon, A. K. Detjen and B. Kampmann (2016). "Why the Convention on the Rights of the Child must become a guiding framework for the realization of the rights of children affected by tuberculosis." BMC Int Health Hum Rights 16(1): 32.

Bauer, T. T., A. Torres, R. Ferrer, C. M. Heyer, G. Schultze-Werninghaus and K. Rasche (2002). "Biofilm formation in endotracheal tubes. Association between pneumonia and the persistence of pathogens." Monaldi Arch Chest Dis 57(1): 84-87.

Bauernfeind, F. G., G. Horvath, A. Stutz, E. S. Alnemri, K. MacDonald, D. Speert, T. Fernandes-Alnemri, J. Wu, B. G. Monks, K. A. Fitzgerald, V. Hornung and E. Latz (2009). "Cutting edge: NF-kappaB activating pattern recognition and cytokine receptors license NLRP3 inflammasome activation by regulating NLRP3 expression." J Immunol 183(2): 787-791.

Bean, A. G., D. R. Roach, H. Briscoe, M. P. France, H. Korner, J. D. Sedgwick and W. J. Britton (1999). "Structural deficiencies in granuloma formation in TNF gene-targeted mice underlie the heightened susceptibility to aerosol Mycobacterium tuberculosis infection, which is not compensated for by lymphotoxin." J Immunol 162(6): 3504-3511.

Beck von Bodman, S. and S. K. Farrand (1995). "Capsular polysaccharide biosynthesis and pathogenicity in Erwinia stewartii require induction by an N-acylhomoserine lactone autoinducer." J Bacteriol 177(17): 5000-5008.

Betts, J. C., P. T. Lukey, L. C. Robb, R. A. McAdam and K. Duncan (2002). "Evaluation of a nutrient starvation model of Mycobacterium tuberculosis persistence by gene and protein expression profiling." Mol Microbiol 43(3): 717-731.

Bharati, B. K., I. M. Sharma, S. Kasetty, M. Kumar, R. Mukherjee and D. Chatterji (2012). "A full-length bifunctional protein involved in c-di-GMP turnover is required for long-term survival under nutrient starvation in Mycobacterium smegmatis." Microbiology 158(Pt 6): 1415-1427.

Bianco, M. V., F. C. Blanco, B. Imperiale, M. A. Forrellad, R. V. Rocha, L. I. Klepp, A. A. Cataldi, N. Morcillo and F. Bigi (2011). "Role of P27 -P55 operon from Mycobacterium tuberculosis in the resistance to toxic compounds." BMC Infect Dis 11: 195.

Bigger, J. W. (1944). "Treatment of Staphylococcal infections with penicillin." Lancet 244: 497-500.

Blanchard, J. S. (1996). "Molecular mechanisms of drug resistance in Mycobacterium tuberculosis." Annu Rev Biochem 65: 215-239.

Bloch, H. (1955). "Virulence of mycobacteria." Bibl Tuberc 9: 49-61.

Bloch, H. and H. Noll (1955). "Studies on the virulence of Tubercle bacilli; the effect of cord factor on murine tuberculosis." Br J Exp Pathol 36(1): 8-17.

Boon, C. and T. Dick (2002). "Mycobacterium bovis BCG response regulator essential for hypoxic dormancy." J Bacteriol 184(24): 6760-6767.

Boon, C. and T. Dick (2012). "How Mycobacterium tuberculosis goes to sleep: the dormancy survival regulator DosR a decade later." Future Microbiol 7(4): 513-518.

Boshoff, H. I., X. Xu, K. Tahlan, C. S. Dowd, K. Pethe, L. R. Camacho, T. H. Park, C. S. Yun, D. Schnappinger, S. Ehrt, K. J. Williams and C. E. Barry, 3rd (2008). "Biosynthesis and recycling of nicotinamide cofactors in mycobacterium tuberculosis. An essential role for NAD in nonreplicating bacilli." J Biol Chem 283(28): 19329-19341.

Bottai, D., M. Di Luca, L. Majlessi, W. Frigui, R. Simeone, F. Sayes, W. Bitter, M. J. Brennan, C. Leclerc, G. Batoni, M. Campa, R. Brosch and S. Esin (2012). "Disruption of the ESX-5 system of Mycobacterium tuberculosis causes loss of PPE protein secretion, reduction of cell wall integrity and strong attenuation." Mol Microbiol 83(6): 1195-1209.

Bourigault, M. L., N. Segueni, S. Rose, N. Court, R. Vacher, V. Vasseur, F. Erard, M. Le Bert, I. Garcia, Y. Iwakura, M. Jacobs, B. Ryffel and V. F. Quesniaux (2013). "Relative contribution of IL-1alpha, IL-1beta and TNF to the host response to Mycobacterium tuberculosis and attenuated M. bovis BCG." Immun Inflamm Dis 1(1): 47-62.

Brauner, A., O. Fridman, O. Gefen and N.G. Balaban (2016). “Distinguishing between resistance, tolerance and persistence to antibiotic treatment.” Nat Rev Microbiol 14(5): 320-330.

Brooun, A., S. Liu and K. Lewis (2000). "A dose-response study of antibiotic resistance in Pseudomonas aeruginosa biofilms." Antimicrob Agents Chemother 44(3): 640-646.

Brosch, R., S. V. Gordon, C. Buchrieser, A. S. Pym, T. Garnier and S. T. Cole (2000). "Comparative genomics uncovers large tandem chromosomal duplications in Mycobacterium bovis BCG Pasteur." Yeast 17(2): 111-123.

Brosch, R., S. V. Gordon, T. Garnier, K. Eiglmeier, W. Frigui, P. Valenti, S. Dos Santos, S. Duthoy, C. Lacroix, C. Garcia-Pelayo, J. K. Inwald, P. Golby, J. N. Garcia, R. G. Hewinson, M. A. Behr, M. A. Quail, C. Churcher, B. G. Barrell, J. Parkhill and S. T. Cole (2007). "Genome plasticity of BCG and impact on vaccine efficacy." Proc Natl Acad Sci U S A 104(13): 5596-5601.

Brosch, R., S. V. Gordon, M. Marmiesse, P. Brodin, C. Buchrieser, K. Eiglmeier, T. Garnier, C. Gutierrez, G. Hewinson, K. Kremer, L. M. Parsons, A. S. Pym, S. Samper, D. van Soolingen and S. T. Cole (2002). "A new evolutionary scenario for the Mycobacterium tuberculosis complex." Proc Natl Acad Sci U S A 99(6): 3684-3689.

Brudey, K., J. R. Driscoll, L. Rigouts, W. M. Prodinger, A. Gori, S. A. Al-Hajoj, C. Allix, L. Aristimuno, J. Arora, V. Baumanis, L. Binder, P. Cafrune, A. Cataldi, S. Cheong, R. Diel, C. Ellermeier, J. T. Evans, M. Fauville-Dufaux, S. Ferdinand, D. Garcia de Viedma, C. Garzelli, L. Gazzola, H. M. Gomes, M. C. Guttierez, P. M. Hawkey, P. D. van Helden, G. V. Kadival, B. N. Kreiswirth, K. Kremer, M. Kubin, S. P. Kulkarni, B. Liens, T. Lillebaek, M. L. Ho, C. Martin, C. Martin, I. Mokrousov, O. Narvskaia, Y. F. Ngeow, L. Naumann, S. Niemann, I. Parwati, Z. Rahim, V. Rasolofo-Razanamparany, T. Rasolonavalona, M. L. Rossetti, S. Rusch-Gerdes, A. Sajduda, S. Samper, I. G. Shemyakin, U. B. Singh, A. Somoskovi, R. A. Skuce, D. van Soolingen, E. M. Streicher, P. N. Suffys, E. Tortoli, T. Tracevska, V. Vincent, T. C. Victor, R. M. Warren, S. F. Yap, K. Zaman, F. Portaels, N. Rastogi and C. Sola (2006). "Mycobacterium tuberculosis complex genetic diversity: mining the fourth international spoligotyping database (SpolDB4) for classification, population genetics and epidemiology." BMC Microbiol 6: 23.

Caceres, N., C. Vilaplana, C. Prats, E. Marzo, I. Llopis, J. Valls, D. Lopez and P. J. Cardona (2013). "Evolution and role of corded cell aggregation in Mycobacterium tuberculosis cultures." Tuberculosis (Edinb) 93(6): 690-698.

Calmette, A., G. Guérin, L. Nègre, and A. Boquet (1926). "Prémunition des nouveaux-nés contre la tuberculose par le vaccin BCG." Ann. Pasteur (Paris) 40: 89-133.

Canetti, G. (1955). Bacillus in the pulmonary lesions of man: histobacteriology and its bearing on the therapy of pulmonary tuberculosis. New York.

Canetti, G. (1955). "[Bacteriological problems in pulmonary tuberculosis treated by excision after chemotherapy]." Strasb Med 6(5): 308-309.

Canetti, G. (1955). "The Tubercle Bacillus in the pulmonary lesions of man: histobacteriology and its bearing on the therapy of pulmonary tuberculosis."

Canetti, G., P. Gay and M. Le Lirzin (1972). "Trends in the prevalence of primary drug resistance in pulmonary tuberculosis in France from 1962 to 1970: a national survey." Tubercle 53(2): 57-83.

Castaneda-Garcia, A., T. T. Do and J. Blazquez (2011). "The K+ uptake regulator TrkA controls membrane potential, pH homeostasis and multidrug susceptibility in Mycobacterium smegmatis." J Antimicrob Chemother 66(7): 1489-1498.

Castaneda-Garcia, A., A. I. Prieto, J. Rodriguez-Beltran, N. Alonso, D. Cantillon, C. Costas, L. Perez-Lago, E. D. Zegeye, M. Herranz, P. Plocinski, T. Tonjum, D. Garcia de Viedma, M. Paget, S. J. Waddell, A. M. Rojas, A. J. Doherty and J. Blazquez (2017). "A non-canonical mismatch repair pathway in prokaryotes." Nat Commun 8: 14246.

Susan E. Cellitti, Jennifer Shaffer, David H. Jones, Tathagata Mukherjee, Meera Gurumurthy, Badry Bursulaya, Helena I. Boshoff, Inhee Choi, Amit Nayyar, Yong Sok Lee, Joseph Cherian, Pornwaratt Niyomrattanakit, Thomas Dick, Ujjini H. Manjunatha, Clifton E. Barry, III, Glen Spraggon, and Bernhard H. Geierstanger (2012). Structure 20, 101–112.

Charlet, D., S. Mostowy, D. Alexander, L. Sit, H. G. Wiker and M. A. Behr (2005). "Reduced expression of antigenic proteins MPB70 and MPB83 in Mycobacterium bovis BCG strains due to a start codon mutation in sigK." Mol Microbiol 56(5): 1302-1313.

Chen, J. M., S. T. Islam, H. Ren and J. Liu (2007). "Differential productions of lipid virulence factors among BCG vaccine strains and implications on BCG safety." Vaccine 25(48): 8114-8122.

Chihota, V. N., B. Muller, C. K. Mlambo, M. Pillay, M. Tait, E. M. Streicher, E. Marais, G. D. van der Spuy, M. Hanekom, G. Coetzee, A. Trollip, C. Hayes, M. E. Bosman, N. C. Gey van Pittius, T. C. Victor, P. D. van Helden and R. M. Warren (2012). "Population structure of multi- and extensively drug-resistant Mycobacterium tuberculosis strains in South Africa." J Clin Microbiol 50(3): 995-1002.

Chopra, T. and R. S. Gokhale (2009). "Polyketide versatility in the biosynthesis of complex mycobacterial cell wall lipids." Methods Enzymol 459: 259-294.

Cimino, M., C. Thomas, A. Namouchi, S. Dubrac, B. Gicquel and D. N. Gopaul (2012). "Identification of DNA binding motifs of the Mycobacterium tuberculosis PhoP/PhoR two-component signal transduction system." PLoS One 7(8): e42876.

Clemens, D. L. and M. A. Horwitz (1995). "Characterization of the Mycobacterium tuberculosis phagosome and evidence that phagosomal maturation is inhibited." J Exp Med 181(1): 257-270.

Cohen, S. N., A. C. Chang and L. Hsu (1972). "Nonchromosomal antibiotic resistance in bacteria: genetic transformation of Escherichia coli by R-factor DNA." Proc Natl Acad Sci U S A 69(8): 2110-2114.

Colangeli, R., D. Helb, C. Vilcheze, M. H. Hazbon, C. G. Lee, H. Safi, B. Sayers, I. Sardone, M. B. Jones, R. D. Fleischmann, S. N. Peterson, W. R. Jacobs, Jr. and D. Alland (2007). "Transcriptional regulation of multi-drug tolerance and antibiotic-induced responses by the histone-like protein Lsr2 in M. tuberculosis." PLoS Pathog 3(6): e87.

Colditz, G. A., C. S. Berkey, F. Mosteller, T. F. Brewer, M. E. Wilson, E. Burdick and H. V. Fineberg (1995). "The efficacy of bacillus Calmette-Guerin vaccination of newborns and infants in the prevention of tuberculosis: meta-analyses of the published literature." Pediatrics 96(1 Pt 1): 29-35.

Cole, S. T., R. Brosch, J. Parkhill, T. Garnier, C. Churcher, D. Harris, S. V. Gordon, K. Eiglmeier, S. Gas, C. E. Barry, 3rd, F. Tekaia, K. Badcock, D. Basham, D. Brown, T. Chillingworth, R. Connor, R. Davies, K. Devlin, T. Feltwell, S. Gentles, N. Hamlin, S. Holroyd, T. Hornsby, K. Jagels, A. Krogh, J. McLean, S. Moule, L. Murphy, K. Oliver, J. Osborne, M. A. Quail, M. A. Rajandream, J. Rogers, S. Rutter, K. Seeger, J. Skelton, R. Squares, S. Squares, J. E. Sulston, K. Taylor, S. Whitehead and B. G. Barrell (1998). "Deciphering the biology of Mycobacterium tuberculosis from the complete genome sequence." Nature 393(6685): 537-544.

Conlon, B. P., S. E. Rowe, A. B. Gandt, A. S. Nuxoll, N. P. Donegan, E. A. Zalis, G. Clair, J. N. Adkins, A. L. Cheung and K. Lewis (2016). "Persister formation in Staphylococcus aureus is associated with ATP depletion." Nat Microbiol 1: 16051.

Conlon, B. P., S. E. Rowe, A. B. Gandt, A. S. Nuxoll, N. P. Donegan, E. A. Zalis, G. Clair, J. N. Adkins, A. L. Cheung and K. Lewis (2016). "Persister formation in Staphylococcus aureus is associated with ATP depletion." Nat Microbiol 1.

Constant, P., E. Perez, W. Malaga, M. A. Laneelle, O. Saurel, M. Daffe and C. Guilhot (2002). "Role of the pks15/1 gene in the biosynthesis of phenolglycolipids in the Mycobacterium tuberculosis complex. Evidence that all strains synthesize glycosylated p-hydroxybenzoic methyl esters and that strains devoid of phenolglycolipids harbor a frameshift mutation in the pks15/1 gene." J Biol Chem 277(41): 38148-38158.

Contassot, E., H. D. Beer and L. E. French (2012). "Interleukin-1, inflammasomes, autoinflammation and the skin." Swiss Med Wkly 142: w13590.

Cooper, A. M. (2009). "Cell-mediated immune responses in tuberculosis." Annu Rev Immunol 27: 393-422.

Cooper, A. M., K. D. Mayer-Barber and A. Sher (2011). "Role of innate cytokines in mycobacterial infection." Mucosal Immunol 4(3): 252-260.

Cousins, D. V., R. Bastida, A. Cataldi, V. Quse, S. Redrobe, S. Dow, P. Duignan, A. Murray, C. Dupont, N. Ahmed, D. M. Collins, W. R. Butler, D. Dawson, D. Rodriguez, J. Loureiro, M. I. Romano, A. Alito, M. Zumarraga and A. Bernardelli (2003). "Tuberculosis in seals caused by a novel member of the Mycobacterium tuberculosis complex: Mycobacterium pinnipedii sp. nov." Int J Syst Evol Microbiol 53(Pt 5): 1305-1314.

Crabbe, A., Y. Liu, N. Matthijs, P. Rigole, C. De La Fuente-Nunez, R. Davis, M. A. Ledesma, S. Sarker, R. Van Houdt, R. E. Hancock, T. Coenye and C. A. Nickerson (2017). "Antimicrobial efficacy against Pseudomonas aeruginosa biofilm formation in a three-dimensional lung epithelial model and the influence of fetal bovine serum." Sci Rep 7: 43321.

Crabbe, A., Y. Liu, S. F. Sarker, N. R. Bonenfant, J. Barrila, Z. D. Borg, J. J. Lee, D. J. Weiss and C. A. Nickerson (2015). "Recellularization of decellularized lung scaffolds is enhanced by dynamic suspension culture." PLoS One 10(5): e0126846.

Crofton, J. (2006). "The MRC randomized trial of streptomycin and its legacy: a view from the clinical front line." J R Soc Med 99(10): 531-534.

Daffe, M. and G. Etienne (1999). "The capsule of Mycobacterium tuberculosis and its implications for pathogenicity." Tuber Lung Dis 79(3): 153-169.

Dagert, M. and S. D. Ehrlich (1979). "Prolonged incubation in calcium chloride improves the competence of Escherichia coli cells." Gene 6(1): 23-28.

Dalton, J. P., B. Uy, N. Phummarin, B. R. Copp, W. A. Denny, S. Swift and S. Wiles (2016). "Effect of common and experimental anti-tuberculosis treatments on Mycobacterium tuberculosis growing as biofilms." PeerJ 4: e2717.

Daniel, J., C. Deb, V. S. Dubey, T. D. Sirakova, B. Abomoelak, H. R. Morbidoni and P. E. Kolattukudy (2004). "Induction of a novel class of diacylglycerol acyltransferases and triacylglycerol accumulation in Mycobacterium tuberculosis as it goes into a dormancy-like state in culture." J Bacteriol 186(15): 5017-5030.

Dartois, V. (2014). "The path of anti-tuberculosis drugs: from blood to lesions to mycobacterial cells." Nat Rev Microbiol 12(3): 159-167.

Davey, M. E. and A. O'Toole G (2000). "Microbial biofilms: from ecology to molecular genetics." Microbiol Mol Biol Rev 64(4): 847-867.

David E. Minnikin, O. Y.-C. L., Houdini H.T. Wu, Vijayashankar Nataraj, Helen D. Donoghue, Malin Ridell, Motoko Watanabe, Luke Alderwick, Apoorva Bhatt and Gurdyal S. Besra (2015). Tuberculosis- Expanding Knowledge, InTech.

Davies, D. (2003). "Understanding biofilm resistance to antibacterial agents." Nat Rev Drug Discov 2(2): 114-122.

Davies, J. and D. Davies (2010). "Origins and evolution of antibiotic resistance." Microbiol Mol Biol Rev 74(3): 417-433.

de la Paz Santangelo, M., L. Klepp, J. Nunez-Garcia, F. C. Blanco, M. Soria, M. C. Garcia-Pelayo, M. V. Bianco, A. A. Cataldi, P. Golby, M. Jackson, S. V. Gordon and F. Bigi (2009). "Mce3R, a TetR-type transcriptional repressor, controls the expression of a regulon involved in lipid metabolism in Mycobacterium tuberculosis." Microbiology 155(Pt 7): 2245-2255.

Deb, C., C. M. Lee, V. S. Dubey, J. Daniel, B. Abomoelak, T. D. Sirakova, S. Pawar, L. Rogers and P. E. Kolattukudy (2009). "A novel in vitro multiple-stress dormancy model for Mycobacterium tuberculosis generates a lipid-loaded, drug-tolerant, dormant pathogen." PLoS One 4(6): e6077.

Deretic, V., S. Singh, S. Master, J. Harris, E. Roberts, G. Kyei, A. Davis, S. de Haro, J. Naylor, H. H. Lee and I. Vergne (2006). "Mycobacterium tuberculosis inhibition of phagolysosome biogenesis and autophagy as a host defence mechanism." Cell Microbiol 8(5): 719-727.

Dhar, N., J. McKinney and G. Manina (2016). "Phenotypic Heterogeneity in Mycobacterium tuberculosis." Microbiol Spectr 4(6).

Draper, P. (1998). "The outer parts of the mycobacterial envelope as permeability barriers." Front Biosci 3: D1253-1261.

Dubos, R. J. and G. Middlebrook (1948). "The effect of wetting agents on the growth of tubercle bacilli." J Exp Med 88(1): 81-88.

Ducati, R. G., A. Ruffino-Netto, L. A. Basso and D. S. Santos (2006). "The resumption of consumption -- a review on tuberculosis." Mem Inst Oswaldo Cruz 101(7): 697-714.

Dunphy, K. Y., R. H. Senaratne, M. Masuzawa, L. V. Kendall and L. W. Riley (2010). "Attenuation of Mycobacterium tuberculosis functionally disrupted in a fatty acyl-coenzyme A synthetase gene fadD5." J Infect Dis 201(8): 1232-1239.

Duque-Correa, M. A., A. A. Kuhl, P. C. Rodriguez, U. Zedler, S. Schommer-Leitner, M. Rao, J. Weiner, 3rd, R. Hurwitz, J. E. Qualls, G. A. Kosmiadi, P. J. Murray, S. H. Kaufmann and S. T. Reece (2014). "Macrophage arginase-1 controls bacterial growth and pathology in hypoxic tuberculosis granulomas." Proc Natl Acad Sci U S A 111(38): E4024-4032.

Edwards, D. I. (1979). "Mechanism of antimicrobial action of metronidazole." J Antimicrob Chemother 5(5): 499-502.

Ehlers, S. and U. E. Schaible (2012). "The granuloma in tuberculosis: dynamics of a host-pathogen collusion." Front Immunol 3: 411.

Eisenach, K. D., J. T. Crawford and J. H. Bates (1986). "Genetic relatedness among strains of the Mycobacterium tuberculosis complex. Analysis of restriction fragment heterogeneity using cloned DNA probes." Am Rev Respir Dis 133(6): 1065-1068.

Epstein, W. (2003). "The roles and regulation of potassium in bacteria." Prog Nucleic Acid Res Mol Biol 75: 293-320.

Evangelopoulos, D., J. D. da Fonseca and S. J. Waddell (2015). "Understanding anti-tuberculosis drug efficacy: rethinking bacterial populations and how we model them." Int J Infect Dis 32: 76-80.

Ewer, K., K. A. Millington, J. J. Deeks, L. Alvarez, G. Bryant and A. Lalvani (2006). "Dynamic antigen-specific T-cell responses after point-source exposure to Mycobacterium tuberculosis." Am J Respir Crit Care Med 174(7): 831-839.

Farhat, M., C. Greenaway, M. Pai and D. Menzies (2006). "False-positive tuberculin skin tests: what is the absolute effect of BCG and non-tuberculous mycobacteria?" Int J Tuberc Lung Dis 10(11): 1192-1204.

Fenton, M. J., M. W. Vermeulen, S. Kim, M. Burdick, R. M. Strieter and H. Kornfeld (1997). "Induction of gamma interferon production in human alveolar macrophages by Mycobacterium tuberculosis." Infect Immun 65(12): 5149-5156.

Fonseca, J. D., G. M. Knight and T. D. McHugh (2015). "The complex evolution of antibiotic resistance in Mycobacterium tuberculosis." Int J Infect Dis 32: 94-100.

Forbes, M., N. A. Kuck and E. A. Peets (1962). "Mode of action of ethambutol." J Bacteriol 84: 1099-1103.

Ford, C. B., R. R. Shah, M. K. Maeda, S. Gagneux, M. B. Murray, T. Cohen, J. C. Johnston, J. Gardy, M. Lipsitch and S. M. Fortune (2013). "Mycobacterium tuberculosis mutation rate estimates from different lineages predict substantial differences in the emergence of drug-resistant tuberculosis." Nat Genet 45(7): 784-790.

Fox, G. J., M. Orlova and E. Schurr (2016). "Tuberculosis in Newborns: The Lessons of the "Lubeck Disaster" (1929-1933)." PLoS Pathog 12(1): e1005271.

Francis, R. J., R. E. Butler and G. R. Stewart (2014). "Mycobacterium tuberculosis ESAT-6 is a leukocidin causing Ca2+ influx, necrosis and neutrophil extracellular trap formation." Cell Death Dis 5: e1474.

Fratti, R. A., J. Chua, I. Vergne and V. Deretic (2003). "Mycobacterium tuberculosis glycosylated phosphatidylinositol causes phagosome maturation arrest." Proc Natl Acad Sci U S A 100(9): 5437-5442.

Frick, M. (2015). "The Tuberculosis Vaccines Pipeline: A New Path to the Same Destination?" Retrieved 25th March, 2017, from http://www.pipelinereport.org/2015/tb-vaccines.

Fridman O, Goldberg A, Ronin I, Shoresh N, Balaban NQ (2014). “Optimization of lag time underlies antibiotic tolerance in evolved bacterial populations” Nature volume 513, pages 418–421.

Fukui, K. (2010). "DNA mismatch repair in eukaryotes and bacteria." J Nucleic Acids 2010.

Fuqua, C. and E. P. Greenberg (2002). "Listening in on bacteria: acyl-homoserine lactone signalling." Nat Rev Mol Cell Biol 3(9): 685-695.

Fux, C. A., J. W. Costerton, P. S. Stewart and P. Stoodley (2005). "Survival strategies of infectious biofilms." Trends Microbiol 13(1): 34-40.

Galagan, J., A. Lyubetskaya and A. Gomes (2013). "ChIP-Seq and the complexity of bacterial transcriptional regulation." Curr Top Microbiol Immunol 363: 43-68.

Gardner, J. K. and M. M. Herbst-Kralovetz (2016). "Three-Dimensional Rotating Wall Vessel-Derived Cell Culture Models for Studying Virus-Host Interactions." Viruses 8(11).

Garnier, T., K. Eiglmeier, J. C. Camus, N. Medina, H. Mansoor, M. Pryor, S. Duthoy, S. Grondin, C. Lacroix, C. Monsempe, S. Simon, B. Harris, R. Atkin, J. Doggett, R. Mayes, L. Keating, P. R. Wheeler, J. Parkhill, B. G. Barrell, S. T. Cole, S. V. Gordon and R. G. Hewinson (2003). "The complete genome sequence of Mycobacterium bovis." Proc Natl Acad Sci U S A 100(13): 7877-7882.

Garton, N. J., H. Christensen, D. E. Minnikin, R. A. Adegbola and M. R. Barer (2002). "Intracellular lipophilic inclusions of mycobacteria in vitro and in sputum." Microbiology 148(Pt 10): 2951-2958.

Garton, N. J., S. J. Waddell, A. L. Sherratt, S. M. Lee, R. J. Smith, C. Senner, J. Hinds, K. Rajakumar, R. A. Adegbola, G. S. Besra, P. D. Butcher and M. R. Barer (2008). "Cytological and transcript analyses reveal fat and lazy persister-like bacilli in tuberculous sputum." PLoS Med 5(4): e75.

Gelman, E., J. D. McKinney and N. Dhar (2012). "Malachite green interferes with postantibiotic recovery of mycobacteria." Antimicrob Agents Chemother 56(7): 3610-3614.

Gerdes & Maisonneuve (2012). “(p)ppGpp controls bacterial persistence by stochastic induction of toxin-antitoxin activity”. Cell. 2013 Aug 29;154(5):1140-1150.

Gey Van Pittius, N. C., J. Gamieldien, W. Hide, G. D. Brown, R. J. Siezen and A. D. Beyers (2001). "The ESAT-6 gene cluster of Mycobacterium tuberculosis and other high G+C Gram-positive bacteria." Genome Biol 2(10): RESEARCH0044.

Gibson, J., A. Sood and D. A. Hogan (2009). "Pseudomonas aeruginosa-Candida albicans interactions: localization and fungal toxicity of a phenazine derivative." Appl Environ Microbiol 75(2): 504-513.

Goloubeva, V., M. Lecocq, P. Lassowsky, F. Matthys, F. Portaels and I. Bastian (2001). "Evaluation of mycobacteria growth indicator tube for direct and indirect drug

susceptibility testing of Mycobacterium tuberculosis from respiratory specimens in a Siberian prison hospital." J Clin Microbiol 39(4): 1501-1505.

Gordon, S., A. Pluddemann and F. Martinez Estrada (2014). "Macrophage heterogeneity in tissues: phenotypic diversity and functions." Immunol Rev 262(1): 36-55.

Gouzy, A., G. Larrouy-Maumus, D. Bottai, F. Levillain, A. Dumas, J. B. Wallach, I. Caire-Brandli, C. de Chastellier, T. D. Wu, R. Poincloux, R. Brosch, J. L. Guerquin-Kern, D. Schnappinger, L. P. Sorio de Carvalho, Y. Poquet and O. Neyrolles (2014). "Mycobacterium tuberculosis exploits asparagine to assimilate nitrogen and resist acid stress during infection." PLoS Pathog 10(2): e1003928.

Groschel, M. I., F. Sayes, R. Simeone, L. Majlessi and R. Brosch (2016). "ESX secretion systems: mycobacterial evolution to counter host immunity." Nat Rev Microbiol 14(11): 677-691.

Grosset, J. (2003). "Mycobacterium tuberculosis in the extracellular compartment: an underestimated adversary." Antimicrob Agents Chemother 47(3): 833-836.

Haile, Y., D. A. Caugant, G. Bjune and H. G. Wiker (2002). "Mycobacterium tuberculosis mammalian cell entry operon (mce) homologs in Mycobacterium other than tuberculosis (MOTT)." FEMS Immunol Med Microbiol 33(2): 125-132.

Halevy, S., A. D. Cohen and N. Grossman (2005). "Clinical implications of in vitro drug-induced interferon gamma release from peripheral blood lymphocytes in cutaneous adverse drug reactions." J Am Acad Dermatol 52(2): 254-261.

Hall-Stoodley, L., J. W. Costerton and P. Stoodley (2004). "Bacterial biofilms: from the natural environment to infectious diseases." Nat Rev Microbiol 2(2): 95-108.

Hall, L., K. P. Jude, S. L. Clark and N. L. Wengenack (2011). "Antimicrobial susceptibility testing of Mycobacterium tuberculosis complex for first and second line drugs by broth dilution in a microtiter plate format." J Vis Exp(52).

Hammond, T. G. and J. M. Hammond (2001). "Optimized suspension culture: the rotating-wall vessel." Am J Physiol Renal Physiol 281(1): F12-25.

Harboe, M., T. Oettinger, H. G. Wiker, I. Rosenkrands and P. Andersen (1996). "Evidence for occurrence of the ESAT-6 protein in Mycobacterium tuberculosis and virulent Mycobacterium bovis and for its absence in Mycobacterium bovis BCG." Infect Immun 64(1): 16-22.

Harris, R. C., P. J. Dodd and R. G. White (2016). "The potential impact of BCG vaccine supply shortages on global paediatric tuberculosis mortality." BMC Med 14(1): 138.

Hett, E. C. and E. J. Rubin (2008). "Bacterial growth and cell division: a mycobacterial perspective." Microbiol Mol Biol Rev 72(1): 126-156, table of contents.

Higginson, E. E., J. E. Galen, M. M. Levine and S. M. Tennant (2016). "Microgravity as a biological tool to examine host-pathogen interactions and to guide development of therapeutics and preventatives that target pathogenic bacteria." Pathog Dis 74(8).

Honer Zu Bentrup, K., A. Miczak, D. L. Swenson and D. G. Russell (1999). "Characterization of activity and expression of isocitrate lyase in Mycobacterium avium and Mycobacterium tuberculosis." J Bacteriol 181(23): 7161-7167.

Honeyborne, I., T. D. McHugh, I. Kuittinen, A. Cichonska, D. Evangelopoulos, K. Ronacher, P. D. van Helden, S. H. Gillespie, D. Fernandez-Reyes, G. Walzl, J. Rousu,

P. D. Butcher and S. J. Waddell (2016). "Profiling persistent tubercule bacilli from patient sputa during therapy predicts early drug efficacy." BMC Med 14: 68.

Houben, D., C. Demangel, J. van Ingen, J. Perez, L. Baldeon, A. M. Abdallah, L. Caleechurn, D. Bottai, M. van Zon, K. de Punder, T. van der Laan, A. Kant, R. Bossers-de Vries, P. Willemsen, W. Bitter, D. van Soolingen, R. Brosch, N. van der Wel and P. J. Peters (2012). "ESX-1-mediated translocation to the cytosol controls virulence of mycobacteria." Cell Microbiol 14(8): 1287-1298.

Houben, E. N., K. V. Korotkov and W. Bitter (2014). "Take five - Type VII secretion systems of Mycobacteria." Biochim Biophys Acta 1843(8): 1707-1716.

Hu, Y. and A. R. Coates (1999). "Transcription of two sigma 70 homologue genes, sigA and sigB, in stationary-phase Mycobacterium tuberculosis." J Bacteriol 181(2): 469-476.

Hu, Y., A. R. Coates and D. A. Mitchison (2008). "Comparison of the sterilising activities of the nitroimidazopyran PA-824 and moxifloxacin against persisting Mycobacterium tuberculosis." Int J Tuberc Lung Dis 12(1): 69-73.

Hu, Y., A. Liu, F. Ortega-Muro, L. Alameda-Martin, D. Mitchison and A. Coates (2015). "High-dose rifampicin kills persisters, shortens treatment duration, and reduces relapse rate in vitro and in vivo." Front Microbiol 6: 641.

Hurdle, J. G., R. B. Lee, N. R. Budha, E. I. Carson, J. Qi, M. S. Scherman, S. H. Cho, M. R. McNeil, A. J. Lenaerts, S. G. Franzblau, B. Meibohm and R. E. Lee (2008). "A microbiological assessment of novel nitrofuranylamides as anti-tuberculosis agents." J Antimicrob Chemother 62(5): 1037-1045.

Indrigo, J., R. L. Hunter, Jr. and J. K. Actor (2002). "Influence of trehalose 6,6'-dimycolate (TDM) during mycobacterial infection of bone marrow macrophages." Microbiology 148(Pt 7): 1991-1998.

Islam, M. S., J. P. Richards and A. K. Ojha (2012). "Targeting drug tolerance in mycobacteria: a perspective from mycobacterial biofilms." Expert Rev Anti Infect Ther 10(9): 1055-1066.

Jayaraman, P., I. Sada-Ovalle, T. Nishimura, A. C. Anderson, V. K. Kuchroo, H. G. Remold and S. M. Behar (2013). "IL-1beta promotes antimicrobial immunity in macrophages by regulating TNFR signaling and caspase-3 activation." J Immunol 190(8): 4196-4204.

Jindani, A., V. R. Aber, E. A. Edwards and D. A. Mitchison (1980). "The early bactericidal activity of drugs in patients with pulmonary tuberculosis." Am Rev Respir Dis 121(6): 939-949.

Jindani, A., C. J. Dore and D. A. Mitchison (2003). "Bactericidal and sterilizing activities of antituberculosis drugs during the first 14 days." Am J Respir Crit Care Med 167(10): 1348-1354.

Jo, E. K., C. S. Yang, C. H. Choi and C. V. Harding (2007). "Intracellular signalling cascades regulating innate immune responses to Mycobacteria: branching out from Toll-like receptors." Cell Microbiol 9(5): 1087-1098.

Juarez, E., C. Nunez, E. Sada, J. J. Ellner, S. K. Schwander and M. Torres (2010). "Differential expression of Toll-like receptors on human alveolar macrophages and autologous peripheral monocytes." Respir Res 11: 2.

Kaldalu, N., A. Joers, H. Ingelman and T. Tenson (2016). "A General Method for Measuring Persister Levels in Escherichia coli Cultures." Methods Mol Biol 1333: 29-42.

Karakousis, P. C., T. Yoshimatsu, G. Lamichhane, S. C. Woolwine, E. L. Nuermberger, J. Grosset and W. R. Bishai (2004). "Dormancy phenotype displayed by extracellular Mycobacterium tuberculosis within artificial granulomas in mice." J Exp Med 200(5): 647-657.

Karumbi, J. and P. Garner (2015). "Directly observed therapy for treating tuberculosis." Cochrane Database Syst Rev(5): CD003343.

Kaur, D., M. E. Guerin, H. Skovierova, P. J. Brennan and M. Jackson (2009). "Chapter 2: Biogenesis of the cell wall and other glycoconjugates of Mycobacterium tuberculosis." Adv Appl Microbiol 69: 23-78.

Kleinnijenhuis, J., L. A. Joosten, F. L. van de Veerdonk, N. Savage, R. van Crevel, B. J. Kullberg, A. van der Ven, T. H. Ottenhoff, C. A. Dinarello, J. W. van der Meer and M. G. Netea (2009). "Transcriptional and inflammasome-mediated pathways for the induction of IL-1beta production by Mycobacterium tuberculosis." Eur J Immunol 39(7): 1914-1922.

Knutson, K. L., Z. Hmama, P. Herrera-Velit, R. Rochford and N. E. Reiner (1998). "Lipoarabinomannan of Mycobacterium tuberculosis promotes protein tyrosine dephosphorylation and inhibition of mitogen-activated protein kinase in human mononuclear phagocytes. Role of the Src homology 2 containing tyrosine phosphatase 1." J Biol Chem 273(1): 645-652.

Kozak, R. A., D. C. Alexander, R. Liao, D. R. Sherman and M. A. Behr (2011). "Region of difference 2 contributes to virulence of Mycobacterium tuberculosis." Infect Immun 79(1): 59-66.

Kubica, T., S. Rusch-Gerdes and S. Niemann (2003). "Mycobacterium bovis subsp. caprae caused one-third of human M. bovis-associated tuberculosis cases reported in Germany between 1999 and 2001." J Clin Microbiol 41(7): 3070-3077.

Kucukyildirim, S., H. Long, W. Sung, S. F. Miller, T. G. Doak and M. Lynch (2016). "The Rate and Spectrum of Spontaneous Mutations in Mycobacterium smegmatis, a Bacterium Naturally Devoid of the Postreplicative Mismatch Repair Pathway." G3 (Bethesda) 6(7): 2157-2163.

Kumar, A., M. Bose and V. Brahmachari (2003). "Analysis of expression profile of mammalian cell entry (mce) operons of Mycobacterium tuberculosis." Infect Immun 71(10): 6083-6087.

Kumar, P., K. Arora, J. R. Lloyd, I. Y. Lee, V. Nair, E. Fischer, H. I. Boshoff and C. E. Barry, 3rd (2012). "Meropenem inhibits D,D-carboxypeptidase activity in Mycobacterium tuberculosis." Mol Microbiol 86(2): 367-381.

Larson, C. L. and W. C. Wicht (1964). "Infection of Mice with Mycobacterium Tuberculosis, Strain H37ra." Am Rev Respir Dis 90: 742-748.

Lawn, S. D. and A. I. Zumla (2011). "Tuberculosis." Lancet 378(9785): 57-72.

Lee, M. H., L. Pascopella, W. R. Jacobs, Jr. and G. F. Hatfull (1991). "Site-specific integration of mycobacteriophage L5: integration-proficient vectors for Mycobacterium smegmatis, Mycobacterium tuberculosis, and bacille Calmette-Guerin." Proc Natl Acad Sci U S A 88(8): 3111-3115.

Leid, J. G., C. J. Willson, M. E. Shirtliff, D. J. Hassett, M. R. Parsek and A. K. Jeffers (2005). "The exopolysaccharide alginate protects Pseudomonas aeruginosa biofilm bacteria from IFN-gamma-mediated macrophage killing." J Immunol 175(11): 7512-7518.

Leistikow, R. L., R. A. Morton, I. L. Bartek, I. Frimpong, K. Wagner and M. I. Voskuil (2010). "The Mycobacterium tuberculosis DosR regulon assists in metabolic homeostasis and enables rapid recovery from nonrespiring dormancy." J Bacteriol 192(6): 1662-1670.

Lenaerts, A., C. E. Barry, 3rd and V. Dartois (2015). "Heterogeneity in tuberculosis pathology, microenvironments and therapeutic responses." Immunol Rev 264(1): 288-307.

Lenaerts, A. J., D. Hoff, S. Aly, S. Ehlers, K. Andries, L. Cantarero, I. M. Orme and R. J. Basaraba (2007). "Location of persisting mycobacteria in a Guinea pig model of tuberculosis revealed by r207910." Antimicrob Agents Chemother 51(9): 3338-3345.

Leung, A. S., V. Tran, Z. Wu, X. Yu, D. C. Alexander, G. F. Gao, B. Zhu and J. Liu (2008). "Novel genome polymorphisms in BCG vaccine strains and impact on efficacy." BMC Genomics 9: 413.

Levin-Reisman, I., I. Ronin, O. Gefen, I. Braniss, N. Shoresh and N.Q. Balaban (2017). “Antibiotic tolerance leads to the evolution of resistance.” Science 355(6327): 826-830.

Lewis, K. (2008). "Multidrug tolerance of biofilms and persister cells." Curr Top Microbiol Immunol 322: 107-131.

Li, L., N. Mendis, H. Trigui, J. D. Oliver and S. P. Faucher (2014). "The importance of the viable but non-culturable state in human bacterial pathogens." Front Microbiol 5: 258.

Li, R., R. Sirawaraporn, P. Chitnumsub, W. Sirawaraporn, J. Wooden, F. Athappilly, S. Turley and W. G. Hol (2000). "Three-dimensional structure of M. tuberculosis dihydrofolate reductase reveals opportunities for the design of novel tuberculosis drugs." J Mol Biol 295(2): 307-323.

Li, W. and Z. G. He (2012). "LtmA, a novel cyclic di-GMP-responsive activator, broadly regulates the expression of lipid transport and metabolism genes in Mycobacterium smegmatis." Nucleic Acids Res 40(22): 11292-11307.

Li, Y. H. and X. Tian (2012). "Quorum sensing and bacterial social interactions in biofilms." Sensors (Basel) 12(3): 2519-2538.

Ligon, L. S., J. D. Hayden and M. Braunstein (2012). "The ins and outs of Mycobacterium tuberculosis protein export." Tuberculosis (Edinb) 92(2): 121-132.

Lim, A., M. Eleuterio, B. Hutter, B. Murugasu-Oei and T. Dick (1999). "Oxygen depletion-induced dormancy in Mycobacterium bovis BCG." J Bacteriol 181(7): 2252-2256.

Limoli, D. H., C. J. Jones and D. J. Wozniak (2015). "Bacterial Extracellular Polysaccharides in Biofilm Formation and Function." Microbiol Spectr 3(3).

Liu, J., V. Tran, A. S. Leung, D. C. Alexander and B. Zhu (2009). "BCG vaccines: their mechanisms of attenuation and impact on safety and protective efficacy." Hum Vaccin 5(2): 70-78.

Loebel, R. O., E. Shorr and H. B. Richardson (1933). "The Influence of Adverse Conditions upon the Respiratory Metabolism and Growth of Human Tubercle Bacilli." J Bacteriol 26(2): 167-200.

Loebel, R. O., E. Shorr and H. B. Richardson (1933). "The Influence of Foodstuffs upon the Respiratory Metabolism and Growth of Human Tubercle Bacilli." J Bacteriol 26(2): 139-166.

Lopez-Castejon, G. and D. Brough (2011). "Understanding the mechanism of IL-1beta secretion." Cytokine Growth Factor Rev 22(4): 189-195.

Lugosi, L. (1992). "Theoretical and methodological aspects of BCG vaccine from the discovery of Calmette and Guerin to molecular biology. A review." Tuber Lung Dis 73(5): 252-261.

Mack, U., G. B. Migliori, M. Sester, H. L. Rieder, S. Ehlers, D. Goletti, A. Bossink, K. Magdorf, C. Holscher, B. Kampmann, S. M. Arend, A. Detjen, G. Bothamley, J. P. Zellweger, H. Milburn, R. Diel, P. Ravn, F. Cobelens, P. J. Cardona, B. Kan, I. Solovic, R. Duarte, D. M. Cirillo, C. Lange and Tbnet (2009). "LTBI: latent tuberculosis infection or lasting immune responses to M. tuberculosis? A TBNET consensus statement." Eur Respir J 33(5): 956-973.

Magdalena, J., P. Supply and C. Locht (1998). "Specific differentiation between Mycobacterium bovis BCG and virulent strains of the Mycobacterium tuberculosis complex." J Clin Microbiol 36(9): 2471-2476.

Mahairas, G. G., P. J. Sabo, M. J. Hickey, D. C. Singh and C. K. Stover (1996). "Molecular analysis of genetic differences between Mycobacterium bovis BCG and virulent M. bovis." J Bacteriol 178(5): 1274-1282.

Malhotra, V., D. Sharma, V. D. Ramanathan, H. Shakila, D. K. Saini, S. Chakravorty, T. K. Das, Q. Li, R. F. Silver, P. R. Narayanan and J. S. Tyagi (2004). "Disruption of response regulator gene, devR, leads to attenuation in virulence of Mycobacterium tuberculosis." FEMS Microbiol Lett 231(2): 237-245.

Mandlik, A., A. Swierczynski, A. Das and H. Ton-That (2008). "Pili in Gram-positive bacteria: assembly, involvement in colonization and biofilm development." Trends Microbiol 16(1): 33-40.

Manganelli, R., E. Dubnau, S. Tyagi, F. R. Kramer and I. Smith (1999). "Differential expression of 10 sigma factor genes in Mycobacterium tuberculosis." Mol Microbiol 31(2): 715-724.

Manjunatha, U., H. I. Boshoff and C. E. Barry (2009). "The mechanism of action of PA-824: Novel insights from transcriptional profiling." Commun Integr Biol 2(3): 215-218.

Martin, C., A. Williams, R. Hernandez-Pando, P. J. Cardona, E. Gormley, Y. Bordat, C. Y. Soto, S. O. Clark, G. J. Hatch, D. Aguilar, V. Ausina and B. Gicquel (2006). "The live Mycobacterium tuberculosis phoP mutant strain is more attenuated than BCG and confers protective immunity against tuberculosis in mice and guinea pigs." Vaccine 24(17): 3408-3419.

Matteelli, A., G. Sulis, S. Capone, L. D'Ambrosio, G. B. Migliori and H. Getahun (2017). "Tuberculosis elimination and the challenge of latent tuberculosis." Presse Med 46(2 Pt 2): e13-e21.

Mawuenyega, K. G., C. V. Forst, K. M. Dobos, J. T. Belisle, J. Chen, E. M. Bradbury, A. R. Bradbury and X. Chen (2005). "Mycobacterium tuberculosis functional network analysis by global subcellular protein profiling." Mol Biol Cell 16(1): 396-404.

McDonough, K. A., Y. Kress and B. R. Bloom (1993). "Pathogenesis of tuberculosis: interaction of Mycobacterium tuberculosis with macrophages." Infect Immun 61(7): 2763-2773.

McKinney, J. D., K. Honer zu Bentrup, E. J. Munoz-Elias, A. Miczak, B. Chen, W. T. Chan, D. Swenson, J. C. Sacchettini, W. R. Jacobs, Jr. and D. G. Russell (2000). "Persistence of Mycobacterium tuberculosis in macrophages and mice requires the glyoxylate shunt enzyme isocitrate lyase." Nature 406(6797): 735-738.

Medzhitov, R. and C. Janeway, Jr. (2000). "Innate immune recognition: mechanisms and pathways." Immunol Rev 173: 89-97.

Meher, A. K., N. C. Bal, K. V. Chary and A. Arora (2006). "Mycobacterium tuberculosis H37Rv ESAT-6-CFP-10 complex formation confers thermodynamic and biochemical stability." FEBS J 273(7): 1445-1462.

Mestre, O., T. Luo, T. Dos Vultos, K. Kremer, A. Murray, A. Namouchi, C. Jackson, J. Rauzier, P. Bifani, R. Warren, V. Rasolofo, J. Mei, Q. Gao and B. Gicquel (2011). "Phylogeny of Mycobacterium tuberculosis Beijing strains constructed from polymorphisms in genes involved in DNA replication, recombination and repair." PLoS One 6(1): e16020.

Middlebrook, G., R. J. Dubos and C. Pierce (1947). "Differential characteristics of virulent and avirulent variants of mammalian tubercle bacilli." J Bacteriol 54(1): 66.

Miller, E. A. and J. D. Ernst (2009). "Anti-TNF immunotherapy and tuberculosis reactivation: another mechanism revealed." J Clin Invest 119(5): 1079-1082.

Miller, M. B. and B. L. Bassler (2001). "Quorum sensing in bacteria." Annu Rev Microbiol 55: 165-199.

Minnikin, D. E. (1982). The Biology of Mycobacteria. London, U.K.

Mishra, A. K., N. N. Driessen, B. J. Appelmelk and G. S. Besra (2011). "Lipoarabinomannan and related glycoconjugates: structure, biogenesis and role in Mycobacterium tuberculosis physiology and host-pathogen interaction." FEMS Microbiol Rev 35(6): 1126-1157.

Mitchison, D. A. (1985). "The action of antituberculosis drugs in short-course chemotherapy." Tubercle 66(3): 219-225.

Mitchison, D. A. (2004). "The search for new sterilizing anti-tuberculosis drugs." Front Biosci 9: 1059-1072.

Mitchison, D. A. (2004). "The Search for New Sterilizing Anti-Tuberculosis Drugs." Frontiers in Bioscience 9: 1059-1072.

Mlynarcik, P. and M. Kolar (2016). "Starvation- and antibiotics-induced formation of persister cells in Pseudomonas aeruginosa." Biomed Pap Med Fac Univ Palacky Olomouc Czech Repub.

Mockler, T. C., S. Chan, A. Sundaresan, H. Chen, S. E. Jacobsen and J. R. Ecker (2005). "Applications of DNA tiling arrays for whole-genome analysis." Genomics 85(1): 1-15.

Moldoveanu, B., P. Otmishi, P. Jani, J. Walker, X. Sarmiento, J. Guardiola, M. Saad and J. Yu (2009). "Inflammatory mechanisms in the lung." J Inflamm Res 2: 1-11.

Monack, D. M., A. Mueller and S. Falkow (2004). "Persistent bacterial infections: the interface of the pathogen and the host immune system." Nat Rev Microbiol 2(9): 747-765.

Monahan IM, M. J., Butcher PD (2001). Extraction of RNA from intracellular Mycobacterium tuberculosis: Methods, considerations and applications. New Jersey, USA, Humana Press.

Morita, Y. S., T. Fukuda, C. B. Sena, Y. Yamaryo-Botte, M. J. McConville and T. Kinoshita (2011). "Inositol lipid metabolism in mycobacteria: biosynthesis and regulatory mechanisms." Biochim Biophys Acta 1810(6): 630-641.

G.V. Mukamolova, O. Turapov, J. Malkin, G. Woltmann, and M.R. Barer (2009). “Resuscitation-promoting Factors Reveal an Occult Population of Tubercle Bacilli in Sputum”. Am J Respir Crit Care Med Vol 181. pp 174–180, 2010.

Mulcahy, H., L. Charron-Mazenod and S. Lewenza (2008). "Extracellular DNA chelates cations and induces antibiotic resistance in Pseudomonas aeruginosa biofilms." PLoS Pathog 4(11): e1000213.

Muller, B., S. Borrell, G. Rose and S. Gagneux (2013). "The heterogeneous evolution of multidrug-resistant Mycobacterium tuberculosis." Trends Genet 29(3): 160-169.

Muller, M. (1983). "Mode of action of metronidazole on anaerobic bacteria and protozoa." Surgery 93(1 Pt 2): 165-171.

Munoz-Elias, E. J. and J. D. McKinney (2005). "Mycobacterium tuberculosis isocitrate lyases 1 and 2 are jointly required for in vivo growth and virulence." Nat Med 11(6): 638-644.

Murugasu-Oei, B. and T. Dick (2000). "Bactericidal activity of nitrofurans against growing and dormant Mycobacterium bovis BCG." J Antimicrob Chemother 46(6): 917-919.

Muttucumaru, D. G., G. Roberts, J. Hinds, R. A. Stabler and T. Parish (2004). "Gene expression profile of Mycobacterium tuberculosis in a non-replicating state." Tuberculosis (Edinb) 84(3-4): 239-246.

Nakae, S., A. Hijikata, T. Tsuji, K. Yonezawa, K. I. Kouyama, K. Mayanagi, S. Ishino, Y. Ishino and T. Shirai (2016). "Structure of the EndoMS-DNA Complex as Mismatch Restriction Endonuclease." Structure 24(11): 1960-1971.

Nalepa, P., M. Strach, M. Rybak-Bak and M. Siedlar (2011). "[Two siblings with an IL-12 and IFN-gamma production disorder diagnosed with pulmonary mycobacteriosis caused by M. kansasii. Mendelian susceptibility to mycobacterial infection: an overview of literature]." Pneumonol Alergol Pol 79(6): 428-436.

Nandakumar, M., C. Nathan and K. Y. Rhee (2014). "Isocitrate lyase mediates broad antibiotic tolerance in Mycobacterium tuberculosis." Nat Commun 5: 4306.

Nayak, S. and B. Acharjya (2012). "Mantoux test and its interpretation." Indian Dermatol Online J 3(1): 2-6.

Ng, V. H., J. S. Cox, A. O. Sousa, J. D. MacMicking and J. D. McKinney (2004). "Role of KatG catalase-peroxidase in mycobacterial pathogenesis: countering the phagocyte oxidative burst." Mol Microbiol 52(5): 1291-1302.

Noll, H., H. Bloch, J. Asselineau and E. Lederer (1956). "The chemical structure of the cord factor of Mycobacterium tuberculosis." Biochim Biophys Acta 20(2): 299-309.

Oettinger, T., M. Jorgensen, A. Ladefoged, K. Haslov and P. Andersen (1999). "Development of the Mycobacterium bovis BCG vaccine: review of the historical and biochemical evidence for a genealogical tree." Tuber Lung Dis 79(4): 243-250.

Ojha, A. and G. F. Hatfull (2007). "The role of iron in Mycobacterium smegmatis biofilm formation: the exochelin siderophore is essential in limiting iron conditions for biofilm formation but not for planktonic growth." Mol Microbiol 66(2): 468-483.

Ojha, A. K., A. D. Baughn, D. Sambandan, T. Hsu, X. Trivelli, Y. Guerardel, A. Alahari, L. Kremer, W. R. Jacobs, Jr. and G. F. Hatfull (2008). "Growth of Mycobacterium tuberculosis biofilms containing free mycolic acids and harbouring drug-tolerant bacteria." Mol Microbiol 69(1): 164-174.

Organisation, T. W. H. (2016, October 2016). "Tuberculosis Fact Sheet." Retrieved 10 March, 2017, from http://www.who.int/mediacentre/factsheets/fs104/en/.

Organisation, T. W. H. (2017). "The Top 10 Causes of Death." Retrieved 10 March, 2017, from http://www.who.int/mediacentre/factsheets/fs310/en/.

Pai, M., L. W. Riley and J. M. Colford, Jr. (2004). "Interferon-gamma assays in the immunodiagnosis of tuberculosis: a systematic review." Lancet Infect Dis 4(12): 761-776.

Pai, M. and G. Sotgiu (2016). "Diagnostics for latent TB infection: incremental, not transformative progress." Eur Respir J 47(3): 704-706.

Pajon, R., D. Yero, A. Lage, A. Llanes and C. J. Borroto (2006). "Computational identification of beta-barrel outer-membrane proteins in Mycobacterium tuberculosis predicted proteomes as putative vaccine candidates." Tuberculosis (Edinb) 86(3-4): 290-302.

Palmer, G. H., T. Bankhead and S. A. Lukehart (2009). "'Nothing is permanent but change'- antigenic variation in persistent bacterial pathogens." Cell Microbiol 11(12): 1697-1705.

Panandiker, A., G. B. Maru and K. V. Rao (1994). "Dose-response effects of malachite green on free radical formation, lipid peroxidation and DNA damage in Syrian hamster embryo cells and their modulation by antioxidants." Carcinogenesis 15(11): 2445-2448.

Pang, J. M., E. Layre, L. Sweet, A. Sherrid, D. B. Moody, A. Ojha and D. R. Sherman (2012). "The polyketide Pks1 contributes to biofilm formation in Mycobacterium tuberculosis." J Bacteriol 194(3): 715-721.

Parish, T., D. A. Smith, S. Kendall, N. Casali, G. J. Bancroft and N. G. Stoker (2003). "Deletion of two-component regulatory systems increases the virulence of Mycobacterium tuberculosis." Infect Immun 71(3): 1134-1140.

Park, H. D., K. M. Guinn, M. I. Harrell, R. Liao, M. I. Voskuil, M. Tompa, G. K. Schoolnik and D. R. Sherman (2003). "Rv3133c/dosR is a transcription factor that mediates the hypoxic response of Mycobacterium tuberculosis." Mol Microbiol 48(3): 833-843.

Patankar, A. V. and J. E. Gonzalez (2009). "Orphan LuxR regulators of quorum sensing." FEMS Microbiol Rev 33(4): 739-756.

Pathak, S. K., S. Basu, K. K. Basu, A. Banerjee, S. Pathak, A. Bhattacharyya, T. Kaisho, M. Kundu and J. Basu (2007). "Direct extracellular interaction between the early secreted antigen ESAT-6 of Mycobacterium tuberculosis and TLR2 inhibits TLR signaling in macrophages." Nat Immunol 8(6): 610-618.

Pendzich, J., W. Maksymowicz-Mazur, U. Mazurek, S. Dworniczak, K. Oklek, J. Kozielski and T. Wilczok (2004). "[Quantitative analysis of sigma genes expression in Mycobacterium tuberculosis cultures exposed to rifampicin and isoniazid]." Wiad Lek 57(5-6): 233-240.

Perez, E., S. Samper, Y. Bordas, C. Guilhot, B. Gicquel and C. Martin (2001). "An essential role for phoP in Mycobacterium tuberculosis virulence." Mol Microbiol 41(1): 179-187.

Polkade, A. V., S. S. Mantri, U. J. Patwekar and K. Jangid (2016). "Quorum Sensing: An Under-Explored Phenomenon in the Phylum Actinobacteria." Front Microbiol 7: 131.

Polmanteer, K. E. (1981). "Current Perspectives on Silicone Rubber Technology." Rubber Chemistry and Technology 54(5): 1051-1080.

Pratt, E. M. S. W. B. (2000). The Antimicrobial Drugs. Ney York, USA, Oxford University Press.

Prescott, L. M., Harley, J.P., Klein, D.A. (2005). Microbiology, McGraw-Hill Publishing.

Pym, A. S., P. Brodin, R. Brosch, M. Huerre and S. T. Cole (2002). "Loss of RD1 contributed to the attenuation of the live tuberculosis vaccines Mycobacterium bovis BCG and Mycobacterium microti." Mol Microbiol 46(3): 709-717.

Rajendran, V. and R. Sethumadhavan (2014). "Drug resistance mechanism of PncA in Mycobacterium tuberculosis." J Biomol Struct Dyn 32(2): 209-221.

Ramamurthy, T., A. Ghosh, G. P. Pazhani and S. Shinoda (2014). "Current Perspectives on Viable but Non-Culturable (VBNC) Pathogenic Bacteria." Front Public Health 2: 103.

Ramaswamy, S. and J. M. Musser (1998). "Molecular genetic basis of antimicrobial agent resistance in Mycobacterium tuberculosis: 1998 update." Tuber Lung Dis 79(1): 3-29.

Ramaswamy, S. V., A. G. Amin, S. Goksel, C. E. Stager, S. J. Dou, H. El Sahly, S. L. Moghazeh, B. N. Kreiswirth and J. M. Musser (2000). "Molecular genetic analysis of nucleotide polymorphisms associated with ethambutol resistance in human isolates of Mycobacterium tuberculosis." Antimicrob Agents Chemother 44(2): 326-336.

Ramu, G., Sreevatsa, U. Sengupta and K. V. Desikan (1981). "Evaluation of multiple regimens in leprosy." Lepr India 53(2): 190-196.

Rangaka, M. X., K. A. Wilkinson, J. R. Glynn, D. Ling, D. Menzies, J. Mwansa-Kambafwile, K. Fielding, R. J. Wilkinson and M. Pai (2012). "Predictive value of interferon-gamma release assays for incident active tuberculosis: a systematic review and meta-analysis." Lancet Infect Dis 12(1): 45-55.

I. Levin-Reisman, I. Ronin, O. Gefen, I. Braniss, N. Shoresh, N.Q. Balaban (2017). “Antibiotic tolerance facilitates the evolution of resistance”. Science 355, 826-830.

Renshaw, P. S., K. L. Lightbody, V. Veverka, F. W. Muskett, G. Kelly, T. A. Frenkiel, S. V. Gordon, R. G. Hewinson, B. Burke, J. Norman, R. A. Williamson and M. D. Carr (2005). "Structure and function of the complex formed by the tuberculosis virulence factors CFP-10 and ESAT-6." EMBO J 24(14): 2491-2498.

Ridell, M., G. Wallerstrom, D. E. Minnikin, R. C. Bolton and M. Magnusson (1992). "A comparative serological study of antigenic glycolipids from Mycobacterium tuberculosis." Tuber Lung Dis 73(2): 101-105.

Ritacco, V. and I. N. Kantor (2015). "[Tuberculosis 110 years after the Nobel Prize awarded to Koch]." Medicina (B Aires) 75(6): 396-403.

Ritz, N., W. A. Hanekom, R. Robins-Browne, W. J. Britton and N. Curtis (2008). "Influence of BCG vaccine strain on the immune response and protection against tuberculosis." FEMS Microbiol Rev 32(5): 821-841.

Roach, D. R., A. G. Bean, C. Demangel, M. P. France, H. Briscoe and W. J. Britton (2002). "TNF regulates chemokine induction essential for cell recruitment, granuloma formation, and clearance of mycobacterial infection." J Immunol 168(9): 4620-4627.

Roberts, M. E. and P. S. Stewart (2005). "Modelling protection from antimicrobial agents in biofilms through the formation of persister cells." Microbiology 151(Pt 1): 75-80.

Rodionova, I. A., B. M. Schuster, K. M. Guinn, L. Sorci, D. A. Scott, X. Li, I. Kheterpal, C. Shoen, M. Cynamon, C. Locher, E. J. Rubin and A. L. Osterman (2014). "Metabolic and bactericidal effects of targeted suppression of NadD and NadE enzymes in mycobacteria." MBio 5(1).

Romling, U., M. Y. Galperin and M. Gomelsky (2013). "Cyclic di-GMP: the first 25 years of a universal bacterial second messenger." Microbiol Mol Biol Rev 77(1): 1-52.

Rose, S. J. and L. E. Bermudez (2014). "Mycobacterium avium biofilm attenuates mononuclear phagocyte function by triggering hyperstimulation and apoptosis during early infection." Infect Immun 82(1): 405-412.

Roth, M. G. (2004). "Phosphoinositides in constitutive membrane traffic." Physiol Rev 84(3): 699-730.

Roy, A., M. Eisenhut, R. J. Harris, L. C. Rodrigues, S. Sridhar, S. Habermann, L. Snell, P. Mangtani, I. Adetifa, A. Lalvani and I. Abubakar (2014). "Effect of BCG vaccination against Mycobacterium tuberculosis infection in children: systematic review and meta-analysis." BMJ 349: g4643.

Russell, D. G., P. J. Cardona, M. J. Kim, S. Allain and F. Altare (2009). "Foamy macrophages and the progression of the human tuberculosis granuloma." Nat Immunol 10(9): 943-948.

Ryndak, M., S. Wang and I. Smith (2008). "PhoP, a key player in Mycobacterium tuberculosis virulence." Trends Microbiol 16(11): 528-534.

Sachadyn, P. (2010). "Conservation and diversity of MutS proteins." Mutat Res 694(1-2): 20-30.

Saleh, M. T. and J. T. Belisle (2000). "Secretion of an acid phosphatase (SapM) by Mycobacterium tuberculosis that is similar to eukaryotic acid phosphatases." J Bacteriol 182(23): 6850-6853.

Salina, E. G., S. J. Waddell, N. Hoffmann, I. Rosenkrands, P. D. Butcher and A. S. Kaprelyants (2014). "Potassium availability triggers Mycobacterium tuberculosis transition to, and resuscitation from, non-culturable (dormant) states." Open Biol 4(10).

Sambou, T., P. Dinadayala, G. Stadthagen, N. Barilone, Y. Bordat, P. Constant, F. Levillain, O. Neyrolles, B. Gicquel, A. Lemassu, M. Daffe and M. Jackson (2008). "Capsular glucan and intracellular glycogen of Mycobacterium tuberculosis: biosynthesis and impact on the persistence in mice." Mol Microbiol 70(3): 762-774.

Saxena, A., R. Kumari, U. Mukherjee, P. Singh and R. Lal (2014). "Draft Genome Sequence of the Rifamycin Producer Amycolatopsis rifamycinica DSM 46095." Genome Announc 2(4).

Scherr, N., R. Jayachandran, P. Mueller and J. Pieters (2009). "Interference of Mycobacterium tuberculosis with macrophage responses." Indian J Exp Biol 47(6): 401-406.

Schildberger, A., E. Rossmanith, T. Eichhorn, K. Strassl and V. Weber (2013). "Monocytes, peripheral blood mononuclear cells, and THP-1 cells exhibit different cytokine expression patterns following stimulation with lipopolysaccharide." Mediators Inflamm 2013: 697972.

Schlesinger, L. S. (1993). "Macrophage phagocytosis of virulent but not attenuated strains of Mycobacterium tuberculosis is mediated by mannose receptors in addition to complement receptors." J Immunol 150(7): 2920-2930.

Schnappinger, D., S. Ehrt, M. I. Voskuil, Y. Liu, J. A. Mangan, I. M. Monahan, G. Dolganov, B. Efron, P. D. Butcher, C. Nathan and G. K. Schoolnik (2003). "Transcriptional Adaptation of Mycobacterium tuberculosis within Macrophages: Insights into the Phagosomal Environment." J Exp Med 198(5): 693-704.

Schweizer, E. and J. Hofmann (2004). "Microbial type I fatty acid synthases (FAS): major players in a network of cellular FAS systems." Microbiol Mol Biol Rev 68(3): 501-517, table of contents.

Seghatoleslam, A., M. Hemmati, S. Ebadat, B. Movahedi and Z. Mostafavi-Pour (2016). "Macrophage Immune Response Suppression by Recombinant Mycobacterium tuberculosis Antigens, the ESAT-6, CFP-10, and ESAT-6/CFP-10 Fusion Proteins." Iran J Med Sci 41(4): 296-304.

Shah, D., Z. Zhang, A. Khodursky, N. Kaldalu, K. Kurg and K. Lewis (2006). "Persisters: a distinct physiological state of E. coli." BMC Microbiol 6: 53.

Shah, S. and V. Briken (2016). "Modular Organization of the ESX-5 Secretion System in Mycobacterium tuberculosis." Front Cell Infect Microbiol 6: 49.

Shah, S., J. R. Cannon, C. Fenselau and V. Briken (2015). "A Duplicated ESAT-6 Region of ESX-5 Is Involved in Protein Export and Virulence of Mycobacteria." Infect Immun 83(11): 4349-4361.

Sharma, D., A. R. Cukras, E. J. Rogers, D. R. Southworth and R. Green (2007). "Mutational analysis of S12 protein and implications for the accuracy of decoding by the ribosome." J Mol Biol 374(4): 1065-1076.

Sharma, I. M., A. Petchiappan and D. Chatterji (2014). "Quorum sensing and biofilm formation in mycobacteria: role of c-di-GMP and methods to study this second messenger." IUBMB Life 66(12): 823-834.

Sharma, I. M., S. Prakash, T. Dhanaraman and D. Chatterji (2014). "Characterization of a dual-active enzyme, DcpA, involved in cyclic diguanosine monophosphate turnover in Mycobacterium smegmatis." Microbiology 160(Pt 10): 2304-2318.

Shi, W., X. Zhang, X. Jiang, H. Yuan, J. S. Lee, C. E. Barry, 3rd, H. Wang, W. Zhang and Y. Zhang (2011). "Pyrazinamide inhibits trans-translation in Mycobacterium tuberculosis." Science 333(6049): 1630-1632.

Shiloh, M. U., P. Manzanillo and J. S. Cox (2008). "Mycobacterium tuberculosis senses host-derived carbon monoxide during macrophage infection." Cell Host Microbe 3(5): 323-330.

Sibille, Y. and H. Y. Reynolds (1990). "Macrophages and polymorphonuclear neutrophils in lung defense and injury." Am Rev Respir Dis 141(2): 471-501.

Simeone, R., A. Bobard, J. Lippmann, W. Bitter, L. Majlessi, R. Brosch and J. Enninga (2012). "Phagosomal rupture by Mycobacterium tuberculosis results in toxicity and host cell death." PLoS Pathog 8(2): e1002507.

Simeone, R., D. Bottai and R. Brosch (2009). "ESX/type VII secretion systems and their role in host-pathogen interaction." Curr Opin Microbiol 12(1): 4-10.

Singh, P., V. M. Katoch, K. K. Mohanty and D. S. Chauhan (2016). "Analysis of expression profile of mce operon genes (mce1, mce2, mce3 operon) in different Mycobacterium tuberculosis isolates at different growth phases." Indian J Med Res 143(4): 487-494.

Sirakova, T. D., V. S. Dubey, C. Deb, J. Daniel, T. A. Korotkova, B. Abomoelak and P. E. Kolattukudy (2006). "Identification of a diacylglycerol acyltransferase gene involved in accumulation of triacylglycerol in Mycobacterium tuberculosis under stress." Microbiology 152(Pt 9): 2717-2725.

Slayden, R. A., R. E. Lee and C. E. Barry, 3rd (2000). "Isoniazid affects multiple components of the type II fatty acid synthase system of Mycobacterium tuberculosis." Mol Microbiol 38(3): 514-525.

Sorensen, A. L., S. Nagai, G. Houen, P. Andersen and A. B. Andersen (1995). "Purification and characterization of a low-molecular-mass T-cell antigen secreted by Mycobacterium tuberculosis." Infect Immun 63(5): 1710-1717.

Sreevatsan, S., K. E. Stockbauer, X. Pan, B. N. Kreiswirth, S. L. Moghazeh, W. R. Jacobs, Jr., A. Telenti and J. M. Musser (1997). "Ethambutol resistance in Mycobacterium tuberculosis: critical role of embB mutations." Antimicrob Agents Chemother 41(8): 1677-1681.

Steenken, W., W. H. Oatway and S. A. Petroff (1934). "Biological Studies of the Tubercle Bacillus: Iii. Dissociation and Pathogenicity of the R and S Variants of the Human Tubercle Bacillus (H(37))." J Exp Med 60(4): 515-540.

Stewart, P. S. (2003). "Diffusion in biofilms." J Bacteriol 185(5): 1485-1491.

Stewart, P. S. (2015). "Antimicrobial Tolerance in Biofilms." Microbiol Spectr 3(3).

Stewart, P. S. and M. J. Franklin (2008). "Physiological heterogeneity in biofilms." Nat Rev Microbiol 6(3): 199-210.

Stockert, J. C., A. Blazquez-Castro and R. W. Horobin (2014). "Identifying different types of chromatin using Giemsa staining." Methods Mol Biol 1094: 25-38.

Stokes, R. W., R. Norris-Jones, D. E. Brooks, T. J. Beveridge, D. Doxsee and L. M. Thorson (2004). "The glycan-rich outer layer of the cell wall of Mycobacterium tuberculosis acts as an antiphagocytic capsule limiting the association of the bacterium with macrophages." Infect Immun 72(10): 5676-5686.

STRING. (2017). Retrieved 25 May, 2017, from www.string-db.org.

Strohmeier, G. R. and M. J. Fenton (1999). "Roles of lipoarabinomannan in the pathogenesis of tuberculosis." Microbes Infect 1(9): 709-717.

Szklarczyk, D., J. H. Morris, H. Cook, M. Kuhn, S. Wyder, M. Simonovic, A. Santos, N. T. Doncheva, A. Roth, P. Bork, L. J. Jensen and C. von Mering (2017). "The STRING database in 2017: quality-controlled protein-protein association networks, made broadly accessible." Nucleic Acids Res 45(D1): D362-D368.

J.D. Szumowski, K.N. Adams, P.H. Edelstein, and L. Ramakrishnan (2013). “Antimicrobial efflux pumps and Mycobacterium tuberculosis drug tolerance: Evolutionary Considerations”. Curr Top Microbiol Immunol 2013; 374

Tan, M. P., P. Sequeira, W. W. Lin, W. Y. Phong, P. Cliff, S. H. Ng, B. H. Lee, L. Camacho, D. Schnappinger, S. Ehrt, T. Dick, K. Pethe and S. Alonso (2010). "Nitrate respiration protects hypoxic Mycobacterium tuberculosis against acid- and reactive nitrogen species stresses." PLoS One 5(10): e13356.

Taype, C. A., J. C. Agapito, R. A. Accinelli, J. R. Espinoza, S. Godreuil, S. J. Goodman, A. L. Banuls and M. A. Shaw (2012). "Genetic diversity, population structure and drug resistance of Mycobacterium tuberculosis in Peru." Infect Genet Evol 12(3): 577-585.

TB Genomes Database. (2017). Retrieved 1 May, 2017, from www.genome.tbdb.org.

Telenti, A., P. Imboden, F. Marchesi, D. Lowrie, S. Cole, M. J. Colston, L. Matter, K. Schopfer and T. Bodmer (1993). "Detection of rifampicin-resistance mutations in Mycobacterium tuberculosis." Lancet 341(8846): 647-650.

Telenti, A., W. J. Philipp, S. Sreevatsan, C. Bernasconi, K. E. Stockbauer, B. Wieles, J. M. Musser and W. R. Jacobs, Jr. (1997). "The emb operon, a gene cluster of Mycobacterium tuberculosis involved in resistance to ethambutol." Nat Med 3(5): 567-570.

Teo, A., A. Mantalaris, K. Song and M. Lim (2014). "A novel perfused rotary bioreactor for cardiomyogenesis of embryonic stem cells." Biotechnol Lett 36(5): 947-960.

Thorel, M. F., M. Krichevsky and V. V. Levy-Frebault (1990). "Numerical taxonomy of mycobactin-dependent mycobacteria, emended description of Mycobacterium avium, and description of Mycobacterium avium subsp. avium subsp. nov., Mycobacterium avium subsp. paratuberculosis subsp. nov., and Mycobacterium avium subsp. silvaticum subsp. nov." Int J Syst Bacteriol 40(3): 254-260.

Tiberi, S., R. Buchanan, J. A. Caminero, R. Centis, M. A. Arbex, M. Salazar, J. Potter and G. B. Migliori (2017). Presse Med.

Timm, J., F. A. Post, L. G. Bekker, G. B. Walther, H. C. Wainwright, R. Manganelli, W. T. Chan, L. Tsenova, B. Gold, I. Smith, G. Kaplan and J. D. McKinney (2003). "Differential expression of iron-, carbon-, and oxygen-responsive mycobacterial genes in the lungs of chronically infected mice and tuberculosis patients." Proc Natl Acad Sci U S A 100(24): 14321-14326.

Trajman, A., R. E. Steffen and D. Menzies (2013). "Interferon-Gamma Release Assays versus Tuberculin Skin Testing for the Diagnosis of Latent Tuberculosis Infection: An Overview of the Evidence." Pulm Med 2013: 601737.

Trivedi, A., P. S. Mavi, D. Bhatt and A. Kumar (2016). "Thiol reductive stress induces cellulose-anchored biofilm formation in Mycobacterium tuberculosis." Nat Commun 7: 11392.

Trunz, B. B., P. Fine and C. Dye (2006). "Effect of BCG vaccination on childhood tuberculous meningitis and miliary tuberculosis worldwide: a meta-analysis and assessment of cost-effectiveness." Lancet 367(9517): 1173-1180.

Tsuchiya, S., M. Yamabe, Y. Yamaguchi, Y. Kobayashi, T. Konno and K. Tada (1980). "Establishment and characterization of a human acute monocytic leukemia cell line (THP-1)." Int J Cancer 26(2): 171-176.

TubercuList. (2017). Retrieved 1 May, 2017, from www.tuberculist.org.

Tudo, G., K. Laing, D. A. Mitchison, P. D. Butcher and S. J. Waddell (2010). "Examining the basis of isoniazid tolerance in nonreplicating Mycobacterium tuberculosis using transcriptional profiling." Future Med Chem 2(8): 1371-1383.

Underhill, D. M., A. Ozinsky, K. D. Smith and A. Aderem (1999). "Toll-like receptor-2 mediates mycobacteria-induced proinflammatory signaling in macrophages." Proc Natl Acad Sci U S A 96(25): 14459-14463.

Vassalli, P. (1992). "The pathophysiology of tumor necrosis factors." Annu Rev Immunol 10: 411-452.

Veerachamy, S., T. Yarlagadda, G. Manivasagam and P. K. Yarlagadda (2014). "Bacterial adherence and biofilm formation on medical implants: a review." Proc Inst Mech Eng H 228(10): 1083-1099.

Vergne, I., J. Chua, H. H. Lee, M. Lucas, J. Belisle and V. Deretic (2005). "Mechanism of phagolysosome biogenesis block by viable Mycobacterium tuberculosis." Proc Natl Acad Sci U S A 102(11): 4033-4038.

Veziris, N., C. Bernard, L. Guglielmetti, D. Le Du, D. Marigot-Outtandy, M. Jaspard, E. Caumes, I. Lerat, C. Rioux, Y. Yazdanpanah, A. Tiotiu, N. Lemaitre, F. Brossier, V. Jarlier, J. Robert, W. Sougakoff, A. Aubry, C. N. R. MyRMA and C. N. R. M. the Tuberculosis Consilium of the (2016). "Rapid emergence of Mycobacterium tuberculosis bedaquiline resistance: lessons to avoid repeating past errors." Eur Respir J.

Vollmer, W., D. Blanot and M. A. de Pedro (2008). "Peptidoglycan structure and architecture." FEMS Microbiol Rev 32(2): 149-167.

Voskuil, M. I., D. Schnappinger, K. C. Visconti, M. I. Harrell, G. M. Dolganov, D. R. Sherman and G. K. Schoolnik (2003). "Inhibition of respiration by nitric oxide induces a Mycobacterium tuberculosis dormancy program." J Exp Med 198(5): 705-713.

Voskuil, M. I., K. C. Visconti and G. K. Schoolnik (2004). "Mycobacterium tuberculosis gene expression during adaptation to stationary phase and low-oxygen dormancy." Tuberculosis (Edinb) 84(3-4): 218-227.

Wakamoto Y, Dhar N, Chait R, Schneider K, Signorino-Gelo F, Leibler S, McKinney JD (2012). “Dynamic persistence of antibiotic-stressed mycobacteria”. Science. 2013 Jan 4;339(6115):91-5

Wayne, L. G. (1976). "Dynamics of submerged growth of Mycobacterium tuberculosis under aerobic and microaerophilic conditions." Am Rev Respir Dis 114(4): 807-811.

Wayne, L. G. and L. G. Hayes (1996). "An in vitro model for sequential study of shiftdown of Mycobacterium tuberculosis through two stages of nonreplicating persistence." Infect Immun 64(6): 2062-2069.

Wayne, L. G. and H. A. Sramek (1994). "Metronidazole is bactericidal to dormant cells of Mycobacterium tuberculosis." Antimicrob Agents Chemother 38(9): 2054-2058.

Wengenack, N. L. and F. Rusnak (2001). "Evidence for isoniazid-dependent free radical generation catalyzed by Mycobacterium tuberculosis KatG and the isoniazid-resistant mutant KatG(S315T)." Biochemistry 40(30): 8990-8996.

Whitfield, M. G., H. M. Soeters, R. M. Warren, T. York, S. L. Sampson, E. M. Streicher, P. D. van Helden and A. van Rie (2015). "A Global Perspective on Pyrazinamide Resistance: Systematic Review and Meta-Analysis." PLoS One 10(7): e0133869.

Wiker, H. G. (2009). "MPB70 and MPB83--major antigens of Mycobacterium bovis." Scand J Immunol 69(6): 492-499.

Wilson, M., J. DeRisi, H. H. Kristensen, P. Imboden, S. Rane, P. O. Brown and G. K. Schoolnik (1999). "Exploring drug-induced alterations in gene expression in Mycobacterium tuberculosis by microarray hybridization." Proc Natl Acad Sci U S A 96(22): 12833-12838.

Woldehanna, S. and J. Volmink (2004). "Treatment of latent tuberculosis infection in HIV infected persons." Cochrane Database Syst Rev(1): CD000171.

World Health Organisation. (2013). Retrieved 07 March, 2017.

World Health Organisation. (2014). "Companion handbook to the HO guidelines for the programmatic management of drug-resistant tuberculosis." Retrieved 15 March, 2017, from http://apps.who.int/iris/bitstream/10665/130918/1/9789241548809_eng.pdf?ua=1&ua=1.

World Health Organisation. (2014). "Global Tuberculosis Report 2014." Retrieved 15 March, 2017, from http://www.who.int/tb/publications/global_report/gtbr14_main_text.pdf.

World Health Organisation. (2016, September 2016). "Antimicrobial resistance fact sheet." Retrieved 15 March, 2017, from http://www.who.int/mediacentre/factsheets/fs194/en/.

World Health Organisation. (2016, October 2016). "Tuberculosis Fact Sheet." Retrieved 10 March, 2017, from http://www.who.int/mediacentre/factsheets/fs104/en/.

Wurmser, A. E., J. D. Gary and S. D. Emr (1999). "Phosphoinositide 3-kinases and their FYVE domain-containing effectors as regulators of vacuolar/lysosomal membrane trafficking pathways." J Biol Chem 274(14): 9129-9132.

Xavier, A. S. and M. Lakshmanan (2014). "Delamanid: A new armor in combating drug-resistant tuberculosis." J Pharmacol Pharmacother 5(3): 222-224.

Yamori, S., S. Ichiyama, K. Shimokata and M. Tsukamura (1992). "Bacteriostatic and bactericidal activity of antituberculosis drugs against Mycobacterium tuberculosis, Mycobacterium avium-Mycobacterium intracellulare complex and Mycobacterium kansasii in different growth phases." Microbiol Immunol 36(4): 361-368.

Zhang, F. and J. P. Xie (2011). "Mammalian cell entry gene family of Mycobacterium tuberculosis." Mol Cell Biochem 352(1-2): 1-10.

Zhang, H. (2006). The Permeability Characteristics of Silicone Rubber. Society for the Advancement of Material and Process Engineering. Dallas, TX, USA.

Zodpey, S. P. and S. N. Shrikhande (2007). "The geographic location (latitude) of studies evaluating protective effect of BCG vaccine and it's efficacy/effectiveness against tuberculosis." Indian J Public Health 51(4): 205-210.

Zumla, A., P. Mwaba, J. Huggett, N. Kapata, D. Chanda and J. Grange (2009). "Reflections on the white plague." Lancet Infect Dis 9(3): 197-202.

Zumla, A., M. Raviglione, R. Hafner and C. F. von Reyn (2013). "Tuberculosis." N Engl J Med 368(8): 745-755.

Zwerling, A., M. A. Behr, A. Verma, T. F. Brewer, D. Menzies and M. Pai (2011). "The BCG World Atlas: a database of global BCG vaccination policies and practices." PLoS Med 8(3): e1001012.